LEABHARLANN CHOLÁISTE NA TRÍONÓIDE, BAILE ÁTHA CLIATH | TRINITY COLLEGE LIBRARY DUBLIN
Ollscoil Átha Cliath | The University of Dublin

Terms and Conditions of Use of Digitised Theses from Trinity College Library Dublin

Copyright statement

All material supplied by Trinity College Library is protected by copyright (under the Copyright and Related Rights Act, 2000 as amended) and other relevant Intellectual Property Rights. By accessing and using a Digitised Thesis from Trinity College Library you acknowledge that all Intellectual Property Rights in any Works supplied are the sole and exclusive property of the copyright and/or other IPR holder. Specific copyright holders may not be explicitly identified. Use of materials from other sources within a thesis should not be construed as a claim over them.

A non-exclusive, non-transferable licence is hereby granted to those using or reproducing, in whole or in part, the material for valid purposes, providing the copyright owners are acknowledged using the normal conventions. Where specific permission to use material is required, this is identified and such permission must be sought from the copyright holder or agency cited.

Liability statement

By using a Digitised Thesis, I accept that Trinity College Dublin bears no legal responsibility for the accuracy, legality or comprehensiveness of materials contained within the thesis, and that Trinity College Dublin accepts no liability for indirect, consequential, or incidental, damages or losses arising from use of the thesis for whatever reason. Information located in a thesis may be subject to specific use constraints, details of which may not be explicitly described. It is the responsibility of potential and actual users to be aware of such constraints and to abide by them. By making use of material from a digitised thesis, you accept these copyright and disclaimer provisions. Where it is brought to the attention of Trinity College Library that there may be a breach of copyright or other restraint, it is the policy to withdraw or take down access to a thesis while the issue is being resolved.

Access Agreement

By using a Digitised Thesis from Trinity College Library you are bound by the following Terms & Conditions. Please read them carefully.

I have read and I understand the following statement: All material supplied via a Digitised Thesis from Trinity College Library is protected by copyright and other intellectual property rights, and duplication or sale of all or part of any of a thesis is not permitted, except that material may be duplicated by you for your research use or for educational purposes in electronic or print form providing the copyright owners are acknowledged using the normal conventions. You must obtain permission for any other use. Electronic or print copies may not be offered, whether for sale or otherwise to anyone. This copy has been supplied on the understanding that it is copyright material and that no quotation from the thesis may be published without proper acknowledgement.

Development of an Antisense Strategy to Down-Regulate Gene Expression in Chronic Myelogenous Leukaemia



A thesis submitted for the degree of

Doctor of Philosophy

Lisa M. O' Connor

Trinity College,

University of Dublin

Trinity Term

2005

TRINITY COLLEGE
10 JUL 2006
LIBRARY DUBLIN
THOSIS
7918

To Mary & Jeremiah

Declaration

I hereby certify that this thesis, submitted for the degree of Doctor of Philosophy to the University of Dublin, has not been previously submitted for a degree or diploma to this or any other university. The work presented here is entirely my own, except where stated.

This thesis may be made available for consultation within the university library and may be photocopied or lent to other libraries for the purpose of consultation.



Lisa O' Connor

Trinity Term 2005

Acknowledgements

I would like to thank my supervisor; Professor Mark Lawler, for giving me the opportunity to do this PhD and for all his guidance and support over the last few years, especially when preparing for talks and presentations, and particularly over the last few months with corrections and advice on this thesis.

Thanks to Professor Shaun McCann and his team of consultants & doctors in the Department of Haematology for their input and advice over the course of the PhD. I'd also like to acknowledge the help of Dr Nicola Gardiner and Dr Patrick Hayden. Thanks also to Richard Giles of the University of Liverpool for his advice with streptolysin-O.

I'd especially like to thank all the great people I've worked with over the course of the project, these include my colleagues in Haematology & Oncology in Sir Patrick Duns Research laboratories, Kathy, Neil, Ludmila, Tony, Jacqui, Prerna, Amjad, Fiona, & Ruth. Mireille gets a special thank you for her essential and much appreciated guidance with the flow cytometer. I'd also like to thank the new gang in the Institute of Molecular Medicine, Antionette, Laure, Martin McGill, Martin Barr, Elaina and Danni. Thanks to Frances who was a tremendous help during the correcting process.

Thanks to Yuri and Basma from Dermot Kellehers group for their help with the fluorescent microscope and also to Eileen Looby for her input. I'd like to express my gratitude to members of the other research laboratories, biochemistry, immunology and vitamin research in the SPD and IMM for their valuable assistance. Thanks to Joe McPartlin and Deirdre Ní Eidhín for their technical advice and practical help with pieces of equipment.

Thanks to my Mom, Mary, for her constant support through all the decisions I've made, and to all the members of my family, for their on-going love & support; especially to Geraldine for her advice on this thesis. Thank you to Neal, for all the support, printing and cups of tea.

Abstract

Since the discovery of mRNA down-regulation by sequences of complementary nucleic acids in 1977, there has been a drive to apply the antisense phenomenon to therapeutic settings. In theory the potential of antisense therapeutics is extensive, however practically, antisense-based therapeutics are not yet widely applied due to limitations and secondary effects of antisense chemistries. This thesis examines the impact of existing and novel antisense backbones on the expression of the Chronic Myelogenous Leukaemia specific protein, BCR-ABL. Novel chemistries examined include the morpholino which prevents the translation of target mRNA transcripts by steric hindrance, and the RNAi approach which utilises anti-pathogenic pathways to mediate mRNA destruction.

For true antisense effects to be induced, the antisense oligonucleotide must down-regulate mRNA expression in a sequence specific manner. Each antisense sequence designed in this study was monitored for complementarity to unintended targets using a bioinformatics approach and antisense effects were measured relative to sequence and chemistry controls. Delivery of oligonucleotide molecules both to target organs and inside the cell presents a significant obstacle to antisense effects. Transient cell permeabilisation using streptolysin-O was used to localise antisense molecules in the cytosol and facilitate their hybridisation to target mRNA. This approach proved highly effective in achieving appropriate delivery of antisense molecules while preserving cellular integrity.

The efficiency of down-regulation achieved by antisense molecules was measured using both real time PCR and Western blotting approaches. It was found to be dependent on both the chemistry employed in the antisense molecule and the secondary structure of both the target and antisense molecule. Additional factors included the mRNA binding site and the use of cellular delivery agents, particularly agents which allowed permeabilisation of cells for efficient antisense delivery. Effective down-regulation of gene expression was achieved using all approaches but morpholino and RNAi based approaches showed particular benefit in relation to lack of non sequence specific effects. Reductions in cell proliferation upon BCR-ABL down-regulation were limited so a second CML protein; cyclin D2 was also

targeted for antisense down-regulation and preliminary results were promising. In summary, novel antisense chemistries show distinct advantages over first generation antisense backbones and display superior ability to mediate specific down-regulation of target gene expression. Coupled with efficient delivery, novel backbone chemistries may prove useful in the down-regulation of BCR-ABL expression and may help limit the oncogenic potential of Chronic Myelogenous Leukaemia cells.

Glossary

aa	amino acid
abl	abelson gene present on Chromosome 9
ABMT	autologous BMT
ALL	acute lymphocytic leukaemia
AML	acute myeloid leukaemia
Ara-C	cytosine arabinoside
ATP	adenosine triphosphate
bcr	break-point cluster region on chromosome 22
bcr-abl	bcr-abl gene / mRNA
BCR-ABL	bcr-abl protein product (p210)
BMT	Bone marrow transplant
CML	Chronic Myelogenous Leukaemia
CDK	cyclin dependent kinase
Cdki	cyclin dependent kinase inhibitor
C elegans	*Caenorhabditis* elegans
DNA	deoxyribonucleic acid
dsRNA	double-stranded RNA
FANA	2'-fluoro-D-arabinonucleic acid
GNEF	guanine nucleotide exchange factor
GFP	Green Fluorescent protein
GVHD	graft versus host disease
GVL	graft versus leukaemia
GTP, GDP	guanine trinucleotide, guanine dinucleotide
IFN	interferon
IL-3	interleukin-3
Kb	kilobases of DNA
KDa	kilodaltons
MFE	minimum free energy
Mg/kg/d	milligrams per kilogram of body weight per day
mRNA	messenger ribonucleic acid
NHL	Non-Hodgkin's Lymphoma
NLS	nuclear localization signal
nt	nucleotide
O(D)N	oligo(deoxy)nucleotide
PI	Propidium iodide
PTGS	post-transcriptional gene silencing
Rb	retinoblastoma
RISC	RNA-induced silencing complex
RNA	ribonucleic acid
RNAi	RNA interference
rRNA	ribosomal RNA
SH	Src homology
siRNA	small interfering RNA
SL-O	streptolysin-O
STAT	signal transduction and activation of transcription
TFO	triple helix forming oligonucleotides
Tm	Melting Temperature
U	Units of SL-O activity, 1U/µl
^{177}Y	tyrosine residue 177 on bcr

Chapter I Introduction

			Page
1.1	Chronic Myelogenous Leukaemia (CML)		2
1.2	The Philadelphia Chromosome		3
1.3	Stages of CML		4
1.4	CML Therapy		4
	1.4.1	Interferon-alpha (IFN-α)	5
	1.4.2	Bone Marrow Transplantation (BMT)	5
	1.4.3	Imatinib Mesylate	7
1.5	The ABL Gene and Protein		9
	1.5.1	Role of ABL in Cell Cycle Regulation	9
1.6	The BCR Gene and Protein		10
1.7	Pathways of BCR-ABL mediated transformation		12
	1.7.1	RAS activation and down-stream effects	13
	1.7.2	Myc Activation	13
	1.7.3	Interleukin-3 (IL-3) Pathways	15
	1.7.4	STAT Family Involvement	15
	1.7.5	Modulation of D-Type Cyclins by BCR-ABL	16
	1.7.6	BAD mediated inhibition of apoptosis	18
1.8	Altered Adhesion of CML cells		19
1.9	Investigational Treatments for CML		20
1.10	Antisense		22
	1.10.1	Overview of Antisense	22
1.11	Steric Hindrance		24
1.12	Enzymatic cleavage of target mRNA transcript		24
1.13	Chemistry of the Antisense Backbone		25
	1.13.1	The Phosphorothioate Backbone	25
	1.13.2	Chimeric Backbones + Subunit Modifications	30
	1.13.3	Sub-unit Modification	31
	1.13.4	RNAse L	32
	1.13.5	RNase H Independent Backbones	33
	1.13.5-a	Morpholino	33
	1.13.5-b	Peptide nucleic acids	35
	1.13.6	Ribozymes	36

page

1.14 Cytosolic delivery of Antisense Molecules 37
1.14.1 Overview of cytosolic antisense Delivery 37
1.14.2 Carrier Agents 38
1.14.3 Cell Permeabilisation Agents 39
1.14.3-a Saponin 40
1.14.3-b Streptolysin-O (SL-O) 40
1.14.3 Peptide-mediated delivery of antisense molecules 41
1.15 Hybridisation 43
1.15.1 Overview of Hybridsiation 43
1.15.2 Secondary Structure 43
1.15.3 mRNA Target Site Selection 44

1.16 RNA Interference (RNAi) 47

1.17 Mechanism of dsRNA induced silencing 48
1.18 Phosphorothioate versus RNAi 50
1.19 Amplification of RNAi and systemic silencing 50
1.20 siRNA design parameters for efficient RNAi induction 52
1.20.1 siRNA modification and specific activity 53
1.21 Induction of endogenous siRNA expression in mammals 54
1.22 Clinical Applications of Antisense Molecules 55

Chapter II Methodologies 58

2.1 Selection of optimal mRNA sites for targeting with nucleic acid molecules 59
2.1.1 Parameters for sequence input 59
2.1.2 Output parameters 60
2.2 Culture of CML Cell Lines 61
2.2.1 Maintaining cell lines 62
2.3 cDNA Preparation 63
2.3.1 TRIzol Method Overview 63
2.3.2 RNA extraction using TRIzol 63
2.3.3 DNase Treatment of isolated RNA 64
2.3.4 RNA Analysis 65
2.3.5 Synthesis of cDNA from RNA template 65

2.4 Saponin Experiments 66

2.4.1 Saponin Permeabilisation Method 1 66

2.4.2 Saponin Permeabilisation Methos 11 66

2.5 Streptolysin-O cell permeabilisation 68

2.5.1 Thiol-activation of *Streptococcus pyogenes* SL-O 68

2.5.2 Permeabilisation of CML suspension cell lines with SL-O 69

2.6 Visualisation of FAM labelled Antisense Uptake using Fluorescent Microscope Analysis 70

2.7 Detection of FAM labelled Antisense Uptake using Flow Cytometric Analysis 71

2.7.1 Preparation of CML cells for Flow Analysis 71

2.7.2 Flow Cytometry Analysis 71

2.8 Treatments of cell lines with Antisense Molecules 73

2.8.1 Experimental Format for Antisense Treatments 73

2.8.2 Nuclear staining of CML cell lines using Hoechst dye 74

2.8.3 Assessment of FAM labelled Antisense uptake following permeabilisation 74

2.9 Detection of Gene Expression Profiles using Real Time PCR 76

2.9.1 TaqMan Fluorescent-based PCR 76

2.9.2 Design of TaqMan reagents using Primer Express ® 77

2.9.3 Determination of target transcript expression levels 77

2.10 Analysis of protein expression 80

2.10.1 Lysis Solution for protein extraction 80

2.10.2 Quantitation of Protein Yields using The Bradford Assay 81

2.10.3 Electrophoretic separation of proteins by SDS PAGE 81

2.10.4 Transfer of protein species to Nitrocellulose Membrane 83

2.10.5 Immuno-detection of Protein expression 84

2.10.6 Stripping & re-probing nitrocellulose membrane 85

2.11 *In vitro* micro-culture assay for cell proliferation / viability Assay 86

2.11.1 Measurement of proliferative capacity 86

2.12 Determining the effect of Novel backbone chemistries on the growth and expansion of Haematopoietic Stem Cells 87

2.12.1 PBMC Isolation 87

2.12.2 Incubation of Primary Haematopoietic cells in methylcellulose 88

Chapter III Selection of Optimal Antisense Molecules for mRNA Down-Regulation 89

3.1 Design of Antisense Molecules 90
3.1.1 SFold 91
3.1.2 SFold output 91
3.2 Statistical Prediction of Optimal Folding Conformation 92
3.3 Secondary structure of bcr-abl mRNA variants 92
3.3.1 Availability of bases for hybridisation 93
3.4 Bcr-abl translational start site positional effects 94
3.5 The b2a2 & b3a2 bcr-abl mRNA breakpoints 95
3.6 Secondary structure of cyclin D2 mRNA 97
3.6.1 Cyclin D2 mRNA positional analysis 97
3.7 Selection parameters for Phosphorothioate backbone Antisense molecules 101
3.7.1 The 'P' Oligonucleotide selection 101
3.7.2 The 'PS' Oligonucleotide Design 103
3.8 Morpholino Molecule Selection: The RNase H Independent Approach 106
3.8.1 bcr-abl targeted Morpholino molecules 106
3.8.2 Cyclin D2 targeted Morpholino molecules 108
3.9 Design of siRNA duplexes 110
3.9.1 bcr-abl directed siRNA molecules 111
3.9.2 cyclin D2 siRNA design 112
3.10 Specificity of Antisense molecules selected for this study 114
3.10.1 Specificity of phosphorothioate molecules 115
3.10.2 Specificity of morpholino molecules 115
3.10.3 Specificity of siRNA duplexes 117
3.11 Discussion 118

Chapter IV Delivery of Antisense Molecules mediated by Cell Permeabilisation Approaches 121

4.1 Introduction to antisense delivery 122
4.2 Investigating pore forming potential of saponin in CML cells 124

4.2.1 Saponin mediated cell toxicity 124
4.2.2 Uptake of fluorescently labelled phosphorothioate molecules using Saponin 125
4.3 Streptolysin-O mediated antisense delivery 128
4.3.1 Presence of 'haloes' using SL-O 128
4.3.2 Delivery of FAM-labelled Antisense Molecules using SL-O 129
4.3.3 Cellular localisation of the antisense molecule using SL-O 131
4.3.4 Monitoring the Toxic Effects of SL-O 132
4.4 Analysis of antisense uptake into CML cells and associated levels of toxicity using flow cytometry 133
4.5 Discussion 134
4.5.1 Saponin cell permeabilisation 134
4.5.2 SL-O cell permeabilisation 136

Chapter V Down-regulation of bcr-abl mRNA transcripts induced by Phosphorothioate antisense molecules 138

5.1 The 'P' Phosphorothioate Oligonucleotides 139
5.1.1 Targeting the bcr-abl mRNA translational start site with P1 139
5.1.2 Targeting the b2a2 bcr-abl mRNA breakpoint with P3 144
5.1.3 Targeting the b3a2 bcr-abl mRNA breakpoint using P2 148
5.2 The 'PS' Phosphorothioate Series 154
5.2.1 PS2 mediated b2a2 down-regulation 155
5.2.2 PS2 mediated mRNA down-regulation in the absence of delivery 157
5.2.3 The effect of non-specific PS2 controls on b2a2 expression 158
5.2.4 PS3 mediated inhibition of b3a2 mRNA expression 159
5.3 Discussion 162
5.3.1 Discussion of 'P' phosphorothioate series 162
5.3.2 Discussion of 'PS' phosphorothioate series 166
5.3.3 Targeting the bcr-abl mRNA with phosphorothioate chemistry antisense molecules 168

Chapter VI Translational Inhibition induced by RNase H-Independent Morpholino Antisense Molecules 170

6.1 Introduction to the Morpholino Backbone Experiments 171
6.2 Cellular Delivery of Morpholino Chemistry Molecules 172
6.3 MPL_bcr induces sequence specific down-regulation of BCR-ABL 173
6.4 MPL_bcr induces dose dependent down-regulation of BCR-ABL 174
6.5. Morpholino Antisense molecules induce enhanced p210 down-regulation relative to the Phosphorothioate in KCL-22 cells 175
6.5.1 Morpholino Antisense Molecules induce enhanced BCR-ABL down-regulation relative to phosphorothioate oligonucleotides over a range of concentrations 176
6.6. BCR-ABL (p210) down-regulation is not accompanied by significant changes in proliferative capacity of CML cells 177
6.7. The influence of morpholino chemistry antisense oligonucleotides on haematopoietic cell proliferation 178
6.8. Discussion 179

Chapter VII RNA-Interference (RNAi)-mediated bcr-abl down-regulation

7.1 Introduction 184
7.2 siRNA mediated bcr-abl mRNA down-regulation 186
7.3 BCR-ABL (p210) protein expression following siRNA mediated bcr-abl mRNA down-regulation 188
7.4 Cell Proliferation capacity of CML cell lines following siRNA down-regulation of bcr-abl mRNA 190
7.5 The efficiency of the siRNA 'pool' to mediate bcr-abl down-regulation in the absence of SL-O delivery 191
7.5.1 mRNA down-regulation 191
7.5.2 Inhibition of proliferative capacity 192
7.6 Correlation of mRNA degradation with target region 193
7.7 siRNA - mediated mRNA down-regulation is sequence specific and not chemistry dependent 194
7.8 Effect of siRNA duplexes on primary haematopoietic cell clonogenicity 195
7.9 Discussion 196

Chapter VIII Cyclin D2 as a novel target to reduce proliferation of Chronic Myeloid Leukaemia cells 199

8.1 Introduction 200
8.2 Cyclin D2 expression in CML cell lines 202
8.3 Cyclin D2 mRNA down-regulation using siRNA molecules 204
8.4 Proliferative capacity of CML cells following siRNA mediated Cyclin D2 down-regulation 206
8.5 The impact of cyclin D2 targeted morpholino molecules on the proliferative capacity of CML cells 208
8.6 The impact of target site selection on siRNA activity 209
8.7 Discussion 210

Chapter IX General Discussion and Future Directions 214

9.1 Introduction 215
9.2 Targeting mRNA transcripts for antisense hybridisation & the role of secondary structure prediction tools 216
9.3 Modes of antisense delivery 220
9.3.1 Cell permeabilisation via polyene antibiotics 222
9.4 Development of phosphorothioate-based antisense molecules 223
9.5 Novel antisense approaches 226
9.5.1 Morpholino antisense molecules 226
9.5.2 siRNA induced gene down-regulation 229
9.5.3 RNAi Potential for Therapeutic Applications 230
9.6 The potential role of Antisense therapeutics in the treatment of CML 233
9.7 Down-regulating cyclin D2 expression in CML 234
9.8 Future directions 235
9.9 'Shooting the messenger' - Concluding remarks 236

Appendix-
Optimisation of TaqMan parameters for determination of gene expression by the comparative method 237

Figures & Tables

Chapter I Introduction

Figure 1.1 Functional regions on the normal ABL Protein (p145)
Figure 1.2 Functional regions on the normal BCR protein
Figure 1.3 Position of breakpoints in the abl gene (green) and the bcr gene (blue), numbers represent exon positions in both genes.
Figure 1.4 Position of exons in abl (green) and bcr (blue) genes following translocations resulting in the e1a2, b2a2, b3a2 and e19a2 transcripts
Figure 1.5 Cellular pathways activated by BCR-ABL to mediate CML cell proliferation, inhibit apoptosis and stimulate early release of progenitor cells into circulation.
Figure 1.6 Induction of cyclin D2 expression by BCR-ABL
Figure 1.7 Antisense mediated down-regulation of mRNA expression
Figure 1.8 Structures of commonly employed antisense backbones
Figure 1.9 Chimeric antisense molecules incorporating RNase H activating phosphorothioate sections and RNase H independent regions at alternative positions
Figure 1.10 Pore formation in a eukaryotic cell membrane by the bacterial toxin streptolysin-O
Figure 1.11 Selection of antisense oligonucleotides to an mRNA target based on their hybridisation ability. Sequences selected by this method are tested for their ability to induce RNase H mediated mRNA transcript cleavage
Figure 1.12 siRNA mediated gene silencing in mammalian systems mediated by the active RNA-induced Silencing Complex
Figure 1.13 The Random Degradative PCR model for prolongation and persistence of RNAi mediated gene silencing.

Table 1.1 Characteristics and properties of backbone and subunit modification of Antisense molecules
Table 1.2 Examples of antisense molecules involved in clinical trials

Chapter II Methodologies

Figure 2.1 mRNA sequence output structure determined using *mfold* web server

Table 2.1 Details of CML suspension cell lines employed in this study
Table 2.2 Components of a cDNA synthesis reaction
Table 2.3 Sub-groups of cells in the four quadrants of the flow cytometry grid following selection of cell population.
Table 2.4 Plate layout for SL-O mediated Antisense Treatment of CML cell lines
Table 2.5 Primer and probe sequences used for TaqMan PCR amplification of the target genes bcr-abl (b2a2 & b3a2), the house keeping gene, GAPDH & Cyclin D2
Table 2.6 Lysis Buffer for extraction of protein from cell lines
Table 2.7 Preparation of Protein Standards for Bradford Assay
Table 2.8 Components of an 8% resolving gel used to separate BCR-ABL and actin
Table 2.9 Components of a 5% stacking gel used to separate BCR-ABL and actin
Table 2.10 Details of antibodies employed in this study to detect protein expression

Chapter III Selection of Optimal Antisense Molecules for mRNA Down-Regulation

Figure 3.1 Secondary structure of the b2a2 bcr-abl mRNA displaying regions of the molecule involved in intra-molecular base pairing predicted using *mfold* software

Figure 3.2 Secondary structure of the b3a2 bcr-abl mRNA displaying regions of the molecule involved in intra-molecular base pairing predicted using *mFold* software

Figure 3.3 A probability profile graph showing the probability of bases surrounding the bcr-abl start site being involved in loops and therefore accessible for antisense hybridisation

Figure 3.4 A probability profile graph showing the probability of bases surrounding the b3a2 breakpoint being involved in loops and therefore accessible to antisense hybridisation

Figure 3.5 A probability profile graph showing the probability of bases surrounding the b2a2 breakpoint being involved in loops and therefore accessible to antisense hybridisation

Figure 3.6 A section of the Cyclin D2 secondary structure (complete mRNA is inset)

Figure 3.7 Probability profile of the cyclin D2 start site (nt 270) incorporating the region targeted by the morpholino molecule (nt 236)

Figure 3.8 Local area secondary structure surrounding the morpholino target region and translational start site of cyclin D2

Figure 3.9 Probability profile of a section of the cyclin D2 mRNA incorporating the region targeted by siRNA molecule 1 (nt 602)

Figure 3.10 Local secondary structure surrounding the target region of the Tuschl motif siRNA molecule (602)

Figure 3.11 Probability profile of a section of the cyclin D2 mRNA incorporating the region targeted by siRNA molecule 2 (nt 859)

Figure 3.12 Local secondary structure surrounding the target region of the aa(n19) motif siRNA molecule (859)

Figure 3.13 Secondary structure of the P1, P2 & P3 antisense phosphorothioate molecules at 37^0C as predicted using the mFold programme

Figure 3.14 Secondary structure of PS2 antisense molecule at 37°C as predicted using the *mFold* software for DNA molecules

Figure 3.15 Secondary structures of the PS3 a & b phosphorothioate antisense molecules at 37°C; calculated using the mFold software for DNA molecules

Figure 3.16 The morpholino molecule directed to the bcr start site showing bases involved in intra-molecular foldings as predicted using *mfold*[1].

Figure 3.17 Secondary structure of the Cyclin D2 directed morpholino antisense molecule predicted using *mfold.*

Table 3.1 Properties of 'P' phosphorothioate antisense oligonucleotides utilised to target the bcr-abl mRNA breakpoint

Table 3.2 Properties of 'PS' phosphorothioate antisense oligonucleotides and their controls targeting the bcr-abl mRNA breakpoint

Table 3.3 Properties and sequences of the Morpholino Antisense Oligonucleotides and their controls targeting the bcr-abl mRNA start site

Table 3.4 Morpholino antisense molecules designed to target the Cyclin D2 mRNA translational start site

Table 3.5 Partial sequence of siRNA duplexes targeted to the bcr-abl mRNA transcript

Table 3.6 Properties of the Cyclin D2 directed siRNA duplexes
Table 3.7 Specificity of phosphorothioate antisense molecules employed to target the bcr-abl mRNA
Table 3.8 Specificity of morpholino antisense molecules employed in this study
Table 3.9 Specificity of siRNA duplexes targeted to the cyclin D2 mRNA transcript

Chapter IV Delivery of Antisense Molecules mediated by Cell Permeabilisation Approaches

Figure 4.1 LAMA-84 cells following permeabilisation with 0.01% saponin
Figure 4.2 Delivery of FAM-labelled antisense molecules to K562 cells in culture mediated by 0.05% saponin in BSA (0.05%)
Figure 4.3 Saponin mediated FAM-labelled antisense molecule delivery to K562 CML cells in culture using 0.05% saponin in PBS
Figure 4.4 Fluorescent photograph showing fluorescent 'haloes' around cells following unsuccessful SL-O delivery
Figure 4.5 Cellular distribution of FAM-labelled phosphorothioate molecules following delivery with SL-O; viewed in cytospin
Figure 4.5 Cellular distribution of FAM-labelled phosphorothioate molecules following delivery with SL-O; viewed in cytospin
Figure 4.6 Cellular distribution of FAM labelled phosphorothioate molecules following delivery with SL-O; viewed *in situ*.
Figure 4.7 Localisation of FAM-labelled phosphorothioate antisense molecules to the nucleus of CML cells
Figure 4.8 KYO-1 cells following treatment with 25U SL-O per 1 X 10^6 cells. A- FAM-labelled antisense uptake into cells. B- PI-positive cells whose membrane integrity was not restored following the permeabilisation procedure
Figure 4.9 Assessment of antisense uptake and cell toxicity in K562 CML cells following SL-O mediated delivery of FAM labelled phosphorothioate molecules

Table 4.1 The effect of a range of saponin concentrations on the viability of and hence the membrane potential of the LAMA-84 cell line

Chapter V Down-regulation of bcr-abl mRNA transcripts induced by Phosphorothioate antisense molecules

Figure 5.1 Uptake of the FAM-labelled P1 phosphorothioate antisense molecule into K562 CML cells using SL-O & associated toxicity levels for the 24Hr time-point
Figure 5.2 Log fold reduction in bcr-abl mRNA expression at 24hrs following delivery of P1 Phosphorothioate molecule to K562 cells using 12U & 14U SL-O
Figure 5.3 Uptake of the FAM-labelled P1 phosphorothioate antisense molecule into K562 cells using SL-O & associated toxicity levels for the 48 & 72Hr time points
Figure 5.4 Log fold reductions in bcr-abl mRNA expression 48Hrs following SL-O delivery of the P1 phosphorothioate molecule to K562 cells
Figure 5.5 Log-fold reduction in bcr-abl mRNA expression 72Hrs following SL-O delivery of the P1 Phosphorothioate molecule in K562 cells

Figure 5.6 Uptake of the FAM-labelled PS3 molecule into KYO-1 cells (% of total) and associated levels of cell toxicity
Figure 5.7 Uptake of 20μM FAM-labelled P3 molecules into KYO-1 cells using SL-O and associated levels of cell toxicity
Figure 5.8 Log fold reduction in b2a2 bcr-abl expression relative to GAPDH following treatment with 20μM P3 phosphorothioate molecule
Figure 5.9 Viability & uptake levels of LAMA-84 cells following SL-O mediated delivery of FAM-labelled P2 phosphorothioate molecules
Figure 5.10 Log fold down-regulation of bcr-abl mRNA expression in LAMA-84 CML cells induced by 10μM P2 phosphorothioate antisense molecule
Figure 5.11 Uptake of the P2 phosphorothioate molecule to LAMA-84 CML cells using 12-16U SL-O & the levels of toxicity associated with permeabilisation
Figure 5.12 Log fold reductions in b3a2 bcr-abl expression following treatment with the P2 phosphorothioate antisense molecule
Figure 5.13 Uptake of the P2 phosphorothioate molecule into K562 cells using SL-O and associated levels of cell toxicity
Figure 5.14 Log fold reduction in bcr-abl b3a2 expression in K562 cells following treatment with the P2 phosphorothioate molecule
Figure 5.15 Uptake of FAM-labelled PS2 antisense molecules into KYO-1 CML cells using 12, 14 & 16U SL-O & associated levels of cell toxicity
Figure 5.16 b2a2 down-regulation induced by the PS2 phosphorothioate antisense molecule over 48, 72, 96 & 120Hrs
Figure 5.17 Log fold decrease in b2a2 expression induced by PS2 molecules in the absence of delivery agents
Figure 5.18 Log changes in bcr-abl gene expression induced by non-sequence specific sense and scrambled controls
Figure 5.19 Uptake of the PS3 a & b phosphorothioate molecules into K562 cells in culture using 12U & 16U SL-O per 1 X 10^6 cells and associated levels of toxicity
Figure 5.20 Log fold bcr-abl down-regulation induced by the b3a2 specific, fluorescently labelled PS3-a and PS3-b phosphorothioate molecules
Figure 5.21 Bcr-abl (b3a2) down-regulation induced by the PS3-a & PS3-b phosphorothioate molecules following 24Hr & 48Hr treatments
Figure 5.22 bcr-abl mRNA log fold reduction induced by P1 after 24, 48 & 72Hrs treatment

Table 5.1 Reductions in b2a2 mRNA expression following treatment with 10μM P3 phosphorothioate molecule, introduced to cells using SL-O

Chapter VI Translational Inhibition induced by RNase H-Independent Morpholino Antisense Molecules

Figure 6.1 a Fluorescent micrograph showing passive entry of morpholino chemistry ODN molecules to K562 cells.
b Fluorescent micrograph illustrating SL-O mediated morpholino ODN molecule entry into K562 CML cells in culture.
Figure 6.2 Down-regulation of BCR-ABL expression using 1 μM MPL_bcr morpholino molecule following 48 hours treatment
Figure 6.3 BCR-ABL (p210) protein down-regulation by bcr start site morpholino molecules is concentration dependent
Figure 6.4 Expression of the BCR-ABL p210 protein in KCL-22 cells following 48 hours treatment with the RNase H competent phosphorothioate (P=S) and the RNase H independent Morpholino Oligonucleotide

Figure 6.5 Comparison of the ability of phosphorothioate and morpholino antisense molecules to mediate inhibition of BCR-ABL protein expression over a range of oligonucleotide concentrations (1μM, 5μM & 10μM)
Figure 6.6 Proliferative capacity of CML cells following treatment with bcr-abl directed morpholino molecules over a range of time-points
Figure 6.7 CFU-GM colony formation following incubation of primary haematopoietic cells in the absence and presence of morpholino antisense oligonucleotides

Chapter VII RNA-Interference (RNAi)-mediated bcr-abl down-regulation

Figure 7.1: Log fold reductions in bcr-abl mRNA expression in KY-01 CML cells following treatment with 4 siRNA molecules targeted to distinct regions of mRNA transcript. Log fold reductions are indicated in brackets (*p<0.01)
Figure 7.2 Log fold reductions in bcr-abl mRNA expression in the K562 cell line following 24 hours treatment with four siRNA duplexes targeted toward the bcr segment on the hybrid oncogene (*p<0.01)
Figure 7.3: p210 protein expression in KYO-1 cells treated with four siRNA molecules following 48Hrs treatment
Figure 7.4 BCR-ABL and actin protein expression in K562 CML cells 72 hours following siRNA treatment
Figure 7.5: The influence of A: Ctrl siRNA molecule delivered with SL-O compared to B: siRNA Pool delivered with SL-O on the proliferative capacity of K562 cells.
Figure 7.6 The impact of a pool of siRNA molecules (P) on bcr-abl mRNA expression in the absence of SL-O mediated delivery over a number of time-points
Figure 7.7 Proliferative capacity of K562 cells following treatment with bcr-abl directed morpholino and siRNA molecules in the absence of a delivery agent
Figure 7.8 mRNA secondary structures surrounding the target binding sites of the S2 and S3 siRNA duplexes
Figure 7.9 The effect of a control siRNA sequence on the expression of bcr-abl mRNA relative to GAPDH expression
Figure 7.10 Colony counts following expansion of primary haematopoietic cells in methylcellulose medium following 14 days incubation.

Chapter VIII Cyclin D2 as a novel target to reduce proliferation of Chronic Myeloid Leukaemia cells

Figure 8.1 Cyclin D2 expression in CML cell lines of lymphoid origin
Figure 8.2 Cyclin D2 and GAPDH expression in the Philadelphia positive LAMA-84 and Philadelphia negative HL-60 myeloid cell lines
Figure 8.3 Cyclin D2 mRNA expression following treatment with the S1 and S2 siRNA molecules singly and in combination following 8 and 12 hrs treatment
Figure 8.4 Cyclin D2 mRNA expression following treatment with S1 and S2 siRNA molecules singly and in combination following 24 and 48 hrs
Figure 8.5 Proliferative inhibition in KCL-22 cells induced following treatment with the S1 siRNA duplex
Figure 8.6 Percent changes in the proliferative capacity of CML cells following treatment with the S2 siRNA duplex over number of time points
Figure 8.7 The proliferative capacity of KCL-22 cells following treatment with 1μM morpholino antisense targeted to the 5' UTR region of the cyclin D2 gene

I

Introduction

1.1 Chronic Myelogenous Leukaemia (CML)

Leukaemia was first identified in 1845 by two independent reports, one by the Scottish physician John Hughes Bennett (1812-1875) (Dougal, 2000); and another by a German intern, Rudolph Virchow (Lowenthal *et al*, 2000). These initial publications by Bennett and Virchow were the first to describe patients with the condition Chronic Myelogenous Leukaemia (CML). Bennett used the term leucocythaemia, while 'Leukaemic' was introduced by Virchow and first used to describe CML in 1865. The term myelogene (myelogenous) was coined by Ernst Neumann due to the concept that the disease originated in the Bone Marrow (Holyoake, 2001).

In Ireland, there are on average 330 new leukaemia cases diagnosed each year. Leukaemia accounts for 1.6% of all cancers registered in Ireland and has a 60% mortality rate (www.ncri.ie). CML has an incidence of 1 to 2 cases per 100,000 head of population per year globally and accounts for 15-20% of all adult leukaemias; which rises to 30% in countries such as India (Pavithran, 2001). CML has been identified in patients of all age groups, however fewer than 10% of cases occur in patients less than 20 years of age and the median age of patients at diagnosis is between 46-53 years. Males are 1.4 times more likely to develop CML than females and females also have a higher five-year survival rate (www.ncri.ie).

Leukaemia is classified into myeloid and lymphoid categories based on the origin of the leukaemic cell. In the case where the cells retain the ability to differentiate, the leukaemia is termed chronic, if the cell loses this ability it is described as an acute leukaemia. CML is a myeloproliferative disorder resulting from the malignant transformation of a haemopoietic stem cell (Faderl *et al*, 1999). It is characterised by the massive expansion of haemopoietic progenitors as well as more differentiated haemopoietic cells and their presence in the circulation. A cause for CML has been difficult to identify. Exposure to radiation, as in patients undergoing radiation therapy and survivors of the atomic blasts in Japan, predisposes to an increased risk; however it is not considered a major effector in CML aetiology.

1.2 The Philadelphia Chromosome

CML is an acquired genetic disease and while our knowledge of the initiating events in CML is limited, the transformation events that lead to the development of CML are more clearly understood. Following refinement of the description of CML at the clinical and laboratory level, Nowell and Hungerford, two scientists based in Philadelphia, USA began investigation into the molecular aspects of CML. In 1960 they observed an abnormal chromosome with an apparent deletion of part of its long arm in specimens derived from CML patients (Nowell *et al,* 1960). This was later recognised as chromosome 22 and termed "The Philadelphia Chromosome" in reference to the city where it was first observed. This chromosome is a disease marker for CML and is observed in virtually all (95%-99%) of diagnosed patients (Di Bacco *et al,* 2000). The introduction of chromosome banding techniques in the 1970s allowed Rowley et al. to show that the acquired genetic abnormality observed was not a deletion of chromosome 22, but a reciprocal translocation involving chromosomes 9 and 22 (Rowley, 1973). Further study identified the key genes that were disrupted in this translocation event - the abelson (c-abl) tyrosine kinase gene on chromosome 9 and the break point cluster region (bcr) gene on chromosome 22.

In the majority of CML patients, the c-abl breakpoint occurs in the first or second exon, usually 5' of the second exon. The breakpoints in bcr occur in three clusters, the major breakpoint cluster region (M-bcr), the minor breakpoint cluster region (m-bcr) and the μ breakpoint cluster (μbcr). All of these sites are located within the 'bcr' gene. The position of the breakpoint in the bcr gene determines the type of leukaemia that subsequently develops, the M-bcr is involved in CML and the m-bcr is involved in acute lymphoblastic leukaemia (ALL) (Kindler *et al,* 2002). Following the juxtaposition of the two chromosomal segments, the abl gene is placed under the influence of the bcr promoter. There is evidence that the BCR portion of the hybrid molecule interferes with the negative regulation of the ABL protein by binding in an intra-molecular fashion to regulatory SRC homology (SH) domains (Cotter, 1995). This results in constitutive activation of ABL tyrosine phosphokinase activity.

1.3 Stages of CML

CML progresses into a biphasic or triphasic condition, beginning with an initial chronic phase, usually of long duration. After a median of 4-5 years in untreated patients, a transition occurs from a chronic phase CML to an accelerated phase of the disease. During the accelerated phase; which is typically of median duration 3-9 months, the patient may be asymptomatic or may display splenomegaly, bone pain, weight loss and fever. The appearance of secondary cytogenetic abnormalities other than the Philadelphia Chromosome is another criterion for accelerated phase CML, these may include such translocations as t(3, 21) or t(15, 17) (Johansson *et al*, 2002). This accelerated phase is marked by a difficulty in controlling white cell counts using conventional chemotherapy. The transition of CML to blast crisis is characterised by the loss of capacity of the malignant clone for terminal differentiation, with transition to a generally fatal acute leukaemia. Approximately 65% of patients evolve to blast crisis with myeloid blasts, 30% with lymphoid blasts and 5% present with undifferentiated or T cell blasts (Kolibaba *et al,* 2000).

1.4 CML Therapy

In 1856 the first specific threrapy for CML; the use of Fowlers solution (arsenicals) was introduced (reviewed in Pavithran, 2000). Radiotherapy was later employed for treatment until the introduction of the oral alkylating agent, busulfan. Busulfan induced prolonged periods of haematological control though toxicity was substantial and it damaged quiescent bone marrow stem cells, leading to secondary leukaemias (Hehlmann *et al,* 1993). Hydroxyurea, a ribonucleotide reductase inhibitor active only in proliferating cells is generally preferred over busulfan, due to increased prolongation of both the chronic phase of the disease and overall survival, coupled with a lower toxicity profile (Singer *et al,* 1998). Though these forms of conventional chemotherapy provide haematological control in greater than 15% of patients, remissions are transient and ultimately the disease progresses to blast crisis.

1.4.1 Interferon-alpha (IFN-α)

Interferon-alpha (IFN-α) was reported to be active in treating CML in 1983 and complete remissions were reported in 1985. Its value to the treatment of chronic phase CML is now undisputed. IFN-α induces haematological remission in 70-80% of patients and complete remission in 5-25% (Greisshammer *et al*, 1993). It functions by induction of FAS and its ligands on CML progenitors, facilitating cell death and induces expression of the pro-apoptotic TRAIL protein which induces apoptosis in cancer cells (Crowder *et al,* 2004). FAS restores integrin mediated adhesion and adhesion-mediated inhibition of proliferation and also augments cellular antigen presentation, increasing recognition of CML progenitors by the immune system. IFN-α increases the 5 year survival rate of patients by delaying blast crisis, the survival rates for patients on IFN-α was 57%, compared to 42% in patients on chemotherapy alone. IFN-α is also used in combination with cytosine arabinoside (ara-c) which selectively suppresses CML cells relative to normal haematopoietic progenitors and this combination improves cytogenetic response and prolongs survival (Mollee *et al,* 2004).

1.4.2 Bone Marrow Transplantation (BMT)

An important advance in the treatment of CML was the use of allogenic bone marrow transplantation (BMT)-the transplantation of normal stem cells from a HLA-matched donor to a leukaemia patient who has undergone chemoradiotherapy conditioning (Goldman, 1995). This is a form of immunotherapy and is suitable for patients less than 50 years of age, where a matched donor, usually a sibling, can be identified (Campbell *et al,* 2001). If the desired graft versus leukaemia (GVL) effect occurs, the donor cells will engraft and will reconstitute haematopoiesis (Kay *et al,* 1985). BMT is currently the treatment of choice for CML and a number of studies have outlined its benefit both in the related transplant and in the unrelated transplant setting (Olsson-Stromberg *et al,* 2004; Maury *et al,* 2001).

The GVL effect is critical to the success of BMT and has been most pronounced in CML, when compared to other forms of leukaemia. While the GVL effect is important to the success of allogenic-BMT, the infusion of immuno-competent donor cells may lead to GVHD which results in significant mortality and morbidity. T lymphocytes in the bone marrow transplant respond to foreign MHC antigens on the recipient's cells and mount an immunological attack (Overfield *et al*, 1999). Harnessing the GVL effect,

while minimising GVHD, has been a goal of many clinicians and scientists in the transplant field. An additional advantage of the GVL effect is the ability to rescue CML patients who have relapsed after allogenic-BMT by donor lymphocyte infusion (DLI). The infusion of donor lymphocytes has been shown to induce remission in 70% of relapsed patients following BMT. The aim of donor lymphocyte infusion (DLI) is to induce a GVL response. However, GVHD is a major treatment related toxicity leading to mortality or serious related side-effects in 25% of transplant patients (Flowers *et al,* 2004).

1.4.3 Imatinib Mesylate

Though empiricism has played a major role in the discovery of valuable new cytotoxic drugs in the 20th century, it is encouraging to note that some active drugs have been identified as a result of a precise understanding of the molecular pathology of malignancy. Imatinib mesylate, an orally active tyrosine kinase inhibitor that is selectively active against the BCR-ABL tyrosine kinase relative to the normal ABL counterpart falls into the latter category (Druker *et al,* 2001). It is an excellent example of the use of targeted molecular medicine in the treatment of malignancy. The active molecule, imatinib mesylate, also actively inhibits c-kit which is over-expressed in gastrointestinal tumours. Imatinib mesylate binds the kinase pocket of the active site of BCR-ABL, preventing binding of its substrate, ATP, whose hydrolysis leads to phosphorylation of downstream effectors of BCR-ABL. The half-life of imatinib mesylate is 16-19 hours, making it suitable for daily doses (Hochhaus, 2004).

Phase I & II clinical trials demonstrated the high levels of efficacy of imatinib mesylate in the treatment of CML, these include significant cytogenetic and haematological responses in all stages of the disease (Borthakur *et al,* 2004). Phase II trials re-affirmed these results and found that haematological and cytogenetic responses were less common in accelerated or blast phase; however these results were favourable relative to existing therapy for these phases of the disease (Savage *et al,* 2002). Recent phase III findings indicate that not only is imatinib better tolerated than IFN-α, it induces significantly greater rates of complete haematological responses (95% versus 56%) and also shows promise in combination with ara-c (Guilhot, 2004). However, while in allogenic-BMT molecular remissions can frequently be achieved; to date relatively few patients have achieved molecular remissions following imatinib mesylate treatment.

The development of acquired resistance to imatinib in a subset of CML patients is the main cause for failure of this treatment. This may be due to BCR-ABL dependent or independent mechanisms (Tauchi *et al,* 2004). Resistance to imatinib mesylate in the blast or accelerated phase is consistent with the theory that secondary mutations are the primary driving force at this stage. Point mutations in the tyrosine kinase domain of BCR-ABL which inhibit binding of imatinib have been identified as a mechanism of resistance (La Rosee *et al*, 2002). The occurrence of resistance indicates that combined therapy with

other chemotherapeutic agents may represent the most appropriate approach for the treatment of CML. This is similar to the principle used for infectious diseases as it is unlikely a single cell will develop resistance to more than one drug (Luzzatto *et al*, 2002). This emphasises the necessity to develop more targeted therapies in CML to complement those already in place. BCR-ABL independent resistance relates to increased intracellular levels of P-glycoprotein and intracellular decreased levels of imatinib. The phosphorylation capacity of BCR-ABL is maintained and loss of imatinib mediated inhibition of proliferation and apoptosis occurs (Illmer *et al,* 2004). While 5-year follow-up data on patients treated with imatinib mesylate is limited; its contribution to CML therapy is guaranteed.

1.5 The ABL Gene and Protein

The normal abl gene is located on chromosome 9, it has 23 exons and spans 230 kilobases (kb) of DNA. C-abl is the human homologue of the oncogenic v-abl derived from the Abelson virus, which induces leukaemia in mice (Sawyers, 1993). C-abl codes for a non-receptor tyrosine kinase which is ubiquitously expressed, with the highest levels found in the spleen, thymus and testes. Two alternative variants are possible due to alternative splicing. One form is myristoylated at the amino terminal, resulting in a cytoplasmic localisation; however, the predominant form lacks the myristilation signal and is found principally in the nucleus. The ABL protein has several distinct features including SH domains required for regulation of its tyrosine kinase activity. They play a crucial role in protein-protein interactions and mediate resistance to a number of chemotherapeutic drugs (Brooksband, 2001). At the carboxy terminal of ABL there is an actin binding domain which is necessary for the cytoplasmic localisation of the BCR-ABL protein, thus ensuring availability to its substrates (Figure 1.1). The actin binding function of ABL is enhanced in BCR-ABL and is required for transformation (Jahagirdar *et al,* 2001).

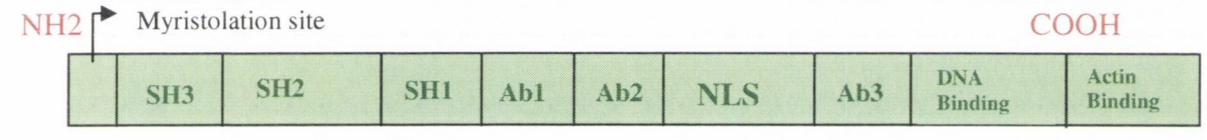


Figure 1.1 Functional regions on the normal ABL Protein (p145)

The SH3 and SH2 domains are involved in protein protein interactions. SH1/Tyrosine Kinase domain is involved in phosphorylation of target proteins. Ab1, ab2 and ab3 are proline rich domains which can bind other SH3 containing proteins. The nuclear localisation sequence (NLS) may localise the ABL protein to the nucleus. The DNA binding domain is a stretch of acidic residues involved in ABL binding to DNA. The actin binding domain is crucial for cytoplasmic localisation of BCR-ABL

1.5.1 Role of ABL in Cell Cycle Regulation

Over-expression of ABL in fibroblasts leads to inhibition of cell growth (Chopra *et al*, 1999) and cell cycle arrest (Thijsen *et al*, 1999), this pattern is reminiscent of tumour suppressor proteins such as retinoblastoma (Rb) and p53. Activation of ABL may be induced by alkylating agents and ionising radiation. During the G_0 phase of cell growth the ABL protein is DNA-bound in complex with Rb. In the G_1-S phase Rb is phosphorylated and dissociates from ABL giving rise to activation of its tyrosine kinase activity (Drummond *et al*, 2001). ABL is then phosphorylated by cdc2 kinase, after which ABL dissociates from DNA and S phase begins.

1.6 The BCR Gene and Protein

The normal bcr gene is located on chromosome 22, it spans 135kb of DNA and is composed of 23 exons. Bcr is a member of a family of genes whose function remains unclear; these include the bcr 2, 3 and 4 genes. Bcr has two possible mRNA transcripts, 4.5 and 6.7 Kb, both of which are translated into a 160 kiloDalton (kDa) protein. The BCR protein is ubiquitously expressed in all human tissues and is composed of a number of distinct functional regions. At the amino terminal site, a dimerisation domain is present; this facilitates oligomerisation of the BCR-ABL protein following auto-phosphorylation, which is considered an essential component of its transforming ability (Chopra *et al,* 1999). Replacement of BCR by other molecules which retain the ability to dimerise has been shown to retain the transforming potential of BCR-ABL (Holyoake, 2001). BCR has two regulatory SH2 binding domains and these mediate binding of SH2 containing proteins, including c-abl. A central portion of the BCR protein is retained in BCR-ABL and shows homology to guanine-nucleotide exchange factors (GNEF's), this may enhance RAS activity by accelerating conversion of GDP to GTP (Kurzrock *et al,* 2003). At the BCR carboxy terminus, there is a region that may be involved in calcium dependent lipid binding, followed by a domain which has homology to and has GTPase activity protein (GAP) function for the RAS like proteins p21 (Figure 1.2). GAP proteins modulate RAS function by accelerating the rate of RAS-bound GTP hydrolysis, thus inactivating RAS. The omission of this region in BCR-ABL may be significant.

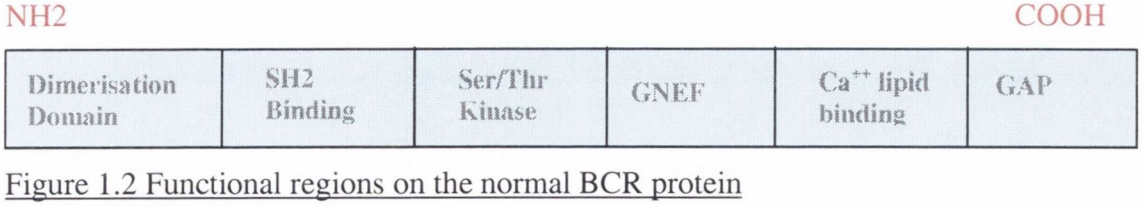


Figure 1.2 Functional regions on the normal BCR protein

Dimerisation Domain – Involved in the oligomerisation of the BCR protein
SH2 Binding domain – may bind SH2 domain of c-abl in a non-phosphotyrosine dependent manner.
Serine/threonine Kinase Domain – Unique serine threonine kinase activity
GNEF – Homology to Rho guanine nucleotide exchange factors (GNEF)
Ca^{++} dependent lipid binding – May be involved in calcium dependent binding of lipids
GAP – Implicated to have GTPase activating protein function for the RAS like proteins p21 rho and p21 rac

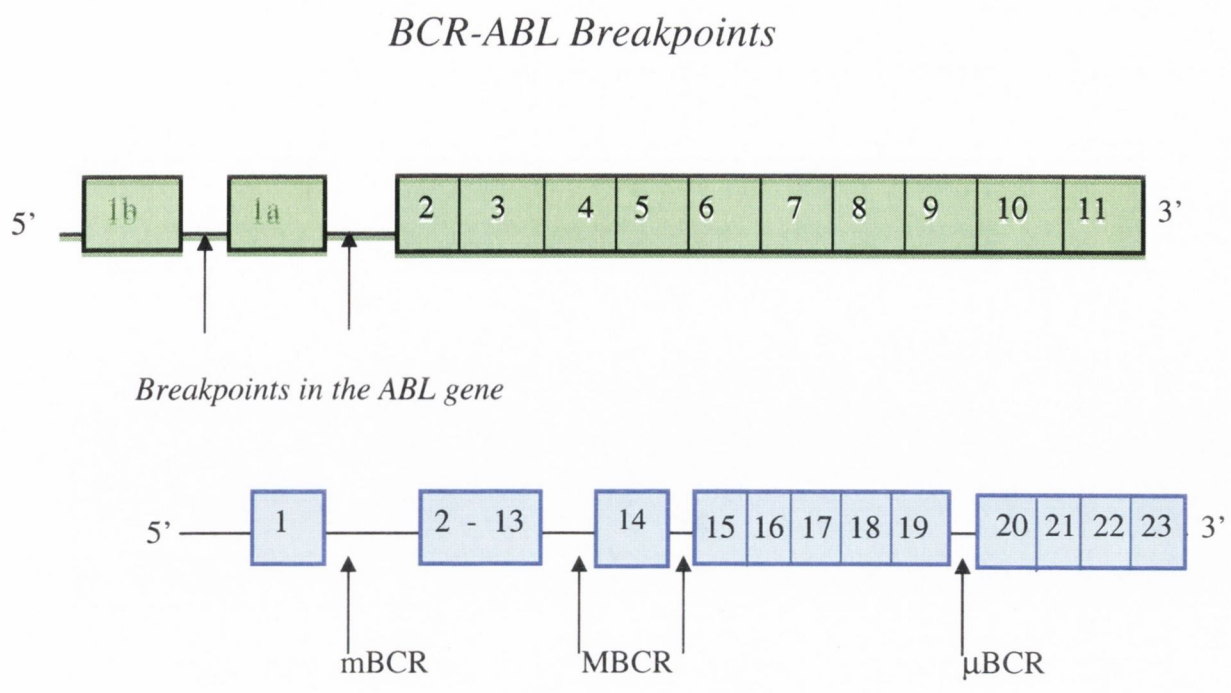


Figure 1.3 **Position of breakpoints in the abl gene (green) and the bcr gene (blue), numbers represent exon positions in both genes.**

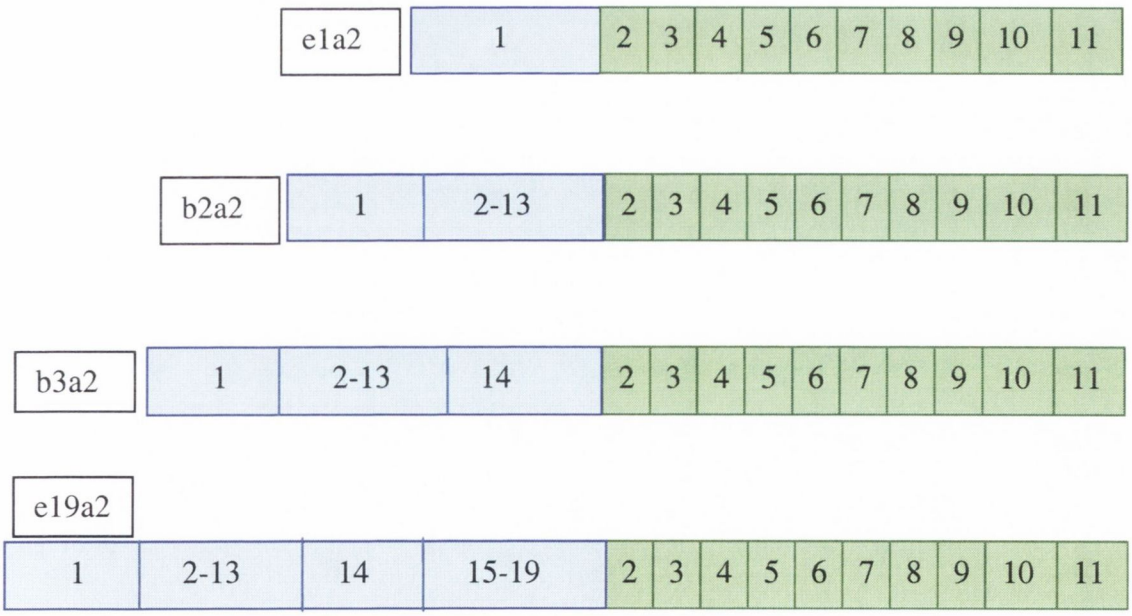


Figure 1.4 **Position of exons in abl (green) and bcr (blue) genes following translocations resulting in the e1a2, b2a2, b3a2 and e19a2 transcripts**

In CML, two breakpoints may occur in the MBCR, either in front of or directly after exon 14 (Figure 1.3); producing either the b2a2 or b3a2 bcr-abl transcript (Figure 1.4). Both mRNAs are translated into a 210kDa protein; however b3a2 is more prevalent than b2a2 and is also 25 amino acids longer. The p210 protein has an elevated tyrosine kinase activity relative to the normal abl (p145) and importantly is constitutively active, requiring no stimulus for sustained activation (Faderl *et al,* 1999). A breakpoint in the m-bcr gives rise to the ela2 fusion gene present in the majority of Philadelphia positive ALL patients and detectable in a sub-group of CML patients (Kurzrock *et al,* 2003). The resulting 190kDa protein has elevated tyrosine kinase activity relative to p210 and is associated with a more aggressive leukaemia. The μ-bcr breakpoint within the bcr gene gives rise to a fusion variant, splicing bcr exon e19 (C3) with abl exon 2 (e19a2) coding for a 230kDa protein (Figure 1.4). This particular fusion protein gives rise to Chronic Neutrophilic Leukaemia. The Philadelphia chromosome is detectable in at least 95% of patients with CML and in other CML cases its detection may be hampered by variant or complex translocations. This chromosomal abnormality is also detectable in 5% of children and 25% of adults with ALL (Kurzrock *et al,* 2003).

1.7 Pathways of BCR-ABL mediated transformation

The structure of the $p210^{bcr\text{-}abl}$ protein allows for the activation of a wide diversity of signalling pathways due to the large number of potential protein-protein interactions. Compared with the normal ABL protein, the tyrosine kinase activity of $p210^{bcr\text{-}abl}$ is elevated, resulting in cross phosphorylation of individual p210 molecules, particularly at the tyrosine 177(^{177}Y) residue (Jahagirdar *et al*, 2001). The ability of BCR-ABL to phosphorylate proteins is key to its transformation ability; as kinase inactive mutants of BCR-ABL are incapable of inducing transformation (Holyoake, 2001). Auto-phosphorylation of tyrosine molecules on BCR-ABL occurs following homo-oligomerisation of BCR and these phosphorylated tyrosines serve as docking sites for the recruitment of cellular adaptor molecules that mediate the transforming potential of BCR-ABL (Van Etten, 2004). Several adaptor proteins including the growth factor receptor-bound protein 2 (GRB2), bind the phosphorylated ^{177}Y region of BCR. Binding of GRB2 induces recruitment of a guanine nucleotide exchange factor (GNEF), SOS; and this forms the complex with which p210 is normally associated (Kindler *et al,*

2002). The GRB2-SOS complex results in increased transcription of important apoptotic genes such as BCL-2, BCL-X_L and the myc transcription factor (Chopra *et al,* 1999). SOS binds the Src homology (SH) domain of GRB2 via its c-terminal proline rich domain and stimulates the exchange of GDP for GTP in RAS, switching it from an inactive to an active form. This complex then mediates signal transduction through the normal RAS pathways; mutation of ^{177}Y abolishes GRB2 binding and inhibits the BCR-ABL mediated activation of the RAS pathway (Weinstein-Oppenheimer *et al,* 2000).

1.7.1 RAS activation and down-stream effects

Mutated or overactive RAS has been implicated in a wide diversity of malignancies such as lung, colorectal and pancreatic cancer (Macaluso *et al*, 2002). Activation of RAS is a key amplification step in the BCR-ABL transformation procedure. RAS activation due to binding of GRB2:SOS to BCR-ABL leads to activation of the Fos/Jun transcription complex (Stewart *et al,* 1995). Fos/Jun form the hetero-dimeric transcription factor, AP-1 and through this BCR-ABL modulates expression of several genes. Dominant-negative mutants of Jun, though not Fos, completely inhibit BCR-ABL transformation, indicating Jun containing transcription complexes other than AP-1 are critical mediators of BCR-ABL signalling (Turhan *et al*, 1998). This highlights Jun as an attractive target for potential therapies. RAS also leads to activation of phosphatidyl inositol-3 kinase (PI-3 Kinase), which is an essential component in bcr-abl transformation (Keeshan *et al,* 2003). Through RAS, BCR-ABL induces expression of the anti-apoptotic protein BCL-2, which contributes to cell survival (Sanchez-Garcia *et al,* 1997). An increase in the AP-1 transcription factor directly results in an increase in the levels of the cell cycle mitogenic, G1/S phase specific, Cyclin D1, inducing its over expression and accelerating G1 progression. Cyclin D1 over-expression alone is insufficient for transformation and may function only to enhance cell cycle progression, indicating it has an auxiliary rather than primary role in BCR-ABL transformation (Takano *et al,* 2000).

1.7.2 Myc Activation

Myc is an oncogenic transcription factor, many of whose target genes are translated to proteins that initiate or maintain the transformed state (Prochownik, 2004). Myc induced pathways are essential for BCR-ABL mediated transformation and myc over-expression restores transforming abilities to a transformation defective SH2 mutant of BCR-ABL, indicating that the SH2 domain sends signals to the myc promoter (Xie *et al*, 2002).

BCR-ABL up-regulates myc expression at the transcriptional stage through an E2F site in the myc promoter (Stewart *et al,* 1995). BCR-ABL induced myc expression is dependent on RAS signalling (Faderl *et al,* 1999) and involves JAK2 (Xie *et al,* 2002). Due to its necessity for transformation, myc may also provide a useful therapeutic target in BCR-ABL related leukaemias.

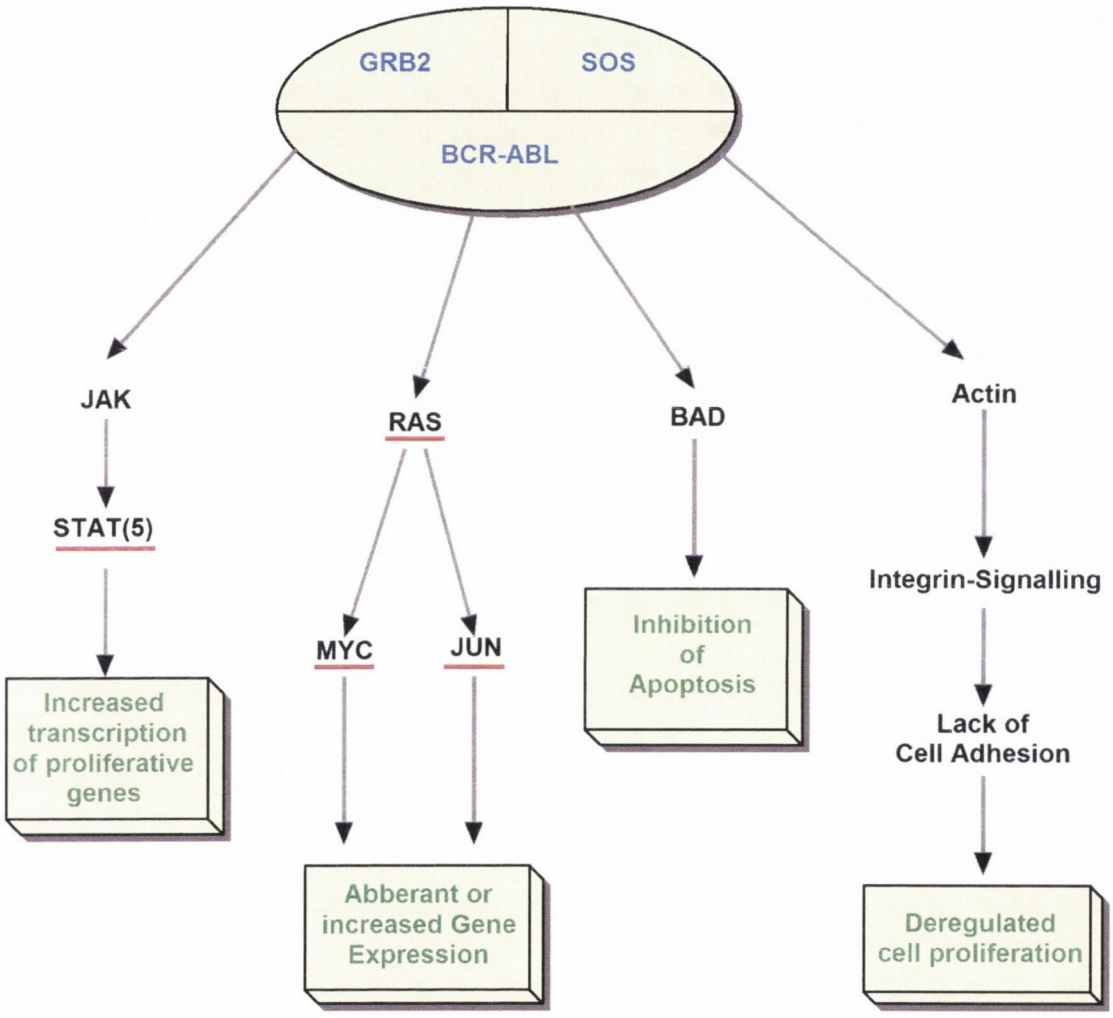


Figure 1.5 Cellular pathways activated by BCR-ABL to mediate CML cell proliferation, inhibit apoptosis and stimulate early release of progenitor cells into circulation.

Each of the factors underlined in red are necessary for BCR-ABL mediated transformation

1.7.3 Interleukin-3 (IL-3) Pathways

IL-3 is an anti-apoptotic regulator of haematopoietic cells; it controls their growth and differentiation through RAS and JAK2 signalling (Wilson-Rawls *et al*, 1997). Over-expression of IL-3 results in hyperplasia similar to that observed in the chronic phase of CML (Parada *et al*, 2001). BCR-ABL cells have an autocrine loop of IL-3 production (Dorsey *et al,* 2002), though its expression is not essential for bcr-abl transformation (Li *et al,* 2001; Wong *et al,* 2003). Direct interaction between BCR-ABL and the common β(C) subunit of the IL-3 receptor has been demonstrated by immuno-precipitation (Wilson-Rawls *et al*, 1997). Through interaction with the IL-3 receptor, BCR-ABL adopts survival and proliferation pathways normally activated by IL-3 in haematopoietic cells. One of the IL-3 mechanisms BCR-ABL activates to promote unregulated cell survival and proliferation is increased cyclin D2 expression (Parada *et al*, 2001).

1.7.4 STAT Family Involvement

Similar to their activation in response to IL-3, BCR-ABL activates "signal transduction and activator of transcription" family members STAT5 and STAT1, which have been demonstrated to play a central role in the inhibition of apoptosis in transformed cells (Sonoyama *et al*, 2002). STAT transcription factors are activated by tyrosine phosphorylation, which is normally a transient and tightly regulated process (Buettner *et al*, 2002). Members of the JAK family phosphorylate STAT members in response to stimulation by IL-3 and GM-CSF and in CML cells both JAKs and STATs are constitutively active (Wilson-Rawls *et al,* 1997). STAT activation is dependent on kinase activity and correlates with growth factor independence, as BCR-ABL substitutes for growth signals normally mediated by cytokines (Shuai *et al*, 1996). BCR-ABL may mediate activation of JAK through RAS resulting in phosphorylation of STAT; however it may also directly phosphorylate STAT1 and STAT5, this results in their dimerisation and translocation to the nucleus where they act as transcription factors (Spiekermann *et al*, 2002). STAT5 directly results in transcription of the anti-apoptotic protein BCL-$_{XL}$ (Gesbert *et al*, 2000) and the cell cycle regulator cyclin D2.

1.7.5 Modulation of D-Type Cyclins by BCR-ABL

To bring about cell transformation, BCR-ABL induces proliferation by driving the cell cycle through its G1/S and G2/M check-points. Cyclin D1 expression is up-regulated via AP-1 however it is not a critical mediator of bcr-abl mediated transformation (Takano *et al,* 2000). A second member of the regulatory D type cyclins; Cyclin D2, has been demonstrated by oligonucleotide array expression profiling to be altered at the transcriptional level by BCR-ABL. A 3.5 fold increase in cyclin D2 mRNA levels was documented in BCR-ABL expressing cells and cyclin D2 was demonstrated to be a necessary component for BCR-ABL mediated transformation as was shown using cyclin D2 deficient mice (Jena *et al*, 2002). The cyclin D2 gene has binding sites for two transcription factors, STAT5 and myc located in its promoter region (Friedrichsen *et al,* 2003; Bouchard *et al,* 2001). Both of these transcription factors are activated by bcr-abl pathways. BCR-ABL mediated cyclin D2 expression is repressed in knock-out models of RAS, PI-3 kinase and STAT5 indicating that each of these factors play a role in the pathway leading to its elevated expression (Sonoyama *et al,* 2002). Cyclin D2 induction by STAT5 is dependent on PI-3 kinase activity and is completely blocked by the PI-3 kinase inhibitor wortmannin (Piatelli *et al*, 2004). C-myc expression is also induced by STAT5 (Moon *et al,* 2004) and this may lead to a continual loop of cyclin D2 expression in bcr-abl cells.

Cyclin D2 is not only up-regulated in BCR-ABL cells but its expression is extended to other phases of the cell cycle other than its normal presence in the G1/S phase, with high expression also noted during the G2/M restriction point (Jena *et al*, 2002). BCR-ABL abrogates the cell cycle variations in cyclin D2 expression and this is another mechanism it employs to by-pass the requirement for external growth signals. The normal functions of cyclin D2 are largely redundant as they are shared with other members of the cyclin D family. However, cyclin D2 activity is essential for the development of normal CD5+ve B lymphocytes and is required for B-cell receptor mediated proliferation (Solvason *et al,* 2000). Particularly high levels of cyclin D2 are detected in CML cells in lymphoid blast crisis and also in Chronic Lymphocytic Leukaemia patients (Deininger *et al*, 2001).

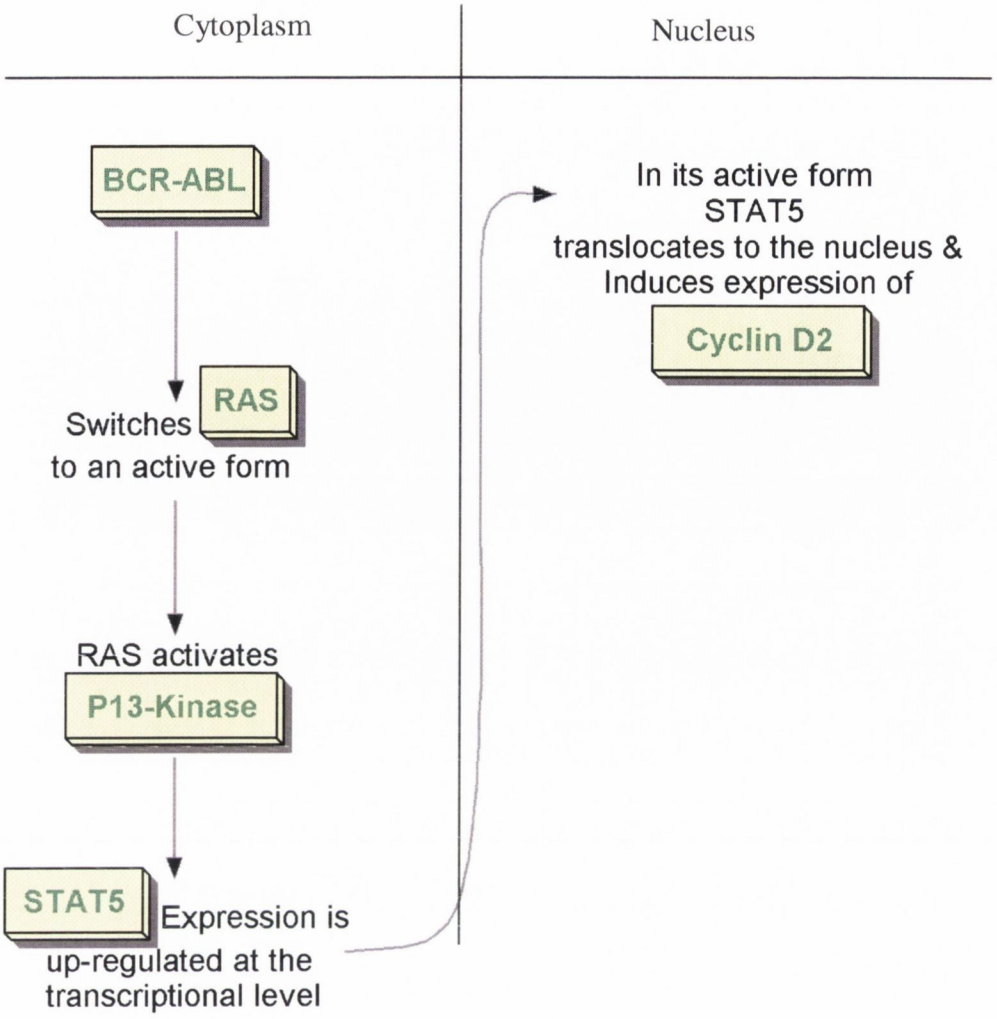


Figure 1.6 Induction of cyclin D2 expression by BCR-ABL

Cyclin D2 is up-regulated by BCR-ABL in a RAS, PI3 kinase and STAT5 dependent manner.

1.7.6 BAD mediated inhibition of apoptosis

BAD, a pro-apoptotic member of a BCL-2 subfamily is inactivated by phosphorylation at serine 112 and 136 residues. De-phosphorylation of BAD leads to induction of apoptosis in response to a wide range of stimuli, and in this active state BAD relocates from the cytoplasm to the mitochondria where it binds the anti-apoptotic factors BCL-2 and BCL_{XL}; inhibiting their function and inducing cell death (Salomoni *et al*, 2000). In bcr-abl null myeloid precursor cells, withdrawal of IL-3 results in Phosphatidyl Inositol-3 (PI-3) kinase-dependent de-phosphorylation of BAD and induction of apoptosis. However, in BCR-ABL cells, BAD remains phosphorylated and localised in the cytoplasm, where it is inactive (Neshat *et al*, 2000). This anti-apoptotic effect of BCR-ABL, at least partially mediated through inactivation of BAD, is a key feature of CML cells, which exhibit decreased levels of cell death. BCR-ABL has also adopted pathways used in normal cells by anti-apoptotic molecules such as IL-3 to reduce apoptosis (Keeshan *et al*, 2002). By activating targets at early stages in a pathway, in the absence of cytokine stimulation BCR-ABL compensates for external stimulation and this provides a key step towards transformation (Neshat *et al*, 2000). Thus, BCR-ABL can act at two discrete levels to control the activity of important anti-apoptotic proteins, not only does it increase their transcriptional levels via the AP-1 transcription factor; it also bypasses an important form of their regulation as indicated above (Salomoni *et al*, 2000).

1.8 Altered Adhesion of CML cells

Interactions due to the adhesion of haematopoietic stem cells to the bone marrow microenvironment are essential for normal cell growth and development. Immature haematopoietic cells attached to the bone marrow matrix, receive signals from anti-apoptotic regulators such as IL-3 to inhibit proliferation and allow progenitor cell differentiation and maturation, while mature cells as they are required are released into circulation. The actin cytoskeleton provides structural support for the stem cell and plays an important role in signal transduction (Blalock *et al*, 1999). BCR-ABL has been shown to induce adhesive and cytoskeletal abnormalities resulting in global dysfunction of CML cells, however this is independent of their tyrosine kinase activity (Wertheim *et al*, 2002). The marked decrease in CML progenitor adhesion is induced by downstream effects of BCR-ABL signalling, resulting in loss of integrin-mediated adhesion to the microenvironment (Bhatia *et al*, 1998).

The actin-binding domain in the ABL portion of BCR-ABL directs re-localisation of the actin cytoskeleton into punctuate structures in the cytoplasm (Telegeev *et al,* 2004). Downstream effectors of actin binding involved in "inside-out" and "outside in" signalling through β-1 integrins are affected due to the increased interaction. Signals transduced from the extracellular matrix by β-1 integrins, particularly α4β1 play an important role in the environmental regulation of normal haematopoietic progenitor proliferation. In normal haematopoietic progenitor cells, β1 integrin engagement increases the levels of $p27^{kip}$, which bind to cyclin dependent kinase 2 (cdk2) and inhibit the G1/S cell cycle progression. BCR-ABL up-regulates $p27^{kip}$ protein levels; however these have a cytoplasmic rather than nuclear localisation and are hence inactive due to their inability to bind cdk2. BCR-ABL mediates $p27^{kip}$ up-regulation by a post-translational modification mechanism; it inhibits formation of the p27/ cyclin/ cdk complex which is required for $p27^{kip}$ degradation mediated by the ubiquitin ligase/proteasome. Lack of $p27^{kip}$ nuclear localisation inhibits its phosphorylation and degradation, leading to an increased life span and higher intra-cellular levels (Jiang *et al*, 2000).

1.9 Investigational Therapies for CML

The prevalence of resistance to currently employed treatment regimens and the occurrence of treatment-related toxicities drive the search for innovative CML therapies. A novel form of IFN-α, pegylated IFN-α has a polyethylene glycol derivative attached which decreases its rate of degradation. Due to its increased half-life, pegylated IFN-α shows strong promise by prolonging the beneficial effects of IFN-α and by reducing the dosage required, thus limiting unwanted side-effects (Grace *et al,* 2001). YNKO1, an oral pro-drug of ara-c is resistant to inactivation by systemic deamination and thus avoids the need for daily injection of ara-c (Reiter *et al, 2001;* Rosti *et al,* 2003). Homoharringtonine (HHT) is a plant alkaloid with antileukemia activity which is used in IFN-α resistant patients (Yinjun *et al,* 2004). It has induced complete haematological remissions and cytogenetic responses and may be used in treatment resistant patients.

A PI-3 kinase inhibitor wortmannin has been shown to selectively inhibit CML colony growth *in vitro* (Klejman *et al,* 2002). Wortmannin may also be employed in imatinib resistant patients as it retains anti-proliferative activity in imatinib-resistant cells (Marley *et al,* 2004). Hyper-methylation of tumour suppressor genes caused by abnormal activity of DNA methyltransferases is an important mechanism that contributes to cancer development (Gowher *et al,* 2004). Decitabine (2'-deoxy-5-azacytidine), can inhibit DNA hyper-methylation and reverse epigenetic silencing of aberrantly methylated genes (Brown *et al, 2004).* A number of investigational approaches currently being explored also exploit the unique presence of the Philadelphia chromosome in CML cells. These include the antisense and ribozyme approaches, which have the potential to specifically reduce levels of the BCR-ABL protein by inhibiting translation of its mRNA whilst having no negative influence on the growth of normal cells. Investigation of these techniques for application in CML will also provide insights into their application in other malignancies and human diseases.

Autologous BMT (ABMT) or stem cell transplantion is currently being explored as a potential therapy. In the chronic phase of CML, while a patient's bone marrow will contain leukaemic stem cells, there may also be normal stem cells present. By treatment of bone marrow cells *ex vivo* to selectively remove or 'purge' CML cells, the remaining

healthy cells may be re-infused into the CML patient following myeloblative chemotherapy to re-colonise the bone marrow. Initial studies carried out using unpurged marrow stem cells resulted in occasional cytogenetic responses, but these were not curative (Singer *et al, 1998*). Recent studies have indicated prolonged patient disease-free survival following ABMT when compared to conventional chemotherapy, but this did not affect the overall survival rate (Nathan *et al,* 2004). However, if all the Philadelphia positive cells are not eliminated, autografting may still reduce the population of malignant cells at risk of further mutation, thereby reducing the risk of or slowing the rate of CML progression to blast crisis. Thus, this avenue is of considerable interest and more efficient methods to selectively purge Philadelphia positive cells are required. *Ex vivo* purging methods may reduce the dependence on allogeneic BMT as a curative option, as unlike BMT, its success is not dependent on the availability of a matched donor and the main cause of BMT-related mortality, the occurrence of GVHD is eliminated. ABMT is also suitable for use in combination with other therapies.

1.10 Antisense

1.10.1 Overview of Antisense

The transformation of a normal cell to one with tumorigenic ability involves changes at the genetic level, usually involving oncogenes or tumour suppressor genes (Lewin, 2003). The mutational event is encoded to the mRNA transcript and this in turn is translated into a mutant protein which may be functional, however with altered or deregulated activity. Following key discoveries which defined mutational events more specifically at the nucleic acid level and in the desire for increased specificity, research began to focus on DNA and RNA as early targets for combating disease (Thurston *et al,* 1999). A classic example of a potential target is the bcr-abl hybrid oncogene. As mRNA transcripts may be translated several times to produce their protein, reducing mRNA levels may have a compound effect on reducing protein expression.

Targeting the mRNA step in order to block protein translation is an attractive approach and has distinct advantages over targeting DNA. mRNA is more readily accessible, as it is present in the cytoplasm as well as the nucleus, thus providing potential for increased interaction with the target. There are less modification groups and proteins associated with mRNA than with DNA, increasing the opportunities for efficient binding. Only genes that are expressed produce mRNA and this facilitates specific targeting, by decreasing the pool of potential mis-targets. DNA is double-stranded in the cell; therefore targeting the mRNA, which is theoretically single stranded, using an antisense approach is much more feasible than the more complex triple-helix forming oligonucleotide (TFO) approach and relies on the simplicity of Watson-Crick bonding to achieve hybridisation to targets. Compared to protein-targeting approaches, nucleic acid-mRNA interactions are more readily predictable due to their sequence-specific nature, and lack the complexity of protein dynamics; this allows greater specificity by facilitating pre-screening of potential mis-targets (Tanaka *et al,* 2001).

Initial mRNA targeting experiments, which were carried out in a cell free system, showed that this approach had potential. In 1977, Paterson et al demonstrated it was possible to inhibit translation of specific proteins with an oligonucleotide which was designed to be complementary to its mRNA (antisense to the sense mRNA) using an *in*

vitro model of translation (Paterson *et al*, 1977). Antisense molecules are sequences of modified nucleic acids complementary to a sequence on the target mRNA which inhibit the translation of the mRNA transcript resulting in specific down-regulation of protein expression. Antisense molecules are routinely 15-20 base pairs in length, although longer sequences, up to 25 base pairs in length can increase efficacy of some backbone chemistries. Statistical calculations predict that a unique DNA sequence of 15-19 nucleotides in length should be found only once in the human genome (Ma *et al*, 2000).

There are two distinct mechanisms by which antisense molecules may interfere with protein production, by physically blocking translation of the appropriate mRNA at the site of the ribosome (steric hindrance) or by directing cellular nucleases to bring about transcript destruction (Figure 1.7). Both strategies initiate with the formation of a double stranded hybrid composed of the mRNA and the antisense. This emphasises the importance of strong antisense binding to target mRNA regardless of which mechanism is utilised.

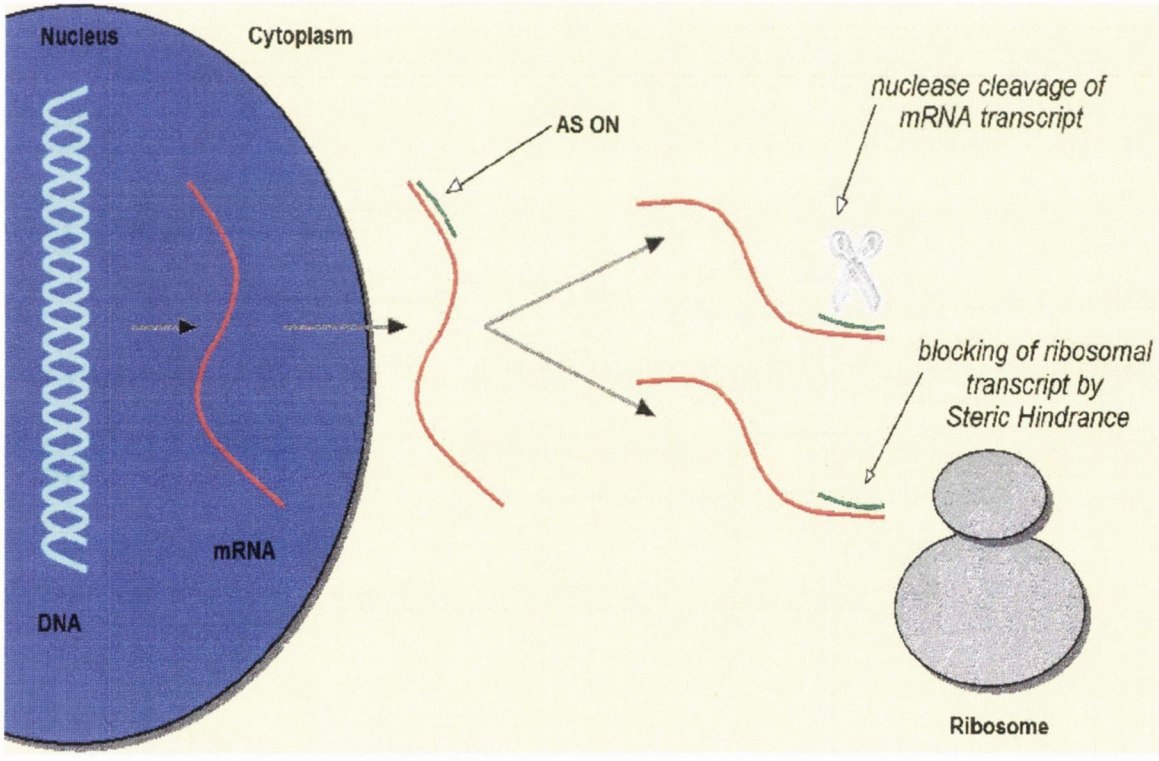


Figure 1.7 Antisense mediated down-regulation of mRNA expression

Following transcription in the nucleus, the mRNA transcript is bound by an antisense molecule in a sequence specific manner. The mRNA : antisense duplex may serve as a substrate for nucleases such as RNase H which mediate transcript cleavage. The antisense molecule may also inhibit translation by blocking ribosomal assembly and progression through the transcript.

1.11 Steric Hindrance

Upon binding of the antisense oligonucleotide to its target mRNA, a double-stranded structure is formed. This hybrid nucleic acid molecule is unreadable by ribosomal machinery hence translation of that particular mRNA is inhibited; this phenomenon is referred to as steric hindrance. The target mRNA is degraded in time by cellular nucleases depending on the half-life of the transcript. Ribosomal subunits possess strong helicase and nuclease activity to displace groups and sequences which may attach to mRNA, to ensure efficient transcript reading. Therefore, antisense molecules employing steric hindrance require strong affinity binding to prevent their dislodgment. While the natural phosphodiester backbone binds to mRNA, its binding affinity is relatively poor and natural DNA is rapidly degraded inside cells. The emergence of novel chemistry backbones displaying strong affinity toward mRNA was an important development in this area. Many of these backbones are strongly nuclease resistant, thus prolonging their antisense effects.

1.12 Enzymatic cleavage of target mRNA transcript

RNase H is an endoribonuclease that specifically degrades the RNA strand in an RNA:DNA hybrid. It is a ubiquitous enzyme whose *in vivo* function is to cleave the RNA primer necessary for initiation of DNA polymerase activity during DNA synthesis (Sohail *et al,* 2001). This cleavage function has been harnessed in the antisense approach to mediate destruction of targeted mRNA sequences once a heteroduplex has been formed. The double-stranded mRNA : antisense hybrid may serve as a substrate for RNase H, which cleaves mRNA at the point where it is hybridised to DNA. This has been recognised as a major form of antisense activity *in vivo (*Summerton, *1999).* It is a highly active enzyme, requiring only 4-6 bases to recognise the duplex and begin cleavage (Dias *et al,* 2002). The RNase H enzyme is RNA specific, thus leaving the DNA-based backbone of the antisense molecule intact. This may allow entry of the antisense molecule into a recurring cycle, following mRNA cleavage and antisense release; the molecule may bind with successive mRNA molecules and thereby mediate the destruction of numerous transcripts.

The formation of a hybrid between mRNA and phosphodiester DNA molecules will induce the activity of RNase H. However, due to the requirement for DNA modification of functional antisense molecules to prevent degradation, only antisense structures that closely resemble that of their parent phosphodiester molecule will retain the ability to activate this pathway. The poor binding affinity of these first generation DNA-based antisense backbones exemplifies the importance of RNase H mediated transcript degradation. Ribosomal sub-units will rapidly displace loosely bound molecules and therefore enzymatic cleavage is vital to arrest translation of the transcript.

1.13 Chemistry of the Antisense Backbone

Due to degradation *in vivo* by endogenous and exogenous nucleases, the natural phosphodiester DNA backbone is unsuitable for use with antisense molecules; therefore suitable modification of the backbone is desirable to prolong its lifespan. The first backbone chemistry to show good stability in a biological system was the methylphosphonate, where a methyl group replaces a non-bridging oxygen atom in the phosphodiester (Figure 1.7). This backbone does not support RNase H activity and relies on steric hindrance alone for the inhibition of translation. Methylphosphonate-linked DNA oligonucleotides were the first to provide resistance to enzymatic degradation, but were limited by poor efficacy of binding and low aqueous solubility (Engelhard, 1998). Methylphosphonate-based molecules are still employed in modified forms and in chimeric oligonucleotides which are composed of more than one chemistry (Prater *et al*, 2004).

1.13.1 The Phosphorothioate Backbone

The introduction of phosphorothioate linked DNA analogs proved a turning point in the development of highly efficient and functional antisense molecules and this superseded the methylphosphonate as the main form of oligonucleotide (ON) employed in antisense studies. In the phosphorothioate backbone, a non-bridging oxygen atom is replaced by a sulphur atom, increasing the molecule's resistance to nucleases, increasing its negative charge and resulting in increased efficacy relative to the methylphosphonate (Figure 1.8-B). As it is chemically similar to the parent molecule, the phosphorothioate retains RNase H activation and induces mRNA transcript destruction. The phosphorothioate

backbone has dominated research in the antisense field, though further experimentation has identified non-antisense effects of this type of molecule.

Like all xenobiotics, antisense molecules have inherent toxicities due to their physical or chemical characteristics. Two major aspects of the phosphorothioate chemistry that led to secondary effects were its polyanionic nature and immune stimulatory properties (Smaglik, 1998). The polyanionic nature of the phosphorothioate is increased relative to that of the natural DNA (which is never normally present in the cytosol) and this may result in interaction with a large number of cellular proteins. Antisense toxicities have been demonstrated to be dependent on their chemistry rather than sequence dependent effects. These toxicities are a result of phosphorothioate protein interactions and are responsible for the majority, if not all of toxicities observed in pre-clinical antisense studies (Cotter *et al*, 1999).

Phosphorothioate molecules have been shown to bind proteins in the micromolar to millimolar range and these binding affinities suggest that at plasma levels attained in toxicity studies, significant protein interactions are possible (Stein, 1996). These non-antisense mediated pathways relate to the phosphorothioate backbone and there is little or no difference between active and non-active sequences with this backbone form. Differences in potency between sequences may be due to sequence motifs which enhance protein binding and hence toxicity. These result in quantitative rather than qualitative differences in toxicity and may be triggered by the presence of a CG flanked by 2 purines at the 3' end and 2 pyrimidines at the 5' end of the sequence (Yuen *et al,* 2000). A G-quartet near the 3' end of a phosphorothioate molecule could also interact with integrins and modify the adhesion properties of cells (Anselmet *et al,* 2002).

The most serious form of acute toxicity due to phosphorothioate treatment is complement activation, which is common when plasma concentrations exceed 40-50μg/ml. The alternative complement pathway is controlled by a circulating regulatory protein; Factor H which is bound by phosphorothioate molecules, leading to its sequestration and inactivation (Bhatia *et al,* 1998). This results in phosphorothioate induced activation of the alternative complement pathway. Clinical dose regimens are carefully designed to prevent plasma concentrations reaching the critical threshold level.

Phosphorothioate oligonucleotides increase levels of liver enzymes and induce a highly transient, concentration dependent prolongation of clotting times (Tamm *et al,* 2001). The prolongation is directly proportional to phosphorothioate plasma levels and once the drug is cleared, the prolongation is completely reversible, showing no residual inhibition following repeated administration. Similar to the effects on complement, activated partial prothrombin times (aPPT) prolongation is independent of sequence and dependent on chemical class and oligonucleotide length. In this case, the binding target of the phosphorothioate was identified as the tenase complex (Bhatia *et al,* 1998). The transient and reversible nature of this aPPT prolongation; indicated it is clinically insignificant for current antisense treatment regimens. Phosphorothioate based oligonucleotides are also being investigated as novel inhibitors of protein clotting function (Agarwal *et al,* 1999).

Other clinical manifestations of side effects observed in mammals following phosphorothioate treatments were a number of haematological changes including a decrease in arterial blood pressure, a transient decrease in total peripheral white blood cells and neutrophils, immunological changes, enlargement of the spleen and histopathological changes to the kidney and liver. The presence of CpG motif in phosphorothioate oligonucleotides added to the severity of toxicity observed. In humans, effects observed included thrombocytopenia and elevation of transaminases; immune stimulation also occurred through induction of mitogen activated protein kinases (MAPK's) (Agarwal *et al*, 1999). However, as the first generation of modified backbones, the phosphorothioate remains the backbone of choice used in a variety of systems and in antisense clinical trials at present.

Table 1.1 Characteristics and properties of backbone and subunit modifications of Antisense molecules

Antisense backbone	Antisense mechanism	Chemistry	Properties	Example of applications
Phosphodiester	RNase H cleavage	Natural DNA backbone	Water soluble Nuclease sensitive	In vitro work & in chimeric molecule with phosphorothioate backbone to target Ha-ras & with methylphosphonate to target HIV(Monia *et al*, 1996)
Phosphorothioate	RNase H cleavage	Non-bridging oxygen is replaced by sulphur	Increased nuclease resistance relative to phosphodiester, negatively charged	BCL-2 studies in a variety of diseases (Hu *et al*, 2002)
Methylphosphonate	Steric hindrance	Non-bridging oxygen is replaced by CH_3 (methyl)	Nuclease resistant, low efficacy, poor hybridisation	bcr-abl breakpoint & in chimera with phosphodiester to target HIV(Giles, Spiller *et al*. 1998; Miller *et al*, 2000)
2'-O-Methyl RNA	Steric hindrance	RNA backbone with oxygen at 2' position	Reduced polyanionic nature relative to phosphorothioate, high affinity to mRNA, strongly nuclease resistant	Protein Kinase A RIα subunit chimera with phosphorothioate centre (Wang *et al*, 1999)
Peptide Nucleic Acid (PNA)	Steric hindrance	Amino acid backbone	High affinity binding, nuclease resistant, difficult to deliver	bcr-abl breakpoint (b2a2)(Ray *et al*, 2000; Rapozzi *et al*, 2002).
Morpholino	Steric hindrance	6-membered ring with nitrogen group	Water soluble, highly nuclease resistant, high affinity binding to mRNA, neutrally charged	TNFα [Qin, 2000]

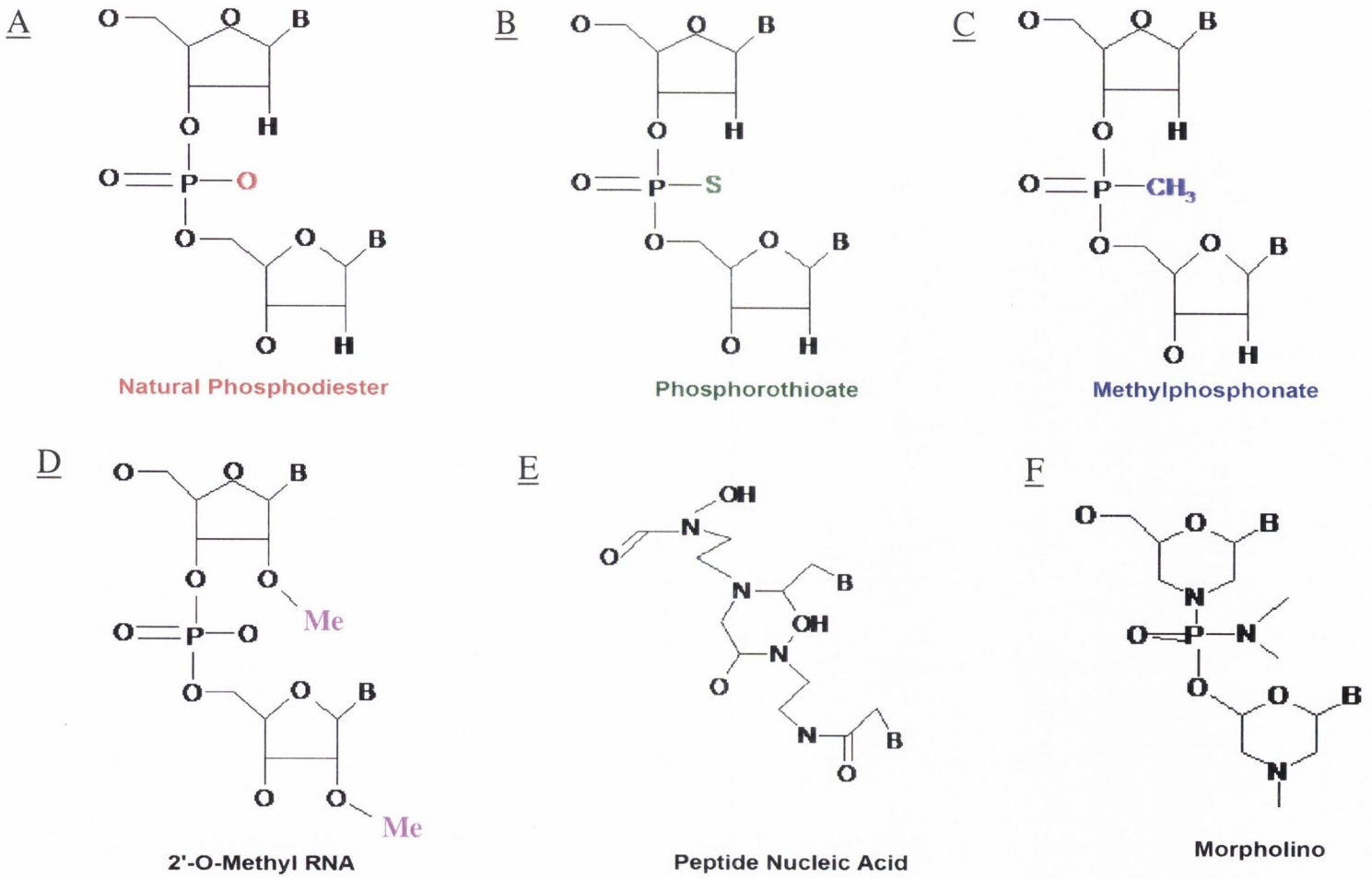


Figure 1.8 **Structures of the commonly employed antisense backbones**

1.13.2 Chimeric Backbones + Subunit Modifications

Due to the drawbacks associated with the phosphorothioate backbone, a second generation of antisense compounds were investigated. In some instances these moved away from the traditional method of RNase H activation, relying only on steric hindrance for prevention of translation. This departure allowed for a greater range of compounds to be employed in the antisense molecule as the phosphorothioate is the only artificial backbone which retains RNase H activation. Although the phosphorothioate backbone confers increased nuclease resistance relative to the phosphodiester backbone, it is still degraded inside the cell in ~72 hours (Cotter *et al,* 1999). RNase H independent backbones may facilitate prolonged stability inside the cell; this is relevant when the half-life of the target mRNA is greater than ~40 hours. The development of chimeras which have both RNase H activating potential and regions of RNase H independence provided a practical alternative.

To combine RNase H mediated antisense mRNA cleavage with the strong binding affinities of RNase H independent backbones, chimeric antisense molecules composed of the phosphorothioate backbone with end or central modification were developed. These may be designed to increase binding stability, reduce polyanionic effects and as only four bases are required for RNase H activation this can be retained within the chimeric molecule (Afar *et al,* 1999). Gapmers combine the diversity of the RNase H independent backbones with the phosphorothioate and seek to harness the positive aspects of both systems, the enzyme activating capacity and strong hybridisation characteristics. These have an internal region composed of an RNase H activating section, flanked on either side by an RNase H independent backbone (Figure 1.9) (Agrawal *et al,* 1998). These flanking sections provide increased nuclease resistance, prolong survival of the antisense molecule in the cell and impart overall higher affinity mRNA binding to the molecule. As phosphorothioate molecules are primarily degraded in a 3' to 5' and less so in a 5' to 3' direction rather than central cleavage, flanking an oligonucleotide on either side with RNase H independent bases should impede its degradation and significantly extend the overall lifespan of the chimeric molecule (Agrawal *et al,* 1997). Chimeras have the advantage of reducing the overall phosphorothioate content of the molecule, thus minimising side effects due to its negative charge (Wang *et al,* 1999). 2' O-methyl RNA modified oligonucleotides

(Figure 1.8) are commonly employed in chimeras due to their high affinity binding and strong nuclease resistance.

An alternative approach to reduce phosphorothioate content is by central modification of antisense molecules, again utilising RNase H-independent chemistries. This design may increase binding stability and reduce polyanionic effects, while phosphorothioate sections at the 5' and 3' ends ensure that once stable hybridisation is mediated by the RNase H independent core of the chimera, RNase H destruction of the mRNA transcript will ensue.

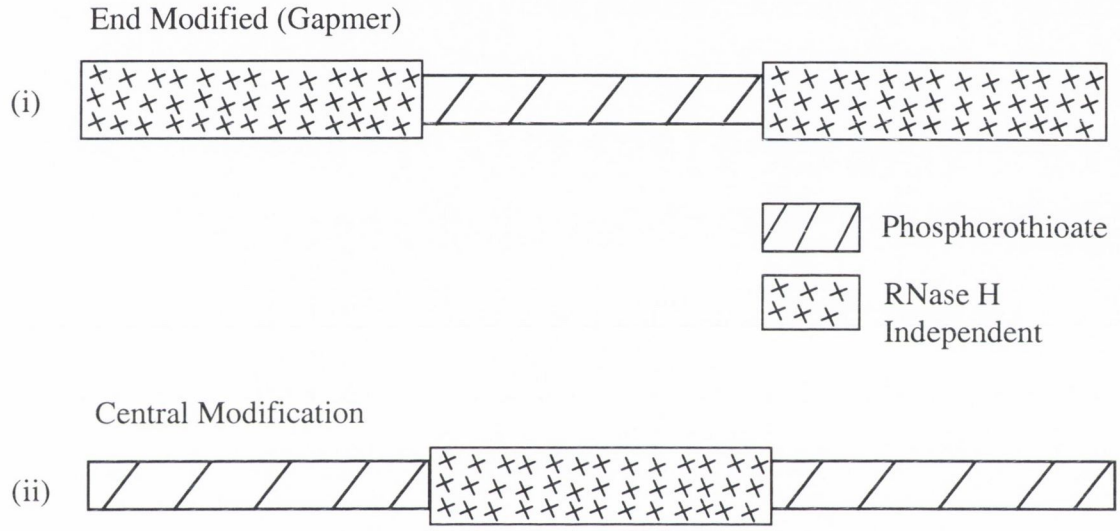


Figure 1.9 Chimeric antisense molecules incorporating RNase H activating phosphorothioate sections and RNase H independent regions at alternative positions

(i) The end modified gapmer has a central portion of RNase H activating phosphorothioate and has protection from nuclease degradation at the 3' and 5' termini in the form of RNase H independent chemistries. These increase binding affinity to mRNA. (ii) Centrally modified molecules contain a central region of RNase H independent backbone to facilitate high affinity mRNA binding

1.13.3 Sub-unit Modification

Based on the theory that the majority of phosphorothioate mediated side-effects were dependent on its negative charge, substitutions to the nucleotide subunits rather than the phosphorothioate backbone were also performed to minimise these effects (Olie *et al,* 2002). The main advantage of using this approach is that the RNase H activation capacity is retained. These studies focus on the feasibility of using phosphorothioate

oligoribonucleotides and phosphorothioate 2´-O-methyloligoribonucleotides at the 3´ and 5´ ends, or in the centre of the molecule, to reduce polyanionic related side effects and increase stability against cellular nucleases (Jiang *et al,* 2000). 2'-O-methyloligoribonucleotides (2'-O Me RNA) significantly enhance the mRNA binding potential of antisense oligonucleotides compared to phosphorothioate molecules.

Unlike other oligonucleotide analogs, arabinonucleic acid (ANA) molecules; in particular 2'-fluoro-ANA (FANA) are capable of inducing RNase H activity though with less potency than phosphorothioate-linked DNA molecules (Lok *et al,* 2002). Though their RNase H activity is not as potent, FANA molecules bind mRNA with significantly increased affinity leading to the formation of thermally stable hybrids (Mangos *et al,* 2003). The binding affinity of chimeric antisense molecules with FANA and DNA portions was directly correlated with the FANA content of the molecule (Min *et al,* 2002). Due to their 'A' conformation FANA : mRNA hybrids show greater resemblance to DNA / RNA hybrids than to RNA /RNA hybrids and this factor facilitates their recognition by RNase H (Wilds *et al,* 2000). Though RNase H binds to RNA / RNA duplexes no cleavage occurs (Denisov *et al,* 2001). Analysis of the exact structural components of FANA molecules which allow RNase H recognition and cleavage may lead to the development of other closely related chemistries as antisense molecules. Due to their conformation, FANA molecules readily form diverse chimeras with a range of oligonucleotides (Minasov *et al,* 2000). Their high binding affinity coupled with reduced or no phosphorothioate content and RNase H activation indicates they are a completely unique form of antisense backbone which show promise (at least theoretically) for broad applicability.

1.13.4 RNAse L

A second ubiquitously expressed ribonuclease, RNase L, has been employed to mediate cleavage of antisense selected targets using specifically constructed sequences (Ueno *et al,* 2003; Cirino *et al,* 1997). The addition of an activating linker allows recognition by RNase L of antisense molecule bound sequences. RNase L is converted from a silent to an active form in response to the presence of a 2' 5' tetraadenylate signal (2-5A), attached via linkers to the 5' terminus of an antisense oligonucleotide (Ueno *et al,* 2004). RNase L mediated cleavage occurs where the 2-5A antisense is hybridised to an RNA target. RNase L has been shown to be a highly active endoribonuclease capable of

selectively cleaving individual RNA molecules in cell-free systems and in human cells. To date, 2-5A antisense molecules when targeted against bcr-abl have shown decreases in mRNA, inhibition of proliferation and growth suppression (Maran *et al*, 1998).

1.13.5 RNase H Independent Backbones

RNase H independent backbones have the potential to exhibit increased specific activity relative to their RNase H competent counterparts (Karras *et al,* 2000). The average antisense molecule is approximately 18-25 base-pairs (bps) in length and the RNase H enzyme requires only 4-6 bases in the duplex for recognition and cleavage (Afar *et al,* 1999). Therefore, before encountering their target, RNase H-activating antisense molecules may form transient duplexes of short duration, leading to non-specific cleavage of targets whose sequences overlap that of the target (Dias *et al,* 2002). Such interactions are difficult to pin point and may result in down-regulation of the expression of more than one gene. This non-targeted mRNA down-regulation may be eliminated by the employment of RNase H independent antisense backbones which can only prevent translation of their target mRNAs when strongly hybridised to a long stretch of bases, normally 25 in length. Another positive aspect of employing RNase H independent chemistries over those that mediate mRNA cleavage is that with RNase H dependent mechanisms the break-down products of the cleavage themselves may participate in secondary effects (Anselmet *et al,* 2002).

A conservative estimate suggests that 35% of all pre-mRNA's are spliced to yield alternative variants and aberrant splicing can be implicated in disease such as cystic fibrosis, β-thalassemia and several types of cancer (Mercatante *et al,* 2002). Aberrant splice variants have been detected in breast cancer (BRCA 1 &2, HER2 genes), neuroblastoma (p73 gene) and leukaemia (WT1). Targeting splice variants with RNase H competent molecules would result in degradation of the mRNA transcript. However, by employing RNase H independent chemistries the spliceosome may be prevented from recognising targeted sites, possibly leading to restoration of the correct splice variant.

1.13.5-a Morpholino

The morpholino is an RNase H independent antisense chemistry whose structure is highly modified relative to the normal phosphodiester backbone (Sazani *et al,* 2002).

The deoxyribose sugar is replaced by a nitrogen containing six-membered morpholine ring joined by phosphorodiamidate linkages and a non-bridging oxygen is replaced by a dimethylamine (Figure 1.7) (Pannier *et al,* 2004). Substitutions of this nature inhibit recognition of the mRNA : antisense duplex by RNase H. However, the morpholino chemistry displays high affinity binding to mRNA and is particularly suited to prevention of ribosomal translation by steric hindrance. Due to its unnatural structure, the morpholino is not recognised by cellular nucleases and is exceptionally stable (Hudziak *et al,* 1996). This is in contrast to RNA and DNA analogs which are degraded by nucleases; albeit at a slower rate than their parent molecules.

The morpholino backbone is non-ionic and as a result of this neutral structure, unlike phosphorothioate molecules, morpholino oligonucleotides do not readily interact with cellular proteins in a non-specific manner (Summerton, 2003). This aspect of the morpholino chemistry is key to its development as a reliable antisense therapeutic. To date, morpholino antisense molecules have demonstrated a strong ability to specifically reduce target protein expression within cells and have been widely harnessed for examination of gene function during embryogenesis and limb regeneration (Corey *et al,* 2001; Schnapp *et al,* 2004). The high affinity mRNA binding of morpholino molecules efficiently blocks expression of target mRNA transcripts when targeted to the areas surrounding the translational start site, where it prevents ribosomal assembly. Its inability to direct target mRNA cleavage may also be manipulated to mediate positive effects such as the re-direction of aberrant splicing. The morpholino and RNase H independent antisense oligonucleotides are suitable for targeting mRNA splice sites and may inhibit or alter formation of mature mRNA transcripts and inhibit capping or polyadenylation resulting in destabilisation of the mRNA (Kole *et al,* 2004).

1.13.5-b Peptide nucleic acids

The most diverse of the artificial backbones is the Peptide Nucleic Acid (PNA). Its atypical, chiral, uncharged polyamide mimic means that it appears to the cell neither as a peptide nor a nucleic acid, rendering it resistant to both proteases and nucleases (Larsen *et al*, 1999). Complete resistance to nucleases means that it has significantly increased stability in biological fluids relative to nucleic acid based backbones (Ray *et al,* 2000). This makes it a particularly useful tool for transcript down-regulation and also a suitable backbone to be used for mRNA targets with prolonged half-lives. Due to the decreased levels of electrostatic repulsion, the uncharged PNA oligonucleotides form extremely strong hybrid duplexes with RNA and DNA (Pooga *et al,* 2001).

PNA hybridisation still follows the normal Watson-Crick bonding rules, due to normal base structure attached via a methylcarbonyl linker. PNA's have been used both in the antigene (TFO) and antisense approaches and have been shown to specifically block expression at both the transcriptional and translational levels (Pooga *et al,* 2001). Antisense efficacy has been demonstrated by nuclear micro-injection of PNA oligomers targeted to the large T Antigen (T Ag) mRNA;, this suppressed T Ag expression, demonstrating a strong antisense effect in intact cells (La Rosee *et al,* 2002). Lack of toxicity at relatively high concentrations suggests that PNA could be considered as highly promising compounds for antisense applications, however PNA's show poor cellular uptake due to their large size. Whilst delivery methods may circumvent this problem in cell culture, it poses a serious obstacle to their application *in vivo*. It has been shown that lipoproteins present in the blood may complex with nucleic acids particularly those with phosphorothioate backbones and mediate their entry into cells *in vivo*, similar to the method employed by carriers such as liposomes *in vitro* (La Rosee *et al,* 2002). This phenomenon is thought to contribute considerably to the success of phosphorothioate molecules *in vivo*. However, it is unlikely to be the true for PNA and successful cell entry is being evaluated by electroporation and by conjugation to peptide and lipophilic moieties (Koppelhus *et al,* 2003). PNA has also demonstrated strong promise in the TFO approach, where PNA molecules bind their target DNA and induce strand displacement leading to formation of an exceptionally stable triplex (Demidov, 2002). PNA pharmacokinetic properties can be modulated by glycosylation; by the substitution of glycine by serine and threonine. These alterations profoundly altered the pharmacodistribution of PNA in mice (Hamzavi *et al,* 2003).

Various other backbone chemistries are being investigated for antisense applications. Locked nucleic acids (LNA) are ribonucleotide analogs with a methylene bridge between the 2' oxygen and 4' carbon of the ribose ring (Braash *et al,* 2002). This modification increases their binding affinity and their melting temperature (Tm) by approximately 10^0C per base. LNA oligomers also retain activation of RNase H which may prove a key advantage in their application. An LNA oligomer may contain as little as one locked nucleic acid residue and is capable of forming chimeras with other monomers e.g. DNA / RNA and 2' O-Me RNA and may also be joined by phosphodiester or phosphorothioate linkages (Vester *et al,* 2004). The introduction of LNA monomers increased the stability of oligonucleotides ten fold in human serum. A comparative study demonstrated LNA molecules out-perform 2'-O-Me RNA phosphorothioate oligodeoxynucleic acid and PNA, though not siRNA (Grunweller *et al,* 2003). Circular antisense nucleic acids are another development which have no ends (3' or 5') and therefore are resistant to exonuclease degradation (Rowley *et al,* 1999), one of the main routes of antisense digestion. Though this form of antisense molecule shows promise in aspects of antisense design, its substantial usefulness yet to be reported.

1.13.6 Ribozymes

Ribozymes, or nucleic acid enzymes, are a form of catalytic mRNA species which can induce site-specific cleavage of the phosphodiester bond within an mRNA molecule (Grassi *et al,* 2004). There are a number of different naturally occurring ribozymes including hammerhead, hairpin and the RNA subunit of RNase P; recent evidence also strongly suggests that ribosomal RNA may function as an enzyme (Khan *et al,* 2003). Allosteric ribozymes have been designed to control the activity of ribozymes and allow regulation of gene expression in response to an externally administered regulatory drug (Khan *et al,* 2003). The catalytic and controllable natures of ribozymes indicate their potential for use as therapeutic tools. However, the nuclease sensitivity of the RNA may prove a drawback to their application. DNAzymes, which are structurally and catalytically similar to ribozymes with a DNA backbone, may improve this aspect (Peracchi, 2004).

1.14 Cytosolic delivery of Antisense Molecules

1.14.1 Overview of cytosolic antisense Delivery

Antisense oligonucleotides are naturally repelled by the lipophilic cell membrane due to their anionic nature; neutrally charged oligonucleotides are also unable to enter the cell freely (Hughes *et al,* 2001). In order to encounter its target mRNA, the antisense molecule must achieve a cytosolic localisation and it has been shown that phosphorothioate antisense molecules present in the cytoplasm are transported to the nucleus, which is the main site of interaction between the antisense molecule and its target (Beltinger *et al*, 1995). Therefore the main barrier to be traversed is the cell membrane and this has been achieved by a variety of approaches. Although the phospholipid bilayer represents a strong barrier to the passive diffusion of ions, there are a number of natural methods by which antisense molecules may be spontaneously taken up by the cell including receptor mediated endocytosis, pinocytosis, and adsorption (Giles, University of Liverpool Antisense Research Group website, 2000). However, these mainly result in an endosomal localisation for the antisense molecule and topologically, oligonucleotide trapped in endosomes is equivalent to oligonucleotide outside of the cell as the antisense molecule is still separated by a membrane from its target mRNA.

Following binding of an oligonucleotide to a cell surface receptor, the active process of internalisation into the endosome compartment occurs. Fluid phase pinocytosis and adsorptive endocytosis also result in endosomal localisations, with similar fates for the oligonucleotide (Broughton *et al,* 1997). The endosome ultimately fuses with a lysosome leading to destruction of the endosomal oligonucleotide, followed by exocytotic efflux (Giles, 2001). Only a relatively low proportion of oligonucleotide, approx 2-5% is released and most of the molecule is destroyed, never having encountered its target. Intracellular injection may be used to deliver antisense molecules directly to the cell cytoplasm and thus by-pass the cell membrane. This is a very successful approach for delivery to embryos for functional studies; particularly for morpholino applications. However, the number of cells which have molecule delivered to them is severely limited and inadequate for significant down-regulation of gene expression as is required in clinical studies. The two main methods of delivery involve the use of delivery agents

which envelop the antisense molecule and carry it across the cell membrane or permeabilisation of the cell membrane.

1.14.2 Carrier Agents

Several carrier agents that bind antisense oligonucleotides and mediate their entry into cells are available. Liposomes are cationic lipids consisting of a phospholipid bilayer surrounding an aqueous compartment, within which the antisense molecule is enclosed. They afford protection to the antisense molecule whilst enhancing its delivery into cells. The most commonly used forms are positively charged and have a high affinity to the negatively charged cell membrane, they gain entry into cells by absorptive endocytosis. However, once inside the cell, the success of carrier agents is highly dependant on release from the endosomal particle (Shi *et al,* 2004). This results in degradation of significant proportions of antisense molecules and this necessitates higher doses of antisense administration. Whilst enclosed in the membrane bound vesicle oligonucleotides are incapable of hybridising to their target and mediating antisense down-regulation.

To facilitate release of the nucleic acid, many liposomes contain a helper lipid such as 1,2-dioleoyl-*sn*-glycero-3-phosphatidylethanolamine; (DOPE) (Garcia-Chaumont *et al*, 2000). This is an inverted cone shaped lipid thought to facilitate cytosolic release through the fusion and/or disruption of the membrane, possibly by the formation of hexagonal lipid structures. Studies have shown that oligonucleotides can readily dissociate from these complexes and are in a bioavailable form within the cell. A second approach to enhance the cytosolic availability of antisense oligonucleotides following intracellular delivery with liposomes is the use of pH sensitive fusogenic liposomes (Hu *et al*, 2001). These are composed of a lipid such as DOPE and an acidic amphiphile. At neutral pH the amphiphile maintains the lipids in a bilayer structure. As the complex moves through the endosome, the pH drops, resulting in protonation of the amphphile. This causes destabilisation and collapse of the endosome, releasing the oligonucleotide free into the cytoplasm. The main drawback is the approach's dependence on natural lipids, which may result in less stable complex formation with the oligonucleotide and decreased interaction with the cell membrane relative to cationic forms.

Liposomes require a high degree of optimisation at the level of the amount of compound, cell number, duration of treatment and complex formation between oligonucleotide and lipid (Dokka *et al,* 2000). Effectiveness has also been reported to rely on such factors as cell type, oligonucleotide chemistry and oligonucleotide length; however liposomes may be considered an option *in vivo* (Lebedeva *et al,* 2000). However, the significant degradation of antisense oligonucleotides by this approach has to be addressed.

Dendrimers are a class of supermolecular delivery system which have attracted interest as delivery agents for both genes and oligonucleotides. They are spherical highly ordered polymers with defined polymerisation activity, resulting in a reproducible product (Hughes *et al,* 2001). It is possible to attach functionally diverse groups during synthesis, thus creating one of the most versatile particulate systems (Akhtar *et al,* 2000). Stable dendrimer:oligonucleotide complex formation can occur in a variety of media including water, serum and PBS and have been shown to enhance oligonucleotide uptake, resulting in nuclear localisation (Hughes *et al,* 2001). They have been demonstrated to provide significantly increased protection to and reduce metabolic degradation of the highly nuclease-sensitive phosphodieter molecule. Polyamidoamine (PANAM) is a commonly employed dendrimer for antisense delivery; it is composed of a hydrocarbon core with charged surface amino groups and a well defined chemistry (Akhtar *et al*, 2000). Delivery using PANAM results in a distribution and specific inhibitory effects of antisense oligonucleotides that are cell cycle dependent, with nuclear localisation occurring predominantly in the G2/M phase. As it is very effective in delivering genes and antisense oligonucleotides into actively dividing cells such as cancer cells, this approach may be particularly relevant to antisense delivery in malignancy.

1.14.3 Cell Permeabilisation Agents

While carrier agents enhance antisense effects, overall they lack efficiency and are limited in the amount of antisense oligonucleotide they can deliver to the cytosolic compartment. This coupled with their innate toxicity results in a less than ideal system for antisense delivery. The alternative form of delivery is via cell permeabilisation; the formation of transient pores in the cell membrane through which the antisense oligonucleotide may pass. This method automatically results in a cytoplasmic localisation for the antisense molecule and bypasses the endosomal pathways,

delivering the molecule to an area where it may interact directly with its target. However, cell permeabilisation agents may also exhibit high toxicity and there is a requirement to allow the permeabilised cells to recover, in order to maintain cell viability. If the pore in the cell membrane isn't resealed, the cells swell and eventually burst.

1.14.3-a Saponin

A plant glycoside, saponin, is known to enhance penetration of proteins and other macromolecules through the cell membrane (Liu *et al,* 1999). Saponins are surfactants with soapy action that can be digested to yield a sugar and saponin aglycone and are used in a wide range of fields including organic gardening, as adjuvants to vaccines and anti-yeast steroidal saponins are used as novel food anti-deterioration agents. Yucca, Ginseng and Agave are herbs with important saponin constituents, however many saponins can be toxic and act as potent haemolytics when injected intravenously. Uptake due to saponin has been shown to be enhanced by the presence of a bis-benzyllisoquinoline alkaloid, TET (Leung *et al*, 1997). Pore formation mediated by saponin is due to complex formation with cholesterol present on the cell surface (Liu *et al,* 1999).

1.14.3-b Streptolysin-O (SL-O)

Streptolysin-O (SL-O), a bacterial cytolysin secreted by members of the Gram positive bacterium *Streptococcus pyogenes* forms pores in red blood cells leading to their destruction during a streptococcal infection (Sierig *et al,* 2003). Streptolysin-O belongs to the highly homologous family of thiol-activated cytolysins, which is remarkable for its strict specificity for cholesterol containing membranes (Meehl *et al,* 2004). Pore formation occurs by binding of the molecule to cholesterol present on the cell surface. Reversible binding occurs at the monomeric level, whereas pore formation coincides with the formation of a large ring shaped, membrane inserted oligomer of approximately 30nm in diameter (Weis *et al,* 2001). Prior to the formation of a full ring, an intermediate, arc-shaped oligomer is formed and is lined on the facing side by a free edge of target membrane. The resulting pore allows passage of the antisense oligonucleotide into the cytoplasm of the cell (Figure 1.10). Resealing of pores is performed by the cell itself and is induced by addition of cholesterol to the cell medium (Spiller *et al,* 1998). SL-O activity is exquisitively sensitive to the presence of cholesterol, which binds to and inactivates any free SL-O and allows cells to recover

their membrane damage (Meehl *et al,* 2004). Repair of lesions is dependent on calcium calmodulin and intact microtubules, thus producing a system of pore formation that can be regulated in healthy cells. While this is a very efficient method of intracellular antisense delivery, it requires a high degree of optimisation with respect to cell type, concentrations used and duration of treatment.

1.14.4 Peptide-mediated delivery of antisense molecules

Short peptides may enhance intracellular concentrations of antisense molecules by binding to them and mediating their passage through the cell membrane. Cationic peptides such as poly-L-lysine complex with oligonucleotides and enhance their cellular uptake via endocytosis (Lochmann *et al,* 2004). The specificity of this approach may be increased by conjugatation of poly-L-lysine to tissue-specific ligands which mediate antisense cell entry by binding to specific cell surface receptors. This includes asialoglycoproteins for hepatocytes and anti-CD5 for T cells (Wagner *et al,* 1998). However, the success of this approach is dependent on release of the antisense molecule from the resulting endosome. Peptides rich in arginine and histidine have endosomolytic potential and may facilitate rupture of the endosomal complex releasing its oligonucleotide cargo into the cell cytoplasm (Moulton *et al,* 2004). Furthermore, peptides with nuclear localisation signals (NLS) may direct intra-cellular trafficking of antisense molecules to the nucleus.

Peptides may also possess cell-penetrating and passive cell permeabilisation properties. Unlike particulate carrier systems, these do not rely on fluid phase endocytosis and deliver the antisense molecule directly to the cytoplasm of the cell. Natural cell-penetrating peptides exist and derivations of these containing α-helical amphipathic sections, enhance cellular uptake of antisense molecules; though the exact mechanism of this is undefined (Oehlke *et al,* 2002). A peptide 'MPG' derived from the hydrophobic fusion peptide HIV1 gp41 and the NLS of SV40 large T antigen interacts with antisense oligonucleotides forming a 'cage-like' structure which protects them from serum degradation and delivers them to an endosome-independent cell location (Morris *et al,* 1999). MPG functions by forming a transient pore in the cell membrane and its protein sequence results in a nuclear localisation for the antisense molecule; it may prove useful *in vivo* depending on its toxicity profile (Deshayes *et al,* 2004).

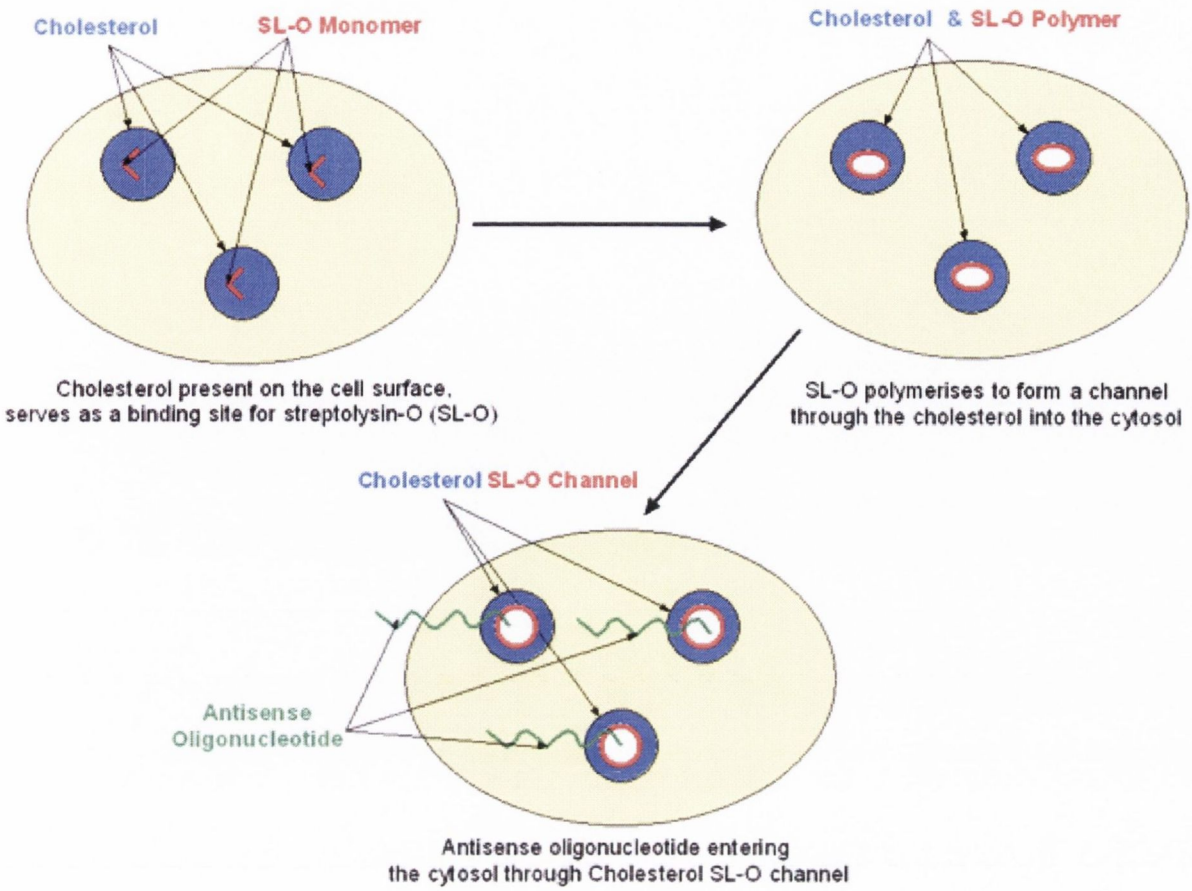


Figure 1.10 **Pore formation in a eukaryotic cell membrane by the bacterial toxin streptolysin-O**

1.15 Hybridisation

1.15.1 Overview of Hybridisation

In order to achieve a strong antisense response, either by steric hindrance or RNase H induction, efficient hybridisation between the antisense molecule and its target is crucial. Efficient hybridisation is required for an active antisense molecule and this is correlated with potency of the response (Sohail *et al,* 2000-b). Efficient binding may be hampered by (A.) mRNA secondary structure, (B.) antisense oligonucleotide secondary structure and (C.) binding of protein groups to antisense binding targets (Agarwal *et al*, 1999).

1.15.2 Secondary Structure

mRNA, once transcribed is considered a single stranded molecule, which theoretically makes it a good target for antisense hybridisation. However, as is likely with most single-stranded sequences of nucleic acid, the mRNA molecule has abundant intramolecular secondary structures due to self-complementarity and annealing by Watson-Crick type bonding forming hairpin loops (Vickers *et al*, 2000). These result in areas of the transcript which are unavailable for binding to antisense molecules and hence serve as poor target regions. Regions of the mRNA which are not involved in intramolecular secondary structures are most suitable for duplex formation with an antisense molecule and produce a more potent antisense response (Sohail *et al,* 2001). However, antisense molecules with high binding affinity backbones may display sufficiently strong binding to overcome limited forms of secondary structure.

To show activity, the antisense molecule should also display minimal levels of secondary structure to allow efficient binding. The secondary structure of the oligonucleotide may be easily deduced using computer programs (such as Primer Express or OligoTech) due to their short length and uncomplicated structure. However, predicting the folding of mRNA molecules to identify suitable regions for targeting is problematic and there are two main, conflicting theories on how this process of folding occurs (Beale *et al,* 2003). Folding of the mRNA following transcription from the DNA strand may occur spontaneously as the strand is transcribed, implying that those sections which are made first are more likely to interact with one another, as the rest of the molecule is not yet available for hybridisation. A second theory is that while the 5'

region of the molecule is being produced, it is 'held' by cellular proteins, preventing interaction with neighbouring sequences (Sohail *et al,* 2000-a). Only when the mature molecule is completed is it released and allowed to interact, ensuring that regions on the sequence distal to each other may bind to one another. These two different methods of folding give two highly variant possible secondary structures to the mRNA molecule. Both present problems to the prediction of secondary structure, however there is evidence that folding occurs by the latter method, with involvement of proteins especially for larger transcripts (Sohail *et al,* 2000).

1.15.3 mRNA Target Site Selection

The success achieved using the antisense approach can vary greatly on the mRNA target area, not only in relation to secondary structure but also in relation to a number of other factors. Targeting around the AUG start site is particularly effective in the case of RNase H independent backbones; if the transcript is blocked at its initiation, it increases the likelihood of successful down-regulation of gene expression, due to the increased ribosomal unwinding activity when it is translating in the centre of the molecule which would displace even strongly bound groups (Dias *et al,* 2002). Regions of an mRNA transcript commonly targeted include the 5' and 3' untranslated areas, splice sites, the translation initiation codon and disease specific targets including hybrid mRNA formation due to gene translocation ('T Hoen *et al,* 2002). Of these, antisense oligonucleotides targeting the AUG start codon have consistently been demonstrated to produce an antisense effect (Ho *et al*, 1996). However, sequences in this area are reasonably conserved and care should be taken to ensure the target is unique (Ho *et al*, 1996).

To successfully predict available hybridisation sites, a number of approaches are employed. These include the "walk the gene" approach, where a large number of oligonucleotides are tested against a target mRNA. It has proved very successful for a number of targets including the discovery of a very potent oligonucleotide targeted against the C-raf kinase mRNA, where 1 of 34 oligonucleotides tested showed >90% inhibition and 4 showed > 70% inhibition (Smith *et al*, 2000). Another more accurate method to detect accessible sites is by RNase H mapping where a library of random or semi random antisense oligonucleotides are allowed to hybridise to the target mRNA of interest. The RNA: DNA hybrids are digested with RNase H, which will cleave the

mRNA at the sites of hybridisation. The resulting fragments are sequenced and analysed to identify accessible regions (Figure 1.11).

All antisense molecules targeted to mRNA regions predicted by RNase H mapping to accessible sites were active (Ho *et al,* 1998). Enzymatic mapping of mRNA may not only be used to identify antisense targets but also to decipher mRNA secondary structure. Some targets may theoretically be overlooked due to steric inaccessibility of RNase H. This is important if the backbone to be used is RNase H independent, however it is a convienent selection procedure in the case of RNase H dependent targets as only those oligonucleotides with RNase H activation capacity are selected. Antisense oligonucleotides to the human multi-drug resistance mRNA with potent activity were selected by this method (Smith *et al,* 2000).

Microarray based approaches can be used to decipher the exact mechanisms of activity of antisense oligonucleotides following incubation with targets cells and they may also be used to aid in identification of sequences that readily participitate in hybridisation. This is a very systematic approach where an array with all possible antisense oligonucleotides against a selected sequence is designed. A large number of potential antisense molecules of varying length and sequence may be tested (Sohail *et al,* 2000). Labelling of mRNA with fluorescent or radioactive labels allows detection of hybridised regions. Duplex yield determined by this method correlated well with antisense activity *in vitro* and RNase H mapping; however secondary structure analysis was not very effective in predicting areas of active hybridisation potential (Ding *et al,* 2001). Using β-globin mRNA as a target, duplex yield on a scanning array using anti β-globin antisense oligonucleotides showed good correlation with antisense activity and *in vitro* translational assays.

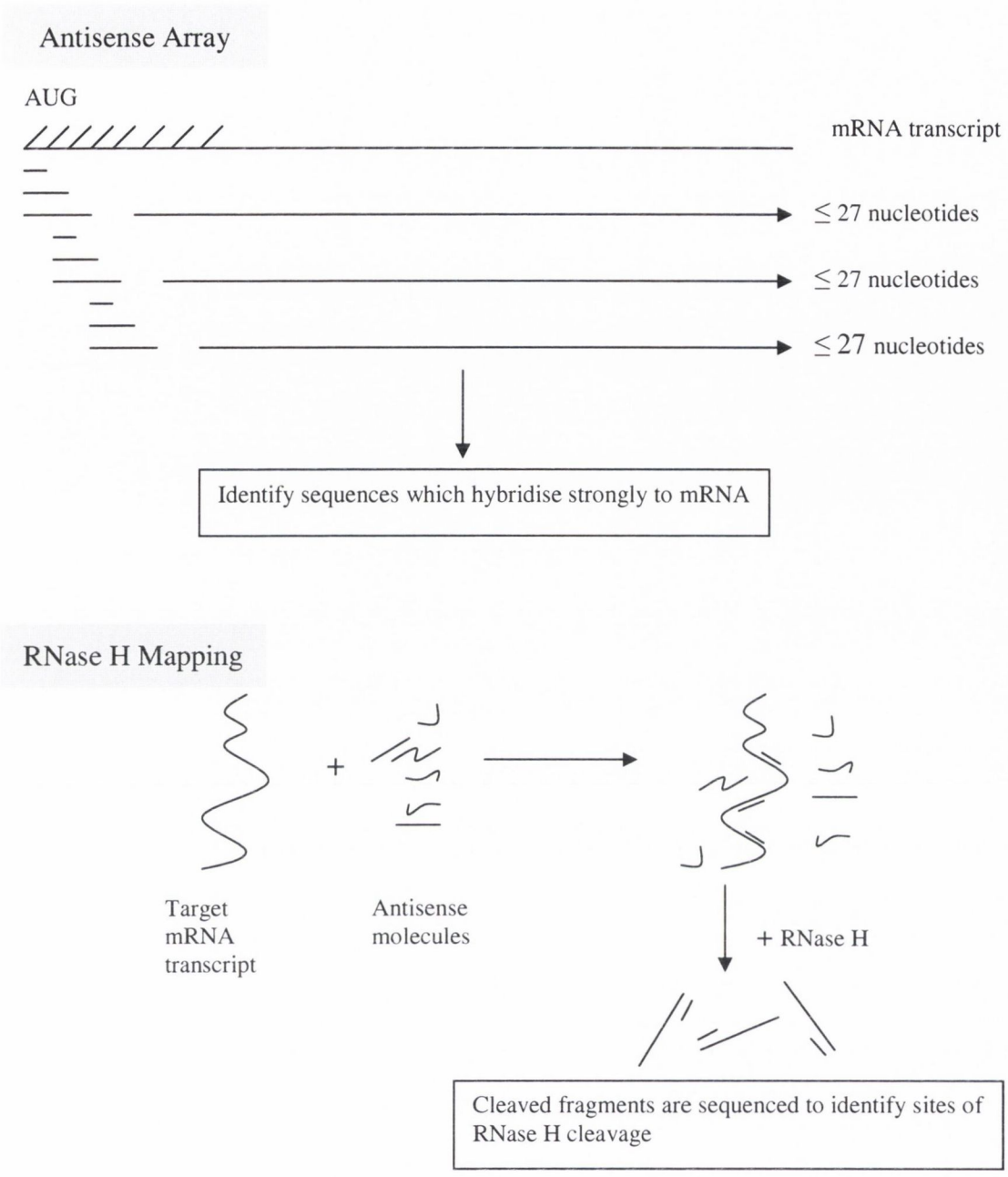


Figure 1.11 Selection of antisense oligonucleotides to an mRNA target based on their hybridisation ability. Sequences selected by this method are tested for their ability to induce RNase H mediated mRNA transcript cleavage

In an antisense array, an array with all possible oligonucleotides less than or equal to 27 base pairs is systematically constructed. Active sequences hybridise to the radio-labelled mRNA transcript which is then detected using phosphor imaging. Hybridising sequences are subsequently analysed for their ability to induce RNase H mediated cleavage of the mRNA transcript. Following antisense hybridisation, RNase H is added and the resulting fragments are sequenced to determine the sites of cleavage.

1.16 RNA Interference (RNAi)

Down-regulation of human gene expression is at best an arduous task. However, natural processes which govern gene expression through translational control have undergone an investigational revolution. Harnessing the cells innate to down-regulate mRNA opens the avenue for intensified and potentially prolonged reductions in specific protein translation. In 1998, Fire et al observed whilst experimenting with petunias that a delivered transgene, designed to accentuate their purple colour not only failed to be expressed but also suppressed expression of the endogenous gene, resulting in loss of colour and appearance of white patches in the flowers (Fire *et al,* 1998). This phenomenon was termed post-transcriptional gene silencing (PTGS) as it occurred following mRNA transcription. Research on the nematode *Caenorhabditis elegans* (*C elegans*), identified a related mRNA down-regulatory mechanism (Elbashir *et al,* 2001), this was termed RNA interference (RNAi). In both instances the trigger proved to be double stranded RNA (dsRNA), which exhibited complementarity to the gene of interest. In 2001, Tomas Tuschl demonstrated this phenomenon also occurred in cultured mammalian cells (Elbashir *et al,* 2001).

In mammalian cells, dsRNA sequences greater than 30 nucleotides trigger non-specific responses. An interferon pathway was shown to induce activation of a dsRNA dependent protein kinase (PKR) upon dsRNA binding. This kinase phosphorylates the α-sub-unit of the protein synthesis initiation factor e1f-2α, resulting in complete inhibition of protein synthesis (Leirdal *et al,* 2002). dsRNA also binds and activates the 2'5'-oligoadenylate synthetase leading to non specific mRNA degradation by RNase L (Der *et al,* 1997). This pathway occurs in response to the presence of low concentrations of long perfectly duplexed RNA molecules and hampers identification of the specific down-regulatory mechanism of RNAi. However, shorter RNA duplexes, small interfering RNA (siRNA) with 3' TT overhangs are capable of circumventing this PKR activation and promote efficient sequence specific gene silencing in mammalian cells.

RNAi is postulated to serve in a protective, anti-pathogen role, through prevention of the integration and translation of transposable elements, such as those of viral or bacterial origin (Czauderna *et al,* 2003). These and other pathogens generate dsRNA upon activation and replication and RNAi is considered an important defence mechanism in

lower organisms (Scherr *et al,* 2003). To maintain genome integrity, an evolutionary conserved system has developed to not only cleave the foreign dsRNA from the cellular milieu, but also to employ this to target the destruction of its homologous and hence likely pathogenic sister sequences. The ancient molecular defence mechanisms employed to carry out this function vary slightly among organisms. However, all are instigated by dsRNA of varying lengths, sharing common pathways and result in specific mRNA down-regulation.

1.17 Mechanism of dsRNA induced silencing

Upon dsRNA exposure, Boulcombe et al observed formation of discrete small RNA's complementary to the target of silencing (Hamilton *et al,* 1999). In *Drosophila* a multidomain RNase III enzyme, Dicer was shown to process long dsRNA, into duplex siRNA molecules 19-21 nucleotides in length. These short dsRNA molecules are the functional effector species, as they are capable of guiding efficient sequence specific mRNA degradation, molecules greater than 30 nucleotides are incapable of activity when added to *Drosophila* cell lysates (Boulta *et al,* 2001; Hutvagner *et al,* 2002). Dicer is unique among RNase III like enzymes to require ATP; this requirement is attributed to the ATP dependent RNA helicase domain at its amino terminus (Der *et al,* 1997). This helicase activity is necessary for duplex siRNA unwinding. As with other RNase III enzyme products, siRNA molecules contain a 5' phosphate and 3' hydroxyl termini and two single stranded residues at the 3' ends. Cells of C *elegans* nervous system are completely refractory to RNAi. This observation prompted the identification of conserved genes active at least in *C elegans* nervous system which negatively regulate RNAi by an siRNA degrading RNase, eri-1 (Kennedy *et al,* 2004). *C elegans* eri-1 encodes a protein with domains homologous to nucleic acid binding and exonuclease proteins and was identified in a screen for mutants with enhanced sensitivity to dsRNA's (Boulta *et al,* 2001).

Due to the interferon pathway and RNase L activation, long dsRNA delivery is unsuitable for mammalian systems. In *Drosophila* extracts synthetic short RNA's induced gene specific inhibition indicating the dsRNA-processing step and the targeting step can be uncoupled (Brantl *et al,* 2002). Following cytoplasmic delivery of these siRNA molecules into mammalian cells, they are recognised by an evolutionary conserved ribonucleoprotein

complex termed the RNA induced silencing complex (RISC). Recognition of this complex was presumed to be due to the presence of 3' overhangs. Following incorporation of the siRNA duplex, the high molecular weight RISC switches from a latent form into an active complex; this involves unwinding of the siRNA using a helicase and strand separation in an ATP-dependent manner. The RISC also contains a number of proteins, including nuclease components, which upon RISC activation are guided by the siRNA molecule to bind to and cleave specific mRNA sequences. The RISC utilises the unwound antisense strand to recognise the target mRNA via Watson-Crick type bonding, at which point cleavage occurs (Figure 1.12). Thus RNAi is considered an antisense mechanism of action, as ultimately binding of an antisense strand to an mRNA recruits cellular components to cleave the transcript. Endonucleolytic cleavage of the mRNA transcript by the re-modelled RISC occurs near the centre of the region spanned by the antisense siRNA strand (Figure 1.12). Further mRNA degradation occurs in an independent reaction by cellular exonuclease cleavage of the transcript (Holen *et al,* 2002).

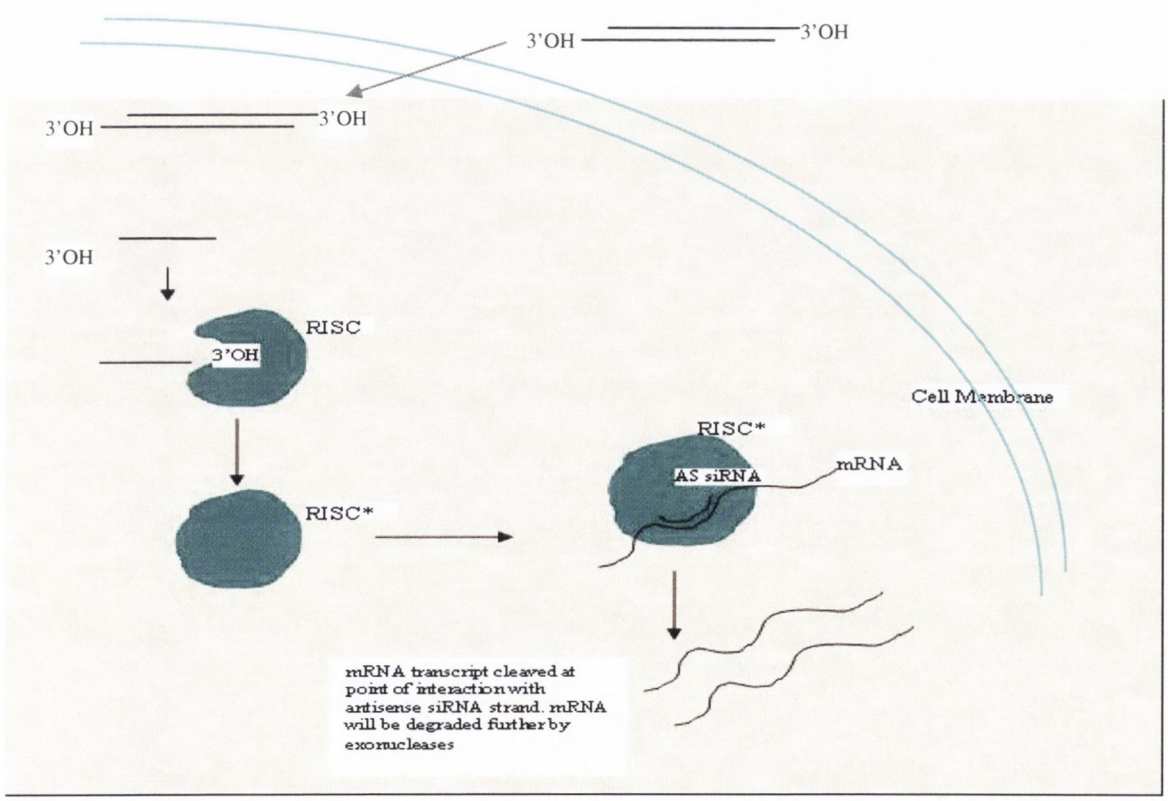


Figure 1.12 siRNA mediated gene silencing in mammalian systems mediated by the active RNA-induced Silencing Complex

The siRNA is recognised by the RISC and following binding the RISC switches to an active state (RISC). The RISC separates the two strands of the duplex in an ATP-dependent manner and uses the antisense strand to direct cleavage of complementary mRNA sequences*

1.18 Phosphorothioate versus RNAi

Several reports indicate siRNA mediated gene silencing to be superior to its RNase H dependent counterpart with respect to levels of mRNA destruction achieved, and concentration of molecule necessary to induce effects (Elbashir *et al,* 2001). However these studies fail to compare down-regulatory responses directly and use published figures as guides to concentrations employed. In 2003, Vickers et al performed a comparative study of optimised antisense oligonucleotides designed to work by RNA interference to oligonucleotides designed to function via RNase H dependent pathways. Molecules were evaluated for relative potency, efficacy, duration of action and sequence specificity. When employing molecules targeted to identical regions on the mRNA transcript, activity of both approaches was correlated to and hampered by the presence of mRNA secondary structure to similar degrees (Vickers *et al,* 2003). A second study targeting protein kinase C-α and GFP indicated similar constraints of target site selection and delivery governed the success of RNAi as a down-regulatory mechanism (Elbashir *et al,* 2001).

1.19 Amplification of RNAi and systemic silencing

An alternative system has been proposed for RNAi mechanisms in *C elegans* and related organisms, where amplification of siRNA effects and persistence of siRNA effects in progeny of treated animals are observed. In this model, following processing of dsRNA by Dicer into siRNA molecules, the siRNA bind their target mRNA via the antisense strand and serve as a primer for extension of the transcript into another long dsRNA molecule, which can re-enter the cycle at the point of cleavage by Dicer (Figure 1.13). SiRNA molecules bind in a 5'-3' orientation and nucleotides are added repetitively to the 3' hydroxyl group. Thus the mRNA molecule itself is then used to produce further siRNA molecules, and the effect is propagated and continued in this manner, ensuring continual supply of these specific siRNA and far enhanced and prolonged down-regulatory effects. The more target transcripts present, the greater the amplification effect induced.

This model is dependent on the activity of an RNA-dependent RNA polymerase (RdRP), and though this is present in *C elegans* and certain plants, no homologues have been identified in the *Drosophila* or Human genomes (Dalmay *et al,* 2000). Following cellular gene silencing by this method, the RNAi effect in *C elegans* is transferable not only from

one cell or tissue to another but also to their progeny, where the effects are prolonged. An RNAi deficient (sid/sid) locus required to transmit the effects of gene silencing between cells using GFP as a marker protein was identified (Winston *et al,* 2002). Sid mutants failed to show any readily detectable mutant phenotype other than failure to exhibit RNAi, and an inability to transfer the RNAi to their progeny. The sid -1 protein is postulated to be a 776 amino acid membrane protein containing a signal peptide and 11 putative transmembrane domains. Based on its structure, sid-1 was proposed to act as a channel for the import and export of systemic RNAi or may act as a receptor, functioning to endocytose the RNAi signal (Winston *et al,* 2002). Lack of systemic RNAi in *Drosophila melangoster* may be attributable to lack of any sid-1 homologues, however, homologues have been identified in humans and mice (Winston *et al,* 2002). Their relevance is unclear as to date no evidence of systemic RNAi has been observed.

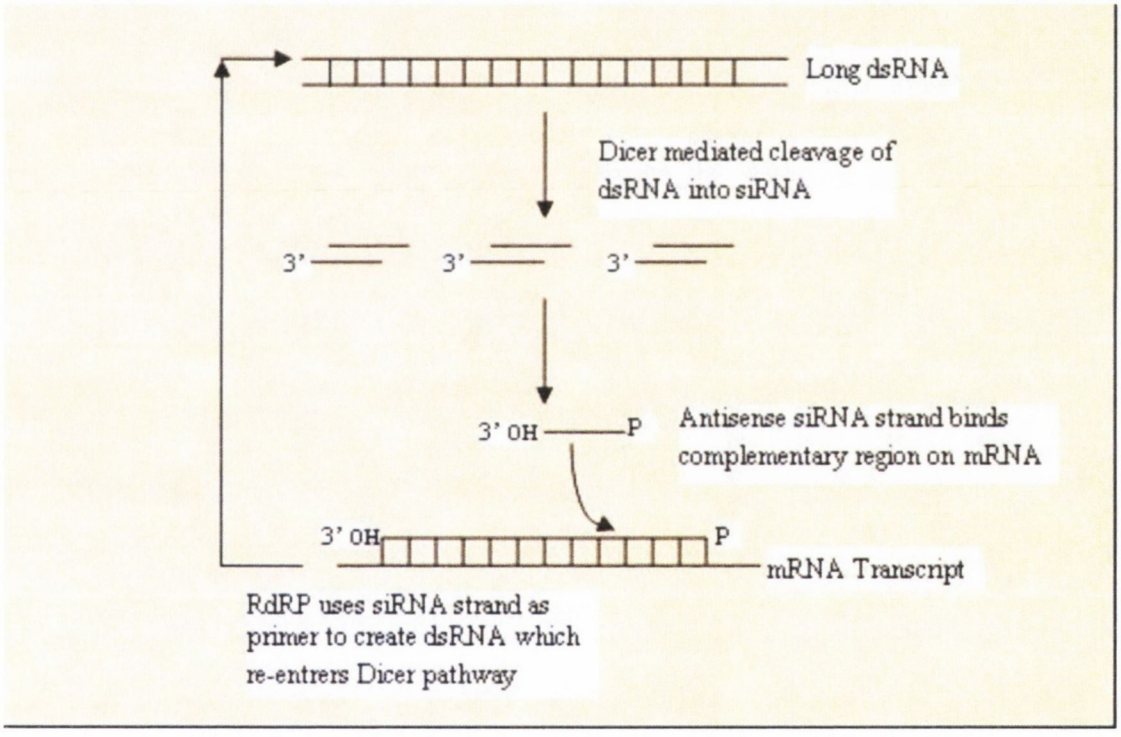


Figure 1.13 The Random Degradative PCR model for prolongation and persistence of RNAi mediated gene silencing.

1.20 siRNA design parameters for efficient RNAi induction

As outlined earlier, target accessibility of siRNA molecules mirrors that of their phosphorothioate counterparts (Vickers *et al,* 2003). However, functional siRNA must be designed to be of particular length, have a degree of overhang and employ suitable chemistries. SiRNA molecules with 3' TT overhangs similar to those naturally generated by Dicer were initially considered the most efficient triggers of siRNA mediated down-regulation (Elbashir *et al,* 2001, Schutze, 2004). However, extension of the overhang length inhibits RNAi; possibly due to ssRNA binding proteins which could associate at these points and interfere with the binding of dsRNA processing factors (Brantl *et al,* 2002). In contrast to observations made in *Drosophila,* no dependence on the presence of an overhang of siRNA duplexes was identified in the mammalian HeLa cell line as siRNA with 3' overhangs did not produce more efficient knock-down of target mRNA expression when compared to those with blunt ends or 5' overhangs (Leirdal *et al,* 2002). This may be related to the lack of Dicer related machinery in human cells and indicates that in these cells, the RISC complex has an alternative recognition system for siRNA molecules.

Length of the RNA duplex is a decisive factor for siRNA recognition by RISC complexes and hence RNAi activity. Optimal siRNA molecule length is species dependent. In mammalian cells, active siRNA molecules have an optimum minimum length of 19 duplexed nucleotides; this was independent of the nature of the 3' overhang (Czauderna *et al,* 2003). While 15nt duplexes did display activity in HeLa cells, it was drastically reduced relative to the 19nt form. Limited activity of a 15nt duplex indicates the length requirement for siRNA molecules in mammalian cells is related to incorporation of siRNA molecules into the RISC complex rather than to limited base pairing between the molecule and its target sequence. Duplexes of 25nt or more show little or no RNAi mediated activity, indicating there is also a maximum length requirement for RISC recognition of siRNA molecules.

Recent evidence supports the theory that antisense siRNA in single stranded form are capable of producing effects akin to those observed with dsRNA, and possibly act through a common pathway. Antisense siRNA is incorporated into the RISC complex in HeLa cell extracts and supports RISC-mediated target RNA cleavage, however, at a lower efficiency than that with the duplex siRNA (Holen *et al,* 2003). A study indicated single stranded

antisense and double stranded siRNA behave in a parallel fashion in regard to mRNA target positional effects, cleavage fragment formation and tolerance for chemical and mutational modifications. As with dsRNA, the antisense siRNA strand activity is inhibited by competition with excess inactive dsRNA, and the activity of both molecules is affected to mirroring degrees by gradual increasing levels of nucleotide methylation. Antisense siRNA has a lower efficiency than its corresponding ds siRNA, indicated by an increased IC50 value, this may be due to the lower intracellular stability of the former. Interestingly, maximum down-regulation induced by antisense siRNA strand occurred by approximately 10 hours and mRNA levels recovered gradually from this point. The delayed onset of double stranded siRNA effects compared to ss siRNA maybe a rate limiting step within the RISC complex, possibly involving unwinding of the RNA strands mediated by one of the putative helicases (Hutvagner *et al,* 2002). This suggests the possibility that the antisense siRNA enters the RNAi pathway at a later stage, closer to the effector nuclease than the ds siRNA.

1.20.1 siRNA modification and specific activity

As discussed earlier with regard to single stranded siRNA species, increasing methylation levels will inhibit RNAi activity (Hamilton *et al,* 1999). The introduction of limited 2'-O-methyl modified residues at selected locations is capable of efficiently inducing RNAi while increasing oligomer stability, however siRNA molecules consisting of one or both strands with 2'-O methyl residues are RNAi inactive (Leirdal *et al,* 2002). Duplex siRNA molecules containing an unmodified antisense strand and a completely modified sense strand were significantly more active than vice-versa, possibly highlighting the essential role the antisense strand plays in either RISC incorporation or in recognising the intended mRNA target. The most efficient modified siRNA molecules to induce mRNA knock-down had stretches of partial modification or were modified on alternating positions on both strands (Amarzguioui *et al,* 2003). This latter form of siRNA modification increased molecular stability significantly when incubated in the presence of serum and coupled with its RNAi activity, indicates alternating 2'-O methyl modified molecules have strong potential as agents of RNAi. 2'-O methyl oligoribonucleotides are well established for forming rapid and stable hybridisation to single stranded RNA and are frequently employed to protect nucleotides from degradation in cell extracts and cultured cells

(Meister *et al,* 2004). Due to their delicate chemistry modifications which stabilise siRNA duplexes may result in the progression of this field closer to clinical trials.

Similar to antisense oligonucleotides, siRNA duplexes should mediate efficient and specific reductions in target gene expression only. This sequence-related property of siRNA molecules is dependent on the minimum number of bases required to induce target cleavage by RISC endonucleases and not on its initial ability to induce RISC mediated cleavage. The incorporation of one or more mis-matches at the 5' hydroxyl of the antisense strand prevents the induction of RNAi, consistent with the important role this region of the molecule plays in RISC recognition and cleavage (Hohjoh *et al,* 2004). Contrastingly, 3' end overhang mis-matches not only retain complete RNAi activity, it has been postulated, based on preliminary evidence that these mis-matches can enhance RNAi activity (Kennedy *et al,* 2004). Though no potential mechanism has been demonstrated, these mis-matches may aid in RISC recognition or in molecular stability.

1.21 Induction of endogenous siRNA expression in mammals

RNAi induced by synthetic siRNA is transient, and in mammalian cell culture re-expression of the target mRNA occurs after a matter of days (Tuschl *et al,* 2002). This block in the utilisation of siRNA may be circumvented by the intracellular expression of short siRNA duplexes. This requires the expression of both the antisense and sense siRNA strands inside the cell, which may be achieved by one of two methods. Generation of siRNA molecules may be achieved using the U6 small nuclear (sn) RNA promoter, the sense and antisense strands are independently transcribed from separate U6 promoters and hybridise inside the cell to form the duplex siRNA with poly-U overhangs at the 3' ends (Scherr *et al,* 2003). The second method employs a single CMV-Pol III promoter system, normally a H1 RNA based Pol III expression cassette or a CMV promoter driven single hairpin RNA, that is subsequently processed to generate the active siRNA with a poly-U stretch (4) at its 3' end (Xia *et al,* 2002; Shen *et al,* 2003).

Viral vectors are routinely employed to transduce target cells with the desired form of siRNA expressing insert. Retroviral and adenoviral vectors have been successfully employed to mediate transcription of siRNA duplexes in mammalian cells using both the U6 sn and the Pol III H1 RNA promoters respectively (Gupta *et al,* 2004; Vickers *et al,*

2003). Intracellular siRNA expression has been demonstrated to induce gene down-regulation for a number of targets including Nuclear Dbf2-Related (NDR) kinase and p53 (Devroe *et al,* 2002; Dalmay *et al,* 2000). Lentiviral vectors have also been employed for siRNA gene knock-down in mouse models where complete inhibition of transduced GFP constructs was achieved (Tiscornia *et al,* 2003). However, a rate limiting step of endogenous siRNA expression is related to low transfection efficiencies, particularly of the high molecular weight expression vectors, when compared to the relative ease of delivery of small RNA molecules (Wilson *et al,* 2003). siRNA molecules face similar obstacles to their antisense counterparts such as the cell membrane barrier and *in vivo* stability. Like phosphorothioate, siRNA molecules are polyanions and present similar delivery issues (Muratovska et al, 2004). Soaking *C elegans* in RNAi solution is sufficient to induce 'heritable' RNAi, in mammals a more complicated system needs to be developed. Systemic delivery via intravenous injection of siRNA using a cationic lipid (N-(1-(2,3-dioleoyloxy) propyl)-N, N, N-trimethyl ammonium chloride has been demonstrated to deliver active molecule to all organs in animal models (Scheiffelers *et al,* 2004).

1.22 Clinical applications of antisense oligonucleotides

The value of antisense in haematological disorders has been investigated principally in the context of *ex vivo* purging of bone marrow cells. Streptolysin-O (SL-O) is unsuitable for application *in vivo* due to its inactivation by cholesterol and loss of its regulation. However, its high rate of efficient delivery coupled with reversible permeabilisation makes it a suitable candidate for delivery of antisense molecules to CML cells in *ex vivo* purging procedures for autologous BMT (ABMT) (Section 1.9). This approach has been undertaken with a degree of success using a small population of Philadelphia chromosome positive patients (Giles, 2001). Pre-clinical SL-O studies in CML patient harvests indicated it could be safely used to enhance intra-cellular uptake of antisense molecules (Broughton *et al,* 1997). In clinical studies chimeric phosphodiester : methylphosphonate molecules delivered by SL-O reduced bcr-abl levels in a b2a2 positive though not in a b3a2 positive patient (Clark, 1999). However, protein levels were unaffected possibly due to the sustained half-life of the BCR-ABL protein. Expansion and honing of these initial positive results may be accomplished through further backbone manipulation.

In a separate study, autografts from eight patients in the advanced phase of CML were treated *ex vivo* with break-point specific phosphorothioate anti-bcr-abl antisense oligonucleotides. The eight patients selected for the study were chosen based on their *ex vivo* response to growth inhibition induced by antisense oligonucleotides. Purging was performed for either 24 or 72 hours, in all cases in the absence of delivery agents. Re-infusion of autografts was carried out following conditioning with busulphan and etoposide. All patients showed haematological reconstitution and two had a karyotypic response, however this did not correlate with a better clinical outcome (de Fabritiis *et al,* 1998). Of the eight patients; one treated in second chronic phase died seven months following ABMT: three patients died in blast crisis 21-39 months following ABMT; one patient died of unrelated BMT complications and three patients were in persistent chronic phase 14-26 months following ABMT. This study demonstrated the potential of antisense molecules to aid in the treatment of patients in advanced phase CML and significantly indicated that antisense oligonucleotides were non-toxic to haematological stem cell populations. Examples of antisense molecules involved in clinical trials are given in Table 1.2.

A number of antisense molecules mainly phosphorothioate-based and phosphorothioate-containing oligonucleotides have entered into large scale clinical trials in a number of diseases. The most prominent of these is the bcl-2-directed phosphorothioate molecule; Genasense. The successful advancement of this molecule through clinical trials in late stage disease of several cancers indicates potential for down-regulation of oncogenic gene expression. However, the lack of approval by FDA and European regulators for Genasense and other phosphorothioate based antisense molecules indicates that several parameters in their implementation remain to be optimised. These trials will be detailed in Chapter 9.

Table 1.2 Examples of antisense molecules involved in clinical trials

Antisense drug	Disease related target	Disease / disorder	Antisense chemistry	Progress
Vitravene	CMV IE2 protein	CMV-induced retinitis in AIDS patients	Phosphorothioate	Approved
Genasense	bcl-2	Wide range of malignancies including melanoma, multiple myeloma and non-small cell lung carcinoma	Phosphorothioate	Phase III clinical trials
Affinitak	Protein kinase C-alpha	non-small cell lung carcinoma, solid tumours	Phosphorothioate	Phase III clinical trials
GEM 231	Protein kinase A-receptor 1- alpha	Solid tumours	Mixed backbone phosphorothioate molecule RNA/DNA composition and four 2'-0-methyl modified bases at 3' & 5' ends	Phase I-II clinical trials
AVI-4557	Cytochrome p450	Drug resistance	Morpholino	Phase I-II clinical trials

II

Materials and Methods

2.1 Selection of optimal mRNA sites for targeting with nucleic acid molecules

Accurate prediction or calculation of mRNA secondary structure is a useful tool to identify suitable regions on the transcript for nucleic acid targeting. Deducing the most likely secondary structure becomes increasingly complex and less accurate with increasing molecule size. This is due to the possibility of subtle variability in potential secondary structures. A number of conflicting theories by which mRNA secondary structures may form are presented as outlined in the Introduction (1.15.2). The only definitive method of determining if sequences are single stranded for antisense purposes is by RNase H mapping (Sohail *et al,* 2000-b). However, this approach requires a large amount of ODN and this was outside the scope of this project.

For secondary structure prediction of mRNA transcripts targeted in this study the web server based statistical software packages; *mfold* and *sfold*, were employed which determine mRNA secondary structures based on thermodynamic principles of nucleic acid interaction and stability. The abbreviated name 'mfold web server' describes a number of closely related software applications which employ algorithms to efficiently predict RNA folding structures dependent on individual sequence alignment (Zuker, 2003). This server is provided on line via a Graphical User Interface (GUI) which circumvents the problem of portability of the software at http://www.bioinfo.edu.rpi/applications/mfold. The *mfold* server operates on a cluster of 36 dual processor 'Intel / Linux' workstations, and comprises a number of separate applications that predict nucleic acid folding and hybridisation, these encompass the *sfold* module.

2.1.1 Parameters for Sequence Input

The default RNA folding form currently uses the latest version 3.1 free energies, which are recommended for most RNA folding. To enter a sequence into *mfold* for folding, a name was first provided for the sequence, if none was given the programme formulated a name based on the exact time and date the sequence was entered. The nucleotide sequence was entered into a 'sequence text area box' where all T's (T's & t's) were converted to U for RNA folding and vice versa for folding DNA. At this point, sequence folding constraints were entered which dictate to the application whether bases were involved in singular or

helical base pairing or were to remain unpaired. Consecutive bases may be forced or prohibited from binding to one another. Using *mfold* 3.1, the nucleic acid sequence may be defined as linear or circular, though the algorithm to fold circular nucleic acids is simpler than that for folding linear nucleic acids. Using the 3.1 software version, the temperature for RNA folding was fixed at 37^0C. However the earlier 2.3 version facilitated folding of RNA at temperatures other than 37^0C and as with DNA can be adjusted to any integral temperature between 0 and 100^0C. The ionic conditions remained fixed at 1M NaCl and $\leq$0.1M Mg^{2+} for RNA folding; these are equivalent to physiological conditions. The percent suboptimality, P, controls the free energy increment ($\delta\delta$G) for displaying base pairs in the energy dot plot and for computing suboptimal foldings. P dictates the number of sub-optimal foldings which will be calculated and displayed, the greater its value the more possible, though suboptimal, interactions will be considered. An upper, absolute limit is applied to the maximum number of foldings permitted, though the actual number of foldings may be considerably lower. The number of permitted computed foldings is controlled by the window parameter, W. This may be considered a distance parameter, where W is the number of bases involved in the interaction, and is at least this number of bases apart from previously computed foldings.

2.1.2 Output Parameters

The output files represent the calculated secondary structures using *jpeg* and *png* documents. These files may be scaled up without loss of quality as the 72 X 72 pixels per square inch resolution remains constant. Bases were numbered according to the length of the sequence, and the frequency of numbering decreased with increased length, from every 10 bases with less than 50 bases to every 50 bases for sequences with greater than 300 base pairs. An energy dot plot which relates the energy of each base to potential interaction candidate bases is also available in text and graphical format. This facilitates analysis of bases individually.

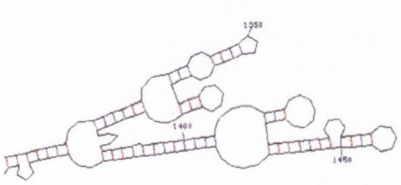


Figure 2.1 mRNA sequence output structure determined using *mfold* web server
The presence of single stranded & double stranded loops and fork-like formations in mRNA secondary structures can be deduced

2.2 Culture of CML Cell Lines

To establish the efficacy of antisense molecules under investigation, cell lines expressing the Philadelphia Chromosome, with either the b2a2 or b3a2 transcipts were employed. These included the Philadelphia Chromosome (Ph) positive BV173, KYO-1, K562, KCL-22 and LAMA-84, along with a control Philadelphia Chromosome negative cell line, HL-60. BV173 KCL-22 and KYO-1 are derived from patients who express the b2a2 translocation, while K562 and LAMA-84 are derived from patients with the b3a2 mRNA version. The main features of these suspension cell lines are outlined in Table 2.1. These cell lines were received as a gift from the Hammersmith Hospital, London.

Table 2.1 Details of CML suspension cell lines employed in this study

Cell Line	*Transcript*	*Origin*	*Cell Type*	*Doubling Time*
K562	b3a2	53 year old female	Erythroid / lymphoblast	26-30 HOURS
LAMA-84	b3a2	29 year old female with CML	Myeloid	~50 HOURS
BV173	b2a2	45 year old male with CML in blast crisis	Lymphoid	48 HOURS
KYO-1	b2a2	Unavailable	Myeloid	20 HOURS
KCL-22	b2a2	32 year old woman with Philadelphia Chromosome positive CML in blast crisis	Lymphoid	~24 HOURS
HL-60	-	35 year old woman with AML in 1975	Myeloid	~25 HOURS

2.2.1 Maintaining cell lines

Cell lines were maintained at 37^0C, 5% CO_2 in RPMI 1640 Glutamax [GIBCO]. FCS and penicillin-streptomycin supplemented the medium and were added by sterile filtering into the solution to give final concentrations of 10% and 1% respectively. PCR based Mycoplasma testing was performed at 6 month intervals to ensure cells were free of these micro-organisms which can strongly affect results of cell culture experiments. Testing was performed using the Mycoplasma PCR ELISA kit from Boehringer Mannheim (# 1 663 925). Cells were maintained at a concentration of 1 X 10^7 - 5 X 10^7 cells per flask in RPMI medium and split 1:2-1:5 depending on confluency.

Freezing Cells

To maintain stocks of cell lines, cells of a confluent flask (>3.0X10^7) were spun down at 1400 rpm for 5minutes. The pellet was re-suspended in 1 part complete medium (10%FCS), followed by the slow addition of 1 part freezing medium (40% DMSO, 40% FCS) whilst mixing over ice. Cells were stored at -80^0C immediately following freezing, and removed to liquid nitrogen (–196^0C) for long-term storage.

Resuscitating Cells

To retrieve cells stored in liquid nitrogen, a vial of frozen cells was removed from the cryovat and placed on ice. Cells were incubated at room temperature for 1 minute and then transferred to a 37^0C water bath until fully thawed. Using a 1ml pipette, cells were aseptically transferred to 10mls of complete medium. It was important to minimise the length of time cells spent in DMSO following thawing, as it is toxic and would reduce cell viability. Cells were centrifuged (Centra GP8 Thermo IEC) at 1400rpm, 5 minutes to remove DMSO, this was repeated once and the second pellet was resuspended in 10mls of warmed, gassed culture media and transferred to the 37^0C incubator.

Cell Counting

When doing a cell count it is recommended to use at least 1% of the total volume of the cells, therefore 200µl is diluted for counting a 20ml flask. 200µl of cells was added to 400µl of ethidium bromide-acridine orange and mixed well. 8µl of this solution was used to fill the chambers of a clean dry haemocytometer with a cover-slip on. Using this dye, viable cells appear green and dead cells orange under the fluorescent microscope.

2.3 cDNA Preparation

2.3.1 TRIzol Method-Overview

Extraction and isolation of total RNA from cells was performed using the commercial reagent TRIzol (GIBCO #15596). This is a mono-phasic solution of phenol and isothiocyanate, and is an improvement to the single step RNA isolation method developed by Chomcynski and Sacchi (Chomczynski *et al,* 1987). During the initial cell lysis or homogenisation step, TRIzol disrupts cell membranes and dissolves cellular components, while stabilising the integrity of the RNA. Addition of chloroform followed by centrifugation separates the heterogeneous solution into its aqueous and organic components, the RNA remains exclusively in the upper, clear, aqueous phase. This is transferred to a fresh tube and the RNA is precipitated by the addition of isopropyl alcohol. Following removal of the aqueous phase, DNA and protein may be precipitated from the interphase and organic phases respectively using alternative protocols.
TRIzol is stored at 2-8^{0}C for optimal performance, however it remains stable if stored at room temperature for up to 1 year. It is a highly versatile reagent and can be applied to extract RNA, DNA and protein from small numbers of cells (5 X 10^6) and tissue (50-100mg) and large quantities of cells(>10^7) and tissue(≥1mg). The reagent is suitable for processing of a large number of samples and may be completed in 1 hour. RNA extracted by this method is free from DNA and protein and is suitable for use in applications such as PCR, RNase protection, and *in vitro* translation. For PCR applications, DNase treatment is recommended when the primers do not span two exons.

2.3.2 RNA extraction using TRIzol

Routinely 5 X 10^6 cells were extracted; these were counted and pelleted at 1,400rpm for 5 minutes (Centra GP8 Thermo IEC). This cell number requires the addition of 1ml of TRIzol reagent, however, with decreasing or increasing cell number the volume was adjusted accordingly. This also applies to each of the reagents added subsequently; their volume was adjusted to retain the same ratio with the amount of TRIzol reagent. After thorough homogenisation of sample, cells were incubated with TRIzol reagent at room temperature for 5 minutes to ensure dissociation of nucleoprotein complexes. 200µl of chloroform per ml of TRIzol was added; tubes were then shaken vigorously for 10-15

seconds and allowed to incubate at room temperature for 3 minutes. Phase separation was induced by centrifugation at 12,000g, 4^0C for 5 minutes (Microlite RF Thermo IEC). The resulting aqueous phase was transferred to a fresh tube and the RNA was precipitated by addition of 0.5mls of isopropyl alcohol per ml of TRIzol originally added to the sample. Samples were incubated for 10 minutes at room temperature, followed by centrifugation at ≤12,000g, 5 minutes, 4^0C as before. Following centrifugation, the RNA formed a small, if not invisible, gel like pellet at the side and bottom of the tube.

This RNA pellet was washed in at least 1ml of 75% ethanol per ml of TRIzol originally used to remove impurities and centrifuged gently. Before re-dissolving, the RNA pellet was allowed to air dry gently for 5-10 minutes, over-drying was avoided as this greatly decreases its solubility. The RNA pellet was dissolved in 87µl of RNase free H_2O and this was facilitated by incubation at 55-60^0C for 10 minutes. After removal of the aqueous phase, DNA and protein may be isolated by further precipitation of the organic phase and interface. Precipitation with 100% ethanol yields DNA from the interphase.

2.3.3 DNase treatment of isolated RNA

TRIzol extraction yields RNA that is DNA free, however if the RNA is to be used in enzymatic reactions where the primers do not span two exons, DNase treatment is recommended. Treatment was carried out with RNase-free DNase from Roche [908746]. 87µl of RNA, 3µl of DNase (10U/µl) and 10µl of 10X DNase buffer were combined and incubated at 37^0C for 30 minutes. Following the incubation period, an equal volume (100µl) of phenol/ chloroform/ isoamylalcohol was added to remove cleaved DNA fragments and samples were spun at 12,000rpm for 5 minutes. The upper phase containing the RNA was transferred to a fresh RNase free 1.5ml tube. RNA was precipitated by the addition of 11µl of LiCl (1M) solution and 250µl of 100% ethanol followed by incubation at -80^0C for ≥20minutes. RNA was recovered by centrifugation at 12,000rpm for 5 minutes and the pellet was washed in 70% ethanol. The RNA pellet was air-dried for 5 minutes with particular care to ensure over-drying did not occur, and resuspended in 30µl of RNase free water. Dissolving was facilitated by incubation at 55^0C for 10 minutes, and the RNA was stored at -80^0C.

2.3.4 RNA Analysis

The quality of extracted RNA was inspected via spectrophotometrical analysis using A_{260} & A_{280} values. This allows estimation of RNA yield and levels of DNA contamination, pure RNA samples have A_{260} / A_{280} ratios of 1.8-2.0. RNA quality was visualised using 2% agarose electrophoresis.

2.3.5 Synthesis of cDNA from RNA template

The DNase-treated RNA served as a template to synthesise the corresponding complementary DNA (cDNA) using a reverse transcriptase enzyme derived from Mouse mammary leukaemia virus (MMLV). This was then employed in Real Time (RT)-PCR reactions to quantify the amount of mRNA present in the original samples. Reverse transcription is carried out in a 30µl reaction as outlined in Table 2.2.

Table 2.2 Components of a cDNA synthesis reaction

COMPONENT	CONCENTRATION	REACTION VOLUME	FINAL CONCENTRATION
5X 1st Strand Buffer (GIBCO-BRL)	5X	6µl	1X
Random Hexamer (Roche)	100µM	2µl	6.5µM
dNTP's (Promega)	4mM	1.5µl	200µM
DTT (GIBCO-BRL)	0.1mM	3.0µl	10mM
DMSO (Sigma)	100%	4.5µl	15%
MMLV-RT (GIBCO-BRL)	200U/µl	1.25µl	250U
RNasin (Promega)	40U/µl	0.6µl	24U
H_2O		5.25	
RNA		6µl	

Synthesis of cDNA was performed by incubation of RNA with the above components at 37^{0}C for one hour followed by storage at -80^{0}C.

2.4 Saponin Experiments

The first permeabilisation agent tested to induce antisense cell entry was saponin, which is commonly employed for intracellular antibody staining in flow cytometry techniques. Two forms of saponin were tested using two permeabilisation protocols; these compounds differed only in their method of purification of saponin. The second protocol uses a more highly refined saponin, which has undergone further purification.

2.4.1 Saponin Permeabilisation Method 1

Cells were seeded at a concentration of 2.5 X 10^4 and 2.5 X 10^5 per well, 24 hours prior to treatment and allowed to grow overnight. Saponin (Sigma S-7900, from Quillaja Bark) was prepared by dissolving in PBS at room temperature followed by sterile filtering.

Cells were incubated in 24 well plates with increasing concentrations of saponin, 0.005%, 0.01% 0.025%, 0.05%, 0.1%, for 24 and 48 hours at 37°C, with 1μM and 10μM antisense oligonucleotide.

Following treatment, the cells were spun down onto cytospin slides, and were examined for changes in morphology and uptake of fluorescent oligonucleotide.

2.4.2 Saponin Permeabilisation Method 11

Due to the similarities in the pore forming mechanisms between Streptolysin-O and saponin, in that both function by binding to cholesterol, a similar procedure for permeabilisation was sought. Though the two agents employ distinct mechanisms, the involvement of cholesterol in both suggested the possibility that removal of FCS may increase the activity and effectiveness of saponin. The protocol was developed from one used for intracellular staining for flow cytometry, which involved fixing the cells with sodium azide. This is unsuitable for our purposes as we require viable cells after the permeabilisation step. Therefore efforts were made to optimise the protocol, without including the sodium azide step. Intracellular distribution, extracellular binding and toxic effects were significant factors relating to the success of the saponin approach, and the vehicle used to dissolve the permeabilisation agent may also affect these approaches. For these set of experiments a more refined form of saponin (Sigma S-4521) was used, which was purified to remove low molecular weight contaminants.

5 X 10^6 cells were used per treatment and these were washed at least three times with FCS-free medium, each pellet was rinsed thoroughly to ensure removal of any cholesterol bound to the cells. To compare the effectiveness of the procedure using only BSA and PBS as vehicles for saponin, substituting the sodium azide, the following experiments were set up with various diluents for the saponin.

Cells were incubated with saponin in (a) PBS
(b) PBS (0.5%BSA) and
(c) PBS/BSA/NaAz (0.1%)

at 37°C for 30 minutes with 10μM FAM labelled antisense oligonucleotide.

Unlike SL-O treatment, where cells require FCS to recover, the pore forming abilities of saponin diminish gradually. However, addition of FCS rapidly terminated the reaction and aided cell recovery. In some instances cells treated with 0.01% saponin were permeabilised twice to increase levels of delivery. Following the initial 30-minute incubation, cells were spun down and resuspended in a fresh saponin medium as outlined above. After the desired period of permeabilisation had elapsed, the cells were resuspended in complete medium containing FCS.

2.5 Streptolysin-O cell permeabilisation

A second permeabilisation agent; streptolysin-O (SL-O) was assessed for its suitability for antisense delivery into CML cells. SL-O requires treatment with the disulphide bond reducing agent DTT for activity. Each batch of SL-O was tested following activation and prior to antisense treatment to determine the volume which induces optimum delivery.

2.5.1 Thiol-activation of *Streptococcus pyogenes* Streptolysin-O

Using a 3 ml syringe, 25,000U of SL-O (Sigma S-5265) was reconstituted in its vial by the addition of 2 ml PBS/BSA (0.05%), and mixed gently by swirling to avoid foaming.
Contents of the vial were transferred to a sterile 50 ml Starstedt tube. This washing step was repeated three times with 1ml PBS/BSA (0.05%), and washings were added to a 25 ml universal. Washing with 1X PBS was repeated 2-3 more times and transferred to the universal.

The SL-O solution was made up to 25 ml with PBS to give a final BSA concentration of 0.01%; this is 1000U/ml (1U/1µl) SL-O. 1M sterile DTT was added to a final concentration of 5mM. Mixing was carried out by inversion with caution to ensure no foaming. Streptolysin-O was activated by incubation at 37^0C for 2 hours. SL-O solution was placed on ice and a permeabilisation experiment (below) was performed to determine activity of individual vials, as high variability is reported. If the SL-O showed sufficient activity, 500µl/1ml was aliquoted per tube and stored at -20^0C. Once reconstituted, Streptolysin-O was not filter sterilised or autoclaved as this abolishes activity and it was stored in aliquots at -20^0C.

2.5.2 Permeabilisation of CML suspension Cell Lines with Streptolysin-O

Overview of SL-O Permeabilisation

The concentration of SL-O required for optimal permeabilisation is cell line dependent, and was optimised for each batch of the active compound. Slight day-to-day variations in activity occur; these can be counteracted by carrying out a test run at the beginning of the day to determine the concentration necessary to give optimal uptake. This is the concentration of SL-O required to give the highest percentage of uptake, whilst maintaining toxicity levels below 5%.

SL-O Permeabilisation Procedure

For the permeabilisation procedure, the cell number has been optimised as between $4X10^6$ and $6X10^6$, due to the toxic and highly active nature of SL-O molecules. $5X10^6$ cells were routinely used per treatment. Cells were pooled and washed twice with FCS-free medium to thoroughly remove all traces of cholesterol bound to the cell surface. SL-O is uniquely sensitive to the presence of cholesterol in the cell medium, as it binds to the molecule and inhibits its activity. Following washing, the supernatant was removed and the cells were resuspended in 300µl of RPMI (No FCS). The volume the cells were present in was accurately measured by increasing the volume on the pipette until it holds all the solution, the cells were then diluted to give an exact concentration of $5X10^6$ cells/200µl.

Permeabilisation was performed in a 24 well plate; fluorescently labelled phosphorothioate oligonucleotide was added to give a final concentration of 10µM in 400µl. Streptolysin-O was added to give the desired number of SL-O units per $5X10^6$ cells. At this stage of the procedure the cells were extremely sensitive and were handled with care. Permeabilisation was carried out at 37°C, 5% CO_2 for 10 minutes. Mixing at regular intervals during the permeabilisation was crucial to ensure certain populations of cells did not become over permeabilised and hence die; and that all cells were permeabilised sufficiently. Mixing of wells was performed at 2 minute intervals during the permeabilisation period by swirling the plate clock-wise and anti-clock-wise. After the permeabilisation step, 1ml of RPMI +FCS was immediately added to each well to terminate the reaction. The cells were returned to 37°C for 10 minutes to allow the cells to recover and were then transferred to flasks containing 9mls of gassed medium at 37°C for the duration of their treatment.

2.6 Visualisation of FAM Antisense Uptake and Toxicity levels using Fluorescent Microscope Analysis

Delivery of fluorescently labelled molecules and determination of cell toxicity levels was initially examined using the fluorescent microscope. Using the fluorescent microscope allowed the examination of the condition of cells following permeabilisation, levels of cell debris and intracellular localisation. Subsequently the flow cytometer was used which allowed more efficient determination of delivery and toxicity with a higher throughput.

Antisense molecules with disparate chemistries display distinct patterns of intracellular localisation. Specific sub-cellular positioning is essential for all antisense molecules, but the desired localisation varies with backbone chemistry employed and its mode of down-regulation. Therefore the fluorescent microscope was an invaluable tool for investigating all these aspects of antisense delivery inside the cell. The investigation of nuclear localisation using Hoechst dye staining was assessed using the fluorescent microscope using 2 of its filter layers that detect the emission of blue and green light.

Analysis of cellular uptake for both *in situ* and cytospin prepared samples was performed using an inverted Nikon TE 300 fluorescent microscope. The excitation light for fluorescent layers was provided by narrow band filters. The excitation filter for Hoescht imaging was at 461nm, the FAM detection filter was at 520nm and the propidium iodide (PI) detection filter at 596nm. White light and fluorescent images were captured using the Leica DC 100 digital camera and were saved and analysed using the Adobe Photoshop 5.0 software which facilitates cell counting using grids, and over lapping of fluorescent microscope filter layers to compare exact cellular locations.

At least 300 cells were counted following each treatment when assessing levels of uptake and toxicity. The number of green (+FAM) and red (+PI) cells were expressed as a percentage of the total cells counted. In some instances, red cells and green cells would overlap, as dead cells (+debris) were observed to bind the oligonucleotide very readily.

2.7 Flow Cytometry Analysis

To increase both the accuracy of the procedure and the number of cells analysed, flow cytometry was employed as a fast and accurate method of detecting both the levels of uptake and toxicity. The fluorescently labelled antisense oligonucleotide can be detected on the FL-1 channel, while necrotic; PI positive cells are detected by the FL-2 channel.

2.7.1 Preparation of cells for Flow Cytometry Analysis

Cells that have taken up the FAM-labelled antisense oligonucleotide will be detected on the FL-1 channel which detects signals in the 500-560nm range. In order to identify dead cells using the flow cytometer, Propidium Iodide (PI) was used to stain cells whose membranes have been irreversibly compromised and are hence non-viable. This signal is then detectable on the FL-2 channel which detects signals in the 560-578nm range. 1000µl of the cell suspension (~5 X 10^5 cells) from each flask was analysed. Cells were incubated on ice for 5 minutes in a 2ml Eppendorf tube, before staining for 5 minutes with propidium iodide (1µg/ml). Staining was carried out on ice to minimise endocytosis of PI by cells, which could produce false negative results. Cells were pelleted at 2000rpm for 5 minutes, and washed 3 times with PBS to ensure complete removal of stain bound to the cell exterior, as the flow cytometer is very sensitive to residual PI. 600µl of Becton Dickinson CellFix solution [BD340181] (1/10 dilution with H_2O) was used to resuspend cells for analysis, and the solution transferred to flow cytometry tubes (Falcon 352052), for flow cytometry analysis. If necessary, tubes were stored overnight at 4^0C in the dark before running on the flow cytometer.

2.7.2 Flow cytometry Analysis

The Becton Dickinson (BD) FACSort flow cytometer was used for analysing the cells which have been prepared as above. The voltage and compensation levels for each cell line was optimised by staining with FITC (FAM) and PE (PI) labelled antibodies, which the cell line is documented to express. This allows the number of cells which contain FAM labelled oligonucleotide, and PI labelled dead cells to be identified.

The parameters were set to give even reporting of the fluorescent signal in the positive channels, and the compensation set so that other signals were entirely negative to ensure no overlap and prevent reporting of false positives. Isotype controls were used to ensure any non-specific binding due to antibody isotype did not occur. Samples were processed and analysed using the CellQuest programme. Settings for the individual cell lines were set and untreated cells were first analysed to check levels were below positive threshold. Cells were scattered and a cell population was selected from the scattered cells. The output of these cells in relation to their FL-1 and FL-2 was examined. A quadrant was drawn to enclose the negative and positive areas as shown in Table 2.3.

Table 2.3 Sub-groups of cells in the four quadrants of the flow cytometry grid following selection of cell population.

Quadrant	**FL-1**	**FL-2**	**Cells**
Lower Left	Negative	Negative	Viable, FAM negative
Lower Right	Positive	Negative	Viable, Taken up FAM oligo
Upper Left	Negative	Positive	Dead cells, no FAM oligo
Upper Right	Positive	Positive	Dead cells, FAM oligo uptake

The co-ordinates for this grid were usually set at 10,10[1]. Negative samples will be below this threshold on the X and Y-axes, whereas positive samples will be above it on one or both axes. During the analysis step, the statistics of each quadrant were displayed and used to assess the percentage of cells in each quadrant; representing the four different states the cells may be in (as above). Quantification of cell populations was also carried out using the histogram plot bar option which relates intensity of signals individually. A significant shift in signal intensity indicates uptake or cell damage.

[1] When appropriate this was increased marginally to ensure negative samples weren't included in the positive selection.

2.8 Treatment of Cell Lines with Antisense Molecules

Antisense treatments were performed on various CML cell lines to assess the effect of the selected antisense molecules on the expression of their target mRNA. The period of mRNA down-regulation depends largely on the half-life of the molecule, and the duration of the effect will depend on the stability of the antisense molecule used.

2.8.1 Experimental format for antisense treatments

Streptolysin-O was used as the uptake agent in the antisense experiments. Cells were treated with various antisense molecules and the levels of uptake and toxicity were assessed. Time course experiments were performed where the cells were left for periods of 0-24, 48, 96, 120 and 144 hours. Cell viability was examined regularly for necrotic rather than apoptotic type death. Cells were fed every 48 hours, and this involved removal of media containing the antisense molecules. However, a large proportion of the molecule would have already been taken up during permeabilisation, and as the phosphorothioate has a half life of approximately 72 hours; its loss from the medium would be of little significance. Treatments were performed in a cell culture 24 well plate format and set-up as outlined in Table 2.4.

Table 2.4 Plate layout for SL-O mediated Antisense Treatment of CML cell lines

Component	**Stock Conc.**	**Volume added**	**Final**
Cells	2.5 X 10^7 /ml	200µl	5 X 10^6
Streptolysin-O	1U/µl	60µl	12U/1 X 10^6 cells
Antisense Oligo	200µM	20µl	10µM
PBS		120µl	
Total		400µl	

Cells were prepared for SL-O permeabilisation as detailed in the SL-O section. Following delivery of the antisense oligonucleotide, cells were removed to flasks and incubated at 37°C for the duration of the treatment. When the time period was completed, RNA and/or protein were harvested as detailed earlier.

2.8.2 Nuclear staining of CML cell lines using Hoechst dye

In order to identify the intracellular localisation of the antisense molecule following delivery with saponin and streptolysin-O, the nuclei of cells were specifically stained with the Hoechst dye, which intercalates with the DNA. Hoechst is a toxic carcinogenic irritant, so extreme caution was employed whilst handling.

Procedure for Hoechst Staining

Initially, the Hoechst stain was performed on cytospins. 2 X 10^5 cells were spun down, re-hydrated by dipping in PBS and stained in the dark for 10 minutes with Hoechst dye (250µg/ml). Slides were stored in a dark box at 4°C for subsequent microscopical analysis. Cellular localisation using Hoechst staining was also viewed in cells *in situ.* Following delivery of FAM labelled antisense molecules; a 200µl aliquot of cells was taken from the 10ml flasks. Cells were stained with 20µl of Hoechst stain (250µg/ml), and incubated at 37°C for 20 minutes in the darkness. Following staining, the cells were spun down at 2,000rpm for 5 minutes, washed once and resuspended in 200µl of PBS or 200µl of Cellfix (Becton Dickinson Cat no. 340181) solution (1/10 with H_2O) for microscope analysis.

2.8.3 Analysis of FAM-labelled antisense uptake and permeabilisation associated toxicity using Microscope Analysis

Following permeabilisation of CML cell lines with both saponin and streptolysin-O, the levels of FAM labelled phosphorothioate antisense uptake and effects on cell viability were assessed. Initially cells were examined on cytospin slides, which was simple and convenient as slides could be stored and examined a later stage. However, examining cells *in situ* gives a better overall idea of the cells condition as they are viewed immediately and while the cells are in their native state. Cytospins were also observed to have a 'mashing' effect on the cells. However, cytospins have the advantage that they can be retained for 4-5 months at 4^0C, allowing direct comparisons to be made with different antisense treatment protocols.

Cytospin Analysis of uptake and toxicity levels

500µl ($2.5X10^5$) of the cell culture was taken from the 10ml flasks shortly following permeabilisation and placed on ice for 5 minutes. Cells were stained with propidium iodide (10µg/ml) and left on ice for a further 5 minutes, followed by spinning at 2000rpm for 5 minutes. Cells were washed twice in PBS to remove any excess stain, and resuspended in 200µl PBS. 200µl of cell solution was added to the cytospin chambers and spun in the Cytospin (Cytospin 3, SHANDON) at 400 RPM for 2 minutes. After spinning, the slides were carefully removed from the cytospin sandwich containers to prevent disruption of the pellet and allowed to air-dry for 3-5 minutes. Cells were fixed by dipping in methanol for 30 seconds, mounted in Dako fluorescent mounting medium (15mM NaN_3, polyvinyl alcohol, aqueous-based) [S3023] and cover-slipped. Slides were stored in the dark at 4^0C to minimise fading of fluorescence.

In situ Analysis of Uptake and Toxicity levels

350µl of the cell culture was taken from the 10ml flasks and stored on ice for 5 minutes. Cells were stained with propidium iodide (1µg/ml) and left on ice for a further 5 minutes. Cells were spun down at 2000rpm for 5 minutes and washed at least twice to remove excess PI. Cells were resuspended in 200µl of PBS and this volume is added to chamber slides for immediate viewing under the fluorescent microscope. Alternatively, cells may be resuspended in 200µl of Cellfix Solution and this will preserve their fluorescence for 24-48 hours. The numbers of cells showing intracellular fluorescence (green) and the number of dead cells, as assessed using propidium iodide (red) staining were counted. The proportion of FAM (+oligo) positive and PI positive cells were expressed as a percentage of the total cell number, either using fluorescent microscopy or flow cytometry.

2.9 Detection of Gene Expression Profiles using Real-Time PCR

2.9.1 TaqMan fluorescence based PCR

In order to sensitively detect alterations in mRNA levels following antisense treatments, a fluorescence-based real time PCR (utilising TaqMan technology) was employed, which uses cDNA sequences reverse transcribed from mRNA as a template. The set-up contains the normal forward and reverse primers used in standard PCR and also employs a fluorescently labelled probe which is used to monitor amplicon production during the course of the PCR cycles. The probe contains a fluorescent reporter molecule at its 5' end and a quencher at its 3' end. Following binding of the probe at 70^0C, the forward and reverse primers bind at 60^0C. During amplification, the 5' nuclease activity of DNA polymerase cleaves the bond between the reporter and quencher molecules.

The 7700 DNA Sequence Detector detects the increase in fluorescence of the reporter dye over the course of the 40-cycle reaction, and the cycle at which its fluorescence reaches a critical threshold level (C_t) is measured. The C_t gives a direct indication of the level of the target transcript initially present in the sample. If there is a decrease in the level of target gene expression, the C_t will occur at a later stage cycle, the converse is true when an increased level is present. This change in expression can be quantified relatively with respect to the level of housekeeping gene. For each gene, the concentration of the primers and probe is optimised to ensure primer limiting does not occur and to ensure primers are balanced to give efficient amplification.

To ensure rates of amplification of target gene primers and probe are comparable to those of the house keeping gene, an efficiency curve was set up with serially diluted cDNA, and the increase in Ct values for the primer sets over each dilution were compared. Similarly to perform duplex or multiplex reactions, with more than one set of primers per well, primer and probe sets were examined singly and in combination over a range of cDNA concentrations to identify any negative impact the presence of another set of primers may have on activity.

2.9.2 Design of TaqMan reagents using Primer Express ®

Primers used in the TaqMan approach must have a Tm of 58°C – 60°C as calculated using the Primer Express software. This is to allow for standard conditions and temperatures to be used in reactions, minimise optimisation procedures and allow for multiplexing with different primer pairs. All primers were designed using the recommended Primer Express software and examined for levels of secondary structure – those with significant levels of secondary structure were excluded. Primers employed in this study to detect bcr-abl, GAPDH and cyclin D2 expression are outlined in the Table 2.5. Probe oligomers had a Tm of 65-70°C and were labelled with two fluorescent labels; a reporter signal e.g. FAM or VIC at the 5' end and a quencher e.g. TAMRA at its 3' tail.

2.9.3 Determination of target transcript expression levels

Analysis of cDNA target gene expression levels by TaqMan:
Following antisense treatments the expression of the target and house-keeping gene was analysed by incorporating cDNA, reverse transcribed from their RNA, into TaqMan reactions. A 25µl or 50µl reaction was performed utilising the optimised primer and probe concentrations as previously determined for each target. In most cases reactions were performed in duplex, i.e. both sets of primers / probes were present in the same well to minimise usage of cDNA and the TaqMan Universal Master Mix and to facilitate as close as possible comparisons in expression. Amplification was performed on the ABI 7700 Sequence Detector System using the thermal cycling conditions outlined above. The fluorescent output of the reaction over the course of 40 cycles and the run data are saved using the Sequence Detector software. From here, the relevant data, containing normalised Ct values for each fluorescent label are exported to Excel for further analysis.

To determine whether the amplification of the target and house-keeping genes were suitable for evaluation using the comparative method, TaqMan primer and probe sets were analysed as outlined in the Appendix p.237

Table 2.5 Primer and probe sequences used for TaqMan PCR amplification of the target genes bcr-abl (b2a2 & b3a2), the house keeping gene, GAPDH & Cyclin D2

B3A2 Amplicon= 85bp				
Oligomer	Sequence 5'-3'	Tm	%GC	Length
Forward	cgt cca ctc agc cac tgg a	59.4	63.2	19
Reverse	act cag acc ctg agg ctc aa g	57.2	57.1	21
Probe (FAM)	agc aga gtt caa aag ccc ttc	66.5	4.6	21

B2A2 Amplicon= 95bp				
Oligomer	Sequence 5'-3'	Tm	%GC	Length
Forward	atc cgt gga gct gca gat g	58.4	57.9	19
Reverse	cgc tga agg gct tct tcc tt	59.6	55	20
Probe (FAM)	cca act cgt gtg tga aac tcc	66.7	52.4	21

GAPDH Amplicon= 76 bp				
Oligomer	Sequence 5'-3'	Tm	%GC	Length
Forward	tgt tcc aat atg att cca cc a	54.9	38.1	21
Reverse	ttg atg aca agc ttc ccg ttc	58.8	47.6	21
Probe (VIC)	ttc cat ggc acc gtc aag gct g	68.0	52	25

Cyclin D2 Amplicon= 81 bp				
Oligomer	Sequence 5'-3'	Tm	%GC	Length
Forward	aag ctg tct ctg atc cgc aag	58.3	52.4	21
Reverse	cgg tgg gta cat ggc aaa ct	59.3	55	20
Probe (FAM)	acc ttc att gct ctg tgt gcc acc g	68.9	56	25

Statistical analysis of TaqMan results

Ct values obtained from the endogenous control gene GAPDH were used to calculate relative changes in the expression of target genes. Initially, bcr-abl expression was normalised to GAPDH expression giving the ΔCt. This facilitates direct inter-sample comparison between different runs and ΔCt will remain constant if expression of neither gene is altered.

ΔCt = Ct value of target gene - Ct value of endogenous control gene

The ΔCt for each sample is normalised to that of the calibrator or control sample, to give the ΔΔCt, which is invariably equal to zero for the calibrator. Any of the controls employed may be selected as the calibrator and expression of all other samples is compared to this sample.

ΔΔCt = ΔCt of each sample - ΔCt of the calibrator sample

The ΔΔCt values were then entered into the formula:

$$2^{-\Delta\Delta Ct}.$$

This normalised the value of the calibrator to one, and all samples which exhibit reduction of target gene expression will be lower than this (ie 0-0.99), and all samples which exhibit increased target gene expression will be greater than this (i.e. >1).

These values may then be converted into logarithmic scale where the calibrator has a value of zero. Samples which showed reductions in target gene expression were in the negative range and those which exhibited an increase in target gene expression were in the positive range.

The significance of the down-regulation mediated by antisense molecules was calculated using GraphPad Prism software (up to version 4). Values were analysed using one-way ANOVA (non-parametric) analysis and Dunnett post-test.

2.10 Analysis of protein expression

2.10.1 Lysis Solution for Protein extraction

A protein lysis buffer was employed for determination of RNase H independent antisense backbone effects. All steps were carried out on ice to minimise degradation by proteases. The lysis buffer is composed of the components outlined in Table 2.6.

Table 2.6 Lysis Buffer for extraction of protein from cell lines

Components:		*Final Concentration*	*Volume added to 1ml*
10mM TRIS-HCl	pH 7.4	100µM	10µl
50mM	NaCl	2.5µM	50µl
10mM	Na4pyrophosphate	1.0µM	100µl
50mM	NaF	2.5µM	50µl
100%	NP-40 (Igepal)	1%	10µl
10%	SDS	0.1%	10µl
Protease components were added fresh to the lysis buffer immediately prior to use :			
10mM	PMSF	1µM	100µl
100mM	Sodium orthovanadate	1µM	10µl
1µg/ml	Leupeptin	2µg/ml	2µl
1µg/ml	Aprototin	1µg/ml	1µl

Protein Isolation

Following treatments, cells were pelleted by centrifugation at 1,400rpm for 5 minutes and resuspended in an appropriate volume of lysis buffer. 80µl of lysis solution was used per 5 X 10^6 cells and following thorough mixing, lysis was carried out on ice for 15 minutes. Samples were centrifuged at 12,000g (11,300RPM) for 20 minutes to remove insoluble cellular components. Soluble proteins are present exclusively in the supernatant which was carefully removed and transferred to a fresh tube. The protein lysates were aliquoted into 12-16µl volumes and stored at -20^{0}C, protein samples remain stable for 6-12 months at this temperature.

2.10.2 Quantification of protein yields using The Bradford Assay

Following extraction of protein lysates outlined above, the Bradford assay was performed to determine protein yield. This was carried out to ensure an appropriate and equal concentration of protein was loaded onto each electrophoresis well. The protein content of each sample was measured spectrophotometrically by comparing its absorbance to that of known concentration standards as outlined in Table 2.7.

Table 2.7 Preparation of Protein Standards for Bradford Assay

0.4mg/ml Stock	Lysis Buffer	H_2O	Conc (ug/500µl)
0	10	990	0
5	10	985	1
12.5	10	977.5	2.5
25	10	965	5.0
37.5	10	952.5	7.5
50	10	940	10
62.5	10	927.5	12.5
75	10	915	15

Bradford Assay Procedure

100µl of each standard and each sample (diluted 1 in 500 with H_2O) were loaded in triplicate into a 96 well reaction plate. An equal volume of Bradford Solution [Sigma B-6916](1 in 2.5 with H_2O) was added using a multi-channel pipette and mixed. Each sample and standard were analysed in triplicate by reading their absorbance at 595nm using the TECAN **SPECTRA***FLUOR* PLUS fluorimeter. Excel Software was used to plot a standard curve from which the concentration of the samples is read.

2.10.3 Electrophoretic separation of proteins by SDS PAGE

Sodium Dodecyl Sulphate (SDS) polyacrylamide gel electrophoresis (PAGE) was performed to separate proteins and facilitate detection of specific protein species. SDS swamps the proteins in negative charge, ensuring the proteins were separated on the basis of their molecular weight alone. Expression of BCR-ABL (p210) was detected using an abl antibody, and β actin expression was detected as a control to ensure equal well loading and specific down-regulation of BCR-ABL expression. The acrylamide gel consists of a lower 8% resolving gel which is optimal for resolving gels of molecular weight >200KDa such as BCR-ABL (p210), and an upper 5% stacking gel to ensure proteins separate smoothly. The resolving gel (8%) was prepared first and its components are outlined in Table 2.8.

Table 2.8 Components of an 8% resolving gel used to separate BCR-ABL and actin

8% Resolving gel		
Component	**Concentration**	**Reaction Volume**
Ammonium Persulphate	(10%)	70µl
SDS	(10%)	70µl
Tris	1.5M pH8.8	1.82ml
Acrylamide	(30%)	1.82ml
TEMED		5.6µl
ddH_2O		3.64ml
Total		7.00

The 8% resolving gel was slowly poured between the two prepared gel plates and overlaid with 500µl isopropanol to facilitate acrylamide polymerisation. The gel was allowed to polymerise for 20 minutes, during which time the upper stacking gel was prepared as in Table 2.9:

Table 2.9 Components of a 5% stacking gel used to separate BCR-ABL and actin

5% Stacking Gel		
Component	**Concentration**	**Reaction Volume**
Ammonium Persulphate	(10%)	20µl
SDS	(10%)	20µl
Tris	0.5M pH6.8	250µl
Acrylamide	(30%)	330µl
TEMED		2µl
ddH_2O		1.4ml
Total		2.00ml

Upon resolving gel polymerisation, the isopropanol was drained off and the 5% stacking gel was poured in between the glass plates. A comb was inserted to induce well formation and the stacking gel was allowed to polymerise before transfer to the gel rig.

Electrophoresis of Protein Samples

35 µg of protein were loaded per well, as calculated from The Bradford Assay. Proteins were loaded in a 10µl volume[2], plus an equal volume of 2X protein dissociation buffer (0.5M Tris-HCl pH 6.8, 10% SDS, 0.2M EDTA, glycerin, bromophenol blue, 2% β-mercaptoethanol). Directly prior to electrophoresis, samples were denatured by heating to 100^0C. 12µl of Biorad Kaleidoscope Pre-stained protein standard (161-0324) was loaded per gel and electrophoresed with samples to determine gel progress and positioning of protein species based on their molecular weight. Protein lysates were electrophoresed in running buffer (0.025M Tris, 0.192M Glycine, 0.2% SDS) at 20mAmp per gel for approximately 1.5 hours. Following electrophoresis the gel rig was dismantled, the glass plates were gently separated and the stacking gel discarded. The resolving gel containing the proteins of interest was retained and the resolved proteins removed to a more robust material, Nitrocellulose.

2.10.4 Transfer of protein species to Nitrocellulose membrane

Immuno-detection of protein species following electrophoresis was performed from a nitrocellulose membrane. Nitrocellulose is a robust membrane suitable for the storage and immuno-analysis of proteins. To efficiently transfer all protein species, a sandwich structure is constructed composed of the gel and membrane between layers of filter paper and transfer pads.

The nitrocellulose membrane, filter paper and transfer pads were pre-soaked in transfer buffer for 30 minutes prior to the transfer. The sandwich structure was assembled and placed in the transfer rig (Consort, E835) so that the membrane is placed at the positive electrode to ensure the negatively charged proteins run in that direction. The transfer was performed in transfer buffer (14.4g/l glycine, 3g/l Tris-HCl, 1g/l SDS) at 60V for 90 minutes, whilst stirring to prevent overheating and to ensure the efficient distribution of ions. Following the transfer the sandwich structure was carefully dismantled, whilst ensuring minimum disruption to membrane and gel. Protein molecular weight markers visible on the surface of the membrane indicate the transfer has been successful.

[2] The 10µl volume is composed of the volume of samples which contains 35µg of protein plus H_2O

2.10.5 Immuno-detection of Protein expression by Chemiluminesence

The nitrocellulose membrane was blocked by soaking in 5% milk (3g/60ml) in 1 X TBS & 0.05% Tween 20 for 1hr whilst shaking (~30 rev/min). During the blocking step, as with the antibody probing steps, the membrane was placed protein side facing upward. Following electrophoresis, the Biorad protein marker indicated the position of each protein on the membrane based on its molecular weight. The two main proteins detected in this study differ significantly in their molecular weight, therefore the nitrocellulose membrane was cut roughly in the middle to divide in two and each half probed for the appropriate protein. The areas of interest are, in the upper portion, the 210KDa region for BCR-ABL, and in the lower portion, the 47KDa region for actin.

Table 2.10 Details of antibodies employed in this study to detect protein expression

Antibody	Source	Specificity	Working dilution
1^0 abl, c-abl	Calbiochem	Mouse anti-human	1 in 200 with 5% milk
1^0 actin, α-actin	Sigma	1gG1 mouse anti-human	1 in 5000 in 5% milk
2^0 antibody	Dako	Rabbit-Anti-mouse HRP conjugated	1 in 1000 in 5% milk

The membrane was probed with the appropriate primary antibody for ninety minutes at room temperature or overnight at 4^0C whilst shaking (Table 2.10). Primary antibody was then removed and the membrane washed three times for three minutes in 1 X TBS & 0.05% Tween 20 whilst shaking. A Horse Radish Peroxidase conjugated anti-mouse secondary antibody, which detected each of the primary antibodies employed was incubated with the membrane for one hour whilst shaking as before.

Following incubation with the secondary antibody, the 1 X TBS & 0.05% Tween 20 washings were repeated three times for three minutes whilst shaking as above. To visualise protein bands using chemiluminescence, a chemiluminescent solution (Pierce) was applied to the nitrocellulose membrane following manufacturers' instructions. The membrane was then exposed to X-ray film (Agfa) and developed using the Agfa Curix 60 developer.

2.10.6 Stripping & re-probing nitrocellulose membrane

Occasionally it was necessary to re-probe a membrane in order to achieve a clearer signal. Briefly, the membrane was incubated at 55^0C in stripping buffer (62.5mM Tris, 2% SDS, pH 6.7 & 70µl β-mercaptoethanol / 10mls) for 20 minutes. The membrane was then washed thoroughly three times in 1 X TBS for three minutes whilst shaking. This was followed by three washes in 1 X TBS & 0.05% Tween 20.

2.11 *In vitro* micro-culture assay for cell proliferative/ viability Assay

To detect changes in the proliferative capacity and viability of treated cells following delivery of antisense molecules, a variation on the previously described MTT non-radioactive colorimetric assay was employed (Alley *et al,* 1988; Scudiero *et al,* 1988). A CellTiter 96® AQueous One Solution Reagent containing a tetrazolium compound [3-(4,5-dimethylthiazol-2-yl)-5-(3-carboxymethoxyphenyl)-2-(4-sulfophenyl)-2H-tetrazolium, inner salt; MTS(a)] and an electron coupling reagent (phenazine ethosulfate; PES) was employed. PES has enhanced chemical stability, which allows it to be combined with MTS to form a stable solution.

2.11.1 Measurement of proliferative capacity

Briefly, 100µl of cells were incubated at 37^0C in a 96 well plate. 20µl of CellTiter96® One Solution Cell Proliferation Assay reagent (Promega, UK) was added per well and incubated at 37^0C, 5% CO_2 in a humidified environment for 2 hours. Following the incubation period, sample absorbance was read at 490nm using the Wallac 1420 multilabel plate reader and analysed using the Wallac 1420 WorkStation Manager Software. Well absorbance values were exported into Excel spreadsheets for further scrutiny.

Samples were analysed in triplicate; a decrease in absorbance of 10% was considered a result, while a decrease of 20% or greater was considered a significant response.

2.12 Determining the effect of Novel backbone chemistries on the growth and expansion of Haematopoietic Stem Cells

The emergence of novel backbone chemistries may prove useful tools in the antisense field. While their introduction has many distinct advantages, it was necessary to assess their effects, if any, on normal haematopoietic stem cell (HSC) populations. The novel backbones employed in this study were evaluated using the CFU-GM colony forming assay. Colony formation is indicative of the proliferative capacity of cells and this is used as a marker to identify chemistry related effects on cell growth. Isolated PBMC populations were cultured for 14 days in a cross-linked methylcellulose based medium which facilitates growth and expansion of haematopoietic progenitors. Normal bone marrow aspirates were obtained with consent from bone marrow transplantation donors.

2.12.1 PBMC Isolation

PBMC cells were isolated by layering the bone marrow sample, usually diluted to an appropriate volume with RPMI, onto a gradient (LymphoPrep AXIS-SHIELD-#1031966) with a density of 1.077±0.001g/ml. Following centrifugation at 500g for 25 minutes with a minimal brake applied, the mononuclear cells were present in the interface between the plasma layer and the LymphoPrep. Cells were removed from this layer using a Pasteur pipette, taking care to minimise collection or disruption of adjacent layers. Mononuclear cells were transferred to a fresh tube and washed with PBS to remove any residual LymphoPrep by centrifugation at 500g for 5 minutes at RT. The PBMC pellet was re-suspended in 10mls of cold (2-8^{0}C) Red Blood Cell Lysis solution, and stored on ice for 5 minutes. Following centrifugation at the conditions outlined above, the pellet was washed once more in PBS and then resuspended in 1 ml PBS. A cell count was performed as outlined previously to assess yield of isolation.

2.12.2 Incubation of Primary Haematopoietic cells in Methylcellulose

Control or untreated cells were diluted to 1 X 10^5 cells in 300µl, this is added to ~3mls of methylcellulose (MC) medium (StemCell Technologies GF H4434) using a 16 gauge blunt ended syringe due to the viscous nature of the medium, and vortexed vigorously to generate a homogenous suspension. Following vortexing, the suspension was allowed to stand for at least 5 minutes to facilitate dispersion of trapped air bubbles.

Treated cells were diluted to 1 X 10^5 cells in 200µl; the backbone chemistry under scrutiny was added to the appropriate concentration (1µM or 10µM) and the volume increased to 300µl with PBS. Cells were incubated at 37^0C for 10 minutes to reflect routine treatment procedure, and transferred to Methylcellulose medium as outlined above.

500µl of the cell suspension was transferred to 3 wells of a 4 well plate and an equal volume of water placed in the fourth well to ensure maximum humidity during the two week incubation. Cells were incubated at 37^0C for 14 days, after which the plates were inspected for colony formation. Colonies were enumerated on the basis that each colony contains at least 40 cells in a clump. Due to the pluripotent nature of the HSC, a number of cell types may be identified. These include the granulocyte-macrophage (GM), granulocyte erythrocyte, macrophage megakaryocyte (GEMM) and each singular cell type colony forming units. All were counted based on the number of cells per colony.

III

Selection of Optimal Antisense Molecules for Down-Regulation of Target mRNA Transcripts

3.1 Design of the Antisense Molecules

Once inside the cell, the antisense molecule faces a series of obstacles before interacting with its target transcripts. These relate to the chemistry dependent sub-cellular trafficking of the molecule, the duration of its lifespan within the cell and its level of competence for mRNA binding. The bulk of these determinants are antisense molecule dependent, however, local mRNA target conformation ultimately dictates the success of individual designs (Vickers *et al,* 2000). To induce optimum mRNA knock-out, antisense design parameters including chemistry, specificity and target location were analysed. During the course of this study, three chemistries that induce antisense effects by diverse pathways were analysed for mRNA down-regulation capacity. The availability of single-stranded regions on the mRNA transcript is a limiting factor for the activity of each chemistry.

The propensity for complementary nucleic acid sequences to form bonds with one another depends on their respective levels of available bases. If a target sequence is held in a loose secondary structure, this can readily be disrupted by hybridisation with a high affinity antisense molecule (Lloyd *et al,* 2001). The tendency to hybridise is dependent on the affinity of the initial binding and on antisense backbone chemistry binding affinity, and not merely on the individual bases involved. mRNA intra-molecular folding presents a challenge to potential antisense agents to compete successfully with binding sequences and induce transcript destruction. In order to recruit RNase H, or successfully block the strong binding activity of the ribosomal subunits, the antisense molecule needs to form a stable duplex with high affinity bonding. In the absence of such a stable double-stranded structure, the molecule will rapidly be displaced and translation of the mRNA will proceed. Hetero-duplex formation requires the presence of a small number of bases (4-6) free from intra-molecular interaction, e.g. in loops, to initiate duplex formation and its progression into double stranded regions (Jayaraman *et al,* 2001).

3.1.1 SFold

SFold is a recently developed software package that utilises a new statistical sampling paradigm based on the Boltzmann ensemble (Ding *et al,* 2004-a) for the prediction of RNA secondary structure (Ding *et al*, 2004-b). Sfold contains three modules; *sirna, soligo* and *sribo* specifically proposed for the rational design of the RNA-targeting nucleic acids, siRNA, antisense agents and trans-cleaving ribozymes respectively. Design is based on in-depth structural analysis including loop free energies and single-stranded probability for each base in the sequence.

Computational derivation of RNA secondary structure is based on the minimal free energy (MFE) of a single sequence. Although free energy models for secondary structure motifs have undergone refinement for more accurate characterisation of folding thermodynamics, inaccuracies are inherent in experimental estimates of the parameters (Ding *et al*, 2003). As with all models based on free energy, minor variations in the free energy parameters may produce a considerable difference in the optimal folding model. The sampling algorithm is unable to encompass external binding factors such as protein groups into its calculations. For these reasons, the sfold package was constructed to explore more in-depth the range and probability of sub-optimal secondary conformations. The most optimal secondary structure identified by this approach is therefore not guaranteed to be the one which occurs *in vivo*.

3.1.2 SFold output

Each mRNA entered is analysed in a base-by-base fashion to decipher its probability of being involved in single-stranded loops and secondary structures. This information is given in text files and displayed graphically in probability profile curves. The package provides the user with a range of suitable siRNA or antisense molecules based on empirical design rules; siRNA duplex thermodynamic properties and RNA target accessibility predictions (Ding *et al*, 2003). Suitable siRNA molecules are categorised according to the motif by which they were designed. These include the Tuschl motif proposed by Tomas Tuschl who has extensively studied the silencing efficacy of siRNA duplexes as a function of their length, the length of their overhangs and the overhang sequences (El Bashir *et al,* 2001).

3.2 Statistical Prediction of Optimal Folding Conformations

The application of computational methods for RNA secondary structure determination is a valuable tool due to difficulties in the crystallisation of large RNA molecules. Crystal structure has been achieved for a small number of RNA molecules; however crystallisation of large RNA for structural determination is extremely difficult and has only been performed for four RNA molecules (Ding, 2002). Models of mRNA secondary structure were produced for each mRNA transcript targeted in this study using a bioinformatics approach. The overall free energy of each structure (dG) is expressed in kilojoules of energy per mole. When this figure lies in the negative range it indicates that the folding is favourable. The greater the magnitude of the negative value; the more favourable and therefore more probable the proposed structure is.

3.3 Secondary Structure of bcr-abl mRNA variants

To facilitate selection of active antisense molecules, a model of the intra-molecular folding and secondary structure of both bcr-abl mRNA variants was calculated based on thermodynamic stability principles. The output graphs for b2a2 and b3a2 are represented in Figures 3.1 & 3.2 respectively. These models signify the optimal binding conformation at 37^0C, based on minimal free energy (MFE) calculations using the *mFold* software.

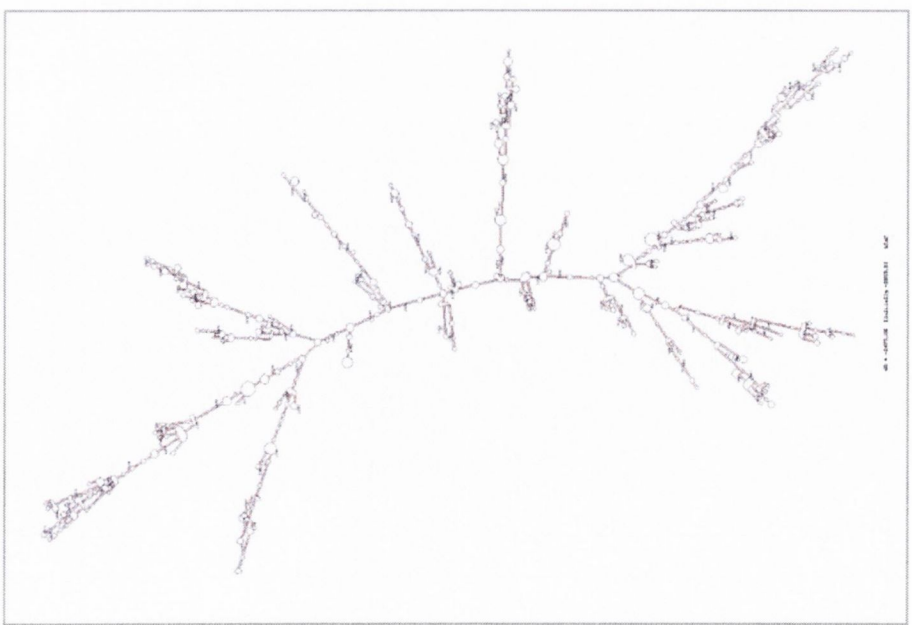


Figure 3.1 Secondary structure of the b2a2 bcr-abl mRNA displaying regions of the molecule involved in intra-molecular base pairing predicted using *mfold* software

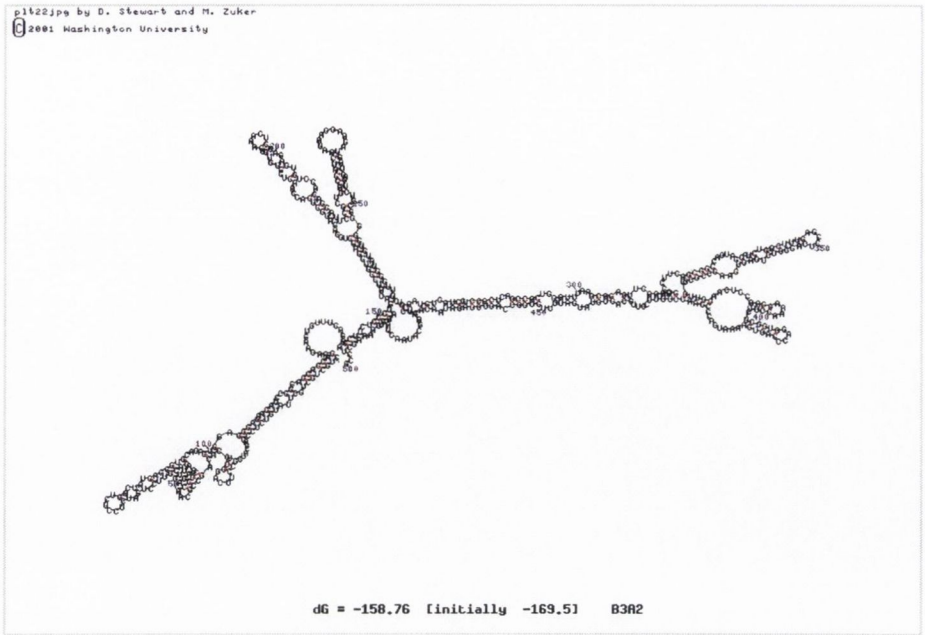


Figure 3.2 Secondary structure of the b3a2 bcr-abl mRNA displaying regions of the molecule involved in intra-molecular base pairing predicted using *mFold* software

3.3.1 Availability of bases for hybridisation

Once transcribed inside the cell, each mRNA adopts a particular secondary structure. The factors that influence this folding are based on the stability of the molecule and this is largely dependent on base composition. As may be seen from Figures 3.1 & 3.2, both bcr-abl mRNAs develop high levels of secondary structure with significant regions of complementary base pairing leading to large stretches of the transcript that are closed for interaction with antisense binding moieties. The binding potential of each antisense-targeted region of the bcr-abl mRNA transcript was examined locally using the *sfold* software. These provide an indication of the ability of antisense oligonucleotides to interact with bases in this region. Both bcr-abl mRNA isoforms were targeted at the translational start site and breakpoint region to induce antisense down-regulation. However, in each mRNA, a number of loops are predicted and these may be up to 20 base pairs in length. The value of statistical approaches in determining secondary structure may lie largely with the accurate prediction of these regions. Interruptions of secondary structure in the form of loops, even of short length represent accessible regions, and logical targets for antisense molecules.

3.4 Bcr-abl translational start site positional effects

The bcr-abl translational start site was targeted using phosphorothioate and morpholino antisense molecules. This complex region is highly conserved and serves as a docking site for translational binding groups (Brown *et al, 2003*). The probability for bases in this region to be involved in loop structures, whether hair-pin, bulge, interior, multi-branched or external loops is depicted in Figure 3.3 below. The closer the graph reaches a value of 1 for each base, the increasing likelihood that this particular base is in a loop structure and indicates availability for binding to exogenous antisense sequences.

Copyright © 2003 Wadsworth Bioinformatics Center

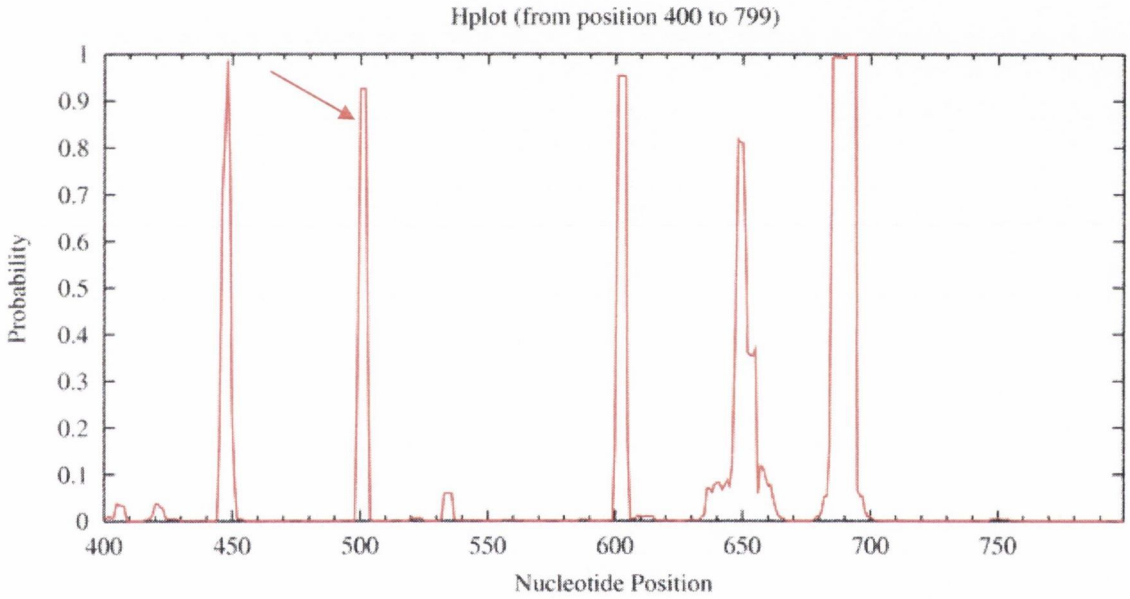


Figure 3.3 A probability profile graph showing the probability of bases surrounding the bcr-abl start site being involved in loops and therefore accessible for antisense hybridisation

The red arrow indicates an area proximal to the translational start site (nt 489) which is likely to contain bases available for hybridisation

The translational start site for bcr-abl is present at position 489 on this sequence and the phosphorothioate and morpholino molecules designed to target this region were 18 and 25 base pairs in length respectively. A high peak is evident around the 500th base pair, indicating that areas of this region are accessible for hybridisation, though the base of the peak is narrow. This graph shows the probability of involvement in all types of loops and it is unknown whether a certain type of loop is more favourable than other loop types for binding by complementary nucleic acids (Ding *et al, 2003*).

3.5 The b2a2 & b3a2 bcr-abl mRNA breakpoints

As the bcr-abl translocation is derived from the juxtaposition of two gene products normally present in healthy cells, the specificity of antisense agents needs to be addressed. The only area of the transcript that is suitable for design of CML specific antisense molecule spans the region lying immediately 5' and 3' of the breakpoint position. The probability of bases surrounding the b3a2 breakpoint being involved in loop formation is displayed in Figure 3.4.

Copyright © 2003 Wadsworth Bioinformatics Center

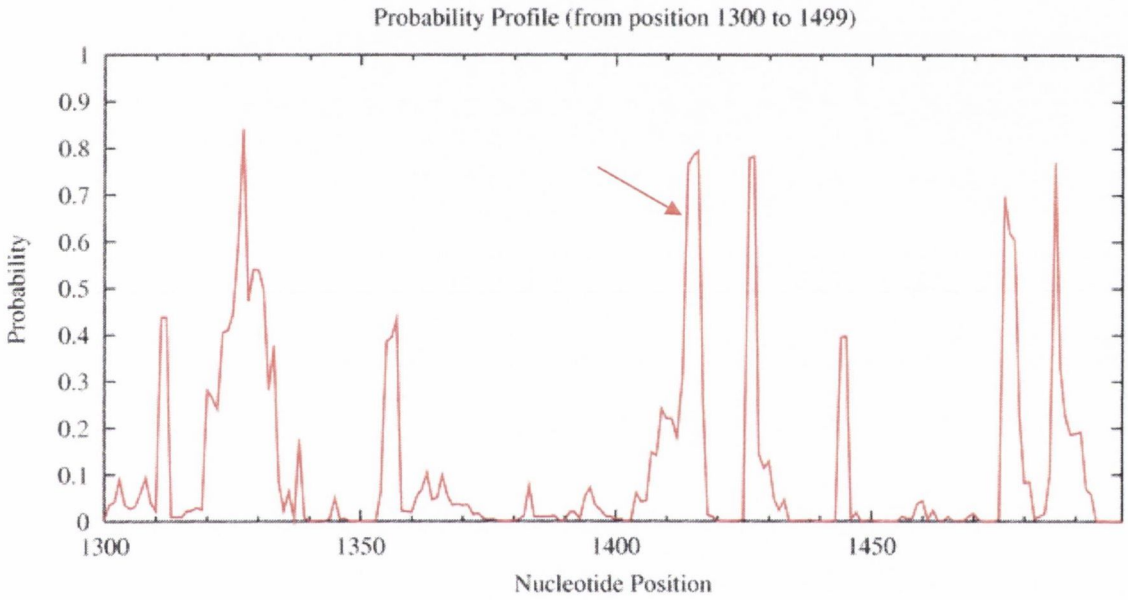


Figure 3.4 A probability profile graph showing the probability of bases surrounding the b3a2 breakpoint being involved in loops and therefore accessible to antisense hybridisation

The red arrow indicates a region surrounding the b3a2 breakpoint which is likely to contain single-stranded bases and be available for hybridisation

A peak in probability, with a value of 0.8 occurs directly 3' of the b3a2 breakpoint at position 1411(indicated by the arrow). A region with broad though moderate likelihood of being involved in loops lies directly at the site of the b3a2 breakpoint indicating its potential for specific down-regulation at this location. However, no bases in this selection have a value of 1, so therefore cannot be excluded from having any secondary structure involvement.

The probability of bases surrounding the b2a2 breakpoint being involved in loop formation is displayed in Figure 3.5 where the b2a2 breakpoint occurs at position 1296.

Copyright © 2003 Wadsworth Bioinformatics Center

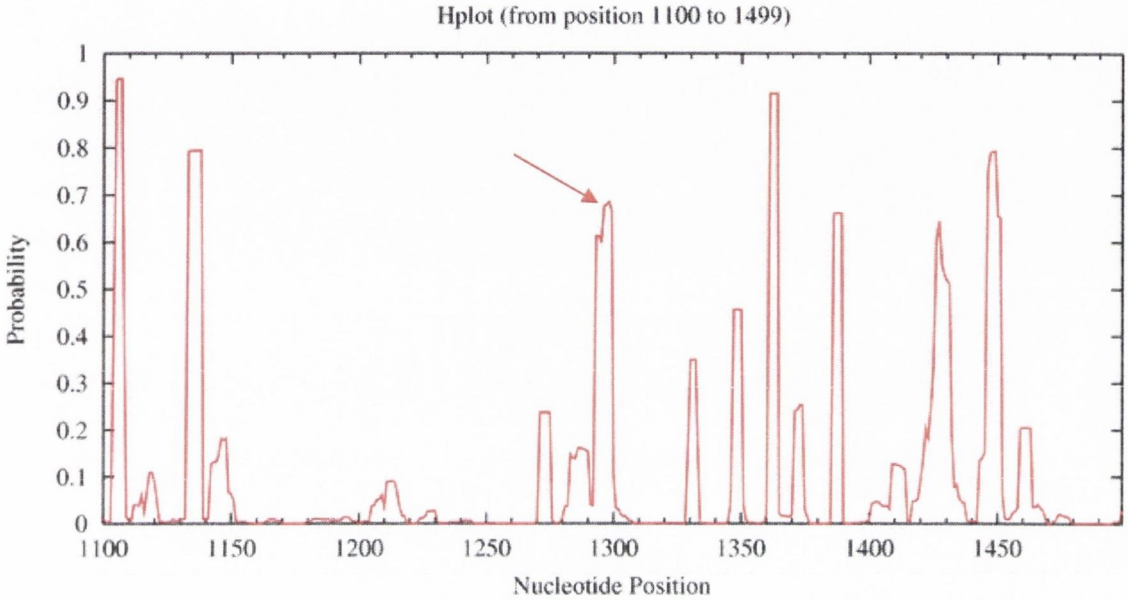


Figure 3.5 A probability profile graph showing the probability of bases surrounding the b2a2 breakpoint being involved in loops and therefore accessible to antisense hybridisation
The red arrow indicates the peak in probability of single-stranded bases surrounding the b2a2 breakpoint

An increase in single-stranded probability with a broad baseline is evident around the b2a2 break-point, this indicates that this mRNA region has moderate potential for hybridisation by antisense agents. The peak in probability occurred at nucleotide position 1298 and had a value of 0.685. If a loop structure is present, this opens up potential target regions in mRNA secondary structure. Certain areas can be highlighted as being highly unsuitable target areas for antisense hybridisation; these include the region spanning 1230-1280, where there is stable intra-molecular bindings effectively blocking invasion by antisense sequences. Also though several peaks are present indicating bases not involved in secondary structure, some stretches are only 2-3 bases in length and are insufficient to permit hybridisation at these sites.

3.6 Secondary structure of cyclin D2 mRNA

The cyclin D2 mRNA secondary structure was determined using the *mfold* software.



Figure 3.6 A section of the Cyclin D2 secondary structure (complete mRNA is inset)

The highlighted region incorporates the translational start site, target regions for the morpholino and siRNA molecules

As may be seen from Figure 3.6, the Cyclin D2 mRNA molecule has a multi-branched and intricate secondary structure; with greater than 90% of bases coupled with their complementary bases. Intermittent loops break up the existing self-complementary sections and offer potential for antisense binding.

3.6.1 Cyclin D2 mRNA positional analysis

The cyclin D2 mRNA was targeted using morpholino molecules that function by binding to the start site and 5' areas of transcripts. The cyclin D2 translational start site occurs at nucleotide 270; see Figure 3.7. This displays the probability profile of bases in the start site and surrounding regions being single stranded, and their potential suitability for morpholino targeting.

Copyright © 2003 Wadsworth Bioinformatics Center

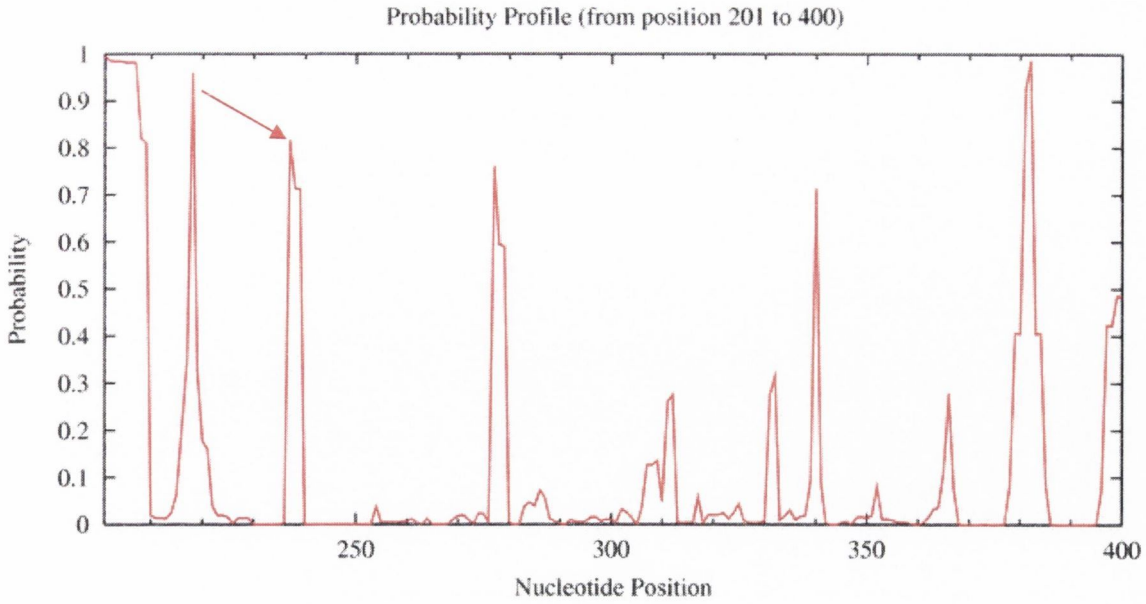
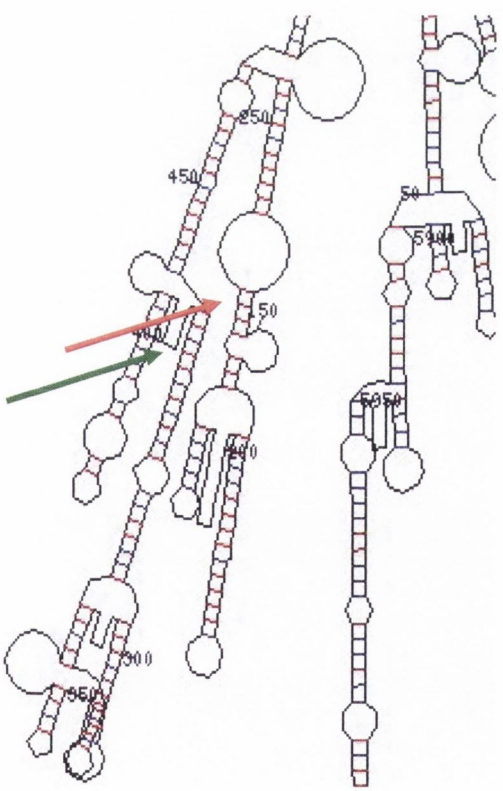


Figure 3.7 Probability profile of the cyclin D2 start site (nt 270) incorporating the region targeted by the morpholino molecule (nt 236)



From the probability profile, the lack of antisense accessible sites surrounding the cyclin D2 translational start site is evident (Figure 3.7). The target position for the cyclin D2 morpholino molecule is base 236 and is indicated by the red arrow (Figure 3.8). The presence of a loop directly at this region with the corresponding bases at position 50 signifies this region may be a feasible hybridisation target. The translational start site is indicated by the green arrow and is surrounded by strong secondary structure that may hamper potential binding groups.

Figure 3.8
Local area secondary structure surrounding the morpholino target region and translational start site of cyclin D2

Copyright © 2003 Wadsworth Bioinformatics Center

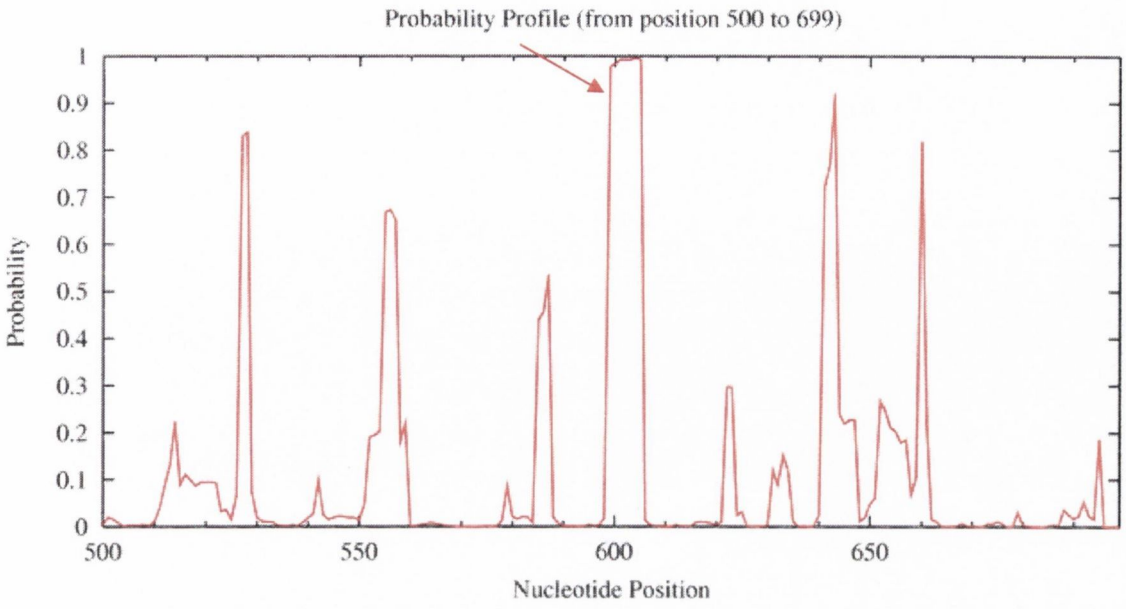


Figure 3.9 Probability profile of a section of the cyclin D2 mRNA incorporating the region targeted by siRNA molecule 1 (nt 602)

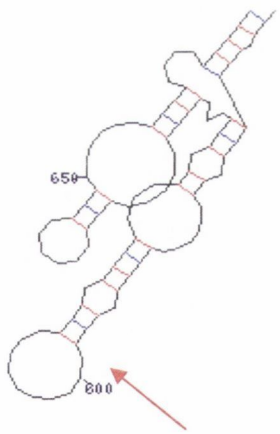


Figure 3.10
Local secondary structure surrounding the target region of the Tuschl motif siRNA molecule (602)

Figure 3.9 shows the availability of single stranded bases surrounding the target site of the Tuschl motif siRNA molecule, CyD2_SA. A dramatic increase in single stranded probability coupled with a broad baseline indicates this is a highly suitable region for binding by exogenous sequences. A number of consecutive bases have a probability of 0.999 / 1, implying this region is almost definitely open for hybridisation. The openness of this region is also seen in the secondary structure in Figure 3.10. A large loop around base 600 opens up this region to hybridisation by antisense molecules, and this site is likely to serve as a suitable target.

Copyright © 2003 Wadsworth Bioinformatics Center

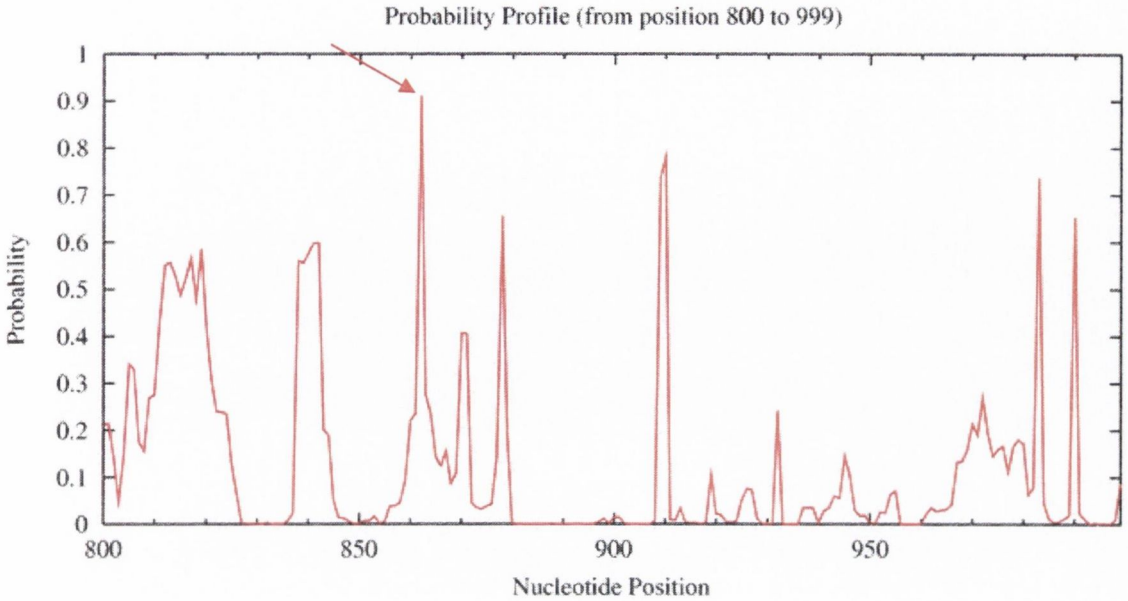


Figure 3.11 Probability profile of a section of the cyclin D2 mRNA incorporating the region targeted by siRNA molecule 2 (nt 859)

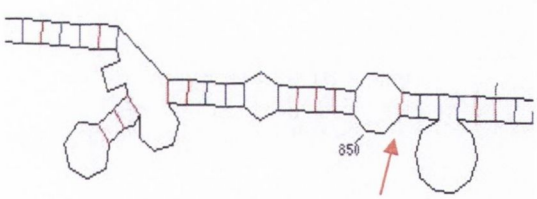


Figure 3.12
Local secondary structure surrounding the target region of the aa(n19) motif siRNA molecule (859)

The second siRNA molecule targeted to cyclin D2 and designed using the aa(n19) motif is targeted to nucleotide 859. The incidence of potential loops surrounding this region is indicated in Figure 3.11. The target area has a broad based peak with a probability of >0.9 around nucleotide 862. Various bases surrounding this location occur in loops and may serve as an initial binding site for the siRNA molecule and mediate its progression into the adjacent regions. The incidence of loops surrounding this region is shown in Figure 3.12.

3.7 Selection parameters for Phosphorothioate Antisense Molecules

The primary objective of this antisense approach was the down-regulation of the leukaemia specific mRNA; bcr-abl. To preserve expression of all normal mRNA's, and hence their gene products, including the normal variants of c-abl and c-bcr, this hybrid molecule was targeted with phosphorothioate molecules precisely at the breakpoint, the only unique sequence of the mRNA in CML cells. Bcr-abl was also targeted at the translational site by phosphorothioate molecules.

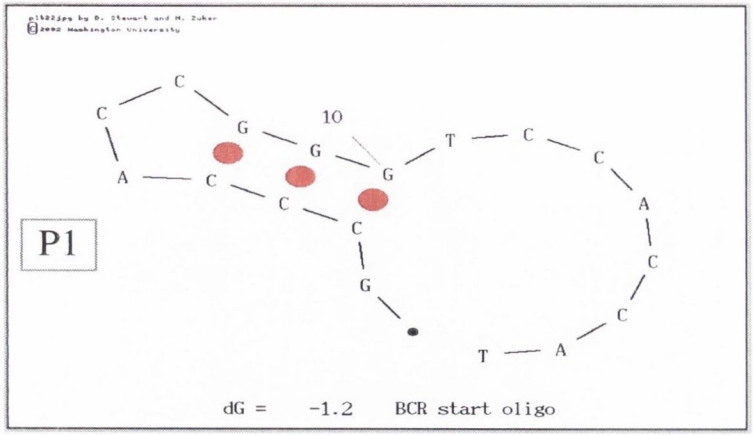
3.7.1 The 'P' Oligonucleotide Selection

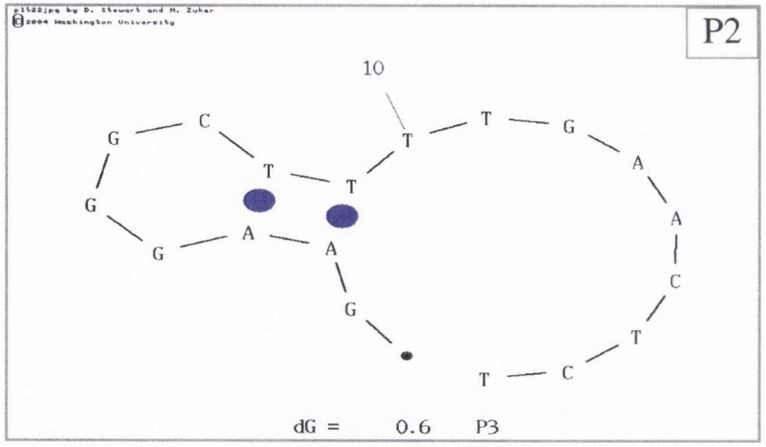
Selecting the translocation breakpoint in bcr-abl provided the opportunity to target a unique oncogene derived sequence not present in any normal cell. Limiting design of the antisense molecules imposed restraints regarding the number of potential antisense sequences to select from, and ruled out the possibility of using RNase H independent backbones at that stage. The first set of antisense molecules used to target the bcr-abl start site, the b3a2 and b2a2 break-points were labelled P1, P2 and P3 respectively, and these are detailed in Table 3.1. Molecule structures are displayed in Figure 3.13.

Table 3.1 Properties of 'P' phosphorothioate antisense oligonucleotides utilised to target the bcr-abl mRNA breakpoint

Oligo-nucleotide	**Target**	**Sequence 5' – 3'**	**Tm**	**%GC**	**Length**	**Bonds**
P 1	BCR	GCC CAC CGG GTC CAC CAT	74.0°C	72.2%	18	3X G:C See P1 diagram
P2	B3A2	GAA GGG CTT TTG AAC TCT	63.2°C	44.4%	18	2 X A:T See P2 Diagram
P3	B2A2	GAA GGG CTT CTT CCT TAT	63.2°C	44.4%	18	2 X G:C, 2 X A:T See P3 Diagram

The b2a2 breakpoint in particular, proved a challenging obstacle in relation to antisense oligonucleotide design, due to the proportions of guanines and cytosines in the sequence. This leads to increased secondary structure in the mRNA and complementary sequences and hence equal levels of intra-molecular folding are found in the complementary sequence antisense molecules.





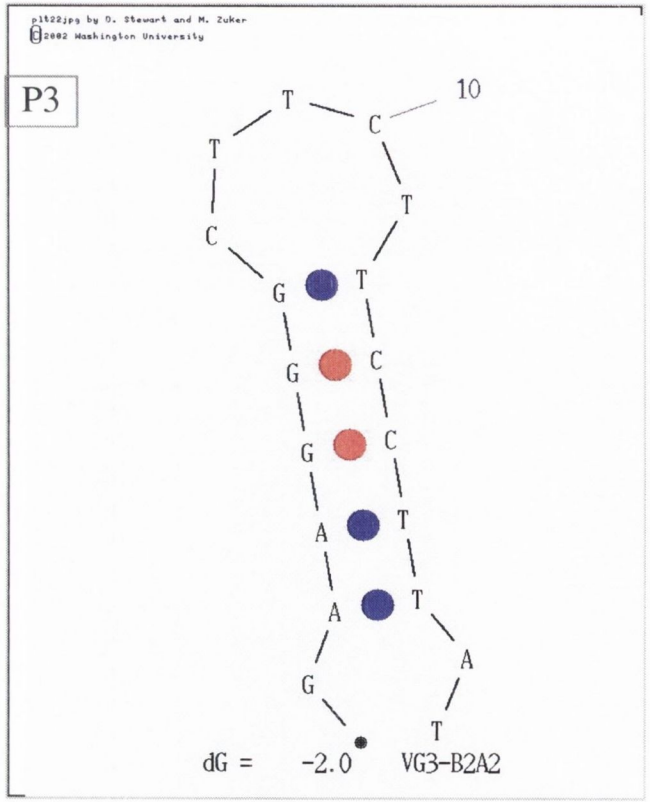


Figure 3.13 Secondary structure of the P1, P2 & P3 antisense phosphorothioate molecules at 37^{0}C as predicted using the mFold programme

3.7.2 The 'PS' Oligonucleotide Design

To further improve the antisense molecules targeted towards the b2a2 and b3a2 breakpoints a second set of phosphorothioate molecules were designed. These molecules were designed based on (i) Lack of secondary structure (ii) Potential for specific down-regulation. Sense and scrambled controls were designed and these represent the antisense molecule in a reverse orientation and in a version containing the same proportion of each base in a different order. These controls allow for allocation of sequence-specific as opposed to sequence-dependent effects to the antisense molecule. They also identify any non-sequence specific, chemistry or sequence dependent (though non-sequence specific) side effects. Their importance is undisputed with the revelation that various antisense effects are observed to be caused by general oligonucleotide effects, rather than the blocking of transcription (Agrawal *et al,* 1999 & Lloyd *et al,* 2001). 'PS' series molecules are detailed in Table 3.2.

Table 3.2 Properties of 'PS' phosphorothioate antisense oligonucleotides and their controls targeting the bcr-abl mRNA breakpoint

Antisense Phophorothioate Oligonucleotide		Sequence 5'-3'	Tm	%GC	Bonds
PS3-a	1.	ctg aag ggc ttt tga act	48.9°C	44.4	2 X A:T
	SE	gac ttc ccg aaa act tga	49.5°C	44.4	2 X A:T
	SR	ttt gag ccg gac tga att	48.9°C	44.4	1 X G:C 1 X G:T
PS3-b	2.	ccg ctg aag ggc ttt tga	58.5°C	55.6	2 X G:C 1 X A:T
	SE	ggc gac ttc ccg aaa act cga act att	56.4°C 58.5°C	55.6 55.6	2 X G:C 2 X G:C
	SR	ctg gcg gtg ctt ctt cct tat tga tgg t			
PS2			45.3°C	36.8	2 X G:C
	SE	gaa gaa gga ata act acc a	42.8°C	36.8	2 X G:C
	SR	tcg tct ttg tga tct att c	45.3°C	36.8	1 X G:C

To provide equal comparison, sequence controls should display equal secondary structure and relatively comparable access to sequences as the antisense oligonucleotide to which it is being compared. The purpose of sequence controls is to show that unrelated or slightly altered sequences do not show the same effect, and to demonstrate this they must have equal access to the target sequences.

Due to the high G:C content of the region, the optimal b2a2-directed phosphorothioate molecule; PS2 that could be designed still contained two G:C bonds (Figure 3.14). However this is not a stable conformation as it has a positive dG (+0.6) and is a significantly less stable secondary structure relative to the P3 molecule whose dG had a value of -2.0 (Figure 3.13). The PS2 structure is displayed in Figure 3.14 below. Secondary conformations for the PS3-a and PS3-b antisense molecules are displayed in Figure 3.15. The PS3-a ODN (Figure 3.15) has a more suitable secondary structure for binding to mRNA compared to the PS3-b ODN (Figure 3.15). This is due to the presence of two strong G:C bonds in the latter.

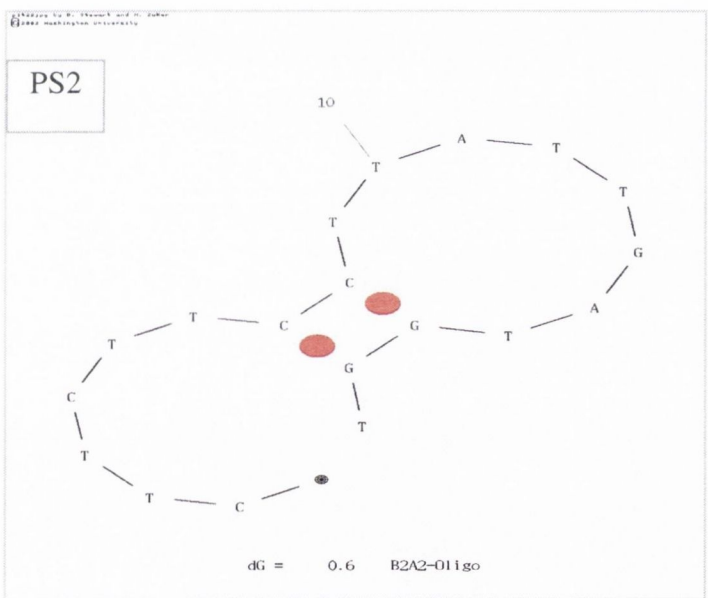
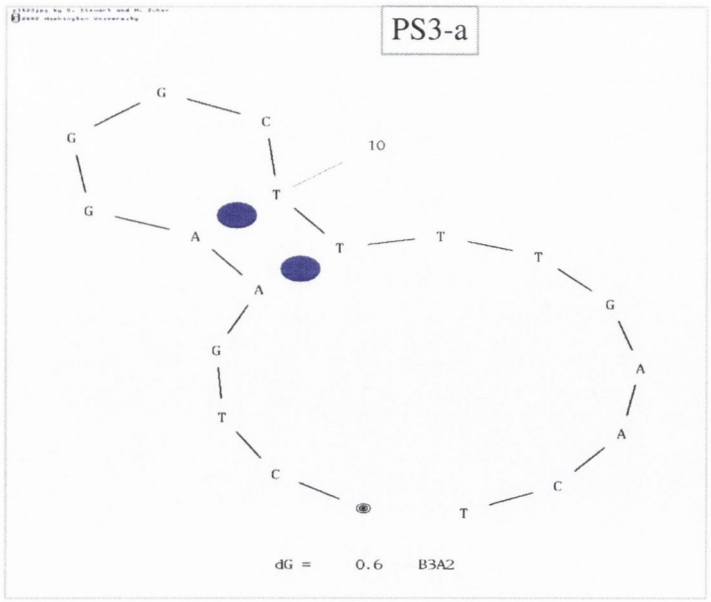


Figure 3.14 Secondary structure of PS2 antisense molecule at 37°C as predicted using the *mFold* software for DNA molecules

Structure of PS2 shows two consecutive GC bonds, hybridising the 5' and central portions of the molecule. Six bases remain in single stranded form at the 3' end.



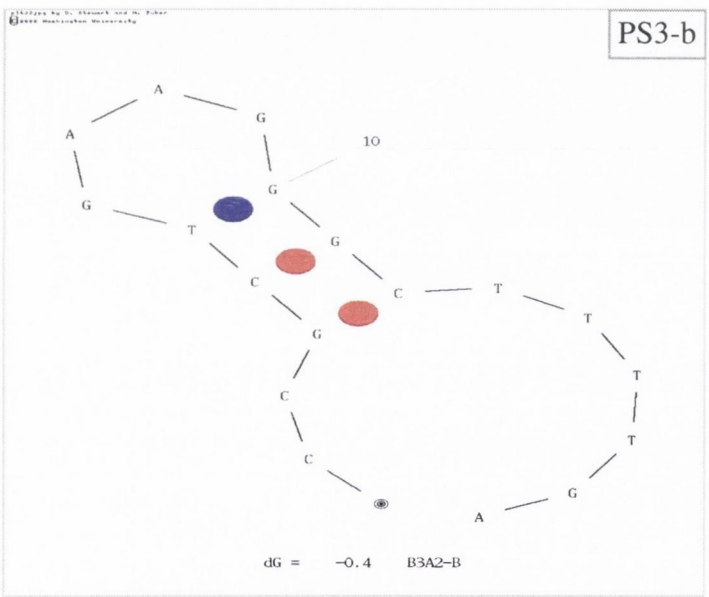


Figure 3.15 Secondary structures of the PS3 a & b phosphorothioate antisense molecules at 37°C; calculated using the mFold software for DNA molecules

These structures indicate that the PS3-b molecule with two GC pairs has much more stable intra-molecular folding relative to PS3-a with a double AT dinucleotide sequence.

3.8 Morpholino Molecule Selection: The RNase H-Independent Approach

3.8.1 Bcr-abl targeted Morpholino Molecules

Limitations in targeting the breakpoint of bcr-abl impose serious restrictions on the type of backbone that may be utilised. Traditionally, targeting mRNA translational start sites has been widely employed, and represents the most successfully targeted area by antisense molecules (Patzel *et al,* 1999). Sequences may be highly conserved in this region, and selection of active and specific oligonucleotides is dependent on the factors already outlined which dictate their design, and also by examining each target region for homology to secondary targets using the BLAST program. One of the unique features of the morpholino is its uncharged backbone, which elicits minimal side effects. Nonetheless, this lack of charge means that the morpholino is unsuitable for delivery using the traditional lipid based methods (Ghosh et al, 2000). However; cell permeabilisation is still a suitable avenue for delivery. Morpholino molecules are reported to require lower concentrations for activity, approximately 20-50 fold lower than their phosphorothioate counterparts (Summerton *et al,* 1997). This chemistry has increased potential for down-regulation of gene expression around the translational start site relative to the RNase H dependent phosphorothioate.

The optimal length for morpholino oligonucleotides has been shown experimentally to be 25 nucleotides (Summerton *et al,* 1997). The efficacy of the antisense molecule improves substantially with increasing length, and longer molecules increase access to single stranded regions of the transcript. As the morpholino represents a completely distinct type of backbone from a chemistry perspective, it no longer activates RNase H, relying only on steric hindrance for inhibition of translation. Reductions in protein expression are examined using western blotting.

Standard and sequence controls were tested concomitantly with the morpholino backbone oligonucleotides. The standard control has the same backbone chemistry but is designed to a universal target not found in mammalian systems. This allows measurement of any non-specific morpholino backbone related effects. The second control is a sequence control, the sense version of the antisense molecule, and allows measurement of any non-specific, sequence dependent effects. This control possesses the same proportion of purine (AG) and

pyrimidine (TC) bases as the antisense sequence. A 5' mis-match control was also assessed to determine the specificity of the bcr-directed morpholino molecule (MPL_bcr); replacing bases present in the active molecule should obliterate antisense effects if activity of the molecule is sequence specific. This is the most stringent sequence control employed. Each of these molecules are detailed in Table 3.3.

Table 3.3 Properties and sequences of the Morpholino Antisense Oligonucleotides and their controls targeting the bcr-abl mRNA start site

Antisense Oligonucleotide	Sequence 5'-3'	Tm (%GC)	%GC	Intra-molecular Bonds
Morpholino bcr ss	CCG CGA AGC CCA CCG GGT CCA CCA T	88°C	76%	4 X G:C[1]
Standard Control	CCT CTT ACC TCA GTT ACA ATT TAT A	50°C	32%	1 X A:T 1 X G:C
Sense Control	ATG GTG GAC CCG GTG GGC TTC GCG G	88°C	76%	3 X G:C
5' mismatch control[2]	CC**c** CG**t** AGC CCA **g**CG GGT C**g**A C**g**A T	88°C	76%	4 X G:C 1 X G:T

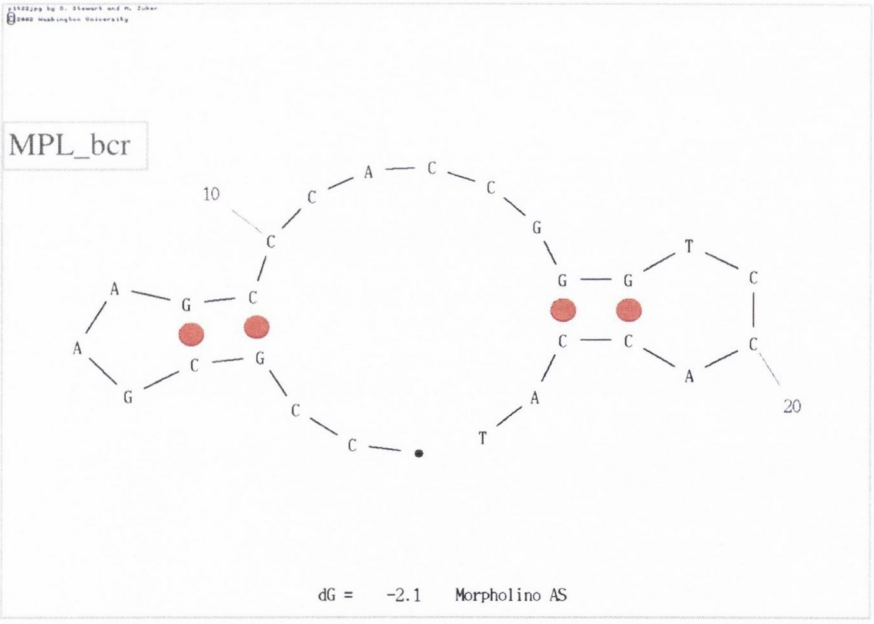


Figure 3.16 The morpholino molecule directed to the bcr start site showing bases involved in intra-molecular foldings as predicted using *mfold*[1].

[1] Folding of morpholino chemistry molecules is not available on *mfold*. The structures were predicted using the DNA algorithm. Therefore, though base composition is the same the actual morpholino folding pattern may be slightly altered relative to the one displayed above.

[2] Mis-matches from the MPL_bcr sequence are indicated in lower-case bold letters

The bcr-abl-targeted morpholino displays relatively strong levels of intra-molecular folding, but also contains stretches of single stranded bases which are not hampered by the interactions from hybridisation to target sequences (Figure 3.16). These sequences may serve as hybridisation initiation sites.

3.8.2 Cyclin D2 targeted Morpholino molecules

Morpholino antisense molecules were designed to a second target for gene down-regulation in CML cells; Cyclin D2. Normally this cell cycle regulator is expressed in a cyclic pattern depending on the stage of the cell cycle (Kehn *et al*, 2004). In CML cells, cyclin D2 expression is deregulated by bcr-abl which mediates its continuous expression (Jena et al, 2002). Table 3.4 details the morpholino molecule designed by Gene-Tools to target cyclin D2 and its 5' mis-match sequence control.

Table 3.4 Morpholino antisense molecules designed to target the Cyclin D2 mRNA translational start site

Antisense Oligo	Sequence	Length	Tm	%GC	Intra-molecular Bonds
Cyclin D2 MPL_CyD2	ggc ggc ccc tct ccc tcc tgc ttt c	25	75.7	72	3 X G:C, 1 X G:T
5'MM_CyD2 Cyclin D2	ggc Cgc ccG tct Gcc tcG tgG ttt c	25	77.2	72	3 X GC

Figure 3.17 displays the secondary conformation of the cyclin D2 morpholino molecule which is targeted to a region 5' of the translational start site. A significant level of intra-molecular bonding is evident including 3 G:C interactions surrounding a G:T interaction. The delta G (dG), though in the negative range which indicates a favourable structure, is of a relatively low magnitude (-0.2). Within the molecule there is a stretch of 12 unpaired nucleotides which are capable of initiating binding to target sequences. However, their ability to interact may be impeded by the abundant secondary structure.

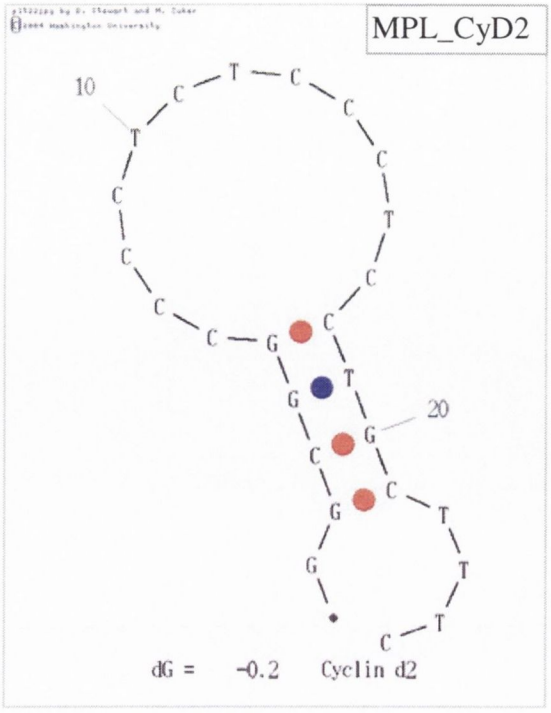


Figure 3.17 Secondary structure of the Cyclin D2 directed morpholino antisense molecule predicted using *mfold.*

The strong secondary structure is induced by the presence of 3 GC base pairs, and this facilitates interaction between GT also. The 12 unpaired nucleotides may be capable of mRNA hybridisation despite these blockades.

3.9 Design of siRNA duplexes

RNA interference (RNAi) involves the introduction of short double stranded (ds) RNA molecules carrying the sense and antisense sequences of the gene to be inactivated. Intracellular presence of these molecules activates the highly conserved RNA induced silencing complex (RISC) pathway that mediates rapid, efficient and repeated target transcript destruction (Grunweller *et al,* 2003). Initial results suggested that siRNA approaches could be designed to any part of the target mRNA, irrespective of secondary structure (Reynolds *et al,* 2004).

However, further analysis indicated that siRNA activity is inhibited by the constraint of strong secondary structure (Kretschmer-Kazemi-Far 2003). Accessibility of siRNA sequences to specific target mRNA regions mirrored that of the antisense oligonucleotides to the same site (Kretschmer-Kazemi-Far *et al*, 2003 & Vickers *et al,* 2003). siRNA is also reported to show high levels of efficacy and potency in down-regulation of gene expression (Akkina *et al,* 2003). High levels of activity need to be balanced with high specificity of target sequence, as there is the potential to induce strong alterations in expression of non-target genes with overlapping sequences. Sequence-related non-specific effects of siRNA need to be analysed and eliminated at the design stage to ensure efficient suppression of the target gene only. Early studies have indicated that a single base pair substitution is insufficient to disrupt siRNA effects and 4 base pairs need to be replaced with mismatches in order to abolish down-regulation of gene expression (Holen *et al*, 2003). Unlike previous antisense chemistries, application of siRNA presents significantly fewer issues in relation to backbone induced side effects. RNA, even in the double stranded form constitutes a naturally occurring chemistry found within the cell. Long double stranded RNA (dsRNA) species will activate non-specific interferon pathways; however this is eliminated by employing shorter stretches of dsRNA which retain capacity for mediating mRNA destruction.

Unlike antisense molecules employed to date, siRNA oligonucleotides need to be double stranded for recognition by the components of the RISC. Activation of these complexes was believed to be based on the presence of 3' overhangs at both ends of the duplex RNA. In Drosophila, siRNA overhangs are naturally generated following cleavage of large RNA

molecules by the RNase III like enzyme DICER. These were considered essential for activity and are thought to serve as recognition sites on the siRNA molecule (El Bashir *et al*, 2001). In 2003, significant gene silencing without these overhangs was reported (Czauderna *et al*, 2003). However, most siRNA still incorporate overhangs in their design.

3.9.1 BCR-ABL directed siRNA molecules

The first set of siRNA molecules designed for this study were directed toward the bcr segment of the bcr-abl mRNA. As with the morpholino, these molecules would potentially induce down-regulation of normal bcr mRNA transcripts, leading potentially to loss of function of this gene. However, bcr down-regulation does not have any significant effects on haematopoietic cell growth (McElwaine PhD thesis, TCD 1999). These molecules were selected by Dharmacon using their patented SMARTselection algorithm and partial siRNA sequences selected on the basis of functionality are outlined in the following table[3]:

Table 3.5 Partial sequence of siRNA duplexes targeted to the bcr-abl mRNA transcript

siRNA	*Sequence 5'-3'*
S1	ACG AGG AAU UUG AG
S2	AGC UCU CGG UCA AG
S3	GCA UUC CGC UGA CC
S4	GAG AAG GAG GCA GU

The siRNA molecules were synthesised using 2' ACE synthesis technology. This involves formation of 3' and 5' intermediates during synthesis and has increased coupling efficiencies to > 99%. This chemistry leads to greater stability of RNA molecules and the patented technology has unlimited modification potential. Each of the duplexes consists of 21 RNA nucleotides in length, forming a 19 base pair duplex and 'UU' overhangs at the 3' ends, and a 5' phosphorylated antisense strand.

[3] Dharmacon SMARTselection uses an algorithm comprised of approximately 30 criteria and parameters that claim to effectively eliminate non-functional siRNAs. Functionality of an siRNA duplex is defined as down-regulation of gene expression by at least 75% 24 hours following transfection of 100μM siRNA.

3.9.2 Cyclin D2 siRNA design

Empirical siRNA design

Several motifs have been proposed for the accurate identification of active siRNA duplexes based on the experience of different groups. Initial empirical rules were established by the Tuschl group for the design of siRNA and these are referred to as The Tuschl motif. These state that the siRNA duplexes should be composed of 21-nt sense and 21-nt antisense strands, paired so as to have 2-nt 3'dTdT overhangs at both ends. The targeted region is 50-100 bases down-stream of the start site (3' UTRs have also been targeted successfully). Nucleotides 1-19 of the sense siRNA strand correspond to positions 3-21 of the 23-nt target motif. The targeted motif is selected in the following order of preference:

i) NAR (N17)YNN (where N=any nt, R= A/G, Y=C/U)

ii) AA(N19)TT

iii) NA(N21)

The target sequence is selected to have approximately 50% GC content and selected siRNA sequences are aligned against EST libraries to ensure only one gene will be targeted.

AA (N19) is a popular motif advocated by two reagent companies, Ambion and Qiagen, and is infrequently represented in the human genome. This motif avoids more than three Gs or three Cs in a row because polyG and polyC sequences can hyper-stack to form agglomerates that may interfere in the siRNA silencing mechanism. SiRNA molecules with 60% G:C content are effective at inducing down-regulation of gene expression. When this is increased to 70% however, the siRNA molecule will loose efficacy (Reynolds *et al,* 2004 & Ding *et al,* 2004). This may be due to increased strength of secondary structure in G:C rich areas, as the G:C pairing is energetically stronger than the A:U pairing. GC content may also delay or impair efficient unwinding of the siRNA duplex by RISC machinery (Reynolds *et al,* 2004).

Sfold aims to provide tools for improved siRNA design by combining secondary structure and accessibility prediction with the established empirical design rules. The Cyclin D2 mRNA was targeted using two siRNA molecules designed by the *sfold* software using different design criteria. These duplexes are detailed in Table 3.6.

Table 3.6 Properties of the Cyclin D2 directed siRNA duplexes

siRNA	*Motif*		*Sequence 5'-3'*	*Target (In relation to Cyclin D2 start site)*	*Antisense siRNA binding energy*
CyD2_S1	Tuschl	Sense AS*	cccaccgucgaugaucgcatt ugcgaucaucgacggugggtt (57% GC)	+589-609 bps (nt859)	-26.4 kcal/mol
CyD2_S2	aa(N19)	Sense AS	acucaaagagaccagcccgtt cgggcuggucucuuugagutt (52% GC)	+331-351 bps (nt601)	-17.7 kcal/mol
Control	-	Sense AS	uucuccgaacgugucacgutt acgugacacguucggagaatt	No target in mammalian cells	-

*AS is the antisense strand of the siRNA duplex

Both siRNA duplexes expressed strongly negative binding energies to their antisense targets. The greater the negative value, the greater affinity binding the molecule has to its selected target. In this case, The Tuschl motif siRNA had a value of -26.4 kcal/mole, and for a molecule of this length this is a very strong binding affinity. In part this is attributable to its increased GC content relative to the AA(N19) motif siRNA. However, at -17.7 kcal/mole, the aa(N19) motif also has potential for capable of strong hybridisation.

A control siRNA sequence was also employed to ensure antisense effects observed were attributable to sequence specific effects and its details are also outlined in Table 3.6.

3.10 Specificity of antisense molecules selected for this study

Confidence in antisense molecule specificity is implicit for their use both in *in vitro* studies and in clinical applications. Previously, non-specific antisense effects have been attributed to the chemistry of the antisense molecule, but lack of sequence specificity may also result in degradation of unintended targets. This sequence-related secondary effect is readily detectable for base-base interactions using bio-informatic approaches as outlined below, and monitoring of potential targets is required in the case of each antisense sequence employed.

Unintended targets of each antisense molecule employed in this study were identified and analysed using the blastn (Basic Local Alignment Search Tool-nucleotide) programme on the NCBI website (NCBI, 2004). This programme, along with others in the BLAST heuristic search algorithm ascribes significance to its findings using the statistical methods of Karlin and Altschul. While this identifies complementary sequences in all organisms, only those of human origin were considered. The EXPECT value relates the likelihood of a particular sequence occurring by chance, and the lower this value (upper limit of 10), the more significant the match. Values of 1 or less were considered significant for assessing interaction between antisense molecules and unintended targets.

Table 3.7 Specificity of phosphorothioate antisense molecules employed to target the bcr-abl mRNA

Antisense Molecule	Length	No. of over-lapping bases	2^0 Target	Form	EXPECT value for 2^0 Target	EXPECT value for antisense target
P1	18	17	DNA on Chromosome 16p13.3	DNA (+/+)	1.1	0.28
P2	18	16	DNA from Chromosome 2	DNA (+/+)	4.3	0.28
P3	18	16	DNA from chromosome 4	DNA (+/-)	4.3	0.28
PS2	19	17	Baculoviral IAP repeat containing 4	mRNA (+/-)	1.1	0.28
PS3-a	18	18	BAC clone from Chromosome 2	DNA (+/-)	0.28	0.28
PS3-b	18	17	Clone from Chromosome 13	DNA (+/-)	4.9	1.2

3.10.1 Specificity of Phosphorothioate antisense molecules

The BLAST results for each phosphorothioate molecule employed in this study are detailed in Table 3.7. While complementary sequences for P1 and P2 are detected in the human genome, they do not serve as targets for binding as the DNA lies in the same orientation as the antisense molecule. The secondary targets identified for the P2 and P3 antisense molecules both have significantly higher EXPECT values than their target sequence; 4.3 compared to 0.28 for their specific target (Table 3.7).

The secondary target identified for the PS3-a antisense molecule is DNA based and no corresponding mRNA was detected (Table 3.7). This molecule is phosphorothioate based and will therefore be translocated into the nucleus upon delivery to the cytoplasm. However, it does not have the ability to intercalate and interact with DNA in a sequence specific fashion. Triple helix forming oligonucleotides recognise and bind to defined sequence motifs within the DNA helix and lack of these factors renders a molecule incapable of intercalation. Secondary structures identified for PS2 and PS3-b both display significantly higher EXPECT values (Table 3.7).

3.10.2 Specificity of morpholino molecules

Morpholino molecules employed in this study were also assessed for their target specificity and the results are detailed in Table 3.8.

Table 3.8 Specificity of morpholino antisense molecules employed in this study

Antisense Molecule	*Length*	*Target*	*2^0 Target*	*over-lap in bases*	*Form*	*EXPECT value for 2^0 Target*	*EXPECT value for antisense target*
MPL bcr ss	25	bcr ss	Phosphatidyl-inositol glycan, class C, pseudogene 1 on chromosome 11	17 / 25	DNA (+/-)	3.9	6e 10-5
Cyclin D2	25	5'UTR of cyclin D2	Erythrocyte membrane protein band	20 / 25	mRNA (+/+)	0.063	7e 10-5

Functionality of morpholino molecules is strongly linked with their increased length. This length increases the affinity for target regions and assures strong hybridisation to prevent ribosomal displacement. Therefore molecules with shorter lengths of complementarity to targets show very reduced activity. This is advantageous as morpholino molecules with stretches of overlapping sequences are unable to prevent ribosomal assembly and do not affect translation of mRNA with partial complementarity.

Both morpholino molecules were identified to have secondary targets with diminished regions of complementarity. For the MPL_bcr molecule, only 68% of the target is accessible and binding is unlikely to be of sufficient affinity to prevent ribosomal displacement (Table 3.8). This coupled with a several log fold increase in the EXPECT value implies that binding may occur occasionally in a transient fashion, but will not have significant effects on gene expression. The secondary target for this molecule was identified as being double stranded (ds) DNA, present only in the nucleus. As the morpholino functions in the cytoplasm and doesn't gain large scale access to the nucleus the interaction is unlikely to be relevant.

80% of the cyclin D2 morpholino target bases are found in the mRNA of the erythrocyte membrane protein band. These sequences occur in the same orientation as the CyD2_mpl molecule and will be unable to hybridise to one another. The EXPECT value for this interaction is also significantly elevated relative to the cyclin D2 target; 0.063 compared to 7e X 10^5 (Table 3.8).

3.10.3 Specificity of siRNA duplexes

Specificity of siRNA molecules is a function of the antisense strand of the duplex as this interacts in a sequence specific fashion with the mRNA target.

Bcr directed siRNA duplexes

As sequence information is limited on the bcr-directed siRNA molecules supplied and selected by Dharmacon, when these molecules were entered into the BLAST-n search tool, no significant secondary matches were identified. Shorter sequences are more likely to occur by chance in the human genome and thus generate high EXPECT values. All matches with an EXPECT value greater of 10 and greater were disregarded.

Cyclin D2 directed siRNA specificity

Specificity of cyclin D2 directed siRNA molecules is shown in Table 3.9. The EXPECT value for the target of each antisense molecule examined using BLAST-n was compared to that of its secondary target. In all cases, secondary targets had significantly higher EXPECT values indicating the interaction with the greatest affinity and the greatest complementarity was with its designated target.

Table 3.9 Specificity of siRNA duplexes targeted to the cyclin D2 mRNA transcript

SiRNA Molecule	Length	Target	2^0 Target	No of over-lapping bases	Form	EXPECT value for 2^0 Target	EXPECT value for antisense target
CyD2_S1	21	Cyclin D2	No secondary target identified in humans.	-	-	-	0.027
CyD2_S2	21	Cyclin D2	Chromosome 16 DNA clone	17 / 21	DNA (+/-)	1.7	0.007

3.11 Discussion

Designing a specific, robust molecule capable of hybridisation with its intended mRNA target is the first step in the preparation of a viable antisense molecule. As efficient hybridisation is strongly correlated with down-regulation of the mRNA transcript (Sohail *et al,* 2000) and this is hampered mainly by intra-molecular folding on the mRNA, suitable regions for antisense hybridisation were examined. Current approaches to accurate mathematical prediction of mRNA secondary structure based on thermodynamic principles were employed. Following experiments to determine activity of these molecules against their targets *ex vivo*, a comparison between target site location and molecule activity can be examined.

In the past number of years, the range and diversity of compounds suitable for inducing antisense effects has expanded, and to reflect this development, different antisense chemistries have been examined in this study. These encompass molecules which reduce mRNA transcript translation by three distinct mechanisms. Diversity in antisense chemistry may provide an as yet unlocked potential to bind to and prevent translation of mRNA sequences. The chemistry of the antisense molecule dictates its mode of action and is chosen to reflect the molecules target location on the mRNA transcript. Molecules with strong hybridisation affinity are selected to target 5' regions of the transcript and prevent ribosomal assembly and progression. Chemistries with lower affinity function by transiently binding to a target sequence and recruiting cellular enzymes to mediate cleavage ensuring that the transcript is not translated.

A total of fourteen active antisense oligonucleotide molecules were selected for this study. Of these nine were designed in-house, four bcr-abl targeted siRNA molecules were selected by Dharmacon based on their functionality and the MPL_CyD2 was selected by Gene-Tools. Of the molecules designed, the PS3-a indicated strongest promise for efficient down-regulation of its target b3a2 expression. This is facilitated by high levels of target accessibility surrounding the b3a2 breakpoint at 1411 (Figure 3.4). In turn, the PS3-a antisense molecule is largely open with few intra-molecular bonds, none of which are strong in magnitude, and the optimal predicted structure has a sequence of seven consecutive bases available for target hybridisation, (Figure 3.15).

Morpholino antisense molecules were designed to target areas surrounding the bcr-abl and cyclin D2 mRNA translational start sites (Table 3.3 & Table 3.4). Of these two targets the bcr-abl directed morpholino may be expected to display a higher level of activity. Despite the presence of four G:C bond pairs in the MPL_bcr structure, the central portion of this molecule contains six successive bases available for hybridisation (Figure 3.16). The GC bonds are located two at each end of the twenty-five base pairs; giving the bcr-directed morpholino three different avenues for initiation of double stranded structures with mRNA targets. In the case of the cyclin D2 directed molecule designed by Gene-Tools, CyD2 _MPL, bonds occur consecutively leaving four bases available for hybridisation at the 3' end, this will facilitate interaction (Figure 3.17). A further twelve bases are sequestered in a loop structure and retain capacity to interact with their target.

Six siRNA duplexes were employed in this study. Limited sequence information curtails in-depth analysis of the four Dharmacon selected molecules. The CyD2_S1 duplex exhibits a high target binding capacity at –26.4 kcal/mol (Table 3.6), coupled with excellent likelihood of consecutive base availability of the target mRNA region (Figure 3.9); this indicates the hybridisation potential of this molecule is extremely high. Absolutely no secondary targets were identified for this molecule in the human genome indicating its high level of specificity (Table 3.9).

The application of mathematical and computational approaches to decipher mRNA transcript conformation has many potential attributes. Folding of mRNA molecules *in vivo* is largely determined by the primary composition of A, U, G and C bases. While this is specific to each mRNA, the nature and stability of their interactions with one another are readily predictable by employing bioinformatic approaches. The reliable delineation of accessible target regions within the full sequence is a problematic hurdle in antisense down-regulation (Toschi *et al,* 2000). This process grows increasingly complex with larger molecules, leading to the formation of more than one possible optimal conformation. By employing *mfold* and *sfold* in this study, an important gap in the antisense hybridisation pathway has been bridged. Using these programs, the mRNA transcripts examined were determined to exhibit a high proportion of bases involved in intra-molecular foldings. Therefore a random selection of oligonucleotides selected without the consideration of mRNA secondary structure may have yielded as little as one active molecule. A previous study performed using randomly selected antisense molecules had a success rate of just 1

in 20 (Patzel et al, 1999), thus showing the value of a bioinformatic approach in selecting optimal antisense oligonucleotides.

IV

Delivery of Antisense Molecules mediated by Cell Permeabilisation Approaches

4.1. Introduction to antisense delivery

A prerequisite for hybridization is the co-localisation of the antisense molecule with its target mRNA; in the nucleus where it is transcribed, or en route to the ribosome in the cytoplasm where it is translated. Phosphorothioate (PS) linked antisense molecules delivered to the cytoplasm of the cell will rapidly locate to the nucleus which is the main site of interaction between RNase H dependent backbones and their targets (Beltinger *et al*, 1995). This translocation effect from cytoplasm to nucleus seen with phosphorothioate molecules is not observed with the non-ionic morpholino backbone. Following its introduction into the cytoplasm, morpholino antisense molecules are observed to have a general cell wide distribution, mainly in the cytoplasm and partially in the nucleus. This is consistent with the mode of action of morpholino oligonucleotides, because they are RNase H independent; they function at the site of the ribosome where they form a physical block in translation. Therefore cytoplasmic localisation of the antisense oligonucleotide is an important step to achieve for both the RNase H –independent approach which requires a mainly cytoplasmic localisation for activity and the RNase H –dependent approach where a cytoplasmic localisation allows trafficking to the nucleus.

Delivery is one of the universal stumbling blocks which affects all antisense approaches. Optimum delivery of antisense in sufficient concentrations will maximise the efficacy of the antisense approach. A natural repulsion occurs between the lipophilic cell membrane and the anionic antisense oligonucleotides and this prevents interaction with the antisense mRNA targets (Hu *et al,* 2002). In the absence of delivery agents, intracellular antisense concentrations are approximately 100-fold lower than the extracellular concentration (Broughton *et al*, 1997). Delivery agents facilitate passage of the antisense molecule through the cell membrane, promoting a cytoplasmic localisation where they may interact with their specific target. An important aspect of these agents is their potential toxicity to normal cells which would undermine any enhanced uptake effects. Toxicity is likely to occur with both the carrier or permeabilisation agents, and is a key factor when determining suitability of antisense delivery agents.

Permeabilisation of cell membranes was selected as the antisense delivery route rather than using carrier agents such as liposomes and dendrimers. Permeabilisation agents were investigated for their suitability to deliver antisense molecules due to the distinct draw-backs present when using carrier systems. Liposomes require a high degree of optimisation with regard to nucleic acid content and carrier to cell ratio. Anionic liposomes which function by encapsulation deliver the nucleic acid to an endosomal compartment which presents further difficulty for release to the cytosol.

Cell permeabilisation is unsuitable for delivery of larger gene loads such as plasmid inserts due to a limiting pore size. Membrane permeabilisation is particularly suited to delivery of antisense oligonucleotides into cells. Antisense molecules, due to their small molecular size, in turn serve as excellent tools for investigation into efficacy of potential pore forming agents. CML cells are non-adherent suspension cells, which are roughly spherical and relatively large. This property gives a large surface area suitable for interaction with SL-O in solution and maximal uptake of oligonucleotides through permeabilisation formed pores. Large available surface area facilitates resealing of pores and makes cells less susceptible to cell rupture than smaller sized cells such as red blood cells (RBC's).

4.2 Investigating pore forming potential of saponin in CML cells

4.2.1 Saponin mediated cell toxicity

Saponins are present in many plants but are most abundant in desert plants such as Yucca and Quillaja; the saponin employed in this study was extracted from the bark of the quillaja tree. Toxicity of saponin over a variety of concentrations (0.001%-0.05%) was initially determined using the LAMA-84 CML cell line. Cell counts were performed manually on the Nikon TE 300 fluorescent microscope. Saponin activity is determined by its ability to induce pore formation; as the cell is permeabilised the cell membrane is compromised and a surrogate marker of saponin potency is the ability of propidium iodide (PI) to enter the cell and detect cell damage. This saponin activity can indirectly be measured by the degree of cell toxicity it induces.

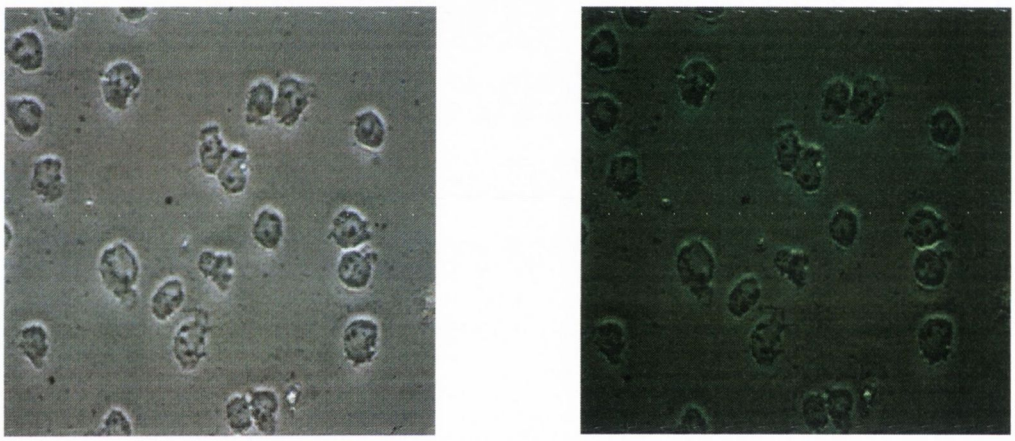
Table 4.1 The effect of a range of saponin concentrations on the viability of and hence the membrane potential of the LAMA-84 cell line

Saponin	**Viability (+24Hrs)**	**Cell Number**
0	100%	1.4 X 10^6/ml
0.001%	95.2%	9.9 X 10^5/ml
0.005%	91.95%	8 X 10^5/ml
0.01%	83.1%	3.54 X 10^5/ml
0.025%	0%	No viable cells remain
0.05%	0%	No viable cells remain

Saponin exhibits minimal membrane permeabilisation potential at concentrations below 0.005% as determined by the proportion of cells whose membranes have been compromised (Table 4.1). Moderate activity was detected when the saponin concentration rose to 0.01%, however, the number of permeabilised cell membranes represents less than a fifth of the total cells present (Table 4.1). At concentrations of 0.025% and 0.05% saponin activity was seen to induce complete permeabilisation of cell populations. Following permeabilisation, the cells are non-viable and unsuitable for further experimentation. This pore formation is irreversible under current conditions. Therefore to perform antisense experiments which require prolonged periods of treatment to induce translational arrest, this aspect of saponin activity needed to be addressed.

4.2.2 Uptake of fluorescently labelled phosphorothioate molecules using Saponin

The ability of 0.01% saponin to mediate antisense entry into CML cells in culture via cell permeabilisation was assessed by fluorescent microscopy using the FAM detection filter at 520nm. Fluorescent micrographs revealed low levels of uptake using saponin protocol I (Methodologies, Section 4.1), as is seen in Figure 4.1 A and B below. Normal cell morphology was observed in the majority of cells; however, these cells did not exhibit an increase in FAM uptake following washing (Figure 4.1)



A B

Figure 4.1 LAMA-84 cells following permeabilisation with 0.01% saponin

Figure 4.1A indicates the morphology of LAMA-84 cells following treatment with 0.01% saponin as viewed under white light. Under the green filter (Figure 4.1B), these cells are FAM negative indicating the lack of antisense entry as a result of saponin permeabilisation.

0.01% saponin exhibited minimal cellular delivery of antisense molecules into viable LAMA-84 cells. Two potential limiting factors are (1) the proportion of cells which were permeabilised; i.e. poor efficiency rates and (2) the lack of viability of the permeabilised cells; this rendered further analysis of antisense effects redundant. In an effort to combat both limiting factors, a higher concentration, 0.05%, was employed and resealing of pores using Protocol II (Methodologies, 2.4.2) was investigated.

Due to a lack of saponin-inducible permeabilisation within a low toxicity concentration range of the compound, an alternative permeabilisation protocol which utilises the cholesterol binding properties of the molecule was employed. This is similar to that used for other cell permeabilisation agents which mediate their effects through cholesterol. The pore forming abilities of saponin diminish gradually, however the addition of FCS immediately terminates the reaction and facilitates membrane resealing and cell recovery. A more purified form of saponin, which has low molecular weight contaminants removed, was also employed for these experiments. The increased purity of this saponin may have a more specific effect on cells and enhance delivery potential.

To retain cell viability during the saponin delivery step, alternative permeabilisation buffers without sodium azide were tested for their ability to facilitate pore formation by saponin whilst allowing cell recovery and avoiding the need for cross-linking of cells (Figure 4.2). Buffers containing 0.5% BSA and PBS alone were used to deliver saponin to cells.

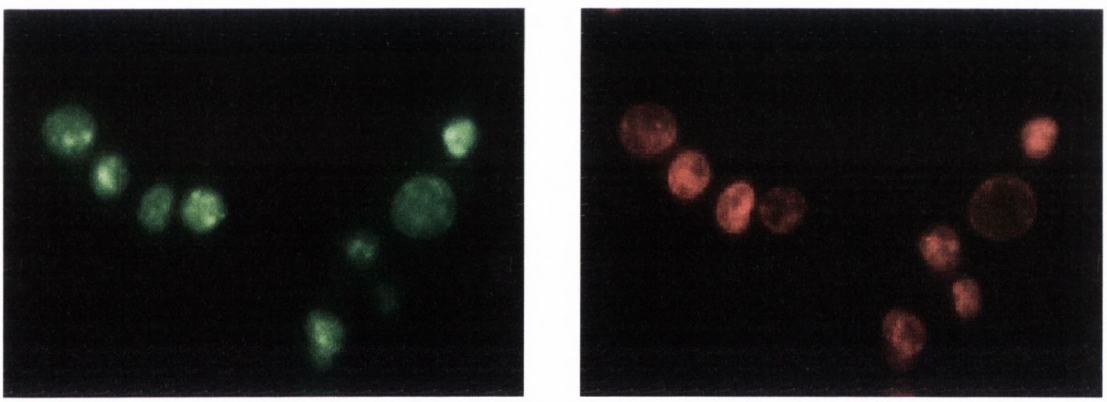


Figure 4.2 Delivery of FAM-labelled antisense molecules to K562 cells in culture mediated by 0.05% saponin in BSA (0.05%) using Protocol II.

Fluorescent images show FAM-labelled phosphorothioate uptake into K562 cells following saponin cell permeabilisation (LHS). Cells stained with Propidium Iodide have had their membranes compromised and were non-viable (RHS).

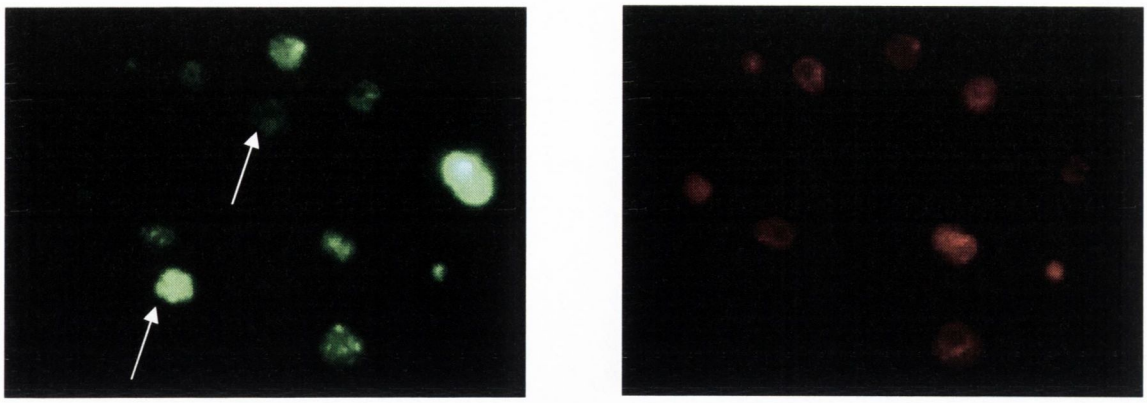


Figure 4.3 Saponin mediated FAM-labelled antisense molecule delivery to K562 CML cells in culture using 0.05% saponin in PBS (Protocol II).

Fluorescent micrographs indicated FAM-labelled phosphorothioate uptake into K562 cells using saponin in PBS diluent. In the view shown two cells have been successfully permeabilised without irreparably compromising the cells viability

Despite including an FCS resealing step and omitting sodium azide from the permeabilisation buffer, cells treated with 0.05% saponin were still observed to be unable to restore their membrane integrity resulting in loss of viability in a large proportion of cell populations (Figure 4.3). Using the more purified form of saponin, a concentration of 0.05% was seen to induce large scale delivery of FAM-labelled phosphorothioate molecules. However, as the cells are non-viable following this procedure, saponin proved to be an unsuitable candidate to employ as a delivery agent in this study. Thus, a second permeabilisation agent streptolysin-O was investigated for its antisense delivery potential in CML cells.

4.3 Streptolysin-O mediated antisense delivery

Streptolysin O (SL-O) is a bacterial toxin whose ability to infiltrate cell membranes has been harnessed to produce resealable pores in eukaryotic cells (Clark *et al,* 1999). It is a highly sensitive thiol activated molecule, produced by strains of beta-haemolytic group A streptococci, and has a molecular weight of 69 KDa. Membrane damage by SL-O is analogous to that mediated by other channel formers, the C5b-9 complement complex and staphylococcal alpha-toxin. Activation requires the presence of whole molecule Bovine Serum Albumin (BSA) and thiol groups provided by DTT which cleave secondary structure in the protein. Different batches of SL-O showed significant fluctuations in activity, and optimum concentrations of active agent varied between batches.

4.3.1 Presence of 'haloes' using SL-O

The second permeabilisation agent tested for its antisense delivery potential was the bacterial toxin, Streptolysin-O (SL-O). SL-O activity was found to be uniquely sensitive to FCS and required strict washings to remove all traces of the compound.

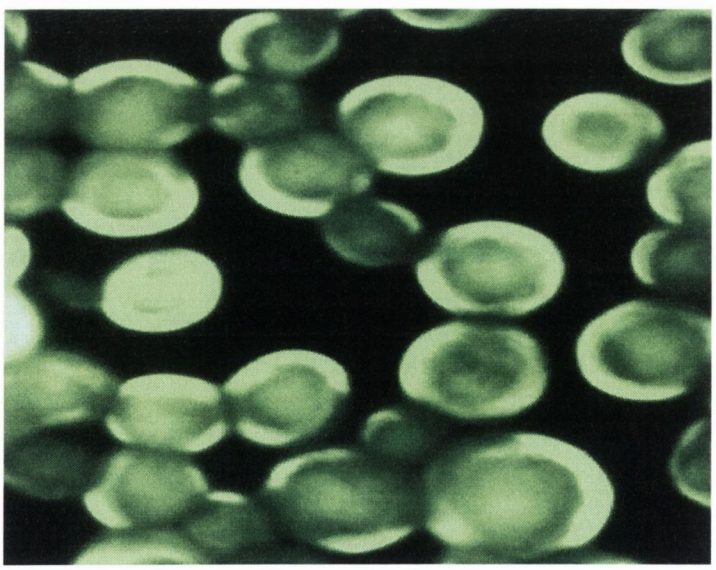


Figure 4.4 Fluorescent photograph showing fluorescent 'haloes' around cells following unsuccessful SL-O delivery

Initial experiments with SL-O, which appeared to show the antisense oligonucleotides localising inside the cell, proved to be the FAM-labelled molecule 'sticking' to the cell exterior (Figure 4.4). Repeated washings were unable to lift these molecules from the cell surface and hence resulted in a 'halo' appearance (Figure 4.4). Research with this particular batch of SL-O indicated that it was inactive at both concentrations used (2U/1 X 10^6 & 20U/1 X 10^6 cells). The halo effect may also be some indirect artefact of the cytospin process, as washed cells when viewed *in situ* did not show haloes.

4.3.2 Delivery of FAM labelled Antisense Molecules using SL-O

Following initial false positives as detailed above, SL-O was successfully employed to deliver antisense molecules to CML cells in culture using a freshly activated batch of the compound. An altered cell distribution, the recognizable punctuate pattern of the phosphorothiate molecule, was detected when cells were subsequently fixed and viewed by cytospins (Figure 4.5).

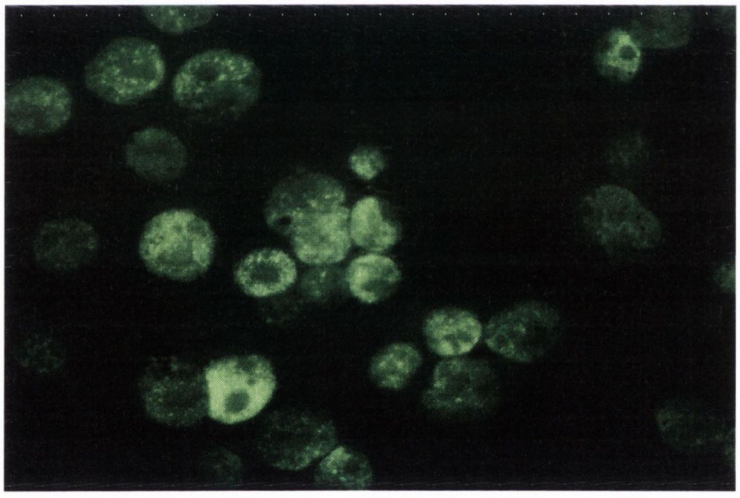


Figure 4.5 Cellular distribution of FAM-labelled phosphorothioate molecules following delivery with SL-O; viewed in cytospin

Figure 4.5 indicates the uptake pattern of FAM-labelled phosphorothioate antisense molecules when viewed following cytospining of cell suspensions onto slides. Uptake using SL-O is evident with the large number of cells exhibiting punctuate intra-cellular fluorescence (Figure 4.5). However; viewing cells following the cytospin process may give an altered reading of cell condition as a result of cytospin-induced cell changes. Cells were permeabilised with SL-O and were viewed *in situ* in chamber slides (Figure 4.6). Fixation protocols have a strong influence on the intracellular localisation of ODN's (Pichon *et al,* 1999). *In situ* the distribution pattern was different, with the labelled phosphorothioate molecules mainly appearing in the nucleus. Delivery of FAM-labelled antisense molecules is apparent in all cells in the view, indicating high levels of cellular uptake using SL-O.

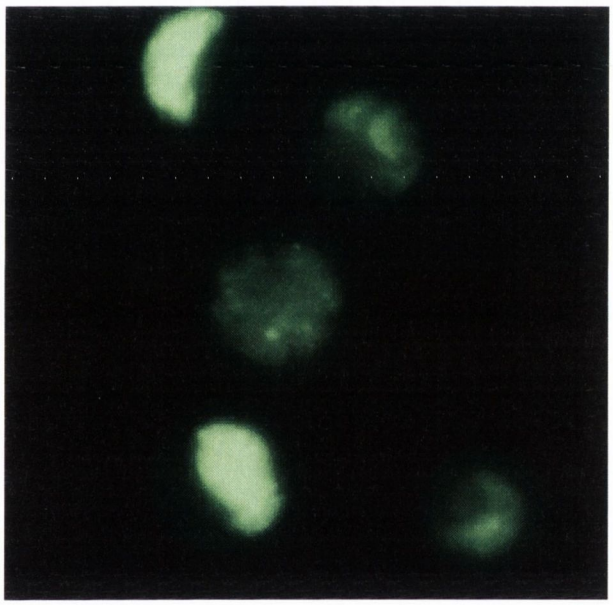


Figure 4.6 Cellular distribution of FAM labelled phosphorothioate molecules following delivery with SL-O; viewed *in situ*.

4.3.3 Cellular localisation of the antisense molecule using SL-O

Once phosphorothioate backbone antisense molecules enter the cytoplasm, they are rapidly transported to the nucleus; which is the main site of interaction between the antisense molecule and its target (Beltinger *et al,* 1995). However, this is prevented if the antisense molecule has been localised to the endosome. Therefore to examine if it is possible to deliver the antisense molecule to a sub-cellular compartment using SL-O where it may ultimately interact with its target; and evade being degraded, the nuclear stain, Hoechst was employed. Hoechst dye will localise to the nucleus, and stains nuclei blue under the UV layer on the fluorescent microscope. The FAM uptake distribution pattern of these cells was examined under the green layer, and overlays of these two layers reveal what proportion of the phosphorothioate antisense molecules localised to the nucleus (Figure 4.7).

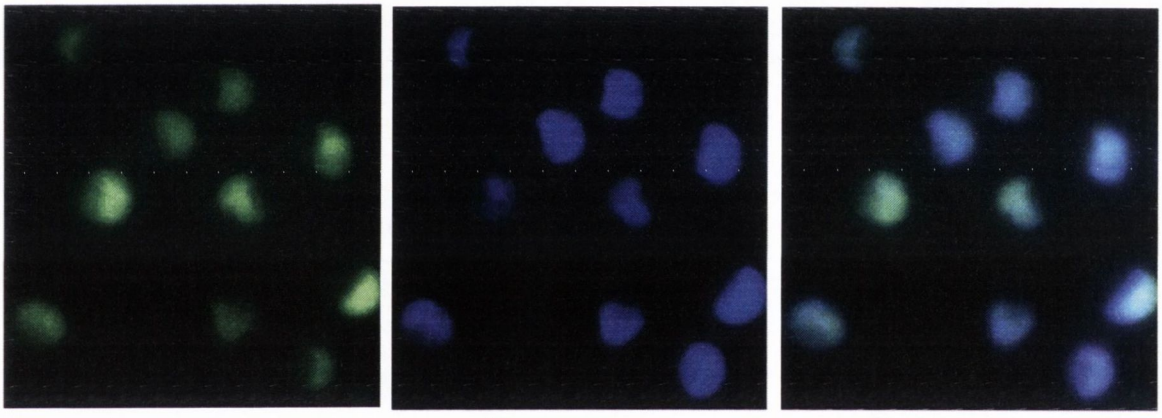


Figure 4.7 Localisation of FAM-labelled phosphorothioate antisense molecules to the nucleus of CML cells

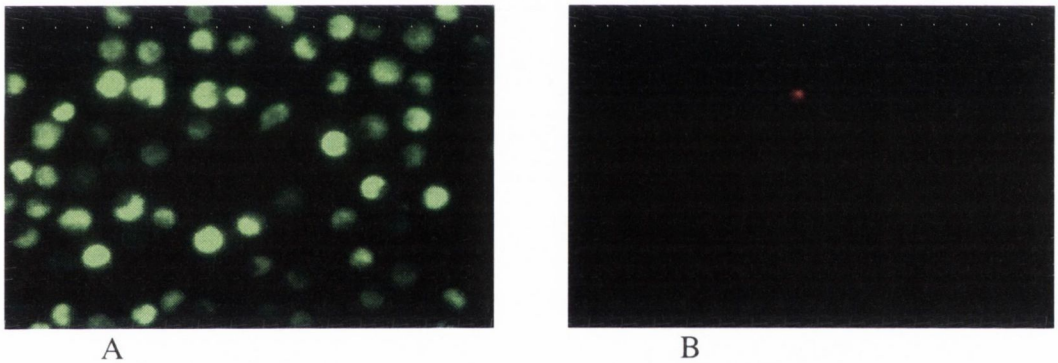
The A micro-graph shows the FAM-labelled molecule delivered to KYO-1 cells. In B, the nuclei of these cells have been stained with Hoechst dye. An overlay of these, C, on the right indicates that the antisense molecule has localised to the nucleus of cells.

The intracellular localisation of the FAM-labelled molecules was observed to coincide with that of the cellular region stained with the Hoechst nuclear dye (Figure 4.7). This indicates that following successful cellular delivery with this cell permeabilisation agent, endosomal localisation and hence antisense molecule destruction may be avoided. This facilitates interaction between the antisense molecule and its mRNA target immediately following transcription.

4.3.4 Monitoring the Toxic Effects of SL-O

The cell permeabilisation properties of Streptolysin-O are closely linked with its ability to cause cell rupture and death (Spiller *et al,* 1998). Thus it is important to monitor for cell toxicity during antisense experiments. Uptake levels of 95% and over are optimal; however, a balance is needed to maintain toxicity below 5%. Staining with propidium iodide (PI) identifies dead cells under the fluorescent microscope, and the proportion of uptake-positive cells to dead cells can be calculated.

Figure 4.8 shows the effect of 25U SL-O on 1 X 10^6 KYO-1 cells. (A) Shows the cells which have taken up the FAM-labelled antisense ODN, while (B) shows the proportion of these cells that have died. This is measured by staining positive with propodium iodide which was detected on the red channel of the fluorescent microscope at 596nm. Using 25U SL-O, viability was maintained at greater than 95%.



A B

Figure 4.8 KYO-1 cells following treatment with 25U SL-O per 1 X 10^6 cells. A- FAM-labelled antisense uptake into cells. B- PI-positive cells whose membrane integrity was not restored following the permeabilisation procedure

Using 25U / 1 X 10^6 cells, viability was maintained at 98.67%. This represents an optimum delivery concentration for this batch of SL-O. Increasing the concentration further tips the balance toward cell death and heightened levels of toxicity. Further batches of SL-O were optimised for each cell line before antisense experimentation to ensure sufficient delivery at sub-toxic concentrations.

4.4 Analysis of antisense uptake into CML cells and associated levels of toxicity using flow cytometry

To facilitate rapid and accurate detection of FAM-labelled antisense uptake into CML cells, flow cytometry was employed to measure the efficiency of delivery reactions and to detect the presence of dead cells following permeabilisation. Cell populations were selected following cell scattering, and the fluorescent output of these cells was examined with regard to FAM positivity on the FL-1 channel and PI positivity on the FL-2 channel (Figure 4.9).

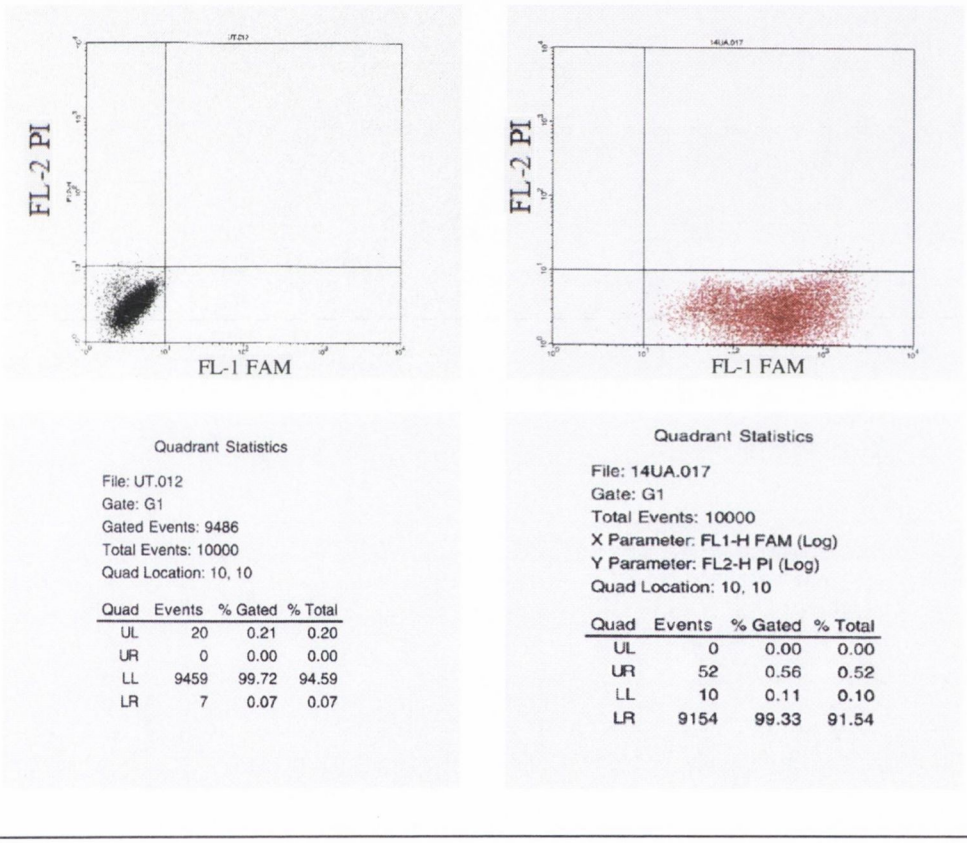


Figure 4.9 Assessment of antisense uptake and cell toxicity in K562 CML cells following SL-O mediated delivery of FAM labelled phosphorothioate molecules

The LHS shows the untreated cells which are negative in the FL-1 (FAM) & FL-2 (PI) channel. Following introduction of the antisense molecule using SL-O, cells are positive in the FL-1 FAM channel (LR=99.33% of cells) indicating antisense uptake & the FL-2 channel remains negative indicating the cells have maintained viability following the permeabilisation procedure (total=0.56% of cells).

4.5 Discussion

Delivery of antisense molecules is recognised as a primary obstacle in the successful application of antisense therapeutics *in vivo* (Eriksson *et al,* 2002). Passage of oligonucleotides through the cell membrane is retarded by their own chemical composition and by the non-polar lipophilic cell membrane (Lebedeva *et al*, 2000). The mode of antisense passage through this barrier will impact strongly on its ability to hybridise to its target mRNA and achieve down-regulation of gene expression. This study focused on the ability of two permeabilisation agents, saponin and streptolysin-O, to mediate cytosolic entry of phosphorothioate antisense molecules into CML cells.

4.5.1 Saponin cell permeabilisation

To assess the suitability of saponin as a potential antisense delivery agent; its toxic effects were examined by incubation with CML cell lines for 24 hours. Results of concentration curves indicate different effects, as may be seen from Table 4.1. At lower concentrations tested using Protocol I (Methodologies, 2.4.1), very little uptake or toxicity was observed, indicating the compound is largely inactive at these concentrations. However, as the concentration of saponin is increased, its effects on cell viability and numbers are marked; at 0.005% saponin, viability is reduced by almost 10% and reduced further to below 15% viability at 0.01% saponin (Table 4.1).

No concomitant increase in uptake of the antisense molecule is associated with this increase in cell toxicity. At these saponin concentrations, fluorescence is mainly confined to debris, with less than 5% of cells showing fluorescence; and this is mainly restricted to dead cells. Between 0.01% and 0.025% saponin, a shift is evident. At concentrations of 0.025% and above, saponin is seen to successfully permeabilise cells but with no reaction limiting factors or resealing mechanisms, this is detrimental to cell membranes and cells die. The uptake capacity of saponin at this concentration is intrinsically limited by its cell toxicity. The lack of antisense delivery using this protocol prompted the development of another protocol with greater emphasis on maintaining cell viability.

This initial work outlined the requirement for a resealing step which allowed the cells, once the oligonucleotide was delivered, to recover and maintain viability. It is known that pore formation mediated by saponin is due to interaction with cholesterol on the cell membrane (Leung *et al,* 1997). Therefore, in line with a similar protocol used for streptolysin-O, FCS was employed as a termination step to 'mop-up' unbound saponin and allow cell recovery. The inclusion of FCS as a resealing agent was performed with 0.05% saponin in a two different buffers, PBS alone and PBS with 0.05% BSA. Results for these approaches were similar, uptake levels rose to 95-100% with a concomitant rise in the levels of toxicity. Though while the inclusion of the resealing step had some effects in reducing cell morphological changes, it proved inadequate in preventing cell death (Figure 3.3).

The removal of pre-existing FCS from the medium had little effect on the activity of saponin and though this was aided by repeated permeabilisations; cells again failed to recover sufficiently. Staining with Hoechst revealed that the nuclei remained intact and no fragmentation of nuclei was observed (data not shown). The levels of toxicity using saponin show that it is unsuitable for antisense purposes, where cells are required to maintain viability. However, it is a useful method of delivery to employ for flow cytometry purposes, where intracellular staining but not viability is essential.

Other members of the saponin family also exhibit cell permeabilisation properties and some show promise in potential therapeutic applications. Digitonin is isolated from the foxglove plant, and expresses cell permeabilisation properties which have been harnessed to probe the mechanism of hormone-regulated nuclear import (Liu *et al*, 1999). Diosgenin, a steroid saponin of Trigonella foenum graecum (Fenugreek), was demonstrated to induce apoptosis in HT-29 colon cancer cells (Raju *et al*, 2004). Another steroid saponin, icogenin, displays cytotoxic effects to the myeloid leukaemia cell line HL-60, which were determined to be due to the induction of apoptosis (Hernandez *et al*, 2004).

4.5.2 SL-O cell permeabilisation

Following experimentation with both forms of cell permeabilisation; SL-O was selected as an overall superior method due to the availability of viable permeabilised cells following the initial introduction of antisense molecules (Figure 4.8). The ability of SL-O molecules to efficiently permeabilise cell membranes and allow passage of the antisense oligonucleotide is evident (Figure 4.5). 90-100% cell permeabilisation was routinely achieved. Along with this high level of cellular uptake, by-passing of endosomal pathways and localising to the nucleus was confirmed using Hoechst nuclear dye (Figure 4.7). This indicates that the antisense molecule reaches the desired cytoplasmic localisation, from where the phosphorothioate backbone ensures it is translocated to the nucleus, its main site of activity (Beltinger *et al, 1995*).

As with saponin, this high activity may be coupled with increasing risk of cell toxicity due to unsuccessful resealing. Strict control over this aspect of SL-O activity is the key to its successful employment. To this end, permeabilisation reactions were monitored both for levels of uptake and toxicity using fluorescent microscopy or flow cytometry. An upper limit of 5% cell toxicity was desirable for antisense experiments.

The employment of SL-O as a cell permeabilisation agent allowed clear assessment of the effect of antisense molecules after their delivery in relation both to hybridisation and activity. Its employment allowed the primary obstacle in the antisense process, i.e. cellular delivery, to be overcome and to focus on further downstream aspects determining what areas of mRNA have minimal secondary structure and serve as suitable targets and also allowed focus on optimal antisense design and backbone. Though its usefulness is limited to *ex vivo* studies, it is an excellent tool for co-localising antisense molecules inside CML cells and investigation into potential down-regulatory properties of antisense molecules.

A key challenge in the antisense field is to avoid the unproductive endocytosis / degradation / exocytosis process and instead achieve delivery into the cytosolic compartment of cultured cells in a manner that does not unduly reduce cell viability or perturb cell metabolism. Antisense molecules at low concentrations are capable of entering cells unaided through non-specific recognition processes such as receptor-

mediated endocytosis and adsorption. This process leads to high variability in cellular uptake. While methods of delivery examined in this study are limited to *ex vivo* applications, they will enhance the activity of each antisense molecule by delivering it to its target mRNA. Application of antisense molecules *in vivo* requires the development of strategic vectors capable of discerning between different organ sites to ensure specific targeting.

In vivo, an ideal antisense agent would display tissue-specific activity, localising the antisense molecule only to its target site. Targeted delivery of therapeutic molecules may confer several advantages. It would allow all antisense molecules to be delivered to the target site thus maximising interactions with the target mRNA. In addition, it would reduce the number of antisense molecules which might interact with non-specific targets in 'normal' cells. Lack of antisense molecules in normal tissues not only decreases the amount of unused molecules, it also reduces complications associated with high doses of active molecules in non-targeted tissues (Hussain *et al*, 2000).

To date, delivery remains one of the most challenging obstacles to the wide-spread application of antisense chemistries. This difficulty is further compounded by diversity of approaches required to mediate efficient delivery to different organ sites. Also much research focuses on *ex vivo* work, which requires a distinct approach to delivery and cannot be easily translated to the *in vivo* setting. The variability in the requirements for efficient delivery divides progress in this area. *In vivo,* the antisense backbone chemistry determines which sites molecules localise to the cell and in the body. While phosphorothioate molecules gain large-scale access to most organs excluding the brain and components of the central nervous system, other antisense chemistries may not exhibit such favourable *in vivo* distributions and this will further impact on their applicability for therapeutic intervention.

V

Down-regulation of bcr-abl mRNA transcripts induced by Phosphorothioate antisense molecules

5.1 The 'P' Series Phosphorothioate Oligonucleotides

Details of the 'P' series of oligonucleotides are outlined in Table 3.1. P1, P2 and P3 are phosphorothioate based molecules which target the bcr-abl start site, the b3a2 and the b2a2 breakpoints respectively. Delivery of 'P' series antisense molecules was induced by cell permeabilisation using Streptolysin-O and the uptake into cells was quantified by flow cytometry and fluorescent microscopy. The 'P' series phosphorothioate molecules were FAM-labelled to track and quantify their uptake into CML cells.

5.1.1 Targeting the bcr-abl mRNA translational start site with P1

Following SL-O mediated delivery of P1 to CML cells the extent of cell toxicity during permeabilisation procedures was determined using propidium iodide staining. Propidium iodide enters cells with compromised membrane integrity and gives a measure of the proportion of non-viable cells following SL-O mediated permeabilisation. The uptake and toxicity levels are displayed in Figure 5.1.

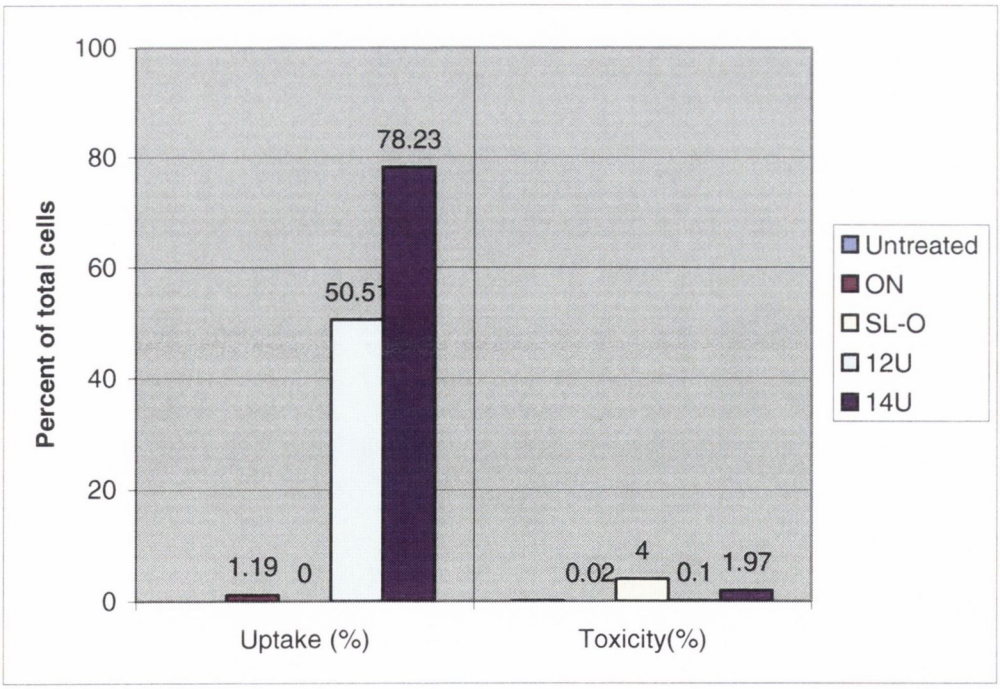


Figure 5.1 Uptake of the FAM-labelled P1 phosphorothioate antisense molecule into K562 CML cells using SL-O & associated toxicity levels for the 24Hr time-point

The 'ON' sample was treated with the antisense molecule in the absence of SL-O. The 'SL-O' sample contained no antisense molecules and determined the level of SL-O toxicity for each experiment. The '12U' & '14U' samples had the antisense molecule delivered to cells at 12U SL-O & 14U SL-O per $1X10^6$ cells respectively

Following the delivery of P1 into K562 cells, the bcr-abl mRNA expression levels were assessed using TaqMan PCR, with GAPDH as a control gene.

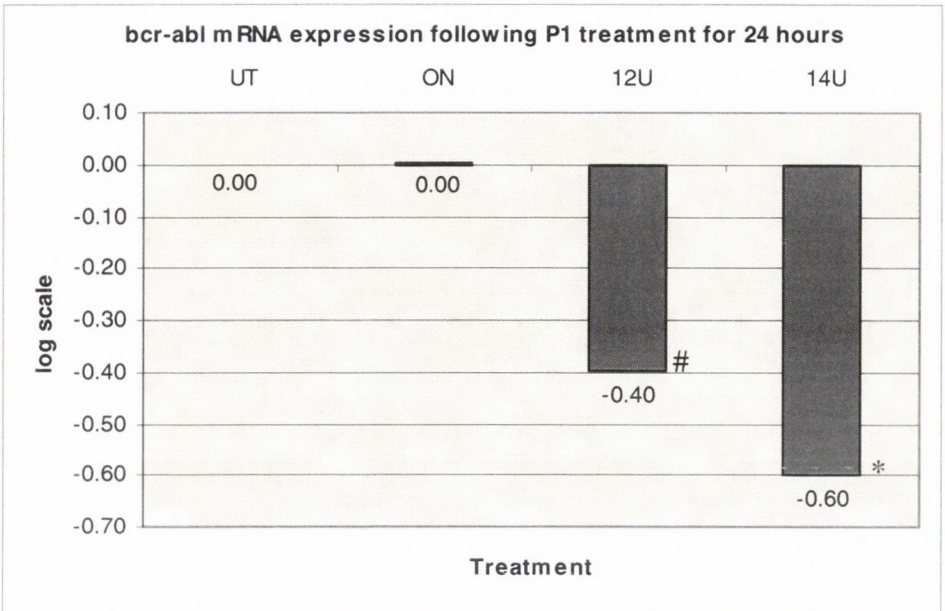


Figure 5.2 Log fold reduction in bcr-abl mRNA expression at 24hrs following delivery of P1 Phosphorothioate molecule to K562 cells using 12U & 14U SL-O

*The untreated sample (UT) shows the change in bcr-abl expression in untreated cells. The 'ON' sample was treated with the antisense molecule in the absence of SL-O. The 12U & 14U SL-O samples were treated with antisense molecule during cell permeabilisation mediated by 12U SL-O/1X10^6 cells and 14U SL-O/1X10^6 cells respectively. Reductions in bcr-abl gene expression were quantified relative to expression of the house-keeping gene; GAPDH (# $p<0.05$, * $p<0.01$). (The 'UT' and 'ON' abbreviations will be used in each graph to indicate the untreated & oligonucleotide-only samples and 'U' will be used to indicate the units of SL-O employed per 1 X 10^6 cells.)*

The P1 antisense molecule was delivered into K562 cells using two different concentrations of SL-O; 12U & 14U per 1X 10^6 cells. Significant levels of uptake were achieved and this was accompanied by low levels of cell toxicity (Figure 5.1). The P1 molecule induced reductions in b3a2 bcr-abl mRNA expression, and increased delivery of the molecule was associated with greater efficacy (Figure 5.2). Using 12U SL-O, uptake was observed in 50.51% of cells and this was accompanied by a 0.4 log reduction in the expression of bcr-abl. When the delivery level was increased to 78.23% using 14U SL-O, the down-regulation increased to 0.6 log units ($p<0.05$) (Figure 5.2).

Significant down-regulation of bcr-abl mRNA was detected using P1 after 24 hours. In order to examine the capability for sustained down-regulation of gene expression, P1 was delivered into cells for 48 & 72 hours before assessing the effects on mRNA expression. The uptake and toxicity levels achieved for this delivery experiment are shown in Figure 5.3.

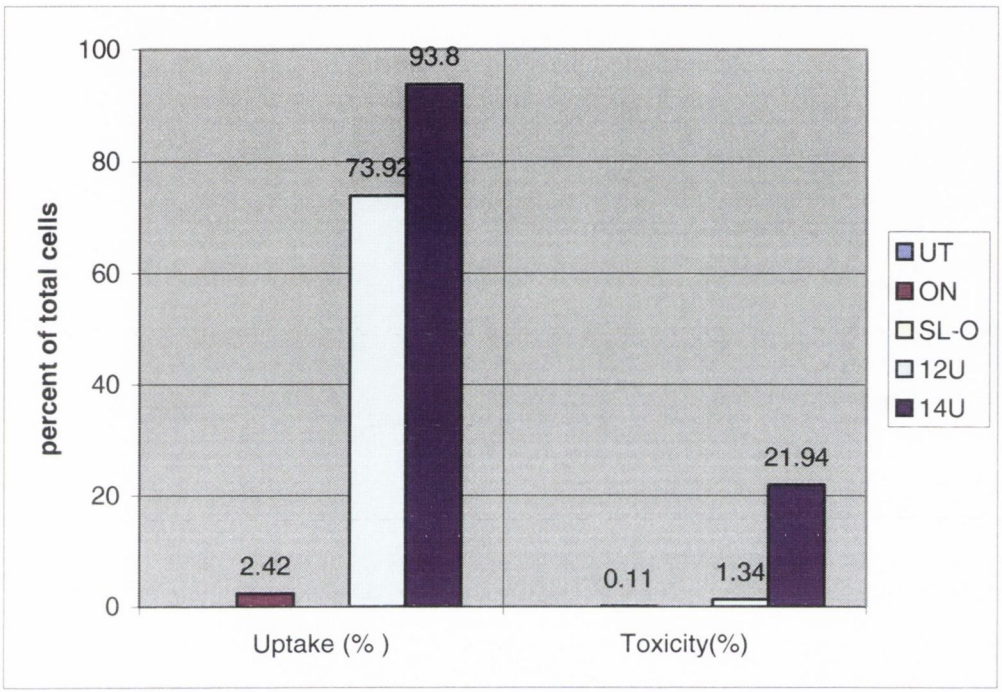


Figure 5.3 Uptake of the FAM-labelled P1 phosphorothioate antisense molecule into K562 cells using SL-O & associated toxicity levels for the 48 & 72Hr time points

The 'ON' sample was treated with the antisense molecule in the absence of SL-O. The 'SL-O' sample contained no antisense molecules and determined the level of SL-O toxicity for each experiment. The '12U' & '14U' samples had the antisense molecule delivered to cells at 12U SL-O & 14U SL-O per $1X10^6$ cells respectively

The bcr-abl b3a2 mRNA expression level was assessed at 48 & 72 hours following delivery with SL-O. The log fold reductions in bcr-abl expression are shown in Figures 5.4 & 5.5 respectively.

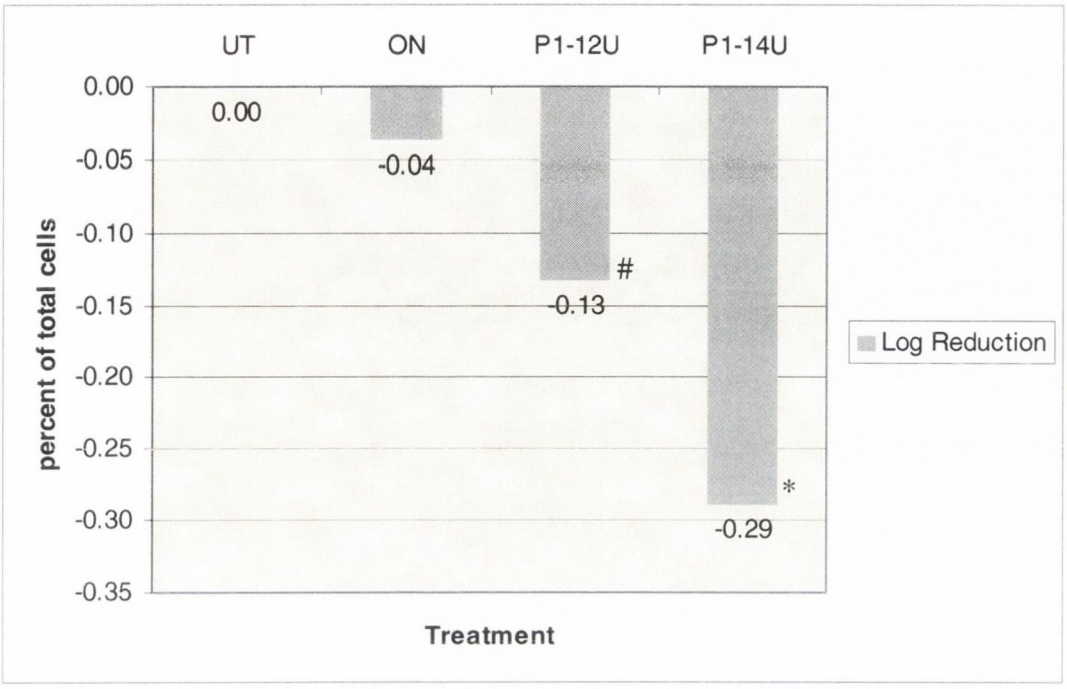


Figure 5.4 Log fold reductions in bcr-abl mRNA expression 48Hrs following SL-O delivery of the P1 phosphorothioate molecule to K562 cells (*p<0.0001)

Reductions in bcr-abl gene expression were quantified relative to expression of the house-keeping gene; GAPDH. The untreated sample (UT) shows the change in bcr-abl expression in untreated cells. The 'ON' sample was treated with the antisense molecule in the absence of SL-O. The 12U & 14U SL-O samples were treated with antisense molecule during cell permeabilisation mediated by 12U SL-O/1X10^6 cells and 14U SL-O/1X10^6 cells respectively.

Following 48 hours treatment with the P1 phosphorothioate antisense molecule in K562 cells, reductions in the level of b3a2 transcripts were still evident. However, they had decreased in intensity from a log value of -0.4 to -0.13 when delivered with 12U SL-O and -0.6 to -0.29 log units when delivered with 14U SL-O. This was despite increased efficiency of delivery (Figure 5.3). At 48 hours, P1 molecules which were incubated with K562 cells in the absence of delivery agent began to have a detectable effect. The level of down-regulation achieved was less than the SL-O delivered P1, and was due to a low level of cell entry of 2.42%.

The level of bcr-abl down-regulation using the delivery conditions in Figure 5.3 was also examined after 72 hours treatment with the P1 molecule. Log changes in gene expression measured using TaqMan fluorescent PCR are shown in Figure 5.5.

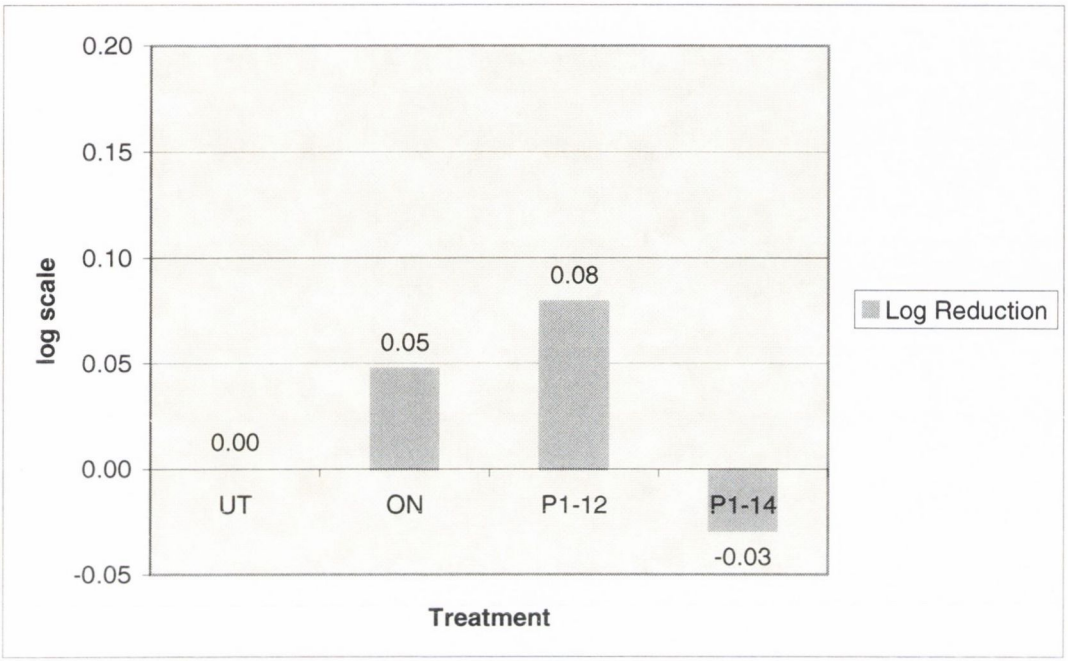


Figure 5.5 Log-fold reduction in bcr-abl mRNA expression 72Hrs following SL-O delivery of the P1 Phosphorothioate molecule in K562 cells

Reductions in bcr-abl gene expression were quantified relative to expression of the house-keeping gene; GAPDH. The untreated sample (UT) shows the change in bcr-abl expression in untreated cells. The 'ON' sample was treated with the antisense molecule in the absence of SL-O. The 12U & 14U SL-O samples were treated with antisense molecule during cell permeabilisation mediated by 12U SL-O/1X10^6 cells and 14U SL-O/1X10^6 cells respectively.

Following 72 hours treatment of K562 cells with the P1 phosphorothioate molecule, no significant down-regulation was observed. The sample delivered using 14U SL-O was seen to retain slight levels of activity. However, these were severely diminished when compared to earlier time-points and did not reach statistical significance. At the mRNA level, bcr-abl expression had recovered and returned to pre-treatment levels of expression. In the case of the 12U delivered sample, a slight increase was observed. This was also true for the undelivered P1 sample which only displayed a brief transient effect on bcr-abl expression.

5.1.2 Targeting the b2a2 mRNA breakpoint with P3

Significant success was achieved targeting the bcr-abl start site with a view to reducing bcr-abl mRNA (Figure 5.2). To increase the specificity of this approach, the bcr-abl mRNA was targeted at the breakpoint region, which is not present in either of the normal abl or bcr molecules. The b2a2 breakpoint was targeted using the P3 phosphorothioate antisense oligonucleotide which is detailed in Table 3.1.

P3 phosphorothioate molecules were delivered to the b2a2 positive CML cell line KYO-1 using SL-O. 10μM P3 was initially delivered to determine its efficacy at down-regulating bcr-abl expression. Optimal levels of mRNA down-regulation were seen following 24hrs treatment for the P1 phosphorothioate molecule, this time-point was also examined for P3. The uptake and toxicity levels are shown in Figure 5.6.

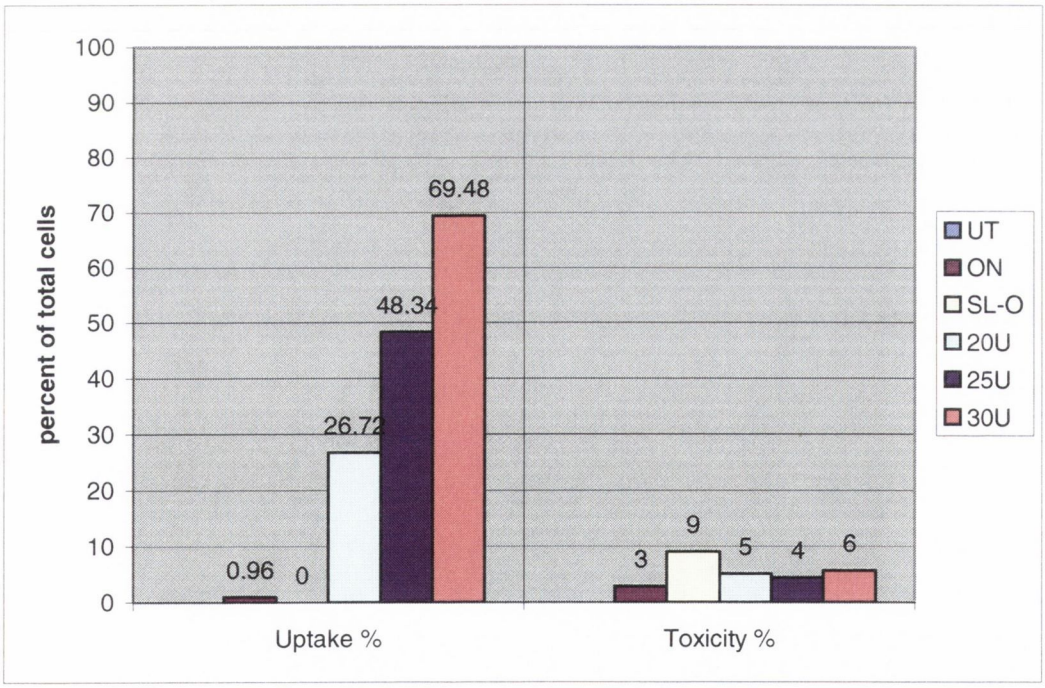


Figure 5.6 Uptake of the FAM-labelled P3 molecule into KYO-1 cells (% of total) and associated levels of cell toxicity

The 'ON' sample was treated with the antisense molecule in the absence of SL-O. The 'SL-O' sample contained no antisense molecules and determined the level of SL-O toxicity for each experiment. The '12U' & '14U' samples had the antisense molecule delivered to cells at 12U SL-O & 14U SL-O per $1X10^6$ cells respectively

A relatively high SL-O concentration range was employed to deliver P3 into KYO-1 cells and a maximum uptake level of 69.48% uptake was achieved. Cell viability remained high, indicating that the concentrations used were not toxic to the cells. Following delivery of the P3 phosphorothioate molecule into KYO-1 cells, b2a2 mRNA expression was assessed using TaqMan fluorescent PCR.

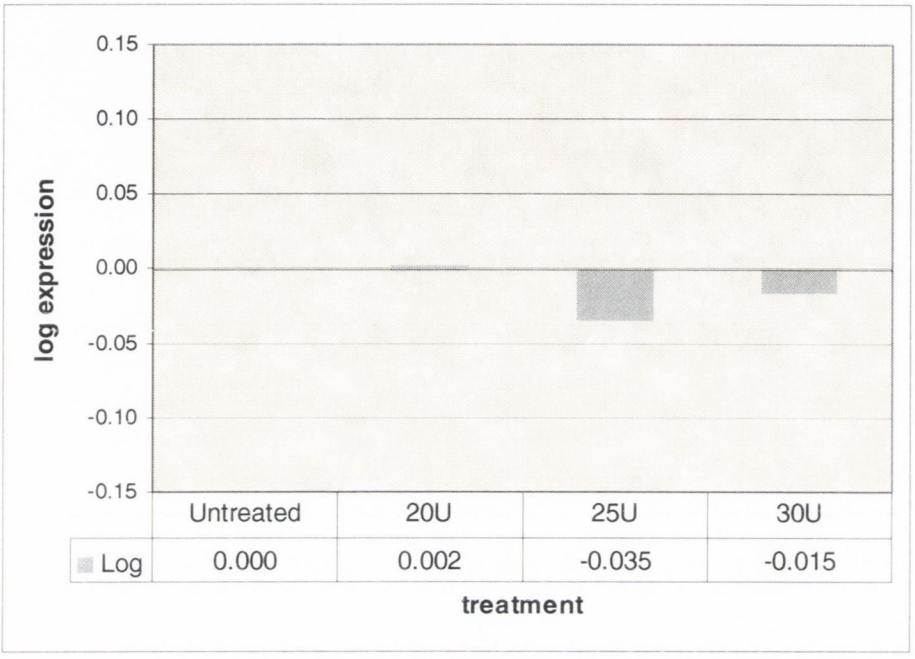


Figure 5.7 Reductions in b2a2 mRNA expression following treatment with 10μM P3 phosphorothioate molecule, introduced to cells using SL-O

Reductions in bcr-abl gene expression were quantified relative to expression of the house-keeping gene; GAPDH. The untreated sample (UT) shows the change in bcr-abl expression in untreated cells. The 'ON' sample was treated with the antisense molecule in the absence of SL-O. The 12U & 14U SL-O samples were treated with antisense molecule during cell permeabilisation mediated by 12U SL-O/1X10^6 cells and 14U SL-O/1X10^6 cells respectively.

As may be seen from Figure 5.7, minimal reductions in the level of b2a2 expression were detected using 10μM P3. The lack of activity is unrelated to low levels of delivery as an increase in delivery levels from 26.72% in the 20U sample to 69.48% in the 30U sample had little impact on mRNA down-regulation. For this reason, the concentration of P3 was increased to 20μM in an effort to promote binding to the b2a2 break-point.

20μM P3 was delivered to the b2a2 expressing KYO-1 cell line, and the uptake and toxicity data are detailed in Figure 5.8.

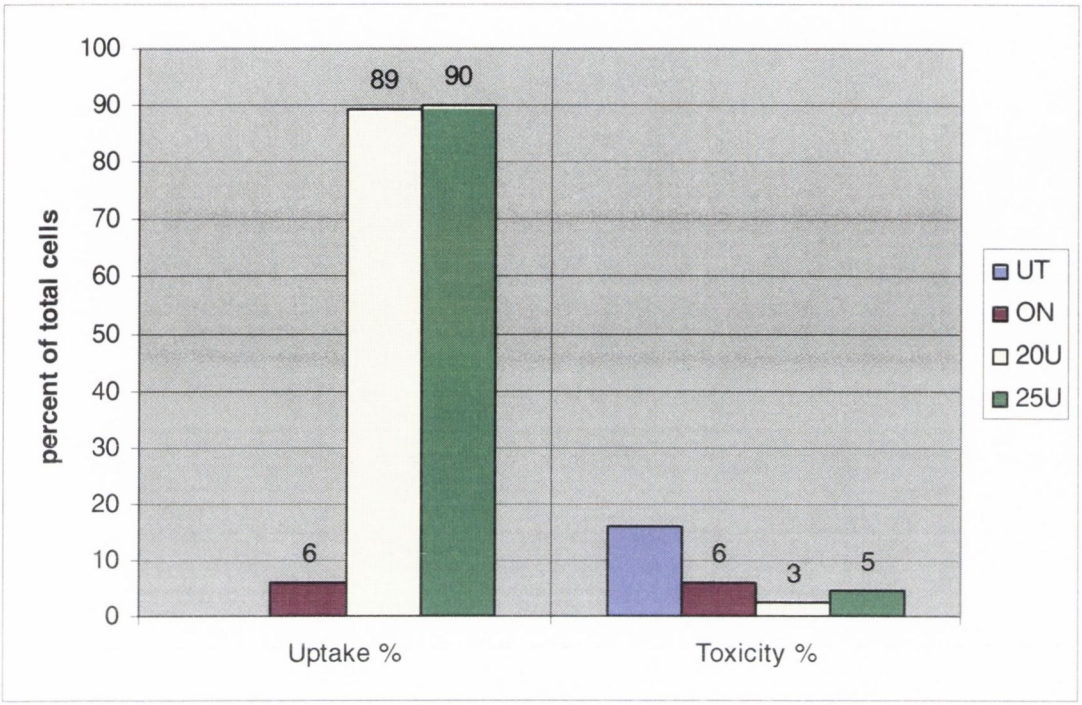


Figure 5.8 Uptake of 20μM FAM-labelled P3 molecules into KYO-1 cells using SL-O and associated levels of cell toxicity

The 'ON' sample was treated with the antisense molecule in the absence of SL-O. The 'SL-O' sample contained no antisense molecules and determined the level of SL-O toxicity for each experiment. The 20U & 25U samples were treated with antisense molecule following cell permeabilisation mediated by 20U SL-O & 25U SL-O/ 1X 10^6 cells. Values expressed are a percentage of the total number of cells in the permeabilisation step.

Following the delivery of 20μM P3 phosphorothioate molecule into KYO-1 cells, strong (0.46 log units) b2a2 inhibition was achieved (Figure 5.8). Increasing the concentration of oligonucleotide significantly increased the activity of P3. This increased effectiveness may have been aided by higher delivery efficiency of the 20μM samples where uptake was more effective than for the 10μM concentration (Figures 5.6 & 5.8).

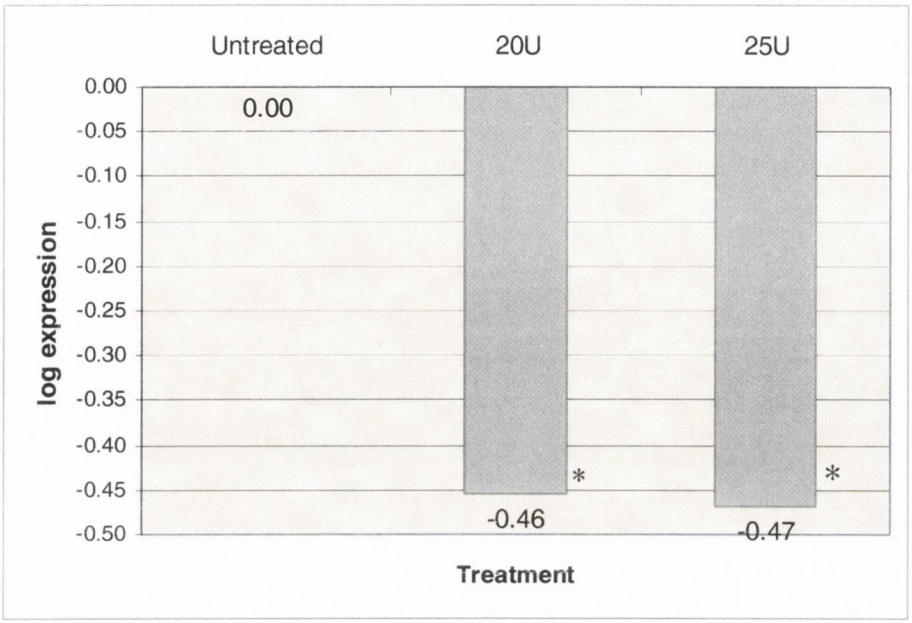


Figure 5.9 Log fold reduction in b2a2 bcr-abl expression relative to GAPDH following treatment with 20μM P3 phosphorothioate molecule (*p<0.01)

Reductions in bcr-abl gene expression were quantified relative to expression of the house-keeping gene; GAPDH. The untreated sample (UT) shows the change in bcr-abl expression in untreated cells. The 'ON' sample was treated with the antisense molecule in the absence of SL-O. The 20U & 25U SL-O samples were treated with antisense molecule during cell permeabilisation mediated by 20U SL-O/1X10^6 cells and 25U SL-O/1X10^6 cells respectively.

5.1.3 Targeting the b3a2 bcr-abl mRNA breakpoint using P2

The b3a2 bcr-abl break-point was specifically targeted using the P2 phosphorothioate antisense molecule (Table 3.1). Delivery was facilitated using the cell permeabilisation agent SL-O. Figure 5.10 details the uptake of P2 into the b3a2 expressing CML cell line; LAMA-84.

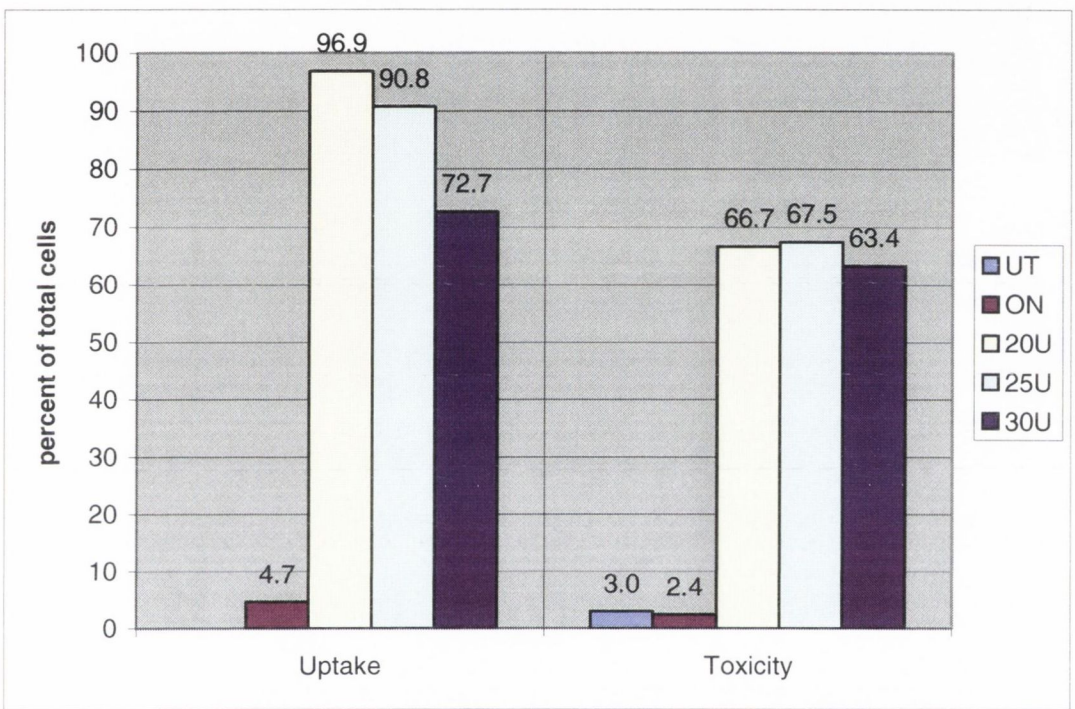


Figure 5.10 Viability & uptake levels of LAMA-84 cells following SL-O mediated delivery of FAM-labelled P2 phosphorothioate molecules

The 'ON' sample was treated with the antisense molecule in the absence of SL-O. The 'SL-O' sample contained no antisense molecules and determined the level of SL-O toxicity for each experiment. The 20U, 25U & 30U samples were treated with antisense molecule following cell permeabilisation mediated by 20U, 25U & 30U SL-O/ 1X 10^6 cells. Values expressed are a percentage of the total number of cells in the permeabilisation step.

At concentrations of 20, 25 & 30U, SL-O induced significant levels of cell toxicity in LAMA-84 cells (Figure 5.10). The viability of samples containing SL-O was reduced dramatically. P2 delivery was achieved in up to 97% of cells treated with an SL-O concentration of 20U. Due to high levels of P2 uptake, these samples were analysed for bcr-abl expression by RQ-PCR analysis.

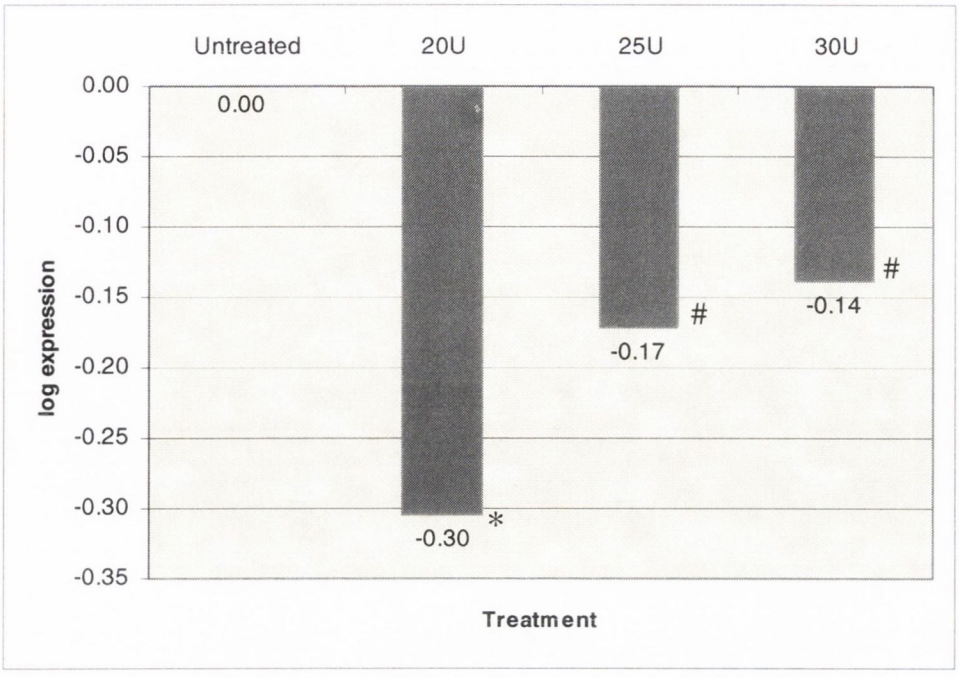


Figure 5.11 Log fold down-regulation of bcr-abl mRNA expression in LAMA-84 CML cells induced by 10μM P2 phosphorothioate antisense molecule

Reductions in bcr-abl gene expression were quantified relative to expression of the house-keeping gene; GAPDH. The untreated sample (UT) shows the change in bcr-abl expression in untreated cells. The 'ON' sample was treated with the antisense molecule in the absence of SL-O. P2 was delivered to LAMA-84 cells using 20, 25 & 30U SL-O per 1 X 10^6 cell, and treatment was performed for 24 hours prior to analysis ($P<0.01$, #$P<0.05$).*

Significant b3a2 mRNA reduction was achieved using the P2 antisense molecules (Figure 5.11). Delivery levels of 96% for the 20U sample resulted in a 0.3 log fold decrease in the levels of mRNA expression.

Due to the SL-O mediated toxicity observed with this range of concentrations, P2 was delivered using a lower range to examine potential down-regulation when the molecule is delivered with sub-toxic concentrations. 12U, 14U & 16U SL-O per 1 X 10^6 cells were employed to investigate P2 effectiveness at these concentrations. Delivery and toxicity results for this set of experiments are displayed in Figure 5.12.

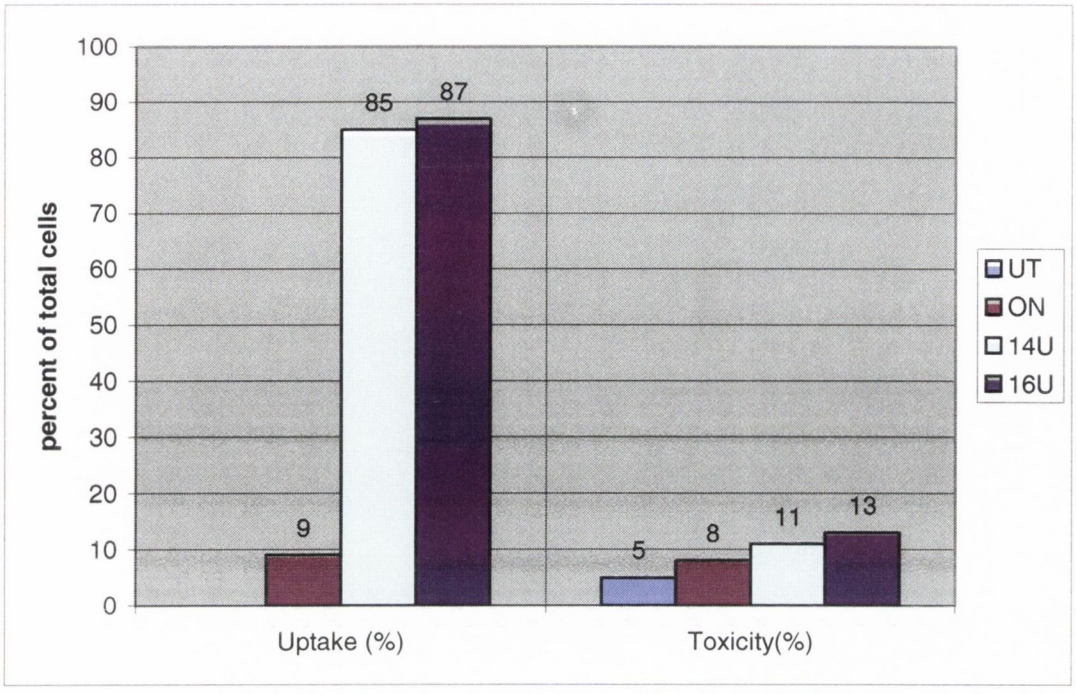


Figure 5.12 Uptake of the P2 phosphorothioate molecule into LAMA-84 CML cells using 14-16U SL-O per 1 X 10^6 cells and the levels of toxicity associated with the permeabilisation

'UT' is the untreated sample. The 'ON' sample was treated with the antisense molecule in the absence of SL-O. The 'SL-O' sample contained no antisense molecules and determined the level of SL-O toxicity for each experiment. Uptake and toxicity levels are expressed as a percentage of the total cells analysed.

Reducing the SL-O concentration to 14U & 16U per 1 X 10^6 cells lead to a significant decrease in cell toxicity. This was accompanied by strong levels of P2 uptake into LAMA-84 cells, where a minimum of 84% of cell uptake was reached. bcr-abl mRNA expression was examined relative to that of the house-keeping gene GAPDH, and the extent of mRNA reduction induced by P2 is shown in Figure 5.13.

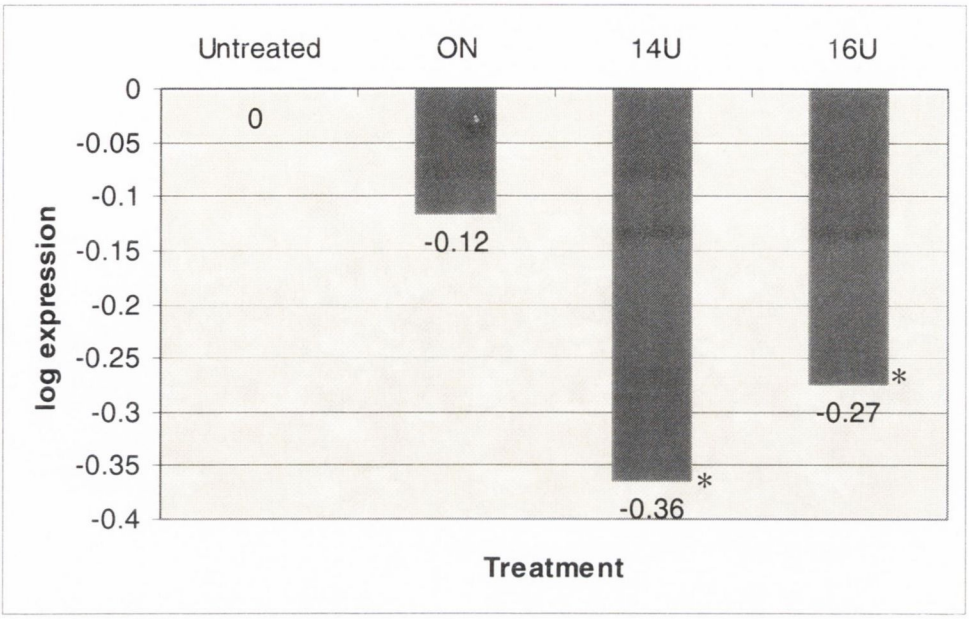


Figure 5.13 Log fold reductions in b3a2 bcr-abl expression following treatment with the P2 phosphorothioate antisense molecule

*Expression levels are expressed relative to those of the house-keeping GAPDH. The untreated sample (UT) shows the change in bcr-abl expression in untreated cells. The 'ON' sample was treated with the antisense molecule in the absence of SL-O. P2 was delivered to LAMA-84 cells using 14-16U SL-O and treatment was carried out for 24 hrs prior to analysis. (*P<0.01)*

The P2 antisense molecule was observed to induce reductions in the expression of b3a2 (Figure 5.13). The strongest down-regulation was seen for the 14U sample, with a -0.365 log fold reduction. The sample treated with P2 in the absence of delivery agent was observed to have entered approximately 10% of cells (Figure 5.12), and this produced a measurable effect on b3a2 expression. As the level of cell delivery was examined following cell permeabilisation, further uptake may have occurred during the incubation period and this would contribute to the down-regulatory effects observed. Though this illustrates the potential for antisense use without the aid of delivery enhancers, the success rate compared to SL-O delivered P2 molecules was minimal. Levels of bcr-abl down-regulation induced by P2 with the lower range of SL-O concentrations were less intense than those observed for the 20-30U samples (Figure 5.11).

A second b3a2-expressing CML cell line, K562 was also investigated to evaluate the efficacy of P2. Delivery of P2 into this cell line is detailed in Figure 5.14.

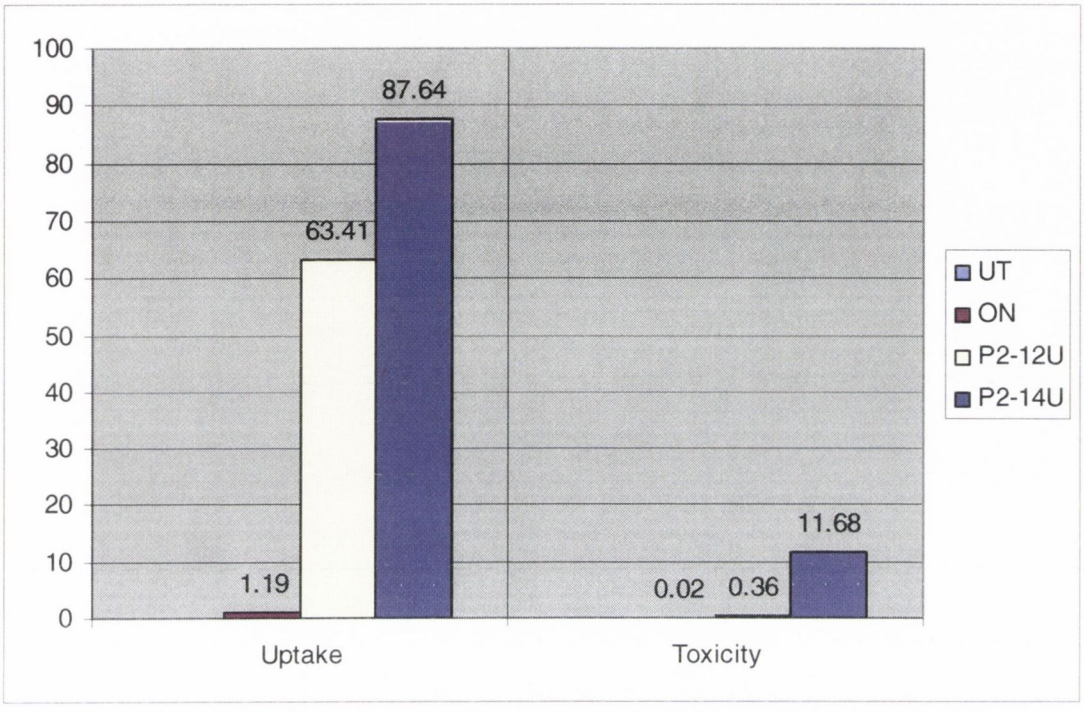


Figure 5.14 Uptake of the P2 phosphorothioate molecule into K562 cells using SL-O and associated levels of cell toxicity

'UT' is the untreated sample. The 'ON' sample was treated with the antisense molecule in the absence of SL-O. The 'SL-O' sample contained no antisense molecules and determined the level of SL-O toxicity for each experiment. Uptake and toxicity levels are expressed as a percentage of the total cells analysed. P2 was delivered to K562 cells using 12U & 14U previously optimised concentrations for this cell line.

SL-O induced high levels of uptake of P2 into K562 cells (Figure 5.14). Increasing the SL-O concentration from 12U per 1X 10^6 cells to 14U per 1X 10^6 cells, induced higher levels of uptake; though this considerably increased the levels of cell toxicity (Figure 5.14).

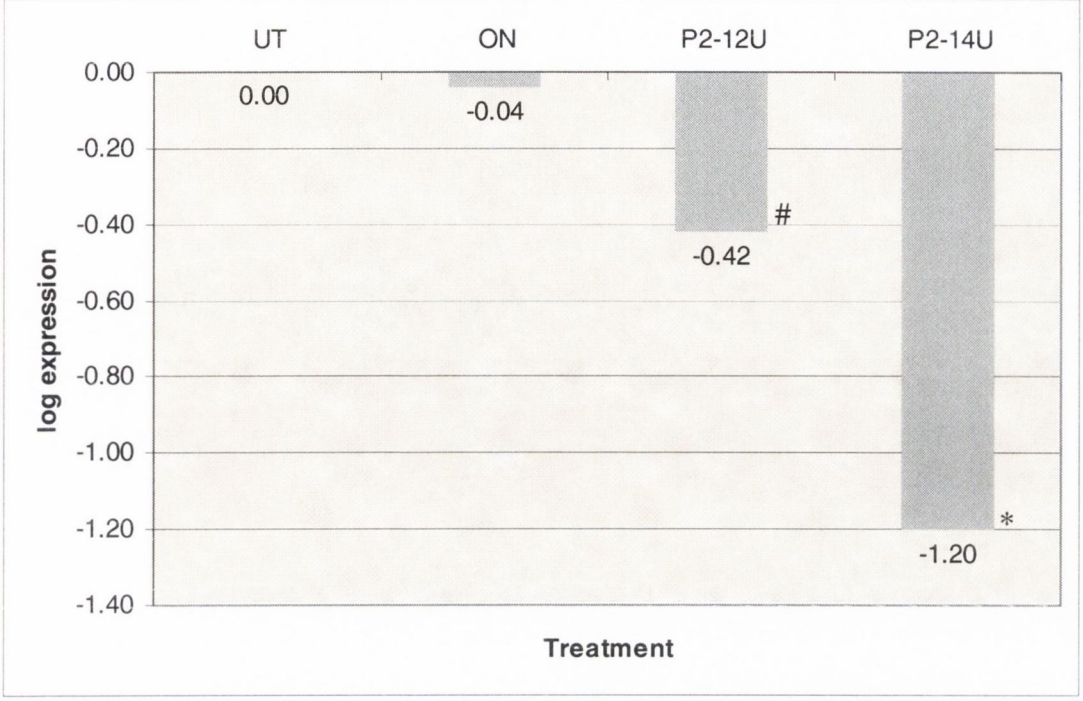


Figure 5.15 Log fold reduction in bcr-abl b3a2 expression in K562 cells following treatment with the P2 phosphorothioate molecule

The untreated sample (UT) shows the change in bcr-abl expression in untreated cells. The 'ON' sample was treated with the antisense molecule in the absence of SL-O. b3a2 expression was analysed using TaqMan fluorescent PCR and levels were normalised to those of the GAPDH house-keeping gene($*p<0.0001$, $\#p<0.05$).

P2 induced strong reductions in the level of bcr-abl expression in K562 cells (Figure 5.15). Increased delivery from 63% uptake with 12U SL-O to 87% uptake with 14U SL-O had a strong impact on the efficiency of P2 to mediate b3a2 down-regulation (Figure 5.15). In the absence of delivery agent the ability of P2 to mediate mRNA down-regulation is severely limited (Column 2-ON).

5.2 The 'PS' Phosphorothioate Series

To improve antisense mediated down-regulation of bcr-abl expression when targeting the CML specific breakpoints a second set of phosphorothioate sequences were designed to target b2a2 and b3a2. These were analysed in conjunction with both sense and scrambled controls to ensure sequence specificity of observed results. Control oligonucleotides were designed to minimise secondary structure and mimic the availability of bases for hybridisation to those present in the targeting antisense molecule.

Antisense activity depends on efficient delivery of antisense molecules for a sufficient length of time to down-regulate mRNA expression such that there is an effect on protein expression. The half-life of both the mRNA and protein are crucial factors in determining the duration and possible frequency of treatment (Spiller *et al,* 1998). For this reason, cell lines were treated with phosphorothioate antisense oligonucleotides for varying lengths of time, before the effects on mRNA expression levels were assessed. Assays were performed at 24-hour intervals, ranging from 24-120 hours, during which cells were supplemented with fresh medium every 48 hours.

Two antisense molecules were selected to target the b3a2 breakpoint, these were tested concurrently. As with the 'P' series of oligonucleotides, the results for each 'PS' experiment were calculated by comparison to the ratio between bcr-abl and GAPDH in the untreated cells. The uptake of the FAM-labelled molecules was monitored by a combination of fluorescent microscopy and flow cytometry.

Delivery of antisense molecules into cells using SL-O provides a convenient method of determining the effect of antisense treatments. However, this form of delivery is not largely applicable, particularly *in vivo,* and most forms of delivery to date show limited efficacy or potential draw-backs. Moderate levels of mRNA down-regulation were observed when antisense molecules in the 'P' series were administered to cells in the absence of delivery agent. The potential for phosphorothioate antisense molecules to gain cell entry and mediate effects unaided was further explored with these molecules.

5.2.1 PS2 mediated b2a2 down-regulation

PS2 was the second phosphorothioate molecule designed to target the b2a2 bcr-abl breakpoint (Table 3.2). The P3 molecule, also designed to target this region exhibited limited ability to down-regulate bcr-abl expression at standard concentrations (Figure 5.7). PS2 molecules were delivered to KYO-1 cells using SL-O and the treatment was performed for various time-points. Uptake and toxicity results are detailed in Figure 5.16.

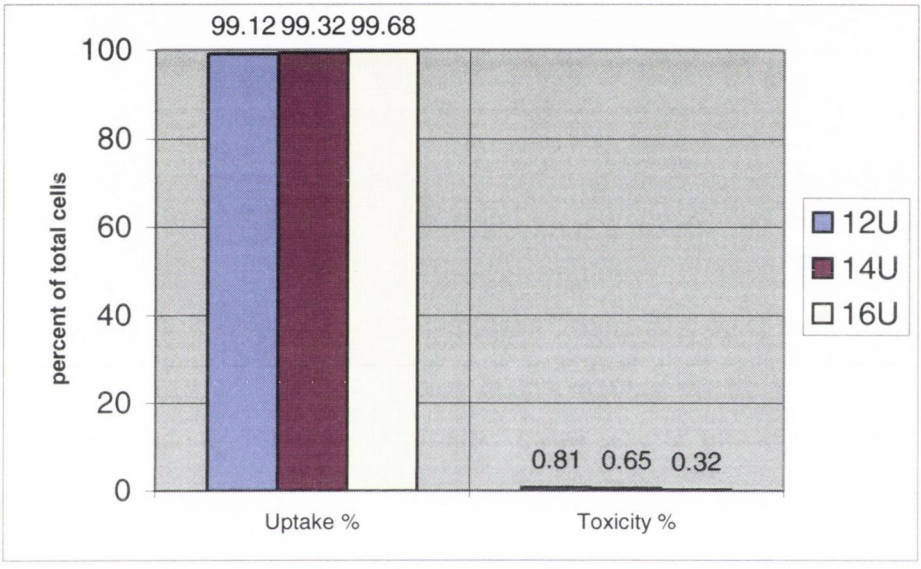


Figure 5.16 Uptake of FAM-labelled PS2 antisense molecules into KYO-1 CML cells using 12, 14 & 16U SL-O & associated levels of cell toxicity

Cellular delivery of PS2 molecules into KYO-1 cells was very efficient with delivery achieved to greater than 99% of target cells using each of three SL-O concentrations (Figure 5.16). The high efficiency uptake was associated with low levels of cell toxicity. In all cases toxicity was below 1%, within the 5% boundary.

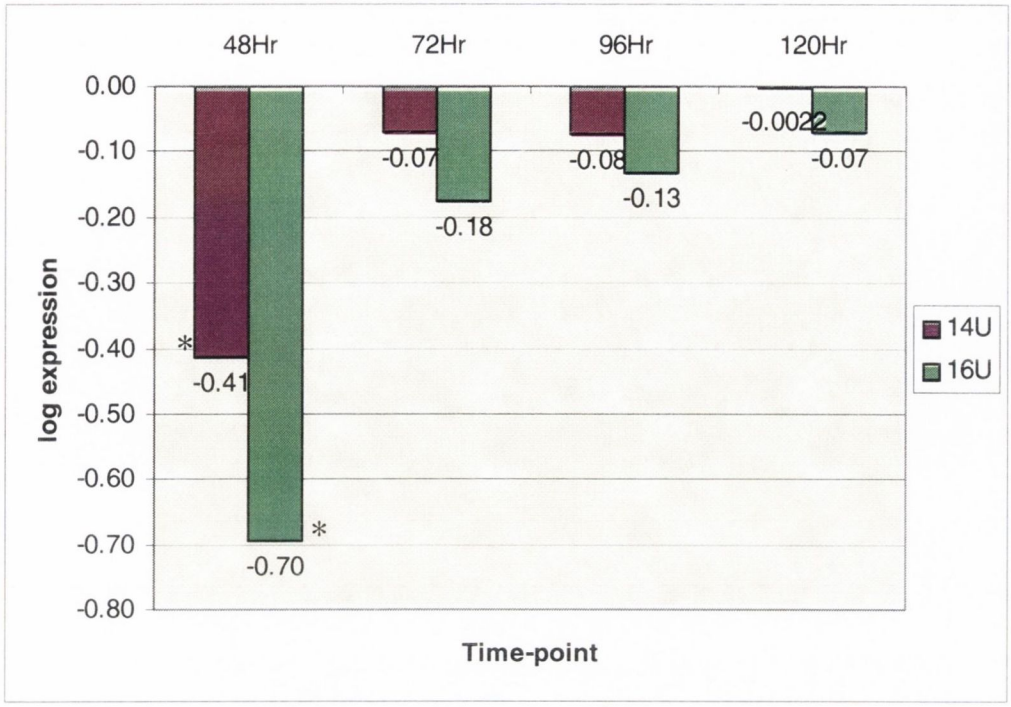


Figure 5.17 b2a2 down-regulation induced by the PS2 phosphorothioate antisense molecule over 48, 72, 96 & 120Hrs

*PS2 was delivered to KYO-1 cells in culture using 14U & 16U SL-O per 1X10^6 cells. mRNA expression analysis was performed on the TaqMan 7700 real-time PCR & expression was normalised to that of the GAPDH house-keeping gene (*14U-$p<0.01$, 16U-$p<0.05$)*

The PS2 molecule mediated significant reduction in b2a2 expression over a number of time-points (Figure 5.17). Maximum down-regulation was detected at 48 hours; however inhibition was evident up to 120 hours for the sample treated with 16U SL-O. During the range of time points investigated, the cells treated with PS2 and 16U SL-O showed increased levels of activity relative to when the PS2 molecule was delivered with 14U SL-O. Thus more effective mRNA down-regulation achieved by the PS2 antisense molecule may persist for longer times.

5.2.2 PS2 mediated mRNA down-regulation in the absence of delivery agent

The ability of PS2 to mediate mRNA suppression in the absence of SL-O mediated delivery was analysed during the 48-120 hour time-course. A peak in down-regulation induced by the naked PS2 occurred following 72 hours treatment, this was significantly later than the peak observed for the SL-O-delivered samples.

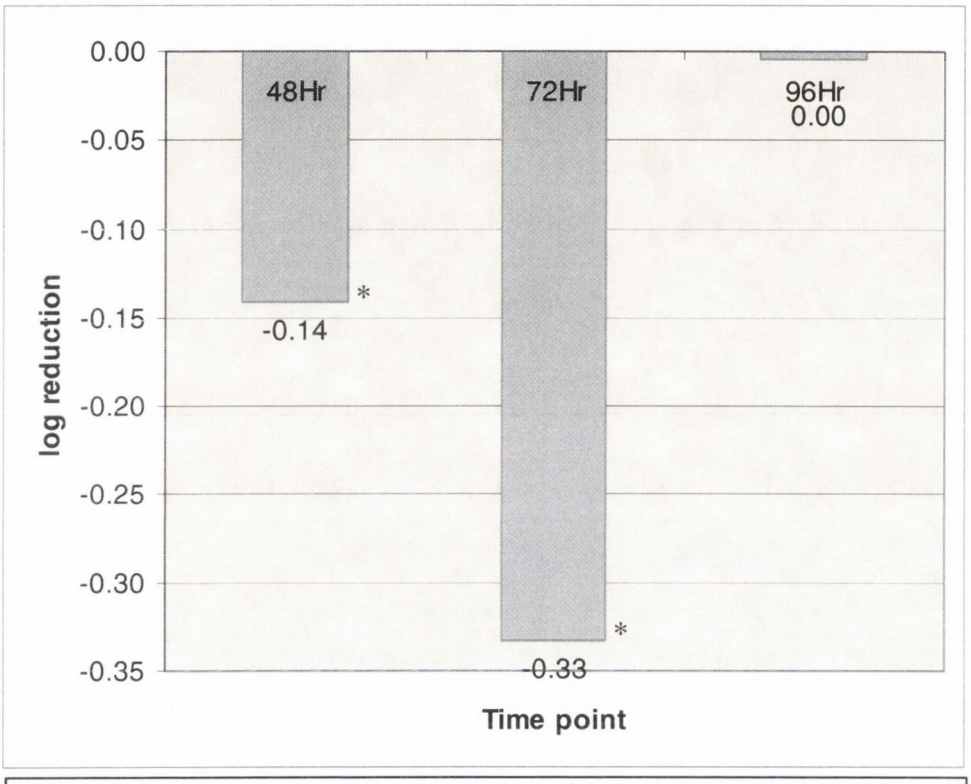


Figure 5.18 Log fold decrease in b2a2 expression induced by PS2 molecules in the absence of delivery agents

PS2 molecules were incubated with KYO-1 cells in the absence of SL-O during the permeabilisation step ($p<0.01$)*

The naked PS2 molecule resulted in a 0.33 log fold decrease in b2a2 expression in the absence of delivery agent (Figure 5.18). By the 96 hour treatment, b2a2 mRNA levels had increased to pre-treatment levels and no further effect was observed thereafter.

5.2.3 The effect of non-specific PS2 controls on b2a2 expression

'Sense' (SE) and 'scrambled' (SR) sequence controls were designed for each set of 'PS' oligonucleotides and tested concomitantly with the antisense molecules (Figure 5.19). Details of 'PS' sequence controls are given in Table 3.2. Antisense down-regulation is a result of sequence specific mRNA interactions and is unrelated to binding of sequence motifs to other cellular components.

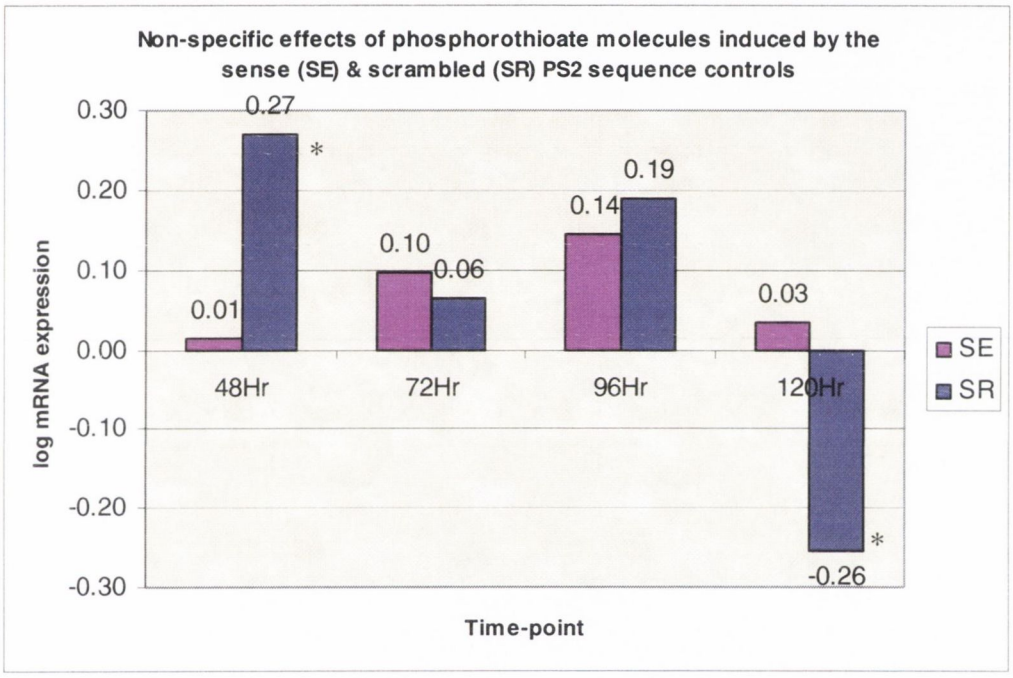


Figure 5.19 Log changes in bcr-abl gene expression induced by non-sequence specific sense and scrambled controls

Changes in gene expression were calculated as for the test samples; with reference to expression of the house-keeping gene GAPDH. Sequence controls were set-up alongside antisense sequences and changes in gene expression for each time-point were analysed on the same plate as antisense test sequences ($p<0.01$).

The PS2 phosphorothioate controls induced variable alterations in the level of bcr-abl expression relative to GAPDH. The strongest of these were induced by the scrambled control which exhibited strong alterations in the gene expression over the range of time-points examined.

5.2.4 PS3 mediated inhibition of b3a2 mRNA expression

The ability of the PS3-a and PS3-b phosphorothioate antisense oligonucleotides to down-regulate gene expression was investigated using the K562 cell line, which expresses the b3a2 translocation. A time-course experiment was carried out examining b3a2 expression at 24, 48 and 72 Hr intervals. Uptake efficiency of the PS3 molecules into K562 cells using SL-O for each of these time-points in displayed is Figure 5.20.

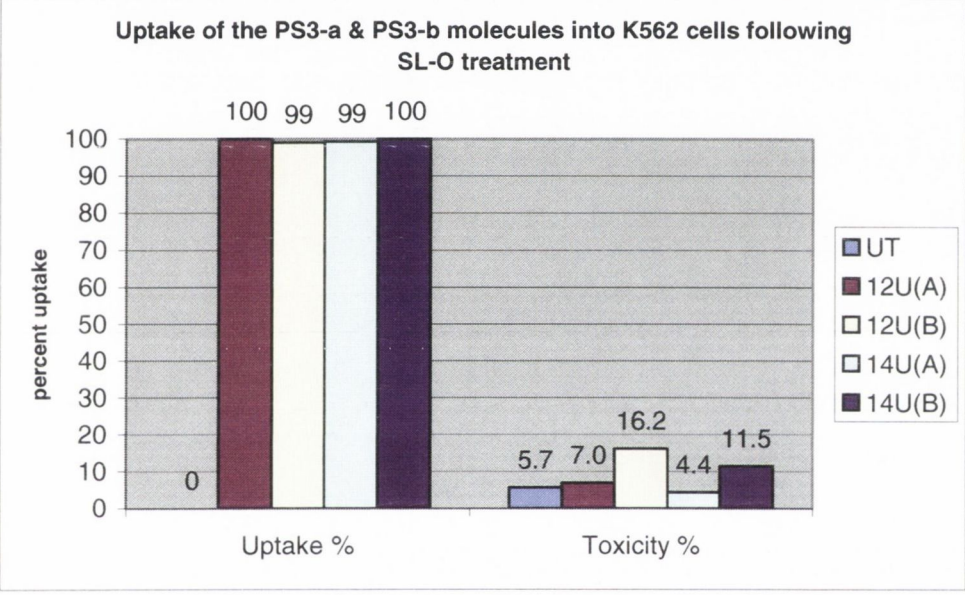


Figure 5.20 Uptake of the PS3 a & b phosphorothioate molecules into K562 cells in culture using 12U & 14U SL-O per 1 X 10^6 cells and associated levels of toxicity

'UT' is the untreated sample. Uptake was induced with 12U & 14U SL-O per 1 X 10^6 cells, and values given are expressed as a percentage of the total number of cells analysed.

Excellent levels of cellular delivery of the PS3 molecules were achieved into K562 cells (Figure 5.20). The main difference between these two molecules; which both target the b3a2 break-point region, was their level of secondary structure, the PS3-a molecule has 2 A:T bond pairs whereas the PS3-b version has 2 stronger G:C bonds plus a partial G:T bonding. However, the latter has a higher G:C content and a resulting higher Tm value.

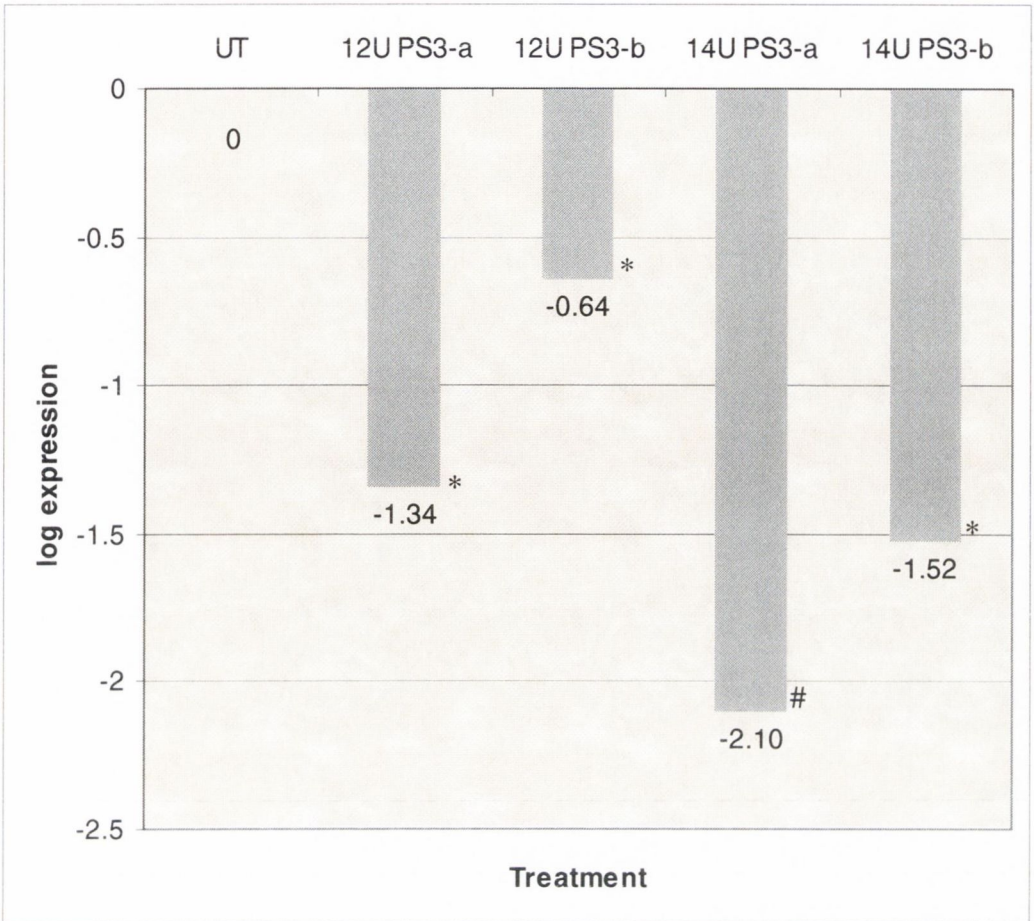


Figure 5.21 Log fold bcr-abl down-regulation induced by the b3a2 specific, fluorescently labelled PS3-a and PS3-b phosphorothioate molecules

The untreated sample (UT) shows the change in bcr-abl expression in untreated cells. Changes in gene expression were analysed relative to those of the GAPDH house-keeping gene and are expressed in log scale. Each molecule was delivered using 12U & 14U SL-O per 1 X 10^6 cells ($p<0.05$, #$p<0.01$)*

Following PS3-a & PS3-b delivery into K562 cells; changes in bcr-abl expression were analysed using TaqMan RQ-PCR (Figure 5.21). Both b3a2 directed phosphorothioate molecules were seen to induce strong levels of target transcript destruction with peak down-regulation of -2.10 log units seen for the PS3-a molecule. High levels of cell delivery were reflected in significant down-regulation of bcr-abl by both PS3-a & PS3-b. Two samples had 100% uptake of molecules into cells following permeabilisation; this reduces the level of molecule degraded outside the cell and internally in endosomal complexes, leading to increased potency for hybridisation and mRNA destruction.

The impact of non-labelled PS3 molecules on b3a2 expression

Previously, antisense molecules analysed in this study were FAM-labelled to detect their levels of cellular delivery and correlate this with effects on gene expression. However, reports indicate that bulky fluorescent labels on antisense molecules may impede molecular interaction and therefore decrease the potency of down-regulatory responses (Holen et al 2003). For this reason, non-fluorescently labelled PS3-a and PS3-b molecules were obtained and their effect on b3a2 expression was determined. Each molecule was examined individually for its ability to reduce b3a2 expression, and the two molecules were combined to examine any additive effects.

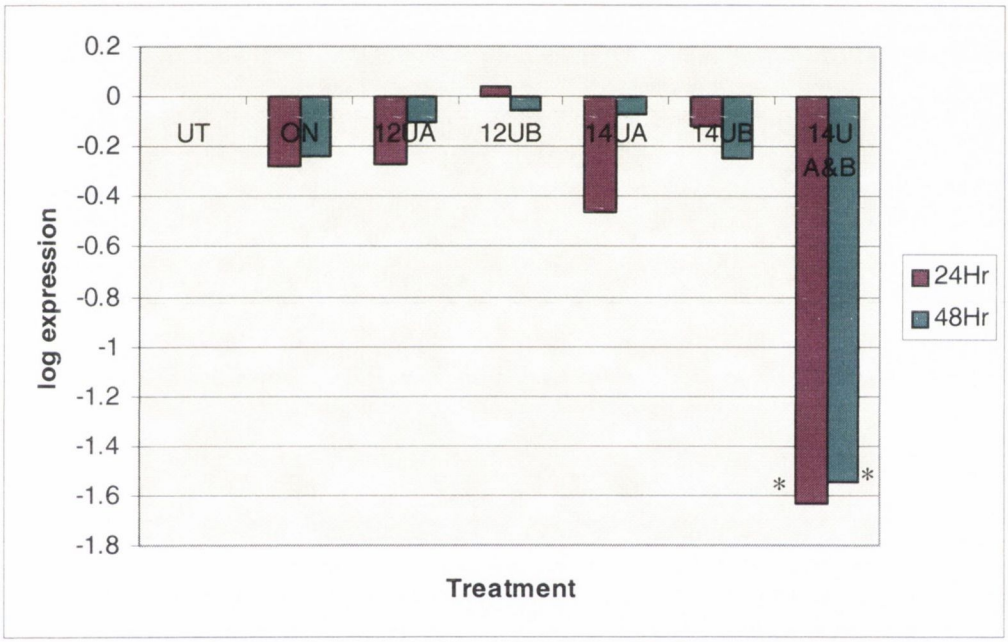


Figure 5.22 Bcr-abl (b3a2) down-regulation induced by the PS3-a & PS3-b phosphorothioate molecules following 24Hr & 48Hr treatments

*The untreated sample (UT) shows the change in bcr-abl expression in untreated cells. Down-regulation is expressed in log scale. Both the PS3-a & PS3-b molecules were delivered to K562 cells using 12U & 14U SL-O, and b3a2 expression has been normalised to that of the GAPDH house-keeping (*p<0.01).*

Levels of down-regulation induced by the two b3a2-targeted molecules are lower than those in Figure 5.21; when uptake was quantifiable and this may relate to decreased levels of uptake. A synergistic effect was observed when the two molecules were combined. As levels of uptake are unavailable it is unclear if this is in part attributable to enhanced delivery.

5.3 Discussion

5.3.1 Summary & discussion of 'P' phosphorothioate experiments

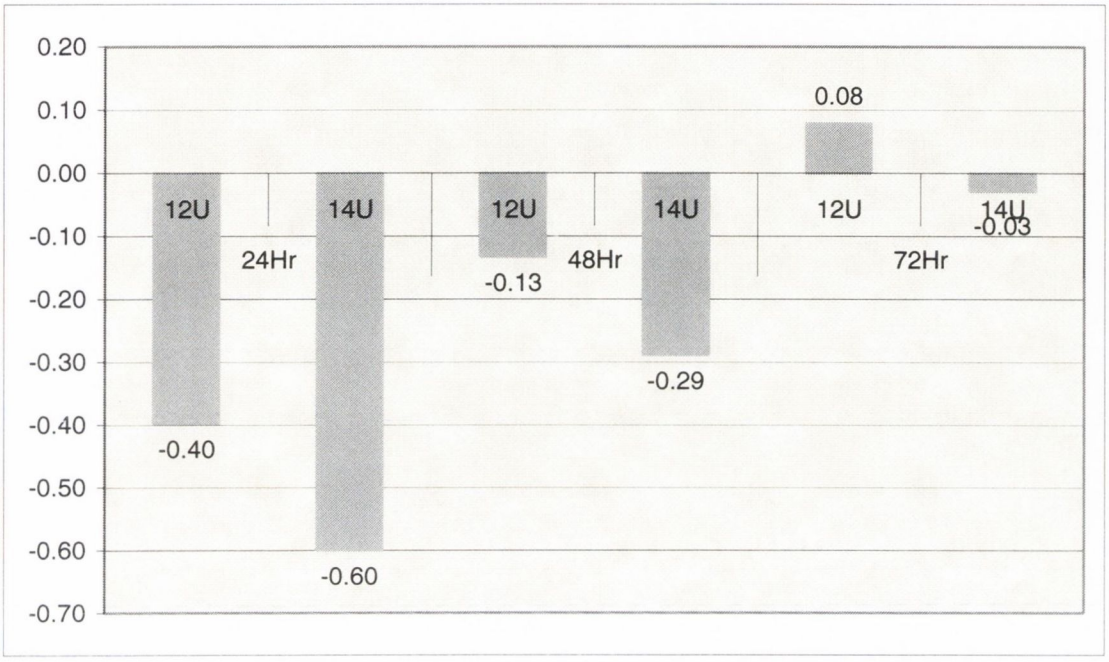


Figure 5.23 bcr-abl mRNA log fold reduction induced by P1 after 24, 48 & 72Hrs treatment

Optimal bcr-abl mRNA down-regulation was evident 24 hours following delivery of the P1 phosphorothioate molecule to K562 cells (Figure 5.23). After this time-point, the down-regulatory effect diminished gradually, though delivery for the 48 & 72 hour experiments was more efficient (Figure 5.1 & 5.3). By 72 hours, the expression levels had recovered completely and no antisense effect could be observed. The lack of antisense activity may be due to degradation of the phosphorothioate backbone at this time-point (Askari *et al,* 1996). These results indicate that increasing the quantity of antisense molecule delivered to the cell had a measurable impact on down-regulation potential. Each of the time-points examined for P1 showed a stronger mRNA down-regulatory response when a higher concentration of delivery agent was employed (Figure 5.23).

The uptake of P3 antisense oligonucleotides into KYO-1 cells was relatively efficient; with low levels of toxicity observed, these samples were examined by TaqMan RQ-PCR to assess the effect of the P3 antisense molecule on bcr-abl b2a2 expression. Relative decreases in bcr-abl gene expression following 10μM P3 treatment were moderate, with a minimum expression index of 0.92 (Log=-0.03) observed.

To determine whether a higher concentration of antisense would improve down-regulatory efficiency of the P3 molecule; a 20μM antisense treatment was employed. A higher concentration would increase the likelihood of interaction between the antisense molecule and its target mRNA and may be expected, at least in part, to overcome the poor binding caused by the presence of secondary structure, or to compensate for low binding affinities of the phosphorothioate backbone. This high concentration of phosphorothioate oligonucleotides would not be suitable for routine antisense treatments due to the potential intensity of secondary effects. The 20μM treatment was employed to identify why P3 shows only moderate down regulation of its mRNA target.

In contrast to the 10μM treatment, significant reductions in b2a2 mRNA expression were achieved when 20μM P3 was employed (Figure 5.9). The reason for this may have been a combination of overcoming poor hybridisation, either at the mRNA breakpoint or in the antisense molecule itself. Another possibility is that the higher concentration of P3 may increase the number of transcripts that can be targeted at any one time. The observed increase in effectiveness would suggest a combination of these factors.

The initial P2 treatments performed on LAMA-84 cells were delivered using 20U, 25U and 30U SL-O / 1 X 10^6 cells. These produced significant down-regulation of bcr-abl relative to GAPDH, with a log value of 0.3 at 20U (Figure 5.11). LAMA-84 cell toxicity at these concentrations of SL-O was substantial (Figure 5.10). These cells are particularly sensitive to the toxic effects of SL-O and viability decreased to less than 40%. A lower range of SL-O concentrations was tested (14U & 16U), for toxicity and effectiveness in down-regulation of gene expression. High uptake levels were reached for these samples

(86%) and toxicity was moderate (Figure 5.12). These SL-O concentrations represent the optimal of those tested for LAMA-84.

Down-regulation in the absence of delivery agents may occur due to escape of antisense molecules from endocytic vesicles following endocytosis (Figure 5.18). The level of down-regulation induced by this route related to the amount of oligonucleotide cell entry immediately following the permeabilisation step, where a high concentration of oligonucleotide was incubated with the cells. However, following this the antisense molecule was still able to gain access through receptor mediated endocytosis and fluid phase endocytosis and this may result in higher levels of uptake of the naked molecule. Complete uptake of this kind was not detected as samples were examined directly following delivery. Antisense down-regulation may also be limited by degradation of oligonucleotides in the endosomal complex. The delay in down-regulation may be associated with the passage of the molecule through these pathways.

The P1 phosphorothioate oligonucleotide, which was targeted towards the bcr-abl translational start site induced strong reductions in bcr-abl mRNA expression. Cytosolic delivery by the permeabilisation protein SL-O strongly enhanced presence of P1 inside the nuclear compartment and played a vital role in the ensuing mRNA degradation. The mRNA start site was one of the more challenging regions for hybridisation by antisense molecules. This evolutionary conserved area poses accessibility and specificity issues relating to sequence specificity and presents limitations to hybridisation in the form of potential secondary structure and binding of tertiary groups e.g. transcription factors to this region (Brown *et al,* 2003).

The most dramatic decrease in bcr-abl mRNA expression was observed using the b3a2 specific P2 molecules (Figure 5.15). This is in contrast to the b2a2 specific P3 molecule where no specific effects were attributable to antisense down-regulation at 10μM (Figure 5.7). This lack of activity may correspond to decreased hybridisation due to mRNA secondary structure and antisense secondary structure. To specifically down-regulate b2a2 expression a more suitable molecule needed to be designed.

The efficacy of P2 was also analysed in the K562 cell line. b3a2 expression was substantially inhibited in K562 cells by the P2 phosphorothioate antisense molecule (Figure 5.15). This down-regulation was more effective than that observed when targeting another b3a2 bcr-abl cell line, LAMA-84 with the same molecule; P2 (Figure 5.13). Comparable levels of cell delivery were achieved for both cell lines using 14U SL-O treatment; however the K562 cell line proved more sensitive to the P2 treatment as a 1.20 log fold reduction was induced compared to 0.3655 log fold reduction in the LAMA-84 sample.

5.3.2 Discussion of 'PS' phosphorothioate molecules

Strong reductions of the b2a2 target mRNA were produced following introduction of the PS2 molecules to KYO-1 cells using SL-O (Figure 5.17). Optimal down-regulation of –0.70 log units was induced 48 hours after PS2 was delivered to KYO-1 cells using 16U SL-O. This down-regulation was approximately 0.3 log units more effective when compared to the sample delivered with 14U SL-O. The intensity of down-regulation was observed to correlate with the length of time required to restore normal levels of expression (Figure 5.17). When b2a2 expression was decreased by 0.4 log units, within 96 hours expression levels had returned to normal. However, when expression was decreased by >0.7 log units, a reduction in gene expression was still observed following 96 hours (Figure 5.17).

The ability of the PS2 molecule to enter the cell and mediate mRNA down-regulation in the absence of delivery agents was assessed in comparison with SL-O delivered molecules. b2a2 down-regulation with a log value of 0.33 was detected following 72 hours treatment in the absence of delivery agents (Figure 5.18). This down-regulation was less than half that observed when PS2 was delivered with SL-O (Figure 5.17). The transient nature of this down-regulation induced by endocytosed molecules is a reflection of the barriers the antisense molecule must overcome to interact with its target, substantial proportions of the molecule were presumably degraded and lost in the process.

Gene expression changes induced by the sense sequence control were low in intensity over the time-course tested. Log values range from 0.01 to 0.14, which was attributable to normal variations in gene expression between wells in the experimental set-up, and is of insufficient intensity to be considered as non-specific alterations (Figure 5.19). This sense control represents the active PS2 sequence in a complementary and reverse orientation; it contains the same percentage GC content and has an identical Tm to the antisense sequence. Application of this control indicated that the observed PS2 mediated down-regulation (Figure 5.17), is not as a result of non-sequence properties of the phosphorothioate molecule and may be attributed in full to sequence specific mRNA interaction.

Over each of the time-points measured, the scrambled 'SR' PS2 sequence control was observed to elicit a degree of non sequence-specific effect and in the majority of these the intensity of effects were significantly greater than those observed for the sense control (Figure 5.19). Changes in gene expression were seen as moderate to strong alterations and did not follow a traceable pattern. While the scrambled control contained the same proportion of GC's as the PS2 molecule and has the same Tm, sequence motifs, induced by the random shuffling of bases may have arisen. Three of the four time-points analysed for the scrambled control indicated an increase in the expression of bcr-abl relative to that of GAPDH, the mechanism for this observation is not clearly understood (Figure 5.19). This observation was in direct contrast to the results seen with the PS2 molecule. At 120 hours the scrambled control was seen to induce reductions in the relative gene expression. This effect did not correlate with the mRNA down-regulation evident for the PS2 molecule at these time-points.

Two phosphorothioate molecules were selected to target the b3a2 breakpoint in the 'PS' series (Table 3.2). These differed extensively in the level of *mfold* predicted secondary conformations (Figure 3.15). Following SL-O mediated delivery, high levels of uptake were achieved for both molecules in K562 CML cells (Figure 5.20). Both the PS3-a and PS3-b molecules were observed to induce strong levels of inhibition of b3a2 expression (Figure 5.21). The PS3-a induced superior levels of mRNA down-regulation when delivered using both 12U and 14U SL-O. This increased activity relative to PS3-b may have been due to the significantly lower levels of intra-molecular secondary structure present in PS3-a (Figure 3.15). However, despite strong levels of intra-molecular folding in PS3-b, including 2 G:C bonds and a G:T interaction, significant levels of down-regulation were still achievable. This activity may have been instigated by the six base pairs at the 3' end of the PS3-b molecule which are capable of hybridisation (Figure 3.15). Undoubtedly, PS3-b activity was enhanced due to the high delivery levels achieved. Levels of b3a2 down-regulation observed with PS3-a were superior to those observed when employing the P2 phosphorothioate molecule (Figure 5.15 & 5.21).

To determine if the presence of the FAM-label negatively impacted on the hybridisation and hence the ability to down-regulate gene expression; an unlabelled version of these molecules was delivered to K562 cells. Down-regulation induced by both PS3 molecules was not of the same level used as that achieved using FAM-labelled oligonucleotides. This is likely to be related to delivery as the ability of these molecules to hybridise and mediate down-regulation has been established (Figure 5.21). Using both PS3 molecules in combination lead to increased down-regulation of b3a2 target expression at both the 24 and 48 hour time-points (Figure 5.22). This augmented effect may be due to enhanced delivery of the sample or may represent a synergistic effect between the two molecules. The main draw-back of this approach was that uptake levels using SL-O; which exhibits variable activity, were unquantifiable.

Following 24 hours treatment with the two b3a2 break-point targeted phosphorothioate molecules; significant reductions in gene expression were evident (Figure 5.21). At this time-point the PS3-a molecule has heightened activity relative to its PS3-b counterpart shown by its stronger ability to mediate mRNA down-regulation. This increased efficiency relates to target binding due to minimal hampering by secondary structure. Combining the PS3-a and PS3-b molecules produces a dramatic drop in the level of b3a2 expression.

At 12U SL-O, the ability of PS3-b to mediate down-regulation appears to be limited by insufficient delivery and increasing the concentration of delivery agent to 14U SL-O had a measurable effect on its activity at both 24 and 48 hours (Figure 5.22). Following 48 hours treatment, the level of down-regulation induced by PS3-a was observed to decrease and the PS3-b molecule exhibited stronger efficiency. Down-regulation induced the PS3-a & PS3-b sample was maintained at a high level (>1.5 log units) following 48 hours.

5.3.3 Targeting the bcr-abl mRNA with phosphorothioate chemistry antisense molecules

Phosphorothioate chemistry oligonucleotides were employed to target the bcr-abl translational start site of bcr and two specific locations that are only present in CML cells;

the b2a2 and b3a2 breakpoints. The b2a2 mRNA breakpoint region presented a strong obstacle to antisense hybridisation due to secondary structure at this point, though a moderate peak in single stranded probability was observed around the breakpoint position (Figure 3.5). The P3 molecule exhibited high levels of intra-molecular secondary structure (Figure 3.13) and this resulted in inhibition of antisense activity (Figure 5.7). A second phosphorothioate based molecule, P2, which displayed significantly less secondary structure, was designed to specifically target b2a2 (Figure 3.14). Redesign of the b2a2 targeted phosphorothioate molecule proved highly successful in mediating down-regulation of this bcr-abl isoform (Figure 5.17). The increased activity of PS2 over P3 was attributable mainly to the level of secondary structure in the molecules, indicating that this factor can negatively impact the down-regulation potential of antisense molecules as well as mRNA target secondary structure.

Using *mfold* the b3a2 breakpoint was predicted to represent an accessible structure to antisense therapeutics (Figure 3.4). All three phosphorothioate molecules targeted to b3a2 induced down-regulation of gene expression (Figure 5.15 & 5.21). As with b2a2, the potency of b3a2 down-regulation was reduced by the presence of intra-molecular antisense base pairing rather than pre-existing mRNA folding. mRNA self-hybridisation did not appear to influence the level of down-regulation induced as both P2 and PS3-a molecules had the same level of secondary structure; 2 AT bonds, but the activity of PS3-a was much enhanced when compared to that of P2 (Figure 5.15 & 5.21). The difference in activity between these two molecules indicates that shifting the target position by even a small number of bases may have a significant effect. The limited activity of PS3-b with 2 GC bond pairs relative to PS3-a is likely to relate to intra-molecular antisense folding rather than mRNA secondary structure.

In summary, this phosphorothioate study identified several active antisense agents against the most suitable targets in CML cells, the bcr-abl translational start site and the b2a2 and b3a2 breakpoints. Though the phosphorothioate chemistry may exhibit distinct draw-backs in terms of non-antisense specific effects it induces, the identified sequence targets may be used to target bcr-abl when combined with alternative backbones.

VI

Translational Inhibition induced by RNase H-Independent Morpholino Antisense Molecules

6.1 Introduction to the Morpholino Backbone Experiments

An RNase H independent chemistry, the morpholino, was investigated as an alternative to the RNase H-dependent phosphorothioate antisense backbone. Morpholino antisense molecules consist of a six membered ring with a nitrogen group at the 3' position (Figure 1.8). This backbone chemistry is unrelated to those naturally occurring *in vivo* and its activity is not readily affected by cellular nuclease activity (Arora *et al,* 2002). It is therefore not subject to degradation by this route and this results in a prolonged life-span *in vivo.* Due to the artificial nature of the morpholino oligonucleotide it is incapable of activating cellular enzymes employed by other antisense backbone chemistries to mediate target destruction (Heasman *et al,* 2002). In the absence of enzymatic cleavage of targeted transcripts, the mechanism of action of morpholino backbone oligonucleotides involves inhibition of ribosomal translation of the target mRNA.

The morpholino chemistry was employed to improve the hybridisation properties of the antisense molecule and also to reduce non-specific interactions encountered when employing the phosphorothioate antisense approaches and thereby to minimise secondary effects (Morcos *et al,* 2001). Due to their uncharged backbone, morpholino molecules have minimal interaction with cellular components (Iversen *et al,* 2001). As the morpholino functions directly at the site of the ribosome, by forming a double stranded block in translation, optimal mRNA degradation induced by type of backbone occurs when it is targeted to the 5' region of the transcript. This limits the design of morpholino antisense molecules to regions of the mRNA which have secondary structure or may be bound by protein factors, however morpholino oligonucleotides offer the possibility of overcoming such structure and striking a balance between selection of targets and improved hybridisation is required.

Morpholino backbone antisense oligonucleotides inhibit translation of their target mRNA in a sequence specific fashion; however this does not reduce the quantity of mRNA transcripts in the cell. Inhibition of mRNA translation occurs and this results in a decrease in the levels of the target protein, therefore it is necessary to employ western blotting to detect antisense activity. Morpholino oligonucleotides analysed in this study are detailed in Table 3.3.

6.2 Cellular Delivery of Morpholino Chemistry Molecules

Upon entry to the cytosol, phosphorothioate oligonucleotide molecules are translocated to the nucleus which is the main site of interaction with their target mRNA (Fisher *et al,* 1993). This is due to the strong chemical similarity of the phosphorothioate linkage to the natural DNA phosphodiester linkages. As morpholino molecules do not translocate to the nucleus, the majority of delivered molecules remain in the cytosol. This cytosolic localisation is suited to the RNase H-independent mode of action of morpholino molecules, where translation of mRNA transcripts is sterically inhibited at the point of ribosomal assembly in the cytosol.

Due to their uncharged backbone, morpholino-based oligonucleotides do not encounter the same level of cell repulsion as the negatively charged phosphorothioate (Sazani *et al*, 2002). Passive entry of morpholino molecules across the cell membrane was reported to be feasible due to their chemistry (Arora *et al,* 2002; Sazani *et al*, 2002). Use of carrier molecules is limited due to the fact that non-ionic morpholino molecules will not complex with cationic lipids (Morcos, 2001). In order to assess the effectiveness of un-aided morpholino entry into cells, fluorescently-labelled morpholino molecules were incubated with CML cells and the level and mode of morpholino uptake was analysed.

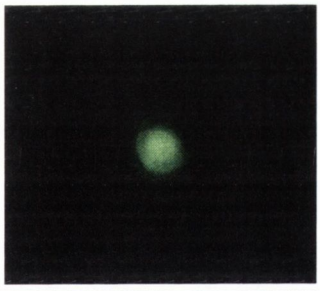
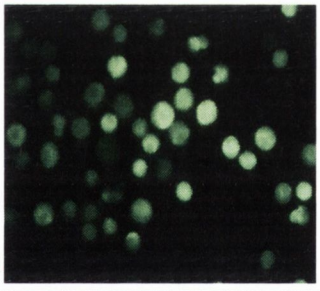
a  b 

Figure 6.1 a Fluorescent micrograph showing passive entry of morpholino chemistry ODN molecules to K562 cells.

b Fluorescent micrograph illustrating SL-O mediated morpholino ODN molecule entry into K562 CML cells in culture.

A non-endocytic sub-cellular localisation was observed for morpholino molecules incubated with K562 cells (Figure 6.1-a). However, levels of cell delivery were strongly enhanced when the cell permeabilisation agent SL-O, was employed (Figure 6.1-b). The diffuse cellular distribution pattern observed indicates that the sub-cellular location is outside the nucleus, allowing access of morpholino molecules to the mRNA in the cytosol.

6.3 MPL_bcr induces sequence specific down-regulation of the BCR-ABL protein (p210)

Following treatment of CML cells with morpholino antisense molecules, BCR-ABL (p210) protein levels were examined using western blotting. The control oligonucleotide employed in this experiment was a standard morpholino control whose sole target is in reticulocytes from thallasemic human cells having a splice generating mutation at position 705 in the β-globin pre-mRNA (Gene Tools). The control oligonucleotide will therefore not affect expression of any genes in normal cells and is employed to determine potential side-effects i.e. non-sequence specific effects of the morpholino chemistry.

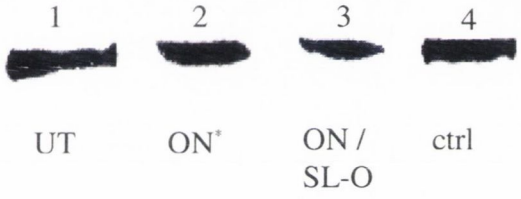


Figure 6.2 Down-regulation of BCR-ABL expression using 1 μM MPL_bcr morpholino molecule following 48 hours treatment

Lane 1 (UT) shows BCR-ABL in the absence of antisense administration
Lane 2 (ON) shows 1μM MPL_bcr in the absence of delivery agent
Lane 3 (1μM) shows BCR-ABL protein levels following introduction of 1μM MPL_bcr molecules with 12U SL-O
Lane 4(ctrl) shows BCR-ABL expression following treatment with a control sequence morpholino chemistry molecule

* *ON denotes oligonucleotide*

Treatment with the MPL_bcr morpholino molecule (at 1μM) induced moderate levels of BCR-ABL down-regulation following 48 hours (Figure 6.2). This was achieved when the MPL_bcr molecule was delivered to K562 cells using a concentration of 12U SL-O per 1 X 10^6 cells. Due to limited ability of morpholino molecules to gain entry to the cell, no down-regulation of BCR-ABL was observed when the cells were treated with morpholino molecules in the absence of delivery agent (Lane 2, Figure 6.2). No down-regulation of protein expression was observed with the standard morpholino control (Lane 4, Figure 6.2).

6.4 MPL_bcr induces dose dependent down-regulation of BCR-ABL

Morpholino targeting of the bcr-abl start site induced p210 protein down-regulation at 1μM (Figure 6.3). To achieve a more effective down-regulation of protein expression and verify the specificity of the morpholino antisense molecule, treatment with a higher concentration of morpholino oligonucleotides was performed. These treatments were analysed in conjunction with the sense sequence control. 1μM and 5μM MPL_bcr was delivered to K562 cells using SL-O and the effects on p210 protein expression were measured (Figure 6.4).

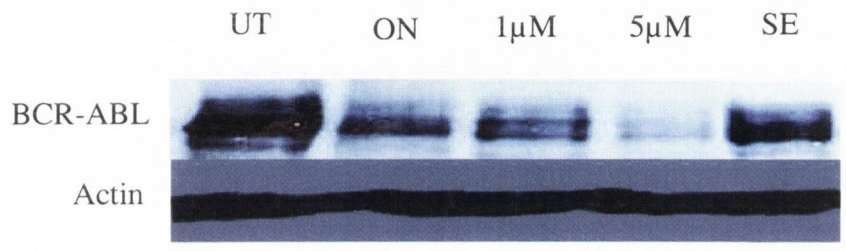


Figure 6.3 BCR-ABL (p210) protein down-regulation by bcr start site morpholino molecules is concentration dependent

Lane 1 (UT) is an untreated sample with no oligonucleotide and no SL-O
Lane 2 (ON) is treated with 5μM bcr start site morpholino and no SL-O
Lane 3 (1μM) is treated with 1μM bcr start site morpholino & 12 SL-O per 1 X 10^6 cells
Lane 4 (5μM) is treated with 5μM bcr start site morpholino & 12 SL-O per 1 X 10^6 cells
Lane 5 (SE) is treated with the sense morpholino sequence control & 12 SL-O per 1 X 10^6 cells

Following cellular delivery of the bcr-directed morpholino molecules, inhibition of BCR-ABL protein expression was detected at 1μM and 5μM concentrations (Figure 6.4). The potency of the morpholino molecule was strongly enhanced when the concentration was increased to 5μM. The level of BCR-ABL down-regulation was enhanced by SL-O delivery, (Compare Lane 2 & Lane 4). The lack of BCR-ABL down-regulation by the sense sequence control indicates the specificity of the antisense effect induced by morpholino chemistry oligonucleotides.

6.5 Morpholino Antisense molecules induce enhanced p210 down-regulation relative to the Phosphorothioate in KCL-22 cells

Potency of down-regulation of gene expression can be correlated directly with hybridisation potential (Sohail *et al,* 2000). The morpholino chemistry demonstrates high efficiency binding to mRNA and has been shown to reduce BCR-ABL protein expression (Figure 6.3). Phosphorothioate backbone antisense molecules also mediate strong reductions in bcr-abl mRNA levels (Figure 5.16). The ability of these backbone chemistries to mediate BCR-ABL down-regulation was compared directly to determine relative efficiencies (Figure 6.4).

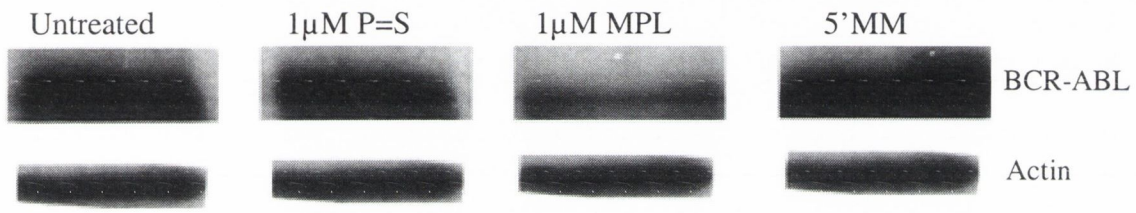


Figure 6.4 Expression of the BCR-ABL p210 protein in KCL-22 cells following 48 hours treatment with the RNase H competent phosphorothioate (P=S) and the RNase H independent Morpholino Oligonucleotide

Lane 1 (UT) is an untreated sample with no oligonucleotide and no SL-O
Lane 2 (P=S) is treated with 1μM P1 phosphorothioate & 12U SL-O / 1 X 10^6 cells
Lane 3 (MPL) is treated with 1μM bcr morpholino & 12U SL-O per 1 X 10^6 cells
Lane 4 (5'MM) is treated with the 5 b.p. mis-match control & 12U SL-O per 1 X 10^6 cells

P1 and MPL_bcr target the same region of the bcr-abl mRNA. P1 has phosphorothioate linkages and is 18 base-pairs in length while the MPL_bcr is morpholino based and is 25 base pairs in length. Comparison of the ability of these two molecules to mediate BCR-ABL down-regulation at the same concentrations indicates that the morpholino shows a higher efficiency (Compare Lane 2 & Lane 3). The 5'MM is the MPL_bcr sequence with 5 base pairs substituted in a manner which retains the same overall GC content and Tm of the molecule (Table 3.3). Lack of a change in gene expression following treatment with this control indicated that the MPL_bcr induced down-regulation in a sequence specific manner (Lane 4, Figure 6.4).

6.5.1 Morpholino oligonucleotides induced enhanced BCR-ABL down-regulation relative to Phosphorothioate oligonucleotides over a range of concentrations

The ability of morpholino oligonucleotides to reduce BCR-ABL protein expression over a range of concentrations was investigated in K562 cells. These samples were run in parallel to and compared to the same range of phosphorothioate concentrations. Oligonucleotides were delivered to K562 cells using 12U SL-O per 1 X 10^6 cells.

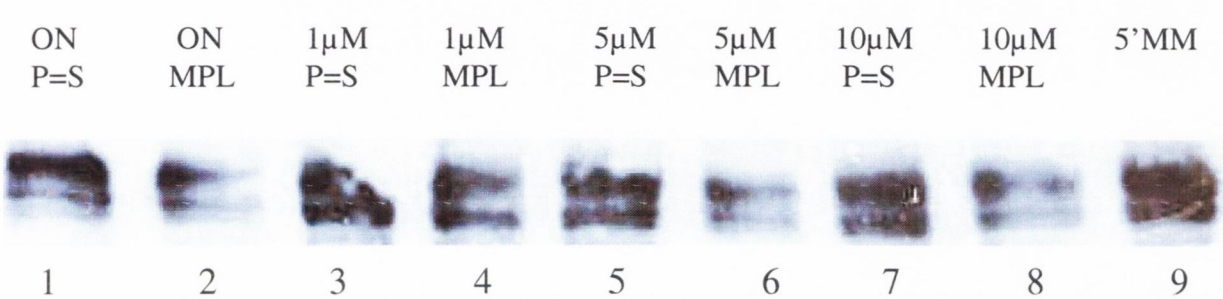


Figure 6.5 Comparison of the ability of phosphorothioate and morpholino antisense molecules to mediate inhibition of BCR-ABL protein expression over a range of oligonucleotide concentrations (1μM, 5μM & 10μM)

Lane 1 *BCR-ABL expression following treatment with 5μM P1 in the absence of delivery agent*

Lane 2 *BCR-ABL expression following treatment with 5μM MPL_bcr in the absence of delivery agent*

Lanes 3, 5 and 7 were treated with 1μM, 5μM and 10μM P1 phosphorothioate molecule respectively and were delivered using 12U SL-O per 1 X 10^6 cells.

Lanes 2, 4, 6, and 8 were treated with increasing concentrations of the MPL_bcr morpholino molecule.

Lane 9 was treated with the morpholino 5 base pair mis-match sequence control 5'MM.

Over the range of oligonucleotide concentrations tested, the morpholino-based antisense molecule induced a more efficient down-regulation of bcr-abl gene expression than its phosphorothioate counterpart (Figure 6.5). The ability of the phosphorothioate based P1 molecule to mediate down-regulation was minimal following 48 hours treatment (Figure 6.5).

6.6 BCR-ABL (p210) down-regulation is not accompanied by significant changes in the proliferative capacity of CML cells

Despite significant reductions in BCR-ABL protein expression at these concentrations, little impact on proliferative capacity was detected. This finding was in contrast to observations by other groups which cite significant reductions in proliferation following p210 down-regulation (Skorski *et al,* 1994). The lack of observed proliferative effects is possibly due to insufficient blocking of p210 expression.

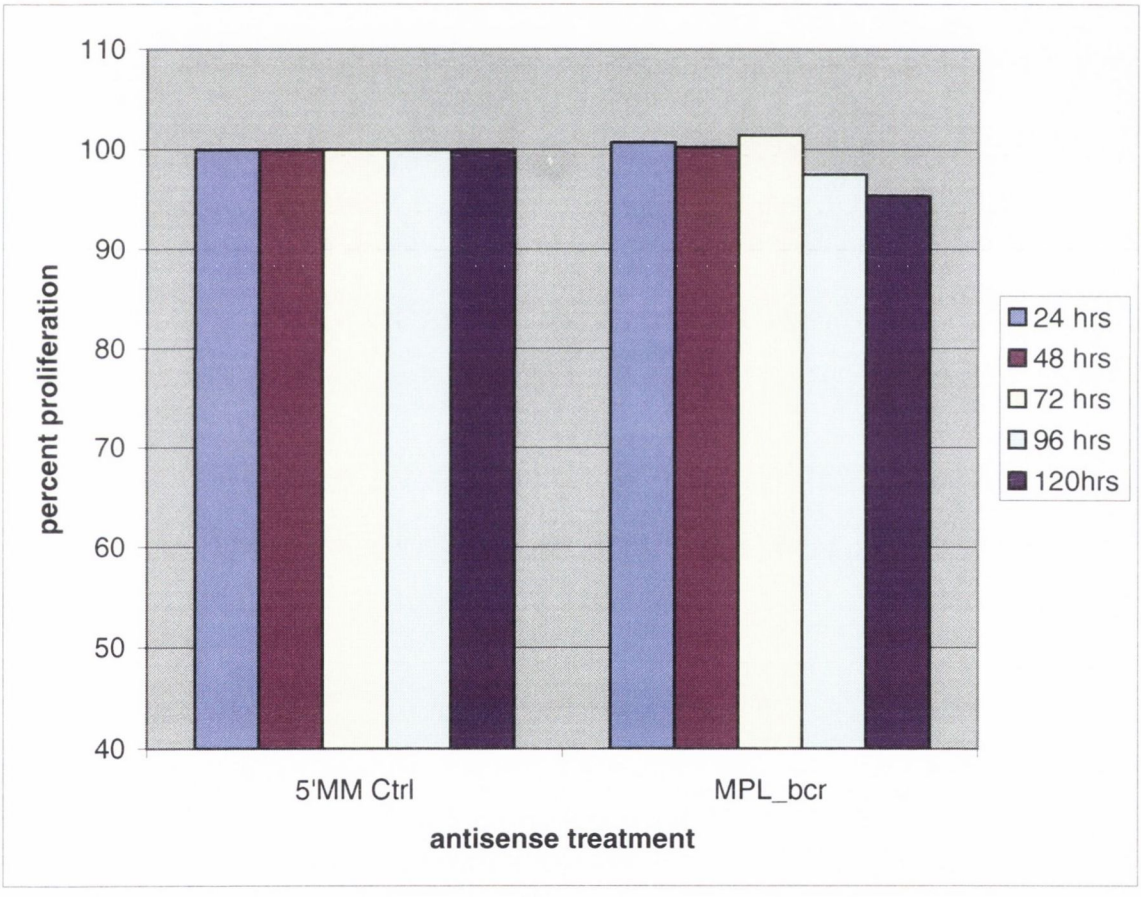


Figure 6.6 Proliferative capacity of CML cells following treatment with bcr-abl directed morpholino molecules over a range of time-points

The levels of down-regulation achieved were compared to the proliferative levels of the standard control morpholino sequence delivered using SL-O at each time-point examined

6.7 The influence of morpholino chemistry antisense oligonucleotides on haematopoietic cell proliferation

The application of novel antisense chemistries necessitates demonstration that they are safe, non-toxic and do not hinder or alter the normal growth cycle of cells. CFU-GM assays, which measure the ability of haematopoietic cells to expand and proliferate *ex vivo,* were used to assess the potential secondary effects of morpholino antisense molecules. No significant changes in colony number were observed for any of the donor samples tested.

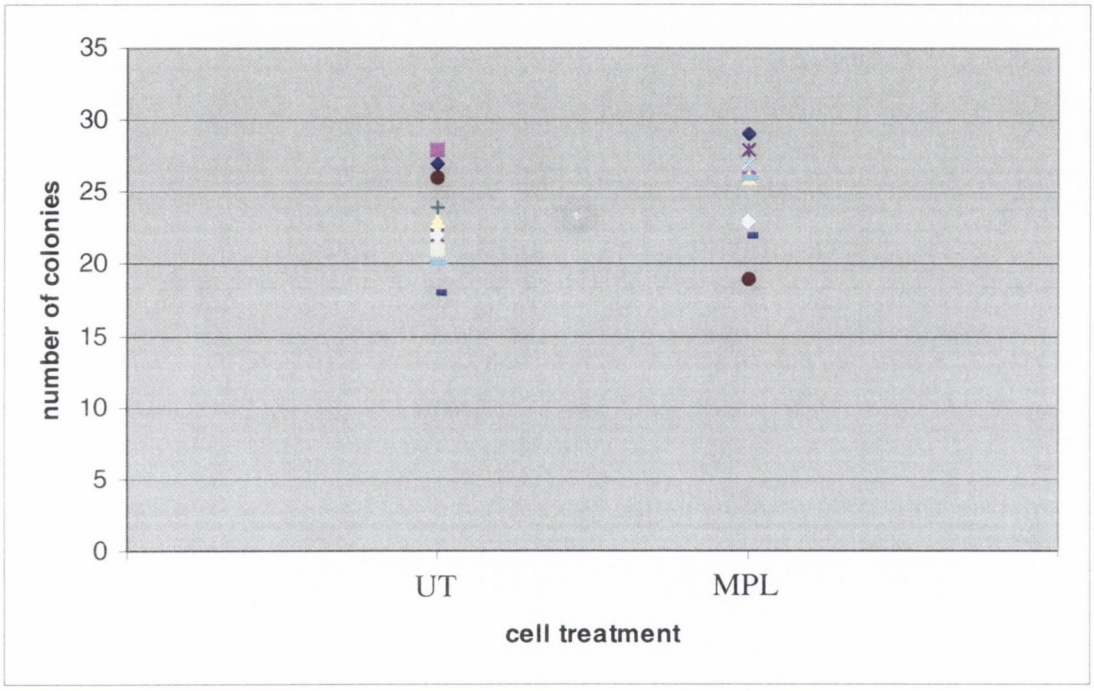


Figure 6.7 CFU-GM colony formation following incubation of primary haematopoietic cells in the absence and presence of morpholino antisense oligonucleotides

Symbols represent the average of three counts from each donor sample (n=10). Colony formation was assessed following 14 days incubation to allow expansion of cells in methylcellulose medium. A colony was defined to contain at least 40 cells.

6.8 Discussion

Facilitation of interaction of morpholino antisense molecules with mRNA requires direct contact and the site of interaction should be predominantly in the cytosol. Due to their non-polar nature, morpholino molecules may passively enter cells to a limited extent, however levels of uptake were found to be strongly enhanced by SL-O cell permeabilisation (Figure 6.1). SL-O mediated rapid entry of morpholino molecules into cells and increased the overall cellular concentrations of morpholino molecules; this undoubtedly resulted in the enhanced down-regulation that was observed. Apart from cell permeabilisation, other methods of delivery have been harnessed to mediate morpholino entry into cells. These include conjugation of morpholino molecules to arginine-rich peptides which significantly enhanced their cellular uptake and antisense activity (Moulton *et al,* 2004).

The MPL_bcr molecule was observed to induce down-regulation of BCR-ABL protein expression (Figure 6.3). Down-regulation at the protein level indicated a strong and prolonged antisense effect at the mRNA level induced by morpholino chemistry oligonucleotides. The intensity of down-regulation was strongly enhanced when the concentration of morpholino molecule was increased to 5μM and this concentration was optimal for BCR-ABL down-regulation (Figure 6.3). When phosphorothioate and morpholino molecules were compared directly, using molecules targeted to the same region on the mRNA, at equal concentrations and under identical delivery conditions, the morpholino antisense molecule was consistently superior to the phosphorothioate based antisense molecule (Figure 6.4). The increased efficiency of the morpholino based molecule remained consistent when the molecules were each examined over a range of oligonucleotide concentrations (Figure 6.5).

The standard morpholino chemistry, sense and 5 base-pair mis-match controls were employed in this study to assess sequence-specificity and potential side-effects of the MPL_bcr molecule. Controls demonstrated no significant decrease in the levels of target protein, indicating the results observed represent a sequence specific down-regulation by the morpholino antisense (Figure 6.3, 6.4, 6.5). This finding is in contrast to effects seen when employing the phosphorothioate controls, which were found to induce non-specific sequence

effects at the mRNA level (Fig 5.20). Partial or transient binding of morpholino molecules to mRNA sequences with partial complementarity will not result in down-regulation of gene expression, as the low affinity interaction will be displaced by ribosomal machinery during translation. The stability of the morpholino sequence controls, indicates that morpholino based compounds may be used *ex vivo* or potentially *in vivo* to induce sequence specific down-regulation. The inert nature of the morpholino backbone also means that binding to other components of the cell e.g. cellular proteins will not occur to any significant degree. Sequences present at the mRNA translational start site are highly conserved in eukaryotic systems (Brown *et al,* 2003). The employment of appropriate morpholino controls may identify chemistry and sequence related secondary effects on the expression of the target and reference protein expression.

Significant reductions in BCR-ABL protein expression were detected following treatment with 5μM MPL_bcr molecule (Figure 6.3). The proliferative capacity of K562 cells following MPL_bcr treatment was assessed using the MTS assay (2.11). However, over a wide range of time-points analysed (24 – 120 hours), no significant reduction in the growth capacity of these cells was detected (Figure 6.6). This finding indicates that in this study, down-regulation of BCR-ABL alone was insufficient to mediate growth arrest. This is in contrast to findings which suggest that as a direct consequence of BCR-ABL down-regulation, apoptosis was induced in CML cells (Skorski *et al,* 1994). However, other research has suggested that transient BCR-ABL down-regulation may not be sufficient to induce reductions in proliferation and down-regulation of other components or chemotherapeutic intervention would be required to drive CML cells into apoptosis (Verfaillie *et al,* 1999).

Morpholino molecules perform consistently well in the presence and absence of serum and may persist for prolonged periods inside the cell as they are highly resistant to enzymatic degradation (Hudziak *et al,* 1996). This is in contrast to the phosphorothioate, which binds albumin and other abundant cellular proteins leading to decreased activity in serum containing mediums (Lebedeva *et al,* 2000). Degradation of phosphorothioate molecules also necessitates repeated dosing; this is likely to present much less of an issue with the morpholino and may aid its suitability for *in vivo* studies. The enhanced down-regulation observed in this study implies an increased hybridisation efficiency of morpholino oligonucleotides compared to phosphorothioate oligonucleotides. While in theory one phosphorothioate molecule can recruit RNase H to potentially degrade numerous transcripts;

the results obtained in this study indicate that this approach did not result in significant protein down-regulation presumably due to an insufficient level of activity for an appropriate period of time (Figure 6.5).

Morpholino antisense oligonucleotides demonstrated no inhibitory effect on the proliferation of normal primary haematopoietic stem cells *ex vivo* (Figure 6.7). This implies that morpholino oligonucleotides may be feasible for employment in *ex vivo* purging of CML cells. Recently, a phosphodiamidate morpholino antisense molecule, AVI-4126 was evaluated in a phase I safely trial in humans (Iversen *et al,* 2003). This trial demonstrated that morpholino molecules administered by the intravenous route were safe to employ and displayed no toxicity or serious adverse effects. This study is an important advance in the progression of antisense research. It represents the first occasion where an antisense molecule without a phosphorothioate component has entered antisense clinical trials. Hopefully the promise it shows in relation to safety will be fulfilled by corresponding success in down-regulating gene expression. The activity of this molecule against its c-myc target has been evaluated in the PC-3 human prostate cancer xenograft murine model. A 75-80% reduction in tumour burden was observed in AVI-4126 treated animals compared to scrambled oligomer controls (Iversen *et al,* 2003).

Hybridisation of antisense molecules to their target sequence is a key step in antisense down-regulation (Sohail *et al,* 2000). This process is limited by the availability of active antisense molecules in specific sub-cellular compartments where they may hybridise with their target. The morpholino backbone displays high affinity binding to mRNA, its hybridisation potential is several fold greater than that of the phosphorothioate backbone based on thermal duplex denaturation experiments (Summerton, 1999). The extent of the down-regulation is significant with almost complete inhibition of target protein following 48 hours treatment (Figure 6.4). This down-regulation can be attributed to the increased hybridisation efficacy of the morpholino backbone. Efficient binding is correlated with an increased sensitivity to antisense activity; therefore antisense molecules with strong binding potential may require lower concentrations to induce down-regulation.

The use of RNase H independent backbones is at present in the early stages of development, particularly in relation to clinical applications. Several research groups have harnessed a combination of positive effects from both RNase H dependent and independent types of

backbone, e.g. the use of a chimeric methylphosphonate - phosphorothioate hybrids have proved successful (Giles *et al,* 2000). However, this retains RNase H activation to mediate mRNA down-regulation. The use of a 'truly' RNase H independent backbone not dependent on enzymatic cleavage has many potential advantages. Primarily, RNase H-independent antisense molecule design is open to novel structures, which could have positive effects on their binding efficiency. More stable and enzymatically resistant structures are feasible leading to increased life span *in vivo.* Lower antisense concentrations could potentially be used to achieve the same degree of down-regulation. This is an expanding and exciting area of antisense research which in time has the potential to surpass its RNase H dependent counterpart by providing a safe, non-toxic and specific mode of gene down-regulation.

VII

RNA-Interference (RNAi)-mediated bcr-abl down-regulation

7.1 Introduction

RNA interference (RNAi) is an endogenous system of regulating expression of mRNA with complementary dsRNA sequences. Target transcript sequences are identified by binding of exogenously derived dsRNA molecules to the RNAi machinery. dsRNA molecules are key intermediates in the genomic replication of many viruses but are not normally found in eukaryotic cells. Upon dsRNA binding the RNAi machinery is activated to cleave mRNA transcripts in a sequence-directed manner. The process occurs in a cyclic manner mediating the destruction of numerous mRNA transcripts containing the target sequence until the RNAi process is complete (Scherr *et al,* 2003).

RNAi was employed to induce bcr-abl mRNA transcript destruction using short interfering RNA (siRNA) molecules. Four siRNA duplexes were employed to target different regions on the bcr-abl mRNA transcript. Using duplexes targeted to distinct regions of the mRNA may facilitate selection of the most appropriate site for siRNA activity. All the siRNA binding sites were located in the bcr segment of the hybrid transcript to avoid disruption of normal c-abl translation. Characteristics of the siRNA molecules used to target bcr-abl in this study are outlined in Table 3.5.

bcr-abl-directed siRNA duplexes were selected by Dharmacon on the basis of their functionality. Active siRNA sequences are considered to have inherent inhibition ability and are capable of reducing target gene expression levels by 50% following 24 hours at low concentrations. Whether or not target site conformation is a factor in the selection process in unclear.

Phosphorothioate and morpholino molecules induced reductions in bcr-abl at the mRNA and protein levels respectively (Figure 5.22 & Figure 6.4). However, reductions in cell proliferation capacity have been limited (Figure 6.6). The application of multiple antisense oligonucleotides to induce increased expression knock-down has been demonstrated with bcr-abl directed phosphorothioate molecules. This indicates that a combined approach targeting discrete and distinct areas of the mRNA transcript either alone or in combination may prove effective.

The cell permeabilisation agent Streptolysin-O (SL-O) was employed to deliver the siRNA duplexes to CML cell lines, using concentrations previously optimised for each of the particular cell lines. As with the phosphorothioate and other antisense chemistries, the attachment of label groups such as FAM to siRNA species has been indicated to have a negative effect on their potential for down-regulation (Holen, 2002/3). For this reason, the siRNA duplexes S1-S4 are not fluorescently labelled, and therefore uptake of these molecules for individual experiments are non-quantifiable.

The main aim of this part of the study was to assess the potential of optimally designed oligonucleotides which function via RNA interference to mediate down-regulation of bcr-abl mRNA species. As well as delivery limitations, the availability and identification of suitable hybridisation targets on the mRNA may impede the effectiveness of antisense molecules.

The mRNA down-regulation of the S1-S4 siRNA duplexes was compared to their *mfold*-predicted hybridisation. Though several publications cite molecules designed by the *mfold & sfold* selection criteria ('t Hoen *et al,* 2002), the best criteria to use when employing molecular prediction approaches to antisense design still needs to be defined. A total of four siRNA duplexes were employed to target the bcr-abl mRNA at distinct sites. Integration of target site analysis with TaqMan determination of mRNA destruction may yield relevant information on the requirements for successful interaction with the target and specific down-regulation of the mRNA sequence.

7.2 siRNA mediated bcr-abl mRNA down-regulation

The impact of the bcr-directed siRNA molecules was assessed in the b2a2 expressing CML cell line, KYO-1. Each siRNA was delivered using a concentration of 14U SL-O and the activity of each duplex was assessed individually. The feasibility of employing naked siRNA molecules (i.e. molecules incubated without a delivery agent) to mediate bcr-abl down-regulation was also explored and results of these experiments are detailed in Figure 7.1.

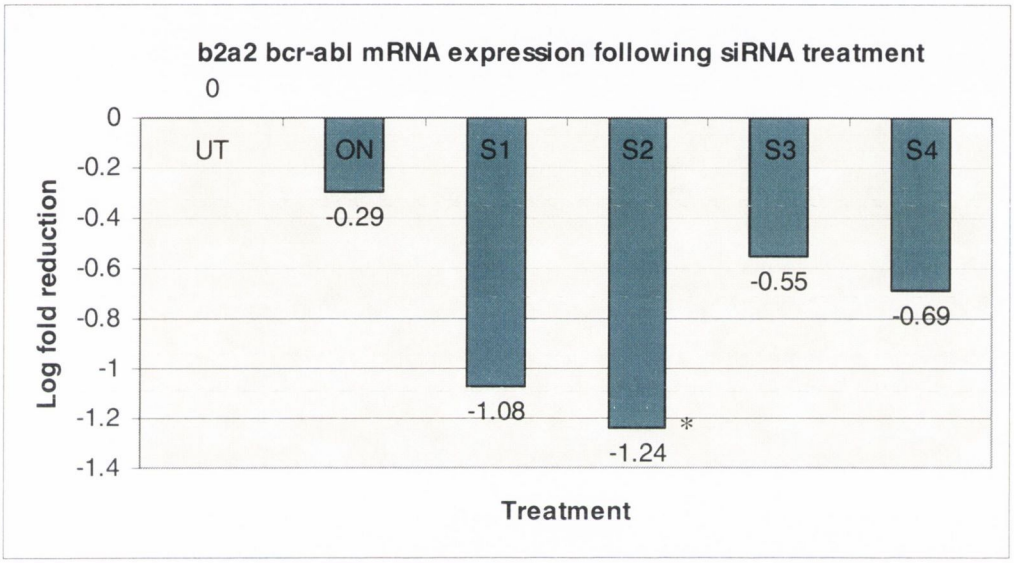


Figure 7.1: Log fold reductions in bcr-abl mRNA expression in KY-01 CML cells following treatment with 4 siRNA molecules targeted to distinct regions of mRNA transcript. Log fold reductions are indicated (*p<0.01)

Column 1(UT) is the untreated sample & has a value of zero
Column 2(ON) is the log-fold change in gene expression induced by a pool of the 4 siRNA duplexes treated without delivery agent (-0.29)
Columns 3-6 represent the log fold change in gene expression induced by individual siRNA molecules S1-S4 (S1-1.08, S2:-1.24, S3:-0.55, S4:-0.69)

Strong reductions in the level of bcr-abl mRNA expression were detected following 24 hours treatment with individual siRNA molecules (Figure 7.1, columns 3-6). The level of transcript destruction varied between the four siRNA molecules and this may be related to accessibility of the siRNA molecules to their target region of the mRNA. Cells were also incubated with a pool of all four siRNA duplexes (1μM) in the absence of delivery agent. This combination was observed to reduce bcr-abl mRNA expression levels to a lesser degree (Figure 7.2, column 2).

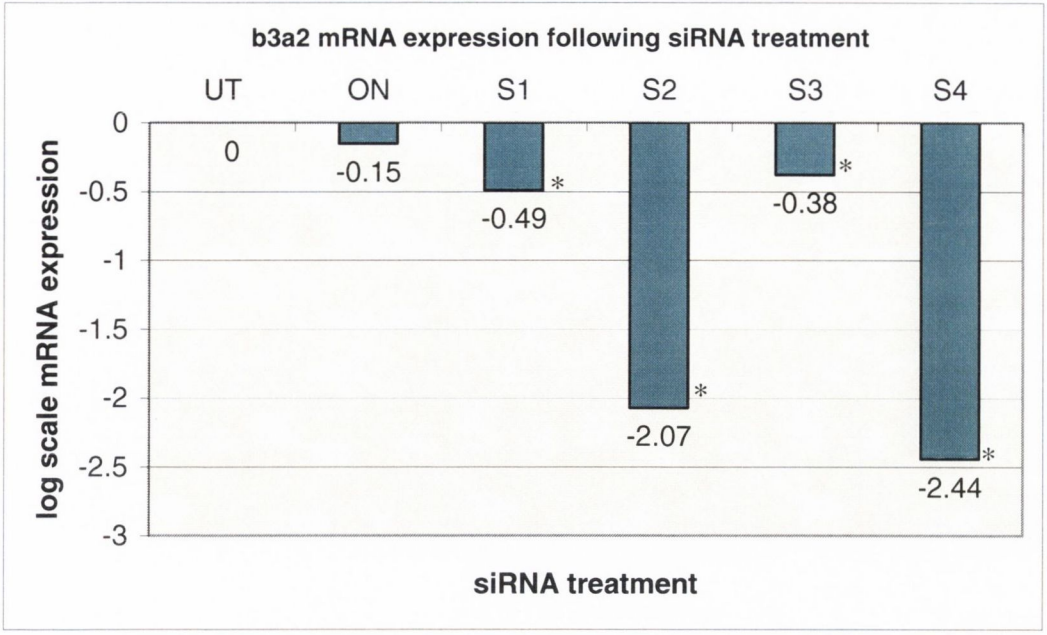


Figure 7.2 Log fold reductions in bcr-abl mRNA expression in the K562 cell line following 24 hours treatment with four siRNA duplexes targeted toward the bcr segment on the hybrid oncogene (*p<0.01)

Column 1(UT) has a value of zero on the log scale
Column 2 (ON) is the log-fold change in gene expression induced by a pool of the 4 siRNA duplexes treated without delivery agent (-0.15)
Column 3-6 represent the log fold changes induced by the S1 (-0.49), S2(-2.07), S3(-0.38) & S4(-2.44) siRNA duplexes

The siRNA duplexes were also observed to induce strong down-regulation of the bcr-abl mRNA in the b3a2-expressing CML cell line; K562 (Figure 7.2). The intensity of down-regulation varied between the different target sites and for the b3a2 cell line, S4 was observed to induce optimum down-regulation. Due to the nature of their chemistry, undelivered siRNA molecules in the extra-cellular fluid are subject to degradation over relatively short time periods. While carrier systems of delivery have the potential to reduce degradation of siRNA molecules by encapsulation, it is evident from the results above that the molecules are sufficiently stable to withstand the SL-O permeabilisation procedure. A pool of the siRNA duplexes incubated with cells in the absence of a delivery agent did not achieve significant down-regulation (Column 2-ON).

7.3 BCR-ABL (p210) protein expression following siRNA mediated bcr-abl mRNA down-regulation

siRNA duplexes targeted to bcr-abl were observed to induce mRNA down-regulation for both b2a2 and b3a2 mRNA variants (Figures 7.1 & 7.2). The main aim of mRNA down-regulation is to reduce translation of the bcr-abl transcript, resulting in lower levels of protein expression. The b2a2 bcr-abl mRNA was down-regulated in KYO-1 cells following 24 hours treatment with siRNA duplexes (Figure 7.1). Cell extracts were analysed for protein expression using western blotting after 48 hours. Figure 7.3 shows the expression of BCR-ABL in KYO-1 cells after treatment with four individual siRNA molecules. The level of protein expression in these siRNA treated cells was examined following 48 hours treatment.

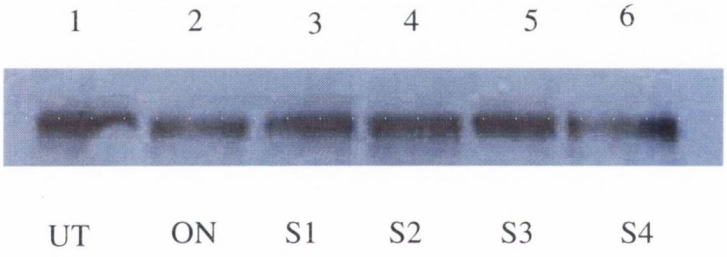


Figure 7.3: p210 protein expression in KYO-1 cells treated with four siRNA molecules following 48Hrs treatment

Lane 1 is the untreated well containing no siRNA duplex & without SL-O
Lane 2 is the oligonucleotide- only sample with no delivery agent
Lanes 3-6 show the bcr directed siRNA molecules S1-S4 delivered using 14U SL-O per 1 X 10^6 cells

Following bcr-abl down-regulation in the b2a2 expressing KYO-1 cell line; minimal reductions in BCR-ABL protein expression were observed following 48 hours treatment (Figure 7.3). At the mRNA level, S2 significantly reduced expression; however this was not reflected in a strong decrease in protein expression at this time-point.

BCR-ABL protein expression in K562 cells was analysed following down-regulation of the b3a2 mRNA variant using siRNA duplexes (Figure 7.2).

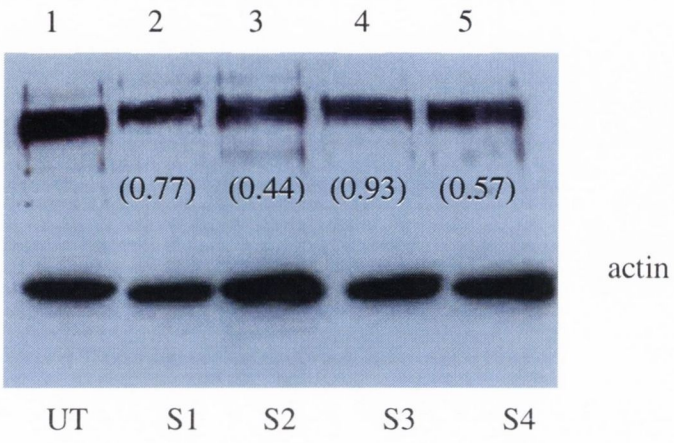


Figure 7.4 BCR-ABL and actin protein expression in K562 CML cells 72 hours following siRNA treatment

Lane 1: BCR-ABL & actin protein expression in untreated K562 cells
Lanes 2-5: BCR-ABL & actin protein expression in K562 cells following treatment with the S1, S2, S3 & S4 siRNA duplexes. Figures in brackets represent the change in BCR-ABL expression when compared to expression of actin.

The four siRNA duplexes were observed to reduce expression of the BCR-ABL protein in K562 cells following 72 hours treatment (Figure 7.4). The intensity of down-regulation varied between each of the molecules tested and was modest in some cases e.g. S3 (Lane 4). S2 induced the greatest reduction in protein expression and this correlates with a strong capacity to mediate down-regulation at the mRNA level (Figure 7.2).

7.4 Cell Proliferation capacity of CML cell lines following siRNA down-regulation of bcr-abl mRNA

Effective RNAi antisense activity results in mRNA destruction and this will induce down-regulation at the protein level. In the case of bcr-abl, protein down-regulation may impact on the proliferative capacity of CML cells. Following treatment with a pool of the four siRNA molecules employed to target bcr-abl, the proliferative capacity of K562 cells was monitored over a number of time-points (Figure 7.5). The level of proliferation in siRNA treated cells was compared to that of control siRNA treated cells (See Table 3.6).

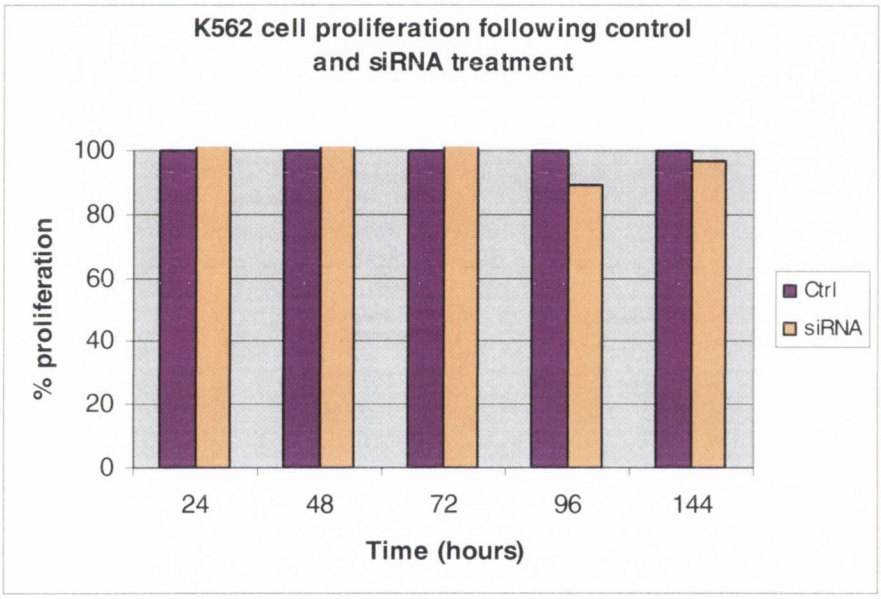


Figure 7.5: The influence of A: Ctrl siRNA molecule ■ delivered with SL-O compared to
B: siRNA Pool ■ delivered with SL-O on the proliferative capacity of K562 cells.

The proliferative capacity of siRNA treated K562 cells was observed to be similar to those of the control-sequence treated cells for greater than 72 hours (Figure 7.5). Following 96 hours treatment a moderate decrease of 10.7% was observed in the proliferative capacity of siRNA treated cells. Following 120 hours, this effect on proliferation is not maintained and proliferation levels have recovered to 3.5% of those of the control siRNA duplex.

7.5 The efficiency of the siRNA 'pool' to mediate bcr-abl down-regulation in the absence of SL-O delivery

7.5.1 mRNA down-regulation

Due to the nuclease sensitivity of the RNA chemistry in cellular systems, the ability of siRNA molecules to mediate mRNA down-regulation in the absence of delivery agents may be restricted (Thompson *et al,* 2002). To examine the efficiency of the siRNA pool to induce bcr-abl mRNA reductions in the absence of SL-O, K562 cells were incubated with the siRNA pool and bcr-abl expression was analysed in relation to GAPDH expression over a number of time-points (Figure 7.6).

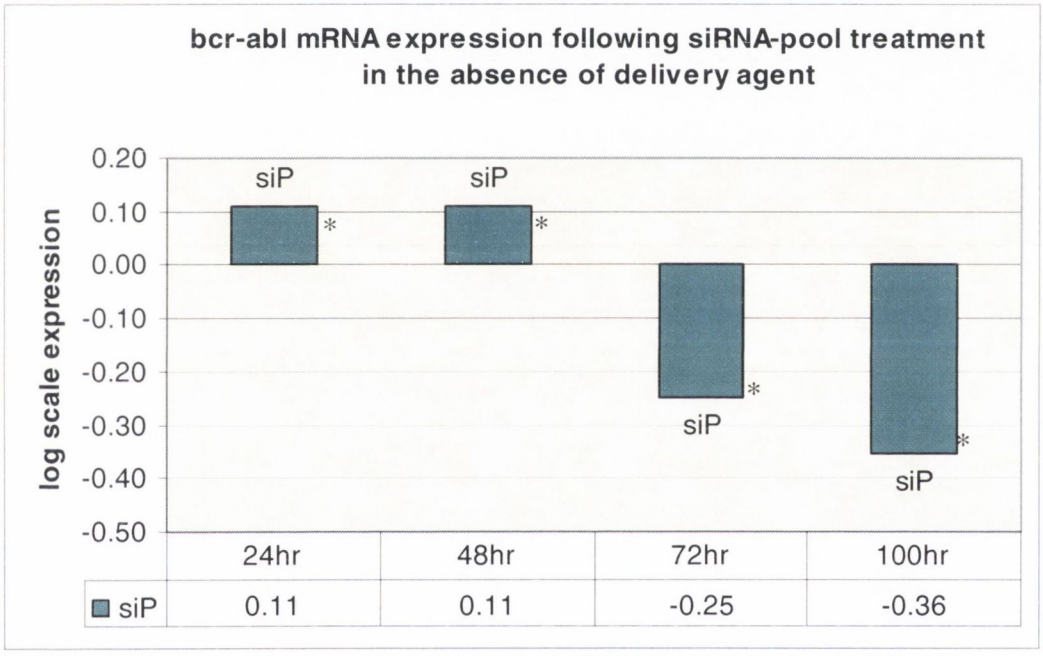


Figure 7.6 The impact of a pool of siRNA molecules (P) on bcr-abl mRNA expression in the absence of SL-O mediated delivery over a number of time-points

*Each result is expressed relative to the untreated sample at that time-point. The impact of siRNA molecules on bcr-abl expression was normalised to GAPDH levels (*p>0.05).*

bcr-abl down-regulation using the siRNA pool was first observed following 72 hours treatment (Figure 7.8). This effect was seen to increase further to -0.36 log units following 100 hours incubation. Activity at 72 hours represents a significant delay in activity relative to the SL-O delivered siRNA molecules which induced down-regulation at 24 hours treatment (Figure 7.1 & 7.2).

7.5.2 Inhibition of proliferative capacity

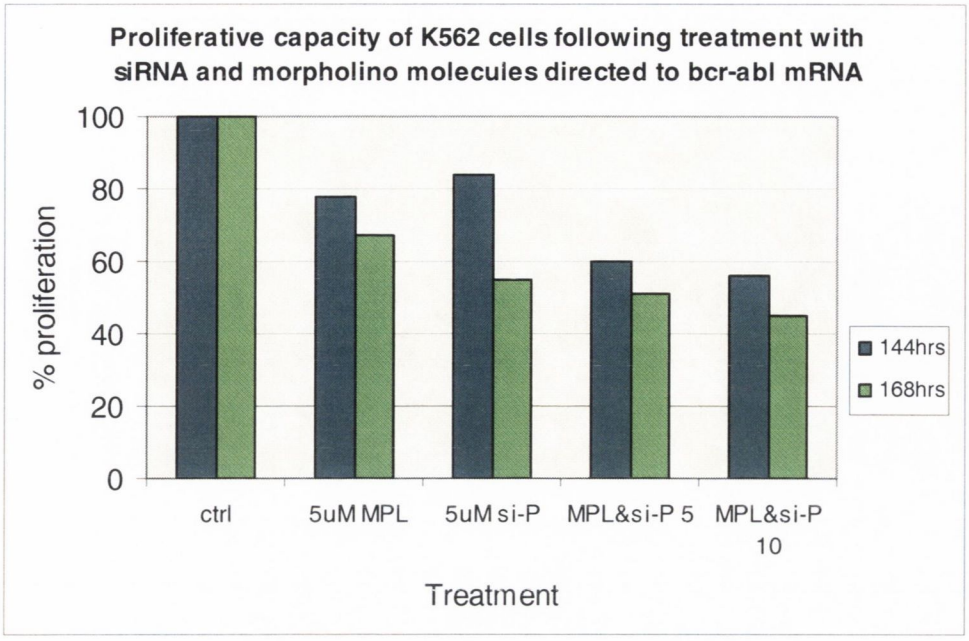


Figure 7.7 Proliferative capacity of K562 cells following treatment with bcr-abl directed morpholino and siRNA molecules in the absence of a delivery agent

Percent reductions in proliferative capacity were measured following 144 & 168 hours treatment with the above antisense oligonucleotides molecules

mRNA down-regulation induced by the siRNA pool in the absence of delivery agent occurred at a later time-point than that for SL-O-delivered molecules (Figure 7.6 & Figure 7.1). This delay in mRNA degradation also had an effect on the time point when differences in proliferative capacity were first detected (Figure 7.7). Significant reductions in the proliferative capacity of cells were not detected until 144 and 168 hours following treatment with siRNA and morpholino molecules, in the absence of enhanced delivery (Figure 7.7). Due to non-overlapping target sites, we decided to examine the effectiveness of combining siRNA and morpholino molecules targeted to bcr-abl. These were observed to induce a strong reduction in the proliferative capacity of CML cells though no additive effect was detected (Figure 7.7, column 5).

7.6 Correlation of mRNA degradation with target region selection

The bcr-abl mRNA transcript was targeted with four siRNA molecules, S1, S2, S3 & S4. siRNA molecules have been found to be limited by mRNA secondary structure to a similar degree to phosphorothioate molecules (Vickers *et al*, 2003). The binding potential of siRNA target areas on the mRNA transcript in this study was examined using *mfold*. The S2 duplex exerted a significant down-regulation of bcr-abl mRNA in both the b2a2 & b3a2 cell lines examined (Figures 7.1 & 7.2). The secondary structure surrounding the S2 target binding site (indicated by the arrow) consists of an open structure with several consecutive bases available for hybridisation. This open region connects to a large open loop and a smaller loop is separated by two G:C bond pairs. Down-regulation induced by S2 is attributable to a large degree by this suitable region for hybridisation.

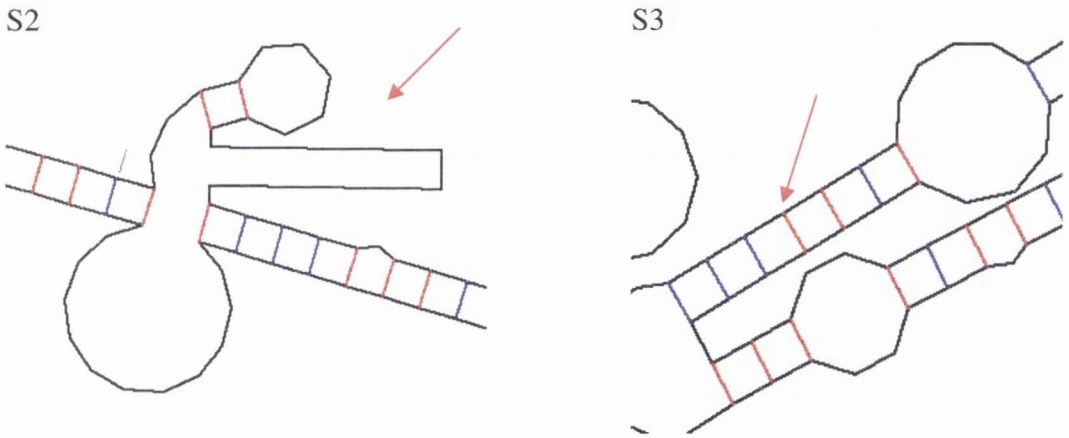


Figure 7.8 mRNA secondary structures surrounding the target binding sites of the S2 and S3 siRNA duplexes

The target sites for S2 and S3 are indicated by the arrows

Of the four siRNA duplexes examined, S3 induced the weakest levels of bcr-abl down-regulation (Figure 7.1 & 7.2). The mRNA target binding region of this molecule occurs in a stretch of hybridised bases, limiting its ability to interact with exogenous binding groups (Figure 7.8, right hand side). In contrast, the S2 binding site lies in a region of the mRNA which was predicted by *mfold* to contain long stretches of nucleic acid available for hybridisation (Figure 7.8, left hand side). Increased levels of down-regulation induced by the S2 duplex may be a result of the accessibility of this site.

7.7 siRNA - mediated mRNA down-regulation is sequence specific and not chemistry dependent

Following identification of secondary effects associated with phosphorothioate molecules, each potential new antisense chemistry needs to be examined for its propensity to induce non-specific effects. This siRNA control sequence employed in this study has no specific mRNA target and therefore should not bind to or induce any changes in bcr-abl mRNA (Table 3.6).

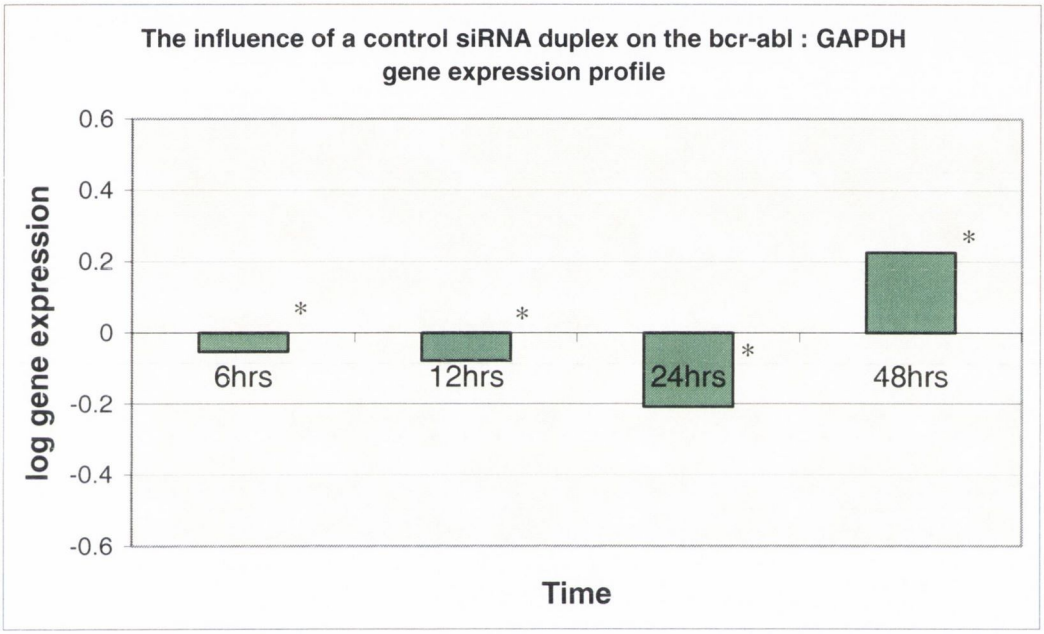


Figure 7.9 The effect of a control siRNA sequence on the expression of bcr-abl mRNA relative to GAPDH expression

The control siRNA sequence was delivered to KCL-22 cells using 12U SL-O ($p>0.05$).

The double-stranded RNA sequence employed as an siRNA chemistry control did not induce significant changes in the bcr-abl : GAPDH ratio (Figure 7.9). Over the four time-points analysed, no significant trend in expression was observed. Any changes in expression were minimal; with a maximum change of 0.2 log units.

7.8 Effect of siRNA duplexes on primary haematopoietic cell clonogenicity

Sequence specificity of siRNA molecules at the mRNA level has been demonstrated (Figure 7.10). To prove valuable for purging CML bone marrow samples *ex vivo*, siRNA duplexes should not hinder the expansion of normal haematopoietic progenitor cells residing in the marrow. Following their isolation from normal bone marrow samples, untreated and siRNA-treated PBMCs were allowed to proliferate in methylcellulose medium for 14 days to assess the effect of siRNA molecules on haematopoietic cell growth.

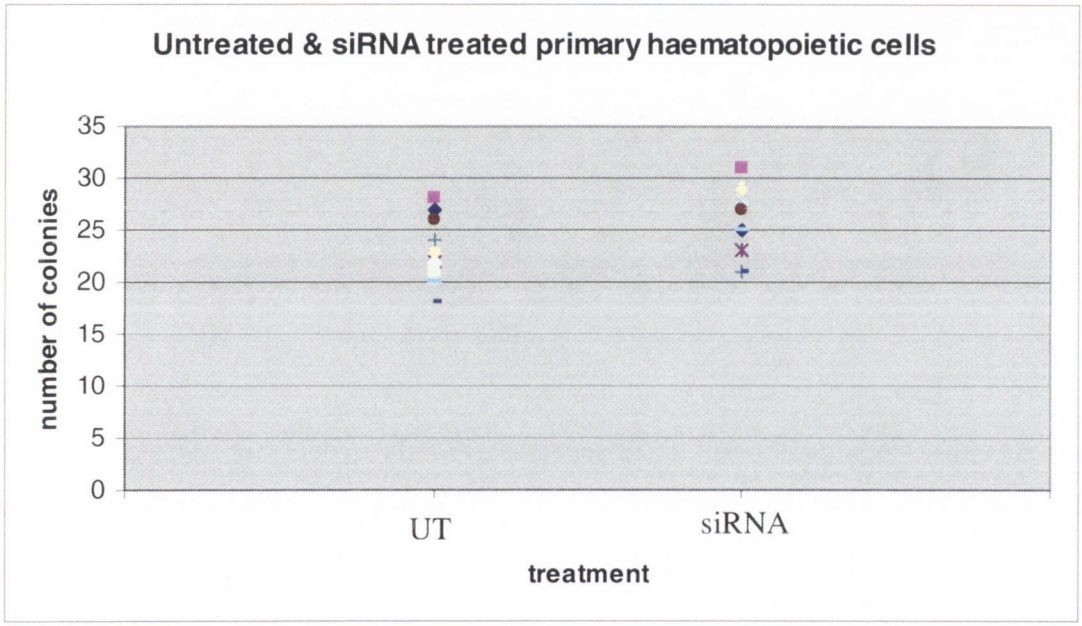


Figure 7.10 Colony counts following expansion of primary haematopoietic cells in methylcellulose medium following 14 days incubation.

Symbols represent the average of three counts from a donor sample (X=10) UT is the colony counts for the untreated cells (mean=24). siRNA (x=10) is the colony count for siRNA treated cells (mean=25)

siRNA duplexes did not negatively effect the expansion of bone marrow mononuclear cells *ex vivo* following incubation of cells with siRNA duplexes for 14 days (Figure 7.10).

7.9 Discussion

RNAi is a novel and promising approach to mRNA down-regulation. Advantages over traditional antisense mechanisms include dependence on and employment of naturally occurring mRNA degradation pathways. siRNA molecules employed in this study were selected by Dharmacon to target the bcr-abl transcript on the basis of functionality. Functionality was defined as the predicted ability of the duplex to mediate greater than 50% inhibition of target mRNA expression in 24 hours using 1μM siRNA. The siRNA duplexes demonstrated strong ability to down-regulate both bcr-abl mRNA variants, with significant log-fold reductions in expression observed (Figure 7.1 & 7.2).

Despite reduction of the bcr-abl mRNA for the KYO-1 cell line, minimal reductions in protein expression were observed following 48 hours treatment. This lack of response is consistent with the finding by the Clarke Antisense research group in Liverpool which found that the p210 protein may persist for approximately 100 hours (email communication RV Giles). To achieve protein knock-out, the antisense molecule half-life must match if not exceed that of its target protein. In addition protein down-regulation will be transient unless a continuous supply of antisense molecule is available to bind to the target. In the case of bcr-abl knock-out where the ultimate goal is to reduce cell growth, transient down-regulation may be insufficient to induce anti-proliferative and apoptotic effects.

The intensity in mRNA down-regulation was seen to be several log greater for the b3a2 positive K562 cells compared to the levels achieved for the KYO-1 cell line; where a maximum reduction of 1.2 log was achieved for KYO-1 when compared to almost 2.44 log reduction for the K562 cell line. This difference in intensity may reflect differences in uptake in the different cell lines. Down-regulation of b3a2 at the mRNA level was seen to produce a quantifiable difference at the protein level. Reductions in BCR-ABL expression were observed 72 hours following b3a2 mRNA down-regulation (Figure 7.4).

Corresponding with the substantial half-life of the BCR-ABL protein, no reduction in cell proliferation was detected until approximately 96 hours following siRNA administration. Here there is a moderate yet significant reduction of 11% in the levels of cell growth; however this figure returns to pre-treatment levels by 120 hours (Figure 7.5). The decrease in RNAi effect at this time may relate to cessation of RNAi activity due to RISC depletion or cell dilution (Scherr *et al,* 2003).

Specificity is a key component to successful antisense approaches. The specificity of the siRNA chemistry was demonstrated at the mRNA level by employing a molecule which has no target in human cells. Over a number of time-points analysed the siRNA control did not induce any significant changes in the expression of the target mRNA (Figure 7.9). siRNA duplexes did not affect cell proliferation of primary haematopoietic cells in culture, indicating they may prove suitable for use in *ex vivo* purging techniques (Figure 7.10).

The relationship between mRNA target location and transcript destruction is complex and not readily identifiable due to the impact of several factors, including different forms of secondary structure and binding of protein groups. However, lack of mRNA accessibility is a significant barrier to the activity of a range of antisense chemistries. The siRNA duplexes employed in this study to target bcr-abl were not designed in-house. To correlate the activity of these molecules with mRNA target parameters, the hybridisation sites of these duplexes were analysed using *mfold.* The design criteria employed by Dharmacon are unknown, however they claim to have a patented SmartSelection ® process. The duplex with the lowest level of mRNA degradation (S3) was found to correspond to a region of the transcript predicted by *mfold* to be involved in intra-molecular folding (Figure 7.8). The duplex with the highest level of bcr-abl mRNA degradation, S2, was predicted using *mfold* to be readily accessible for hybridisation. These findings lend credence to the use of mathematical methods for mRNA structure determination and antisense design.

Prompt delivery of siRNA into cells induces enhanced down-regulatory effects, coupled with efficient application of the siRNA molecules, by minimising degradation of the RNA chemistry. By mediating rapid cell entry, SL-O minimises degradation of delicate siRNA molecules by extra-cellular nucleases. Once inside the cell, incorporation of the duplex siRNA molecules protects the siRNA from further

interaction with cellular enzymes. Therefore, successful delivery confers several advantages on the activity of this chemistry *ex vivo*.

The RNA interference mechanism is regulated in a time dependent manner and its effects are diminished following 72-96 hours (Wall *et al,* 2003).

VIII

Cyclin D2 as a novel target to reduce proliferation of Chronic Myeloid Leukaemia cells

8.1 Introduction

BCR-ABL (p210) alters cellular pathways involved in the growth, proliferation, adhesion and apoptotic properties of CML cells. p210 affects cell transformation through modulation of key cellular mediators. The involvement of several of these factors e.g. cyclin D1 is redundant and BCR-ABL mediated transformation will proceed in their absence (Turhan *et al,* 1998). However, a small number of cellular components, including those involved in the RAS signalling pathway, are uniquely relied on to transmit BCR-ABL signals throughout the cell and to maintain its transformation of cells (Figure 1.5).

Cyclin D2 is a member of the highly conserved D-type cyclin family (Yu *et al,* 2002). D-type cyclins are expressed in a lineage specific manner (Teramoto *et al*, 1999). Cells of lymphoid origin express high levels of cyclin D2 including proliferating B-lymphocytes which have been demonstrated to express both cyclin D2 and D3 though not D1 (Solvason *et al*, 2000). It is the accumulation of cyclin D2 and not D3 which has been suggested as the critical event in passage of cells through the G1/S restriction point (Tanguay *et al*, 1996). In differentiated lymphoid cells, Stat 5 and Sp1 transcription factors mediate expression of cyclin D2 is response to IL-2 stimulation (Martino et al, 2001). Due to its decisive role in cell proliferation, cyclin D2 expression is tightly regulated at the transcriptional level (Fischer *et al,* 2002). Expression is repressed by methylation (Virmani *et al,* 2003), histone deacetylation, p16 and by the Mad-Max complex (Bouchard *et al*, 1999). Cyclin D2 promoter repression by Mad-Max is de-repressed by Myc via a single highly conserved E-box element (Bouchard *et al*, 2001) (See also section 1.7.5).

BCR-ABL has been recognised to adopt and manipulate expression of cellular mediators normally regulated through IL-3 expression (Wong *et al*, 2003). IL-3 is a pleotrophic cytokine which regulates various cellular functions including proliferation, survival and differentiation in a variety of haematopoietic cells (Dorsey *et al*, 2002). Expression of cyclin D2 is IL-3 dependent in haematopoietic cells and declines rapidly in the absence of this growth factor (Ando *et al,* 1993). Investigation into pathways by which BCR-ABL compensates for IL-3 withdrawal identified the involvement of cyclin D2 in BCR-ABL mediated proliferation (Parada *et al*, 2001). In

order to maintain cells in a proliferative state, BCR-ABL positively manipulates cell cycle regulators to overcome cell cycle blockades at the G1/S and G2/M phases of the cell cycle. Cyclin D2 plays a critical role in BCR-ABL induced proliferation of haematopoietic cells at this point (Jena et al, 2002).

At the G_1/S phase of the cell cycle; Cyclin D2 expression activates the cyclin dependent kinases' (CDK's) which then ensure entry of cells into the cell cycle (Brooks, 1996). Cyclin D2 expression is manipulated by BCR-ABL to overcome this G1/S cell cycle blockade (Parade *et al,* 2001). A 3.5 fold increase in cyclin D2 mRNA transcript expression was also observed in bcr-abl expressing cells at the G2/M phase of the cell cycle, where expression of the D-type cyclins is normally low (Jena *et al,* 2002). Cyclin D2 is also subject to abnormal regulation at the protein level in bcr-abl positive cells (Jena *et al,* 2002). Normally cyclin D2 displays a cyclic pattern of cell cycle expression (Lukas *et al,* 1995), however it is present at all stages of the cell cycle in BCR-ABL transformed cells (Jena *et al,* 2002). BCR-ABL stabilisation of cyclin D2 at multiple stages of its expression highlights its reliance on this cyclin.

Both cyclin D2 -/- and the hemi-zygous cyclin D2 +/- bone marrow cells are resistant to BCR-ABL transformation. This indicates that a threshold level of cyclin D2 protein is required for BCR-ABL induced cell cycle progression (Jena *et al,* 2002). Thus cyclin D2 may serve as a suitable target for therapeutic intervention as a partial reduction in cyclin D2 protein levels may inhibit transformation of haematopoietic cells by BCR-ABL. One of the aims of this study was to examine the expression of this cell cycle regulator in CML cell lines. Philadelphia positive cells with of both lymphoid and myeloid origin were investigated as was the Philadelphia negative cell line HL-60. siRNA and morpholino antisense molecules were subsequently designed to target the cyclin D2 mRNA transcript at distinct target sequences. Following treatment the effect of mRNA down-regulation on the proliferative capacity of CML cells was analysed. In the case of the cyclin D2 target, the definitive functional assay is the assessment of cell proliferative capacity.

8.2 Cyclin D2 expression in CML cell lines

Cyclin D2 mRNA was assessed in CML cell lines using TaqMan PCR to determine levels of expression. The lymphoid-derived cell lines BV173, KCL-22 and K562, a myeloid cell line LAMA-84 and a non-CML cell line; HL-60 were analysed. CML cells which present as lymphoid during blast crisis have been reported to express higher levels of cyclin D2 than their myeloid counterparts, and to be more highly dependent on its expression for disease progression (Deininger et al, 2001).

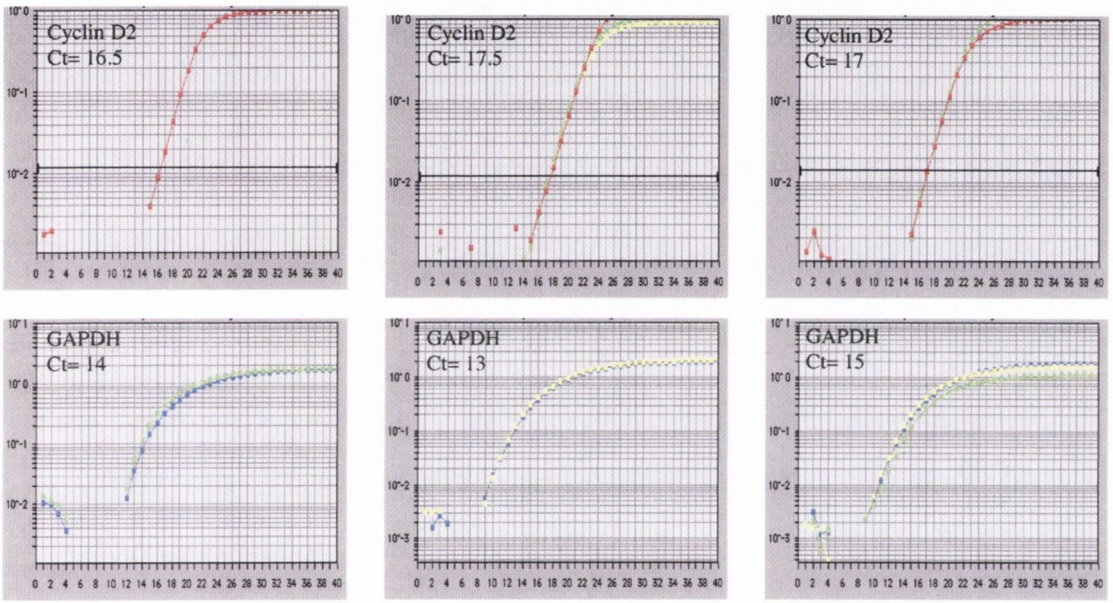
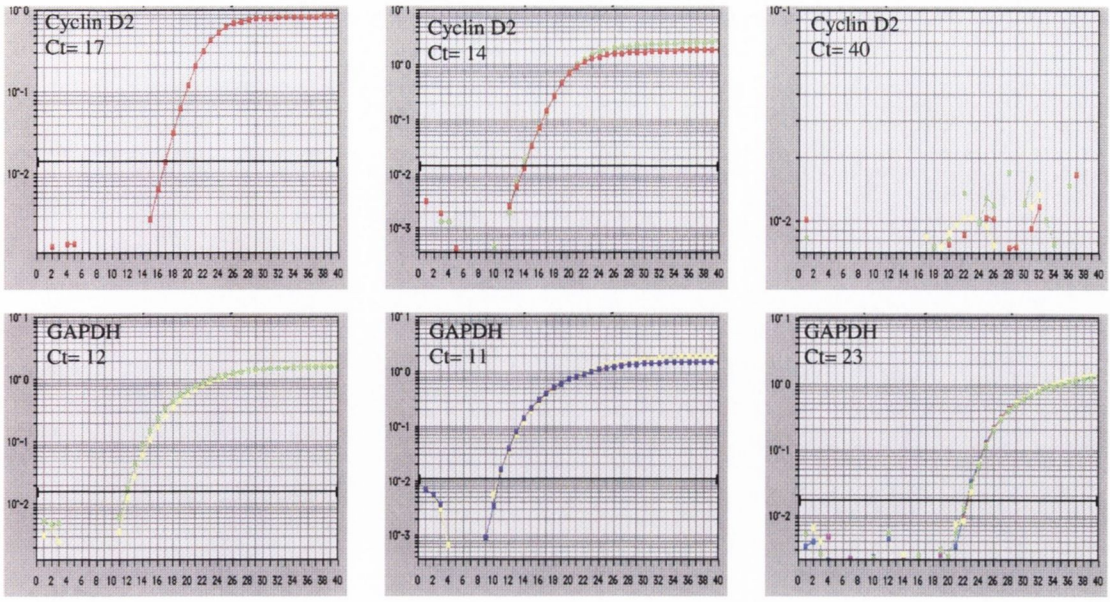


Figure 8.1 Cyclin D2 expression in CML cell lines of lymphoid origin

The upper graph shows cyclin D2 expression in each of the cell lines, while the lower level shows the corresponding expression of the GAPDH house-keeping gene. Each of the three lymphoid cell lines examined expressed cyclin D2 to a strong extent.

As may be seen from Figure 8.1; all three of the lymphoid-derived CML cell lines analysed expressed high levels of cyclin D2 mRNA. Cyclin D2 mRNA was also examined in the myeloid-derived Philadelphia positive LAMA-84, and in the Philadelphia negative cell line HL-60. Cyclin D2 and GAPDH expression from these samples are indicated in Figure 8.2.



LAMA-84 HL-60 HL-60

Figure 8.2 Cyclin D2 and GAPDH expression in the Philadelphia positive LAMA-84 and Philadelphia negative HL-60 myeloid cell lines

Figures indicate cyclin D2 (upper graphs) and GAPDH (lower graphs) expression in the indicated cell lines. On the LHS is the BCR-ABL expressing myeloid LAMA-84 cell line. The central graphs represent gene expression in actively proliferating HL-60 cells, while the graph on the RHS indicates expression of the cyclin D2 and GAPDH genes in highly confluent HL-60 cells. A Ct value of 40, indicates that no expression of the target gene was detected on the TaqMan following 40 cycles of amplification

The myeloid-derived LAMA-84 CML cell line, as with the lymphoid cell lines examined, showed high levels of cyclin D2 expression (Figure 8.2). This was consistent over a range of cell growth conditions analysed, and was comparable in intensity with the lymphoid cell lines with a Ct value of approximately 17 (Figure 8.2). Strong cyclin D2 expression was observed in actively proliferating cells of the bcr-abl negative cell line; HL-60 (Figure 8.2, middle graphs). These HL-60 cells were then allowed to grow for a further 5 days past the normal splitting point. When expression was assessed in the over-confluent HL-60 cells, which due to exhaustion of nutrients were no longer actively proliferating, no cyclin D2 was detectable using TaqMan PCR (Figure 8.2; right-hand side).

8.3 Cyclin D2 mRNA down-regulation using siRNA molecules

The essential nature of cyclin D2 in BCR-ABL mediated transformation has been established in cyclin D2 negative bone marrow cells (Jena *et al,* 2002). BCR-ABL reliance on the cell cycle regulator provides a potential target for modulation of bcr-abl pathways. Due to its essential role in BCR-ABL mediated transformation of cells, cyclin D2 was targeted for down-regulation at the mRNA level using siRNA based antisense molecules.

Cyclin D2 mRNA expression was analysed at different time intervals following the siRNA treatment using TaqMan PCR and the level of log down-regulation in expression following 8 hour and 12 hour treatment are displayed in Figure 8.3.

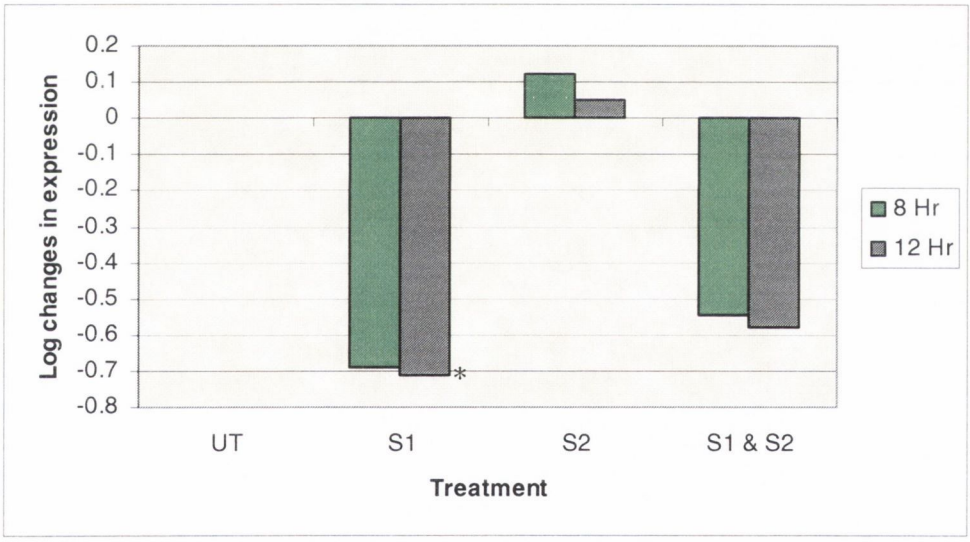


Figure 8.3 Cyclin D2 mRNA expression following treatment with the S1 and S2 siRNA molecules singly and in combination following 8 and 12 hrs treatment (*p<0.01)

Log changes in gene expression are indicated, following treatment with 1μM S1 & S2 siRNA molecules after 8 and 12hrs. Changes in cyclin D2 expression are relative to those of the GAPDH gene. The untreated sample had a value of zero on this scale following $2^{(-\Delta\Delta Ct)}$ *calculations. The combination sample has a final siRNA concentration of 1μM. siRNA molecules were introduced to KCL-22 cells using 12U SL-O*

As may be seen from Figure 8.3, significant reductions in cyclin D2 mRNA levels were induced by the S1 siRNA molecule at 8 & 12 hour treatments. S1 was designed using the Tuschl motif and is targeted to nucleotide 859 on the cyclin D2 mRNA. mRNA expression was monitored up to 48 hours following initial delivery.

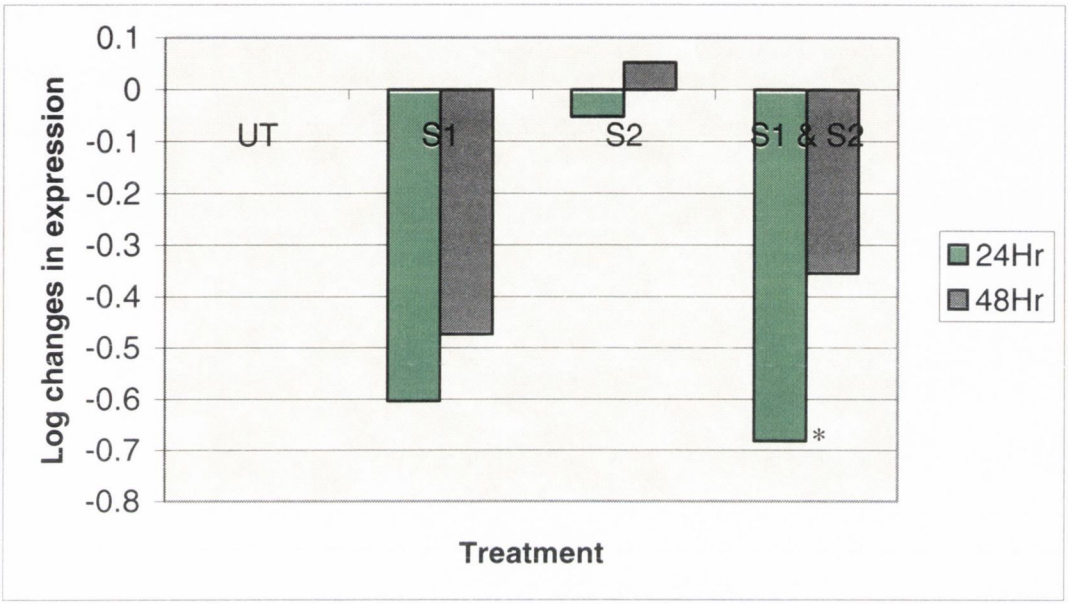


Figure 8.4 Cyclin D2 mRNA expression following treatment with S1 and S2 siRNA molecules singly and in combination following 24 and 48 hrs (*p<0.05)

Log changes in gene expression are indicated, following treatment with 1μM S1 & S2 siRNA molecules after 24 and 48 hrs. Changes in cyclin D2 expression are relative to those of the GAPDH gene. The untreated sample has a value of zero on this scale following $2^{(-\Delta\Delta Ct)}$ *calculations. The combination of S1 & S2 has a final siRNA concentration of 1μM. siRNA molecules were introduced to KCL-22 cells using 12U SL-O.*

S1 continued to induce reductions in the level of cylin D2 mRNA expression following 24 and 48 hours treatment (Figure 8.4). S2 demonstrated little or no ability to mediate cyclin D2 degradation at any of the time-points analysed (Figure 8.3 and 8.4). When applied in combination, the level of S1 mediated inhibition was not enhanced by the addition of S2. Combining the two molecules ended in a lower concentration of S1 present in the experiment and this appeared to reduce its ability to down-regulate expression of cyclin D2 (Figure 8.3).

8.4 Proliferative capacity of CML cells following siRNA mediated Cyclin D2 down-regulation

Following treatment with both siRNA and morpholino antisense molecules designed to down-regulate expression of the cyclin D2 mRNA, effects on the proliferative capacity of these cells were assessed using the modified MTT method; the MTS (Methodologies 2.11). The cell permeabilisation agent SL-O was employed to deliver molecules to the cells; therefore effects on proliferative capacity were expressed in relation to the effects of this agent. The decrease in the proliferative status of KCL-22 cells following treatment with the S1 siRNA molecule is outlined in Figure 8.5.

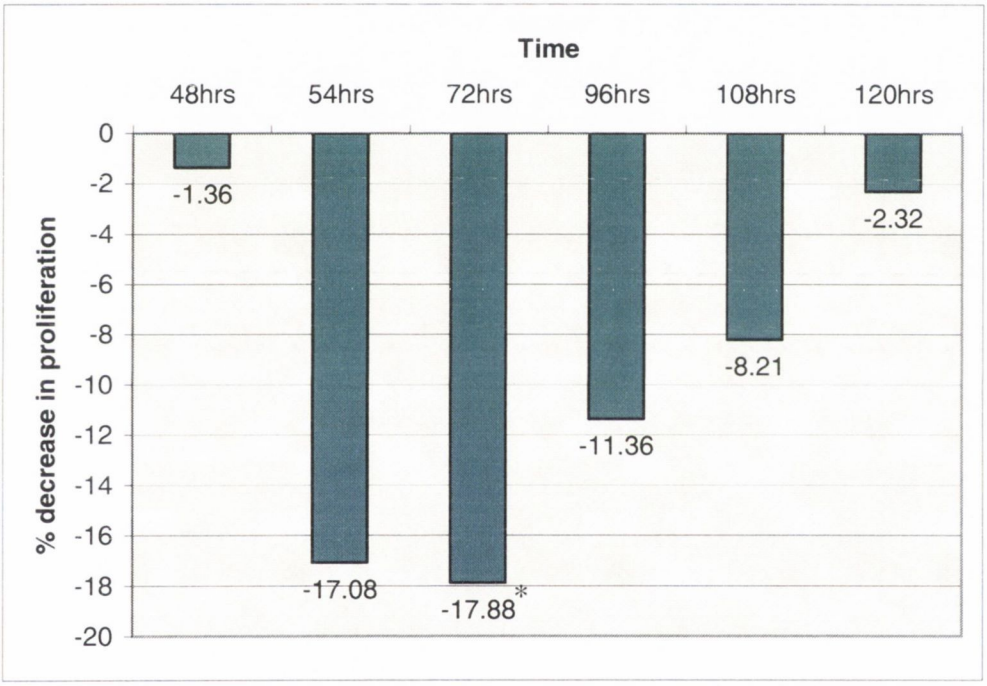


Figure 8.5 Proliferative inhibition in KCL-22 cells induced following treatment with the S1 siRNA duplex

*Cells were treated with 1μM siRNA duplex for the periods indicated on the graph. Each proliferative reading is expressed relative to any changes observed with the SL-O control (*p<0.05)*

Inhibition of cyclin D2 mRNA transcript expression was observed to have a moderate impact on the proliferative status of the S1-treated cells. The most significant effect was detected following 72 hours treatment; however levels of inhibition do not reach 20%.

The S2 siRNA duplex designed using the aa (N19) design motif was observed to induce minimal interruption in cyclin D2 mRNA expression over a number of time points following its introduction into KCl-22 cells using SL-O (Figure 8.3 & 8.4).

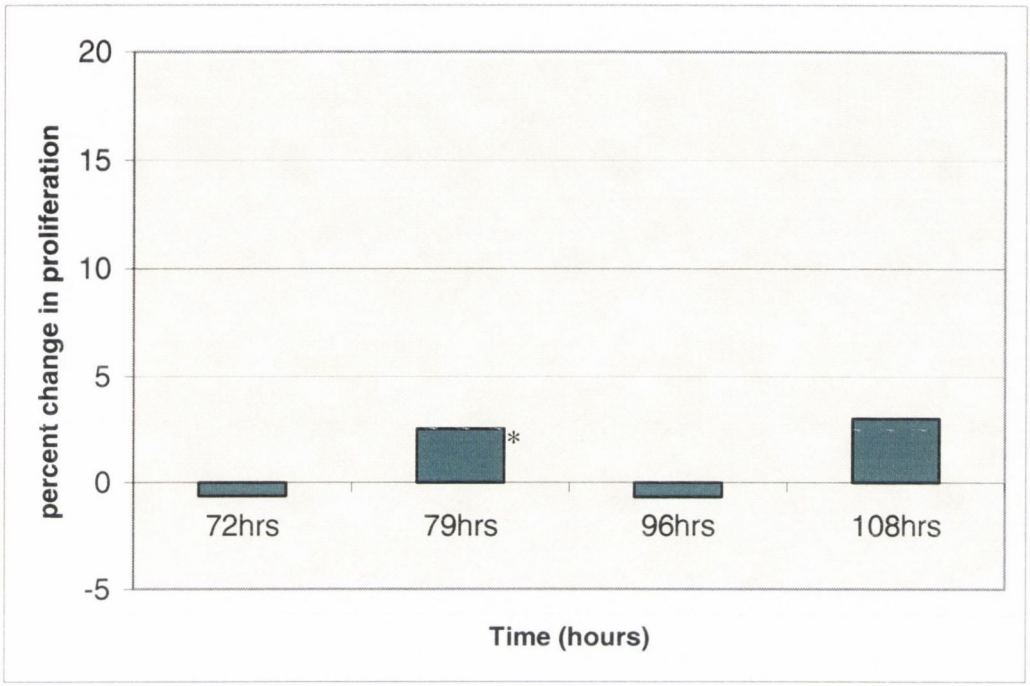


Figure 8.6 Percent changes in the proliferative capacity of CML cells following treatment with the S2 siRNA duplex over number of time points (*p>0.05)

The S2 duplex was delivered to KCL-22 cells using 12U SL-O, and the levels of proliferation are expressed relative to the SL-O control.

Proliferative down-regulation following introduction of S2 siRNA molecules to CML cells was minimal, with no significant effect evidenced at any of the time-points examined (Figure 8.6). This lack of proliferative effects was attributable to the lack of mRNA down-regulation mediated by this molecule and may relate to lack of hybridisation of the S2 molecule. The lack of proliferative effects with S2 indicates that the effects seen with S1 relate to its ability to down-regulate mRNA expression.

8.5 The impact of cyclin D2 targeted morpholino molecules on the proliferative capacity of CML cells

A morpholino antisense molecule was designed to a region 5' of the cyclin D2 mRNA translational start site (See section 3.4.2). Despite attempts to standardise the quality of the cyclin D2 primary antibody no reproducible results were obtainable making it unfeasible to assess protein down-regulation.

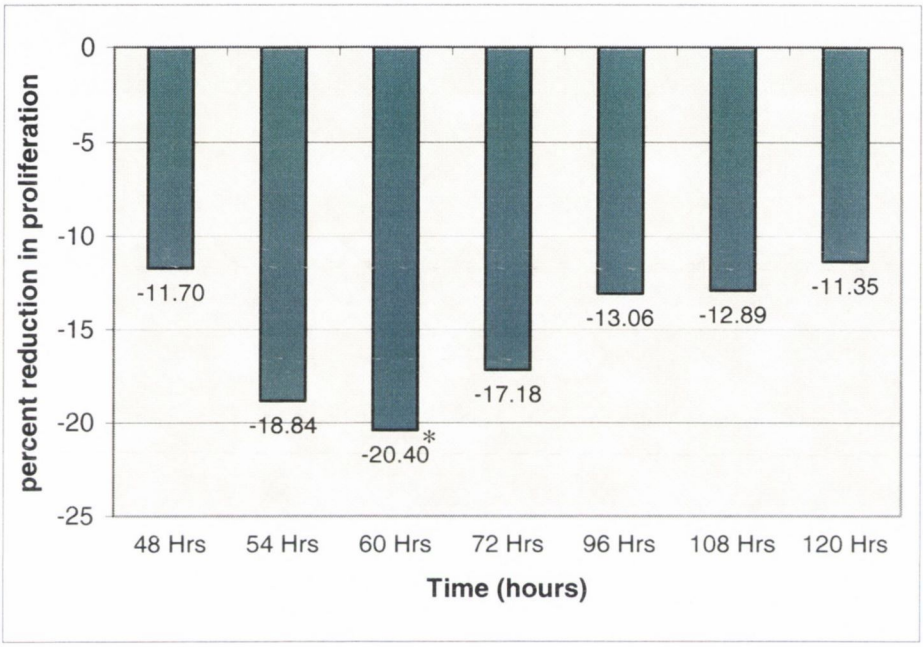


Figure 8.7 The proliferative capacity of KCL-22 cells following treatment with 1μM morpholino antisense targeted to the 5' UTR region of the cyclin D2 gene (*p<0.05)

KCL-22 cells were treated for the periods indicated above with 1μM cyclin D2-directed morpholino antisense molecules. Oligonucleotides were delivered to KCL-22 cells with 12U SL-O per 1 X 10^6 cells. Proliferative capacity is expressed relative to levels seen with the 5' mis-match morpholino delivered using 12U SL-O

Following 48 hours treatment with the cyclin D2-targeted morpholino antisense molecule MPL_CyD2, the proliferative levels of KCL-22 cells decreased (Figure 8.7). The decrease in proliferation was most apparent following 60 hours compared to 72 hours with the S1 siRNA molecule (Figure 8.7 & 8.5). Though decreased in magnitude, a decrease in proliferative capacity persisted and was greater than 10% when the final 120 hour time-point was examined (Figure 8.7).

8.6 The impact of target site selection on siRNA activity

To reach its target site the antisense molecule must overcome a number of obstacles, including cellular delivery and antisense design. However, each mRNA develops its own individual conformation resulting in sections of the transcript which act as suitable targets for hybridisation by antisense molecules and areas which are resistant to binding by exogenous groups and are therefore unsuitable antisense targets. Deciphering the suitability of a particular region prior to performing antisense experiments is problematic. Prediction tools based on mathematical determination of folding constraints play a role in aiding recognition of accessible sites; however these have inherent inaccuracies (Doshi *et al,* 2004).

Despite judicious selection of the S2 siRNA molecule, facilitated using the *sfold* software and antisense design parameters, no significant reductions in mRNA levels were detected following delivery with SL-O. This was noted throughout the time-points examined and over a variety of different delivery conditions. Using the *sfold* software, S2 was calculated to exhibit a target binding efficiency of –17.7 kilojoules/mole, indicating a strong and stable binding. However, due to the lack of mRNA destruction the binding efficiency of this siRNA is likely to be low. Unlike their single-stranded phosphorothioate antisense counterparts, siRNA molecules do not form intra-molecular bonds due to their double-stranded nature, and the two strands are efficiently separated by the unwindase activity of the RNA Induced Silencing Complex, RISC. This may imply that the mRNA transcript is unavailable for hybridisation at this point despite what was predicted using *sfold.*

The S1 siRNA duplex; designed using the highly recognised Tuschl motif was determined to exhibit an mRNA binding capacity of -26.4 kJ/mole using *sfold.* This is a stronger target affinity than that expressed by S2; however this relatively small difference in affinity lead to a large difference in activity. While mRNA secondary structure prediction approaches have an important role to play, the only way to definitively ascertain if a target area is suitable for antisense hybridisation is by experimental validation. Modulation of mRNA structures by protein binding *in vivo* cannot yet be considered in predictive modelling and suggests the possibility that inaccessible sites due to protein binding may be identified as suitable targets (Amarzguioui *et al,* 2000).

8.7 Discussion

Cyclin D2 expression was targeted for down-regulation in CML cells due to its role in maintaining cells in a dividing state. Cyclin D2 is over expressed in CML cells and knock-out of its expression inhibits bcr-abl transformation (Jena *et al,* 2002). To reduce the proliferative status of CML cells, morpholino and siRNA molecules were designed to down-regulate cyclin D2 mRNA (Tables 3.4 & 3.6). Down-regulation of cyclin D2 has the potential to severely weaken the ability of bcr-abl to induce continued cell proliferation and may increase the effectiveness of bcr-abl directed antisense molecules.

Conflicting results have been reported regarding the role of cyclin D2 in CML cells. A critical role for cyclin D2 has been suggested for bcr-abl mediated transformation of haematopoietic cells (Jena *et al,* 2002). However an earlier study suggested that cyclin D2 was only over-expressed in a subset of CML cells which reach lymphoid blast crisis and in acute lymphoblastic leukaemia (ALL) cells; with expression low or absent in Philadelphia-positive myeloid cells (Deininger *et al,* 2001). No consistent over-expression of cyclin D2 was detected in acute myeloid leukaemia (AML) cells compared to three lymphoid malignancies where a 5-10 fold over-expression was detected (Delmer *et al,* 1995). Cyclin D2 mRNA expression was investigated in the cell lines employed in this thesis. These included myeloid and lymphoid CML cell lines and a bcr-abl negative cell line; HL-60.

Strong expression of cyclin D2 was detected in each of the three lymphoid – derived CML cell lines examined; BV173, KCL-22 and K562 (Figure 8.1). The myeloid bcr-abl cell line; LAMA-84, also expressed high levels of cyclin D2 mRNA and these levels were comparable with those detected for the lymphoid CML lines assessed (Figures 8.2 & 8.1). The BCR-ABL negative cell line HL-60 was also found to express high levels of cyclin D2 mRNA (Figure 8.2, middle graphs). However, this expression was seen to diminish to below the TaqMan threshold detection level when RNA was extracted from over-confluent HL-60 cells grown to high-density (Figure 8.2). Taken together these results indicate that cyclin D2 expression is similar in lymphoid and myeloid derived BCR-ABL cell lines. Expression in non-CML cell lines exhibits a cyclic pattern of expression and is not indicative of prolonged or de-

regulated expression. Low or absent expression of cyclin D2 has been reported in mouse cells grown to high cell densities which induced cell cycle arrest. If these cells are then split to normal cell densities cyclin D2 expression is restored to normal levels (Turchi *et al,* 2002).

At the mRNA level, the S1 siRNA duplex induced significant reductions in cyclin D2 expression, with a peak value of -0.72 log fold change in expression occurring following 12 hours treatment (Figure 8.3). mRNA inhibition was still evident at the 24 and 48 hour time-points; however following the peak at 12 hours, the level of inhibition decreased gradually over time (Figure 8.4). Given the level of mRNA down-regulation following 48 hours (Figure 8.4), down-regulation may still be achievable for several hours following this time-point. The duration and intensity of cyclin D2 mRNA degradation indicates that translation of the cyclin D2 protein whose half-life is approximately 24 hours would have been interrupted (Parada *et al,* 2001).

In contrast to the S1 siRNA duplex, S2 was not observed to significantly reduce cyclin D2 mRNA transcript levels at any of the time-points analysed (Figure 8.3 & 8.4). No significant changes in gene expression were observed when this molecule was employed. When S2 was combined with the S1 duplex, enhanced down-regulation was not observed (Figure 8.3). Combing two duplexes which target distinct sites on the cyclin D2 mRNA transcript may enhance the down-regulation of active siRNA molecules singly due to decreased competition for target site binding. Due to a lack of S2 efficacy; the two molecules together did not induce improved down-regulation (Figure 8.3).

Of the four time-points analysed, the earlier times indicate a more proficient antisense mRNA effect, with a -0.69 log fold reduction of cyclin D2 expression after 8 hours and an optimum mRNA down-regulation of -0.72 log units after 12 hours (Figure 8.3). This peak in RNAi effects at 12 hours decreases gradually to -0.60 log fold reduction at 24 hours and -0.47 log reduction after 48 hours. This RNAi-mediated inhibition of expression may have been sustained for a period beyond this but will presumably have been diminished completely at 72-96 hours due to the transient nature of siRNA mediated silencing (Brummelkamp *et al,* 2002).

Following reduction of cyclin D2 mRNA transcripts by S1, changes in the cell proliferation capacity were analysed over a number of time-points using the MTS assay. The reduction in mRNA transcript levels resulted in a decreased proliferative level in S1 treated cells (Figure 8.5). Growth inhibition was significant with a greater than 17% reduction over 54 and 72 hours (Figure 8.5). This transient decrease occurred following down-regulation at the mRNA level (Figures 8.3 & 8.4). In normal haematopoietic stem cells the cyclin D2 protein is tightly regulated and has a short half-life due to ubiquitin-mediated proteolysis (Bashir *et al,* 2003). In CML cells, the cyclin D2 protein may have prolonged stability, increasing its half-life and requiring greater knock-out of mRNA expression for further functional effects (Jena *et al,* 2002).

Following siRNA mediated cyclin D2 down-regulation at the mRNA level, treated cells demonstrated reduced levels of proliferation (Figure 8.5). However, cells recovered their pre-treatment growth capacity, indicating that although cell proliferation slowed it did not induce cell cycle arrest. Given the crucial nature of cyclin D2 expression for bcr-abl mediated transformation, it may reflect insufficient duration or intensity of the antisense effect. This may be caused by a number of factors including the continual production of fresh mRNA transcripts or may be due to depletion of the RNAi at the later time-points.

A morpholino chemistry antisense molecule was also designed to target the cyclin D2 mRNA transcript, and its efficiency to mediate down-regulation was assessed by measuring the cells' proliferative capacity. The MPL_CyD2 morpholino molecule was observed to reduce proliferative capacity of treated cells relative to the 5'MM control morpholino treated cells (Figure 8.7). This reduction was due to morpholino mediated inhibition of translation of the cyclin D2 mRNA transcript. Reductions in the proliferative capacity of CML cells are significant with > 20% inhibition evident following 60 hours treatment. This peak in activity occurs at an earlier time-point in morpholino-treated cells relative to siRNA treated cells (Figures 8.7 & 8.5).

Identification of antisense molecules which down-regulate cyclin D2 may be combined with antisense molecules and potentially other agents which decrease BCR-ABL expression. By eliminating both of these mediators simultaneously this approach could significantly reduce the proliferation potential of CML cells. These interesting

early results which indicate reduced proliferative capacity of BCR-ABL positive cells upon cyclin D2 down-regulation need to be followed up by further investigation into the usefulness of reducing this target for therapeutic intervention. The next step is to identify if the moderate effects on CML cell proliferation by cyclin D2 inhibition can be used in combination with bcr-abl-directed antisense molecules to overcome the inherent resistance of CML cells to apoptosis induced by etoposide and gamma irradiation.

IX

General Discussion And Future Directions

9.1 Introduction

Expression of the bcr-abl hybrid oncogene in CML and Philadelphia-positive ALL has long been identified as an attractive target for therapeutic intervention. This disease-specific marker has an essential role to play in the pathogenesis of CML and is not present in normal cells (Van Etten, 2004). Studies indicate that the levels of BCR-ABL protein within the cell have a measurable effect on its growth capacity (Cambier *et al,* 1998). As bcr-abl produces a leukaemia specific mRNA, it represents a highly suitable target for antisense mediated down-regulation of gene expression. However, down-regulation of bcr-abl and of the proliferative potential of CML cells requires that a number of criteria be fulfilled for potential therapeutic benefit. These include delivery of the antisense molecule to an area inside the cell where it can interact with its target mRNA to down-regulate protein expression and potentially induce anti-proliferative or cell death effects.

In addition to bcr-abl, a number of other targets may also be appropriate for down-regulation in CML; these include the c-myc transcription factor whose over-expression is implicated in a variety of malignancies (Prochownik, 2004). Also, antisense molecules which mediate c-myb down-regulation in CML have entered clinical trials. In this thesis cyclin D2 was chosen as a secondary antisense target as up-regulation of this protein by BCR-ABL maintains cells in a proliferative state. Targeting other molecules in the CML signalling pathway may also have untapped potential in reducing the proliferative potential of CML cells.

To date, one antisense-based therapeutic drug, Vitravene® used for the treatment of CMV-induced retinitis in AIDS patients has been marketed. One of the main advantages of down-regulating expression of pathogenic proteins in infectious diseases is that the target is exogenous; foreign to the normal cellular milieu. Down-regulation of the oncogenic potential in cancer cells is commonly dependent on the inhibition of endogenous mRNA expression and therefore may also result in negative effects to normal cells. bcr-abl provides the opportunity to down-regulate a disease-generating and disease-specific component of CML. However, due to its lengthy half-life, down-regulation of the BCR-ABL protein is a challenging goal,

which requires efficient delivery methods to be used and a highly stable backbone to be implemented.

9.2 Targeting mRNA transcripts for antisense hybridisation & the role of secondary structure prediction tools

In this thesis, the development of an antisense approach was performed in a number of steps. Initial consideration of potential secondary structure in mRNA targets prompted a bioinformatic approach to predict potentially accessible targets within an mRNA molecule. Theoretically single-stranded inside the cell; mRNA transcripts develop secondary structure due to self-complementarity, which may lead to the development of regions which are inaccessible to antisense hybridisation. Targeting these sites on an mRNA transcript can compromise activity of an otherwise active antisense molecule (Ding *et al,* 2004). This aspect of antisense activity is unique for each mRNA target and design of antisense molecules represents a fresh challenge for each transcript.

The *mfold* and *sfold* bioinformatics packages were employed to facilitate selection of antisense molecules targeted to accessible regions on the mRNA transcript. Encouragingly the majority of antisense molecules designed by this method proved efficient at mRNA down-regulation. One notable exception was the S2 molecule designed to down-regulate cyclin D2 via an RNAi mode of action. The inability of S2 to induce antisense down-regulation highlights an inadequacy of the currently available prediction techniques that are unable to incorporate all factors that can affect binding of antisense sequences to mRNA. The main factors not incorporated in the algorithm at present and which may impact antisense hybridisation include the binding of protein groups involved in the regulation or functionality of RNA.

The minimal free energy (MFE) calculations employed by *mfold* for RNA secondary structure determination rated poorly when compared to both the comparative method and the recently established high-resolution crystal structures for ribosomal RNA (rRNA) subunits (Doshi *et al,* 2004). Comparative analysis is based on the theory that homologous RNA sequences are capable of folding into the same secondary and tertiary structures and that during evolution, while the primary sequence may have altered significantly; the secondary and tertiary structures of the

molecule are essentially unchanged. This method of RNA structure determination proved very accurate when applied to the rRNA subunits with 97-98% verification by the crystal structure determination. However, the accuracy of each RNA structure determined by *mfold* was strongly related to its size, with structures of smaller molecules being determined more accurately (Doshi *et al*, 2004). The *mfold* predicted structure for 5S RNA was 71% that of the actual structure, and this dropped to 41% for the 23S rRNA subunit. This indicates that inadequacies in the folding algorithm rather than lack of incorporation of protein binding may be limiting its ability to consistently and accurately predict accessible sites. Results in this thesis indicate that while the bioinformatics approach proved very useful and selected ten antisense molecules that were functional to varying degrees, the minimal free energy parameters in conjunction with the mfold folding algorithm are unable to accurately predict mRNA secondary structure and empirical methods remain the most reliable route to success.

The task of identifying folding sites within coding regions of mRNA is decidedly different from that of functional RNA molecules such as rRNA species and is less applicable to determination by comparative analysis. RNA-DECODER is a novel computational approach to RNA secondary structure prediction. It uses phylogenetic substitution models to decipher over-lapping evolutionary constraints to predict conserved secondary structure elements in both coding and non-coding regions of an mRNA transcript. RNA-DECODER claims to display higher sensitivity than *mfold* when scanning the complete genomes of both the hepatitis C and polio viruses (Pedersen *et al,* 2004). The success of currently available bioinformatic approaches to mRNA secondary structure prediction may be enhanced by deciphering protein binding regions of the mRNA transcript however the most useful step would be an improvement of the algorithm determining the folding patterns of larger molecules.

The most successful method of selecting accessible target sites is an experimental approach; by RNase H mapping or by antisense oligonucleotide arrays where the accessible regions of the transcript are detected by hybridisation (See Figure 1.11). However, in the absence of these experimental approaches, bioinformatics has the potential to aid in the selection of regions which are single-stranded and thereby limit the design of non-hybridising antisense molecules. This is particularly

beneficial when a range of molecules are being tested against a single target mRNA transcript. Molecules are rapidly identified and selected on the basis of high binding affinity criteria, to a variety of targets on a transcript. Inefficient molecules targeted to regions of high mRNA self-hybridisation potential can be eliminated, and identification of a highly active molecule is more probable. Though they may exhibit strong activity, oligonucleotides identified by this method may not always represent the best potential molecule to target the transcript, as may practically be identified using antisense arrays.

The main steps in identifying an active antisense molecule and verifying its suitability for therapeutic applications are outlined overleaf.

Identify a suitable mRNA target for the antisense approach

↓

Select a target region on mRNA transcript
(Based on secondary structure or experimental analysis)

↓

Choose an antisense chemistry which will allow hybridisation to and destruction of this target

↓

Select sequence of antisense molecule to ensure specificity and strong hybridisation

↓

Deliver the antisense molecule to the cell cytosol to facilitate interaction with its target mRNA

↓

Assess efficacy of specific mRNA down-regulation of gene expression

↓

Confirm specific protein down-regulation following degradation of target mRNA relative to stringent chemistry and sequences controls

↓

Perform appropriate functional assay to detect specific cellular effects of mRNA down-regulation relative to stringent chemistry & sequence controls

↓

Analyse impact of antisense molecule delivery on global gene expression using micro-array

↓

Proceed to preclinical *in vivo* models

9.3 Modes of antisense delivery

Adequate delivery of antisense molecules to the appropriate cell type remains an important and difficult challenge. This study employed the highly efficient cell permeabilisation agent streptolysin-O (SL-O) which allowed the activity of antisense molecules and novel antisense chemistries to be assessed inside the cell, where they can hybridise to their target mRNA transcripts. While SL-O cell permeabilisation is highly effective in cell culture, this mode of antisense entry is limited to *ex vivo* applications as opposed to *in vivo* delivery approaches. Antisense delivery *in vivo,* particularly the use of systemic delivery, is a highly complex and challenging task.

The main barrier to the application of the antisense approach in the clinic remains the limited ability to deliver sufficient antisense molecules to the precise target. The only antisense drug currently approved by the FDA to date targets the eye area and is administered locally, by-passing the need for systemic administration (Filmore, 2004). The single most promising development in the field of antisense delivery is the development of a capsule which facilitates oral delivery of morpholino molecules. Following oral administration, the morpholino molecule in question (AVI-4557) successfully down-regulated the activity of the cytochrome P450 liver enzyme which metabolises commonly employed drugs (AVI BioPharma Press Release, March 2004). This is the first reported efficacy in humans of an antisense compound delivered by the oral route and represents a significant advancement in the development of successful morpholino and antisense therapies.

The challenge of effective siRNA delivery poses chemistry specific issues and due to their delicate nature, oral delivery may not be a feasible option. Potential approaches include hydrodynamic delivery and the use of viral delivery vectors to induce siRNA expression in target cells. Hydrodynamic injection involves high pressure administration of siRNA molecules either locally to a tumour site or via intravenous delivery. In the case of the mouse hydrodynamic tail injection inhibited expression of a kidney gene at the mRNA and protein level (Hamar *et al,* 2004). The prospect of successful delivery of siRNA following hydrodynamic injection as in the mouse remains unclear and may prove unfeasible in humans (Zender *et al,*

2004). It is undefined if there are selective sites for siRNA uptake *in vivo* or if there could be system wide delivery as is reported (Stevenson, 2004).

Systemic *in vivo* delivery of nuclease sensitive siRNA molecules can be circumvented by siRNA expression in target cells following transduction with viral vectors. Due to their ability to infect a broad spectrum of cell types, availability of high virus titre, and independence on the stage of cell growth, adenoviral vectors have been suggested as the optimal method for delivery of siRNA expression cassettes (Shen *et al,* 2004). An *in vivo* mouse model demonstrated the ability of siRNA molecules transduced by recombinant adenovirus to inhibit GFP expression following direct injection in the brain (Leirdal *et al,* 2002). In a separate study, adenoviral-siRNA constructs designed to inhibit the anti-apoptotic Survivin protein produced a strong reduction in tumour growth and extended the survival of treated subjects following hydrodynamic injection to solid tumours in nude mice. (Uchida *et al,* 2004). A recent review suggested that the application of viral vectors was limited due to safety issues associated with their usage (Schutze *et al,* 2004). The ability to deliver siRNA past the cell membrane using viral vectors is clear; however delivery to the tissue site limits their applicability for systemic delivery compared to the oral delivery route now feasible for morpholino chemistry molecules.

A novel method of siRNA delivery is the employment of Penetratin1, a membrane transporter protein which can be conjugated to an siRNA molecule via a disulphide bond. This link is cleaved in the reducing environment of the cytoplasm, releasing the bioactive-siRNA molecule. The Penetratin1 peptide has demonstrated a strong ability to deliver siRNA molecules to whole populations of primary neurons (Davidson *et al,* 2004). siRNA activity following Penetratin1 mediated cell entry is superior to that following Lipofectamine 2000 delivery in a number of cell lines and successful delivery is not associated with cell toxicity (Muratovska *et al,* 2004). The potential of molecules of this type for clinical application in a local or systemic context has yet to be explored. However Penetratin1 may reduce degradation of siRNA molecules and not only assist in their delivery but also in siRNA activity *in vivo*. Penetratin1 holds a high degree of promise and confers several advantages relative to the currently available liposomal approaches.

9.3.1 Cell permeabilisation via polyene antibiotics

A novel cell permeabilisation approach involves the use of sublethal doses of the polyene antibiotics. One of the derivatives of this family is the cationic amphotericin B 3' dimethylaminopropylamide (AMA), and is known to perturb plasma membrane permeability and this increase in permeability allows passage of antisense oligonucleotides into the cell (Garcia-Chaumont *et al,* 2000-a). Vectorisation of oligonucleotide into cells occurs whilst complexed with the antibiotic and aggregation of AMA occurs in response to a 20mer oligonucleotide. In this complex the nucleic acid is protected from serum degradation and RNase 1 attack and this may prove a fundamental advantage for clinical use. Unlike SL-O, which has been optimised and intended for use as an *ex vivo* purging tool, AMA has shown potential for direct injection into tumour tissue. Once inside the cell, AMA delivery results in a nuclear localisation for the antisense molecules (Kocisova *et al,* 2004). The transient nature of its permeabilisation coupled with the fact that it is a derivative of a widely applied clinical drug, implies it has several distinct characteristics. It can act as both a cell permeabilisation and oligonucleotide vector in one, and recent successes with AMA whilst targeting the multi-drug resistance gene have been published (Garcia-Chaumont *et al,* 2000-b). AMA may require a degree of optimisation to regulate the charge ratio between it and the oligonucleotide and while significantly less is required compared to other cationic vectors; this may limit its use.

9.4 Development of phosphorothioate-based antisense molecules

The phosphorothioate is by far the most characterised antisense backbone; its nuclease resistance and RNase H activation capacity facilitated its wide application in antisense studies leading to the development of several clinical trials. Even with the considerable number of clinical trials, to date only one antisense formulation has achieved market approval and that is the phosphorothioate-based Vitravene product which locally targets CMV retinitis. Another phosphorothioate-based compound which has undergone several phase II and phase III trials and is seeking approval by the FDA and European regulators is Genasense (G3139). This compound has demonstrated therapeutic activity in a wide-range of malignancies including stage II trials in B-cell Non-Hogkins Lymphoma (NHL), Acute Myeloid Leukaemia, Small Cell Lung Carcinoma (SCLC) and prostate cancer. Phase III Genasense trials are being performed in diseases such as melanoma, multiple myeloma, B-CLL, and Non-Small Cell Lung Carcinoma (NSCLC) (Tamm, Antisense Therapeutics, 2004). The applicability of Genasense over a broad range of malignancies is attributable to its selective choice of target, bcl-2, which is consistently up-regulated in a wide variety of cancers.

The efficacy of Genasense as a single chemotherapeutic agent has been demonstrated in a variety of diseases including prostate cancer and CLL (Orr *et al,* Antisense Therapeutics, 2004) however the majority of applications focus on its ability to chemo-sensitise cancer cells to currently employed chemotherapeutic agents by down-regulating the anti-apoptotic bcl-2 gene. These include carboplatin and etoposide in SCLC; dacarbazine in malignant melanoma, fludarabine and cyclophosphamide in CLL, and dexamethazone in multiple myeloma (Rudin *et al,* 2004). Dose-limiting toxicities associated with Genasense treatment were observed to be disease dependent and different protocols for antisense administration (in terms of dose required) need to be optimised and tested prior to clinical studies. The variability in sensitivity to Genasense between diseases may reflect bcl-2 expression levels.

Despite advancement to Phase III clinical trials in a number of diseases, the antisense mechanism of the Genasense molecule has recently been questioned. siRNA-mediated bcl-2 down-regulation in DU145 prostate cancer cells did not produce the cytostatic

effects induced by Genasense mediated down-regulation and suggested the functioning of the G3139 molecule may be bcl-2 and antisense independent (Raffo *et al*, 2004). Genasense recently received a significant set-back in its clinical trials when a trial was demoted from priority status due to a lack of efficacy in part due to the added risk of the intravenous mode of delivery (Winkler, 2004). The FDA review panel agreed that the Genasense molecule improved tumour response rate, but stated it was not satisfied this was solely due to an antisense mechanism and may be due to the presence of CpG motifs (Winkler, 2004).

Affinitak®, another phosphorothioate-based molecule involved in clinical trials, targets protein kinase C-α, an enzyme widely implicated in malignant transformation and proliferation (Villa-Calero *et al,* 2004). Following successful transition of Affinitak® through a phase I safety trial, a phase II trial in NSCLC indicated significantly enhanced survival rates from a median of 15.9 months for patients receiving Affinitak® compared to 8.3 months in patients receiving chemotherapy alone (carboplatin & paclitaxel). Following this promising finding, a large scale randomised phase III trial was initiated with 616 NSCLC patients to assess the ability of Affinitak® to prolong survival when combined with chemotherapy. However, in this large scale trial the survival of Affintak® patients was only marginally increased relative to those on chemotherapy alone (10 months versus 9.7), and the trial was discontinued (Orr, Antisense Therapeutics, 2004). Affintak® has since entered phase II clinical trials in NSCLC in combination with docetaxol, and two patients who had previously demonstrated resistance to paclitaxel had partial responses (Villa-Calero *et al,* 2004). However, the future of this agent in the treatment of cancer is uncertain due to the failure of the phase III trial.

Similar phase II trials using ISIS 5132 phosphorothioate based molecules to target c-raf expression failed to show therapeutic responses in a range of solid tumours. No clinical activity of this as a single agent was recorded leading to its discontinuation in clinical trials (Tamm, Antisense Therapeutics, 2004). The phosphorothioate remains the most dominant antisense backbone in clinical studies though uncertainty still surrounds its application *in vivo*. The emergence of novel backbone chemistries into clinical trials represents a significant advancement in the application of active molecules which function solely by an antisense mechanism of action. Though secondary effects of the

phosphorothioate are considered substantial and disadvantageous; they are well defined and this remains a drawback to the application of novel compounds.

The ability of the phosphorothioate-based oligonucleotides investigated in this study to down-regulate mRNA expression when targeting the bcr-abl start site and breakpoints was found to be affected by levels of secondary structure in the target binding region and to a large extent on intra-molecular antisense foldings. Though strong levels of bcr-abl mRNA down-regulation were observed, these were over-shadowed by non-specific effects induced by sense and scrambled sequence controls. Given the reported system-wide phosphorothioate side-effects, and in the context of the non-sequence dependent phosphorothioate mediated effects observed in this study; phosphorothioate oligonucleotides were considered to be unsuitable for the sequence specific down-regulation of bcr-abl.

9.5 Novel antisense approaches

9.5.1 Morpholino antisense molecules

Morpholino molecules are one of the few antisense chemistries to reliably induce an antisense response via steric hindrance. Others include the peptide nucleic acids (PNA)'s which have a peptide linked oligonucleotide chain. The efficacy of morpholino antisense molecules has been strongly established in the field of functional genomics and appears to hold significant promise for clinical applications (Corey *et al,* 2004; Suwanmanee *et al,* 2002). Aberrant pre-mRNA splice sites result from mutations within the β-globin gene and lead to the anaemic condition, β-thalassemia. Morpholino molecules targeted to the aberrant splice sites of the pre-mRNA form inhibited the recognition and splicing of the mRNA at this point and the splicing machinery was re-directed to the normal splice site, restoring the normal splicing pathways and correcting expression of the mutated gene (Schmajuk *et al*, 1999). However, if an RNase H competent backbone had been chosen it would have mediated destruction of the mRNA transcript. An anti-TNF-α morpholino antisense oligomer has been evaluated in an *in vivo* mouse model following intranasal insufflation. Anti-TNF-α treated populations showed reduction in TNF-α expression by approximately 30% compared to sequence control treated populations and reduced polysaccharide mediated pulmonary fibrosis. Another finding of this study was that following intranasal insufflation 80% of cells had taken up the FAM-labelled morpholino molecule (Qin *et al*, 2000).

Due to their nuclease resistance and sequence specific effects, the morpholino chemistry is particularly suited to various oligonucleotide applications. The sister technology of antisense is the antigene or triple-helix forming oligonucleotide (TFO) approach; both aim to disrupt expression of target genes normally involved in disease progression. TFO molecules function by forming a triple helical structure with sequences of genomic DNA and preventing their recognition and expression by transcription factors. Degradation due to oligonucleotide stability is also a limiting factor in their performance (Re *et al,* 2004). Unlike forerunning antisense

chemistries, morpholino molecules are particularly suited to TFO applications due to their strong nuclease resistance and high affinity binding (Torigoe *et al,* 2003).

Limited morpholino clinical data are available; *in vivo* bioavailability studies in mice indicated intact AVI-4126 morpholino molecules were present in PC-3 tumours 4, 8 and 24 hours following intravenous administration. The level of intact oligonucleotide diminished over time, however, no evidence was detected of truncated or partially degraded molecules (capable of detecting N-1 nucleotides) (Iversen *et al,* 2003). Expression of the AVI-4126 target c-myc was significantly reduced in treated mice relative to sequence controls and apart from the tumour site, the liver and kidney were identified as the main locations of morpholino accumulation following intravenous administration (Iversen *et al,* 2003).

A phase I clinical trial to evaluate the safety of the AVI-4126 morpholino molecule in humans was performed using a range of morpholino concentrations intravenously administered to healthy volunteers from different ethnic backgrounds. A number of dose-independent side effects, graded as mild by the NCI clinical trial criteria were reported, however no effects were attributable to the morpholino treatment (Iversen *et al*, 2003). Though limited in scale this study was significant as it displayed the potential for the safe administration of morpholino molecules to humans for therapeutic purposes.

One finding of this study was the detection of elevated levels of the split complement component C3a in serum of treated individuals. This is a characteristic commonly observed following phosphorothioate molecule treatment and was considered a feature of its chemistry (Orr, Antisense Therapeutics, 2004). The finding that this also occurs following treatment with morpholino molecules signifies that this complication is less related to their backbone chemistry and is possibly generated by the presence of oligonucleotide bases alone, indicating it may be an essential factor to monitor following oligonucleotide administration. Other secondary characteristics of phosphorothioate administration were not observed following AVI-4126 treatment.

The AVI-BioPharma corporation has entered a number of morpholino-based compounds termed NeuGene® into phase I and II clinical trials following their

successful transition through preclinical models (AVI BioPharma website, 2004). A total of nine different molecules are currently being evaluated and a phase III trial analysing the effectiveness of the c-myc-targeted Resten-NG molecule compared to current therapies for restenosis, is in the planning stages. Other trials in the pipeline include a NeuGene® molecule to target the ebola virus and another to sensitise patients to chemotherapeutic drugs by targeting the role of cytochrome p450 in drug metabolism (Arora *et al,* 2002). Oral delivery provides a promising mode of delivery for the morpholino molecules which lie in the early stages of clinical development, though only one phase III trial is planned at present. While phosphorothioate trials have predominated it is now clear that there is potential for new approaches using non-RNase H dependent molecules.

Arguably the biggest recent advance in antisense therapeutics has been the positive results reported in the down-regulation of drug metabolism following oral administration of AVI-4557 in humans (AVI BioPharma Press Release, March 2004). The success of this approach has been aided in part by the morpholino properties of strong nuclease resistance even at low pH as the morpholino capsules were designed to release in the small intestine (Iversen *et al,* 2001). Progress of this type was unlikely to have been achieved by the phosphorothioate due to the nuclease sensitivity of its chemistry. Oral administration of AVI-4557 resulted in an increase in drug effectiveness and decrease in the concentration of midazolam required to elicit the most beneficial effect. As the target of AVI-4557 is in the human liver its activity was inferred following increased sensitivity to therapy rather than direct evidence of protein knock-down. Clear verification that its observed effects are 100% attributable to antisense down-regulation of cytochrome protein would be valuable.

The morpholino molecule designed in this study to target the bcr-abl translational start site down-regulated BCR-ABL protein expression and this was attributable to strong hybridisation of the morpholino molecule at the target site. Significantly for their application in CML *ex vivo* purging, morpholino molecules exhibited no inhibitory or negative impact on the proliferation of healthy haematopoietic cells. The morpholino mediated dose-dependent decrease in BCR-ABL expression was found to be sequence specific, however the morpholino molecule displayed limited ability to reduce the growth of CML cells following its down-regulation and this

indicates that a combined approach with chemotherapy or other antisense agents may prove necessary.

9.5.2 siRNA induced gene down-regulation

RNAi was labelled 'Breakthrough of the Year' by Science in 2002 (Couzin, 2002). Adopting RNAi to an antisense approach, by employing short double stranded RNA molecules holds promise for the development of RNA-directed therapeutics. Given that the first reported demonstration of activity of siRNA in eukaryotes was in 1998, there have been considerable advances to its first application in mammals in 2001 (Fire *et al,* 1998). *In vivo* mouse models have demonstrated siRNA mRNA degradation activity in liver, kidney, spleen, lung and pancreas (Phillips *et al,* Antisense Therapeutics, 2004) following intravenous administration in mice. This is in contrast to phosphorothioate molecules which are distributed to all parts of the body bar the brain and components of the central nervous system following injection (Phillips *et al,* Antisense Therapeutics, 2004).

Due to their greater flexibility in chemistry, usually lower synthesis costs and comparative ease of delivery *in vivo,* antisense oligonucleotides are considered to be more suitable for antisense approaches. The high nuclease sensitivity of siRNA based molecules may prove the greatest draw-back to their application *in vivo.* Limited siRNA modifications have been reported to enhance their resistance and binding potential (Chiu *et al,* 2003). However, the main concern is that activation of the endogenous RNAi machinery will not occur due to lack of RNA recognition and this confines modification of siRNA molecules to very minor alterations. Another draw-back of harnessing the RNAi pathway by siRNA molecules is that the down-regulatory effect is transient (Scherr *et al,* 2004). However, unlike morpholino mediated inhibition of gene expression the RNAi mechanism may be triggered by endogenous siRNA expression cassettes, and this may lead to more diverse applications and the development of niche fields such as cancer vaccines where siRNA may dominate.

9.5.3 RNAi Potential for Therapeutic Applications

To date, considerable success has been demonstrated in the down-regulation of gene expression in mammalian cells using siRNA molecules. For the development of this strategy into a therapeutic tool which can knock-down or abolish disease-associated gene expression, further experimentation to elucidate fully the mechanism of action needs to be performed and further information regarding intra-cellular behaviour gathered. Preliminary results targeting the bcr-abl mRNA using the RNAi approach have demonstrated the ability of siRNA to down-regulate mRNA, whilst not affecting expression of either normal c-abl or c-bcr expression. BCR-ABL protein down-regulation was confirmed using immuno-blotting. However, consistent with RNAi activity in mammalian cells, effects were highly transient and transfection of primary CML cells with siRNA failed to inhibit cell proliferation or CML colony formation (Scherr *et al,* 2003).

This failure may be connected to the transient nature of down-regulation induced by this form of RNAi; or may be accountable by secondary effectors in CML which retain the ability to drive the cell cycle for periods following bcr-abl deprivation. This siRNA mediated reduction in mRNA without concomitant effects on cell proliferation or colony formation is in contrast to the effects of the selective tyrosine kinase inhibitor, imatinib mesylate, the active agent in the CML drug, Imatinib. However, pre-treatment of bcr-abl expressing cells with anti-bcr-abl siRNA was found to induce a 3.4 fold reduction in the IC_{50} value of imatinib (Wohbold *et al,* 2003). This increased sensitivity is determined by the quantity of BCR-ABL protein inside the cell and is affected by siRNA treatments. Anti-bcr-abl siRNA resulted in a reversion in bcr-abl positive cells resistance to DNA damage and strongly sensitised cells to the effects of γ-irradiation (Wohbold *et al,* 2003).

In this study four siRNA molecules employed to target the bcr region of the bcr-abl hybrid mRNA indicated different abilities to down-regulate bcr-abl mRNA and protein expression. The ability of siRNA molecules to mediate mRNA down-regulation was correlated with levels of secondary structure surrounding the target binding sites, which inhibits hybridisation at these points. The impact of siRNA

molecules on the proliferative capacity of CML cells was measured using a pool of the four siRNA duplexes. This approach may facilitate enhanced hybridisation due to non-saturation of binding sites. However, the ability of the siRNA pool to reduce the proliferative capacity of CML cells was limited. On a positive note, the siRNA duplexes did not display toxic effects toward normal haematopoietic cells, and re-designing the siRNA duplexes in-house may prove more useful.

In the non-malignant disease setting, the HIV virus responsible for the AIDS condition has been the focus of several gene specific targeted therapies. This is a particularly suitable target for gene knock-down systems due to the difference in viral sequence targets and the substantial availability of information regarding genes whose expression is vital for viral infectivity. siRNA molecules targeting different steps in the HIV-1 life cycle have been shown to induce RNAi in $CD4^+$ T lymphocytes and inhibit expression of virally encoded genes using a GFP reporter model (Jacque *et al,* 2002). The viral gag gene, whose polypeptide is cleaved to yield the main structural components of the HIV-1 virus, the p24, p17 & p15 proteins; was targeted by siRNA agents at the p24 region. The resultant four fold reduction in the levels of the viral protein was accompanied by silencing of the full length viral mRNA transcript after 48 hours. Viral particle production measured by ELISA at 120 hours demonstrated a 25 fold reduction in the p24 titres (Novina *et al,* 2002).

An alternative approach to the transient down-regulation of viral genes is the stable introduction of anti-HIV-1 siRNA constructs into haematopoietic stem cells. A third generation lentiviral vector system has been utilized to produce siRNA transducing vector viruses (Akkina *et al,* 2003). Lentiviral vectors have an advantage due to their ability to integrate into non-dividing haematopoietic stem cells. Specific sense and antisense sequences were positioned in tandem and driven by Human U6 snRNA promoters to express the anti-rev gene siRNA. Colony forming assays indicated CD34+ cell populations' transfected with siRNA constructs (at > 90% transduction levels) did not inhibit growth or differentiation relative to the non-transfected counterparts (Holen *et al,* 2003). Although protection from infection was not absolute, this is akin to what is desirable in a clinical setting and provides a proof of concept for stem cell gene therapies in the treatment of human disease.

Sequence specificity of nucleic-acid based therapies is paramount. While some reports suggest a single mis-match in the central region of the molecule is sufficient for inactivation of RNAi (Czauderna *et al,* 2003) others suggest this is insufficient to affect activity and four mutations are necessary to completely abolish its effects (Amarzguioui *et al,* 2003). Micro-array experiments have shown a large number of non-targeted genes with as few as eleven continuous nucleotides with identity to the siRNA were affected by siRNA treatment. This rules out the use of siRNA molecules in the treatments of single nucleotide mutation disorders, and indicated the strong need for thorough pre-treatment testing of all molecules for non-specific targets. At a concentration of 100μM siRNA molecules significantly induced the expression of several genes involved in apoptosis and stress response pathways. However, this effect is eliminated by reducing siRNA levels to 20μM (Sioud *et al,* 2003).

9.6 The potential role of Antisense therapeutics in the treatment of CML

The advent of imatinib has led a new era on the treatment of CML, however the occurrence of resistance can limit its success and BMT remains the only curative therapy for CML. The use of autologous BMT (ABMT) is being investigated in a number of leukaemias due to the dependence on a matched bone marrow donor for allogenic BMT. The main concern in the application of ABMT is that clonogenic tumour cells contained in the haematopoietic stem cell transplant can contribute to disease relapse following transplantation (Alvarnas *et al,* 2004). Auto-grafting has been performed with chemotherapeutic drugs, monoclonal antibodies and complement; however the development of novel efficient purging approaches which can selectively reduce tumour cell populations will drive this promising field.

Antisense strategies hold a high degree of promise for molecular intervention in CML and there are a variety of therapeutic targets other than bcr-abl to consider. To date clinical trials targeting bcr-abl in CML have been limited to two reported cases with small patient numbers (De Fabritis *et al,* 1998 & Clarke *et al,* 1999). Both studies employed *ex vivo* purging to circumvent the delivery issue, despite success achieved in intravenous injection of Genasense (Orr *et al,* Antisense Therapeutics, 2004). A phosphorothioate antisense oligonucleotide designed to down-regulate c-myb has entered clinical trials with CML patients in blast crisis (Zhang *et al,* Antisense Therapeutics, 2004). The c-myb transcription factor is a relevant antisense target; though its expression is not CML specific. C-myb is up-regulated in a variety of leukaemias and thus an antisense approach could be employed in a number of haematological malignancies similar to the application of Genasense. Down-regulation of c-myb led to depletion of bcr-abl expression (Orr *et al,* Antisense Therapeutics, 2004) and this phosphorothioate molecule has also demonstrated strong efficacy in autologous *ex vivo* purging procedures (Luger *et al,* 2002). The application of antisense therapy to CML is a promising start and the development of active antisense molecules with suitable backbones has the potential to advance this therapy through the stages of clinical trials.

A potential advantage of using c-myb as a target in CML rather than bcr-abl is that it has a short half-life (30-50 minutes); compared to BCR-ABL (half-life ~48 hours) (Luger *et al*, 2002). This aspect of BCR-ABL may reduce effectiveness of antisense molecules and necessitates the application of an antisense chemistry which can withstand degradation for prolonged periods within the cell. The bcr-abl directed morpholino molecule used in this thesis reduced BCR-ABL protein levels and as this chemistry has been formulated for oral delivery, this may prove a feasible option for adjuvant treatment of CML patients outside the context of ABMT. Down-regulation of the proliferative capacity of CML cells following treatment with bcr-abl directed siRNA molecules indicates the feasibility of employing this approach in purging ABMT harvests; however translation of this *ex vivo* effect to CML cells *in vivo* may prove problematic.

9.7 Down-regulating cyclin D2 expression in CML

Down-regulation of BCR-ABL by both the morpholino and siRNA approaches had limited impact on the CML cell proliferation capacity. As previously discussed, cyclin D2 is a down-stream target of bcr-abl; possibly through RAS mediated signalling (Section 1.7.5). Cyclin D2 expression was investigated as a potential target to facilitate a reduction in the proliferative capacity of CML cells as it is essential for bcr-abl mediated transformation and is relied on by bcr-abl to induce continued cell proliferation (Jena *et al,* 2002). Down-regulation of cyclin D2 has the potential to severely compromise the transformation ability of bcr-abl by preventing continued cell proliferation. Morpholino and siRNA molecules were designed to target the cyclin D2 mRNA in order to reduce the proliferative status of CML cells (Table 3.4 & 3.6). Down-regulation of cyclin D2 induced a strong decrease in the growth capacity of CML cells (Chapter 8). Inhibiting cyclin D2 expression in normal cells has limited effects due to its overlapping role with other members of the cyclin family (Brooks *et al,* 1996). However, its expression has been linked to myeloid reconstitution *in vivo* (Sasaki *et al,* 2004).

9.8 Future directions

In this thesis, down-regulation of oncogenic mRNA expression was demonstrated by a variety of antisense chemistries. Translating these effects into reductions in the oncogenic potential of CML cells remains a challenging task which may be tackled by a number of approaches. To decrease the level of CML cell proliferation significantly, down-regulation of BCR-ABL alone is probably insufficient and a combined approach is required. This is due in part to the sustained half-life of BCR-ABL, which limits effectiveness of mRNA down-regulation and requires a highly stable backbone to mediate prolonged down-regulation. Reducing expression of cyclin D2 in CML cells had a significant effect on their proliferative capacity. The next step would be to examine if down-regulation of bcr-abl and cyclin D2 in combination can enhance the anti-proliferative effects on CML cells. As both morpholino and siRNA approaches reduced the BCR-ABL protein load, both may be applied in combination with anti-cyclin D2 oligonucleotides. However, the morpholino has a very stable structure leading to sustained effects and this may prove an advantage.

Streptolysin-O proved a very efficient method of delivering antisense oligonucleotides to cells in culture and may have therapeutic application in the context of *ex vivo* purging. However, since the commencement of this project a number of compounds suitable for antisense delivery *in vivo* has been identified including the peptide based Penetratin1 and the antibiotic based AMA. These compounds have broader applicability *in vivo* and may have a reduced potential to mediate cell toxicity, which is a limitation to the use of streptolysin-O. Unlike other currently employed delivery approaches these compounds mediate non-endocytic cellular delivery and facilitate interaction between antisense molecules and their target mRNA transcripts.

9.9 'Shooting the messenger'- Concluding remarks

Twenty-seven years following the initial identification of mRNA down-regulation by sequences of complementary nucleic acids, the application of the antisense approach to therapeutic intervention strategies remains a challenging goal (Paterson *et al*, 1977). Limited success has been achieved in the area of adjuvant therapy for AIDS-related CMV retinitis, where an antisense molecule is employed to down-regulate viral gene mRNA sequences. The success of this approach has shown that the initial promise of specific gene down-regulation could be translated to the clinical setting.

Currently, the main application for antisense molecules in the clinical context is their potential role as chemo-sensitisation agents for chemotherapeutic drugs e.g. Genasense. The development of antisense agents beyond this application, where further treatment is not required is not currently a realistic option. Using antisense as a single agent requires the implementation of a backbone chemistry which can induce sustained down-regulation of target protein expression. To facilitate the functioning of active antisense chemistries, the long-standing issue of delivery needs to be resolved, and recently positive steps in this direction have been achieved.

Antisense technology has emerged as a new source of potential products for use in therapeutics, diagnostics and research applications. The identification of genes involved in disease initiation and progression provides a vast resource for potential targets for antisense therapeutics. Active antisense sequences combined with stable chemistry formulations and efficient delivery approaches could allow the development of novel drugs, and possibly drugs that can compete with current drugs by specifically preventing expression of mutant proteins implicated in the development of disease.

Appendix 1

Optimisation of TaqMan parameters for determination of gene expression by the comparative method

A.1 Optimisation of primers for TaqMan amplification

To bind to their targets within the TaqMan amplifying conditions primers are required to have a Tm between 58^0C and 60^0C. Following design of an appropriate set of primers for each target gene, a range of concentrations were tested to determine the concentration that yields the minimum Ct value. The threshold cycle or Ct value is the cycle at which a statistically significant, increase in ΔR_n is first detected. ΔR_n is the difference between the emission intensity of the no amplification control and that of the positive sample. As the forward and reverse primers may bind to their target sequences with unequal affinity different combinations of forward and reverse were examined for optimal amplification.

Table A.1 Results of the Primer Optimisation experiment carried out for the b3a2 primers. The Ct values are an average of 4 readings.

Primer Concentration (nM)		Ct Value
Forward	Reverse	
50	50	20.25
300	50	18.5075
900	50	19.5525
50	300	20.49
300	300	19.8525
900	300	19.4775
50	900	20.67
300	900	20.0725
900	900	19.7225
non-template control		40
no probe control		40

All primer concentrations tested displayed good amplification of target and the the 300:300 concentration combination was selected for routine experiments. The earliest Ct value detected was 18.5075 for the 300:50 combination. Increasing the concentration of forward primer improved the performance of the primers, however increasing the concentration of the reverse primer had little or no effect on Ct, indicating that it was binding efficiently even at low concentrations. The non-template controls and no probe controls both displayed no increase in fluorescence after 40 cycles; indicating the amplification was b3a2 specific and there was no contamination present in the set-up. Determination of the appropriate probe concentration was performed following primer optimisation and concentrations ranged between 25nM to 225nM.

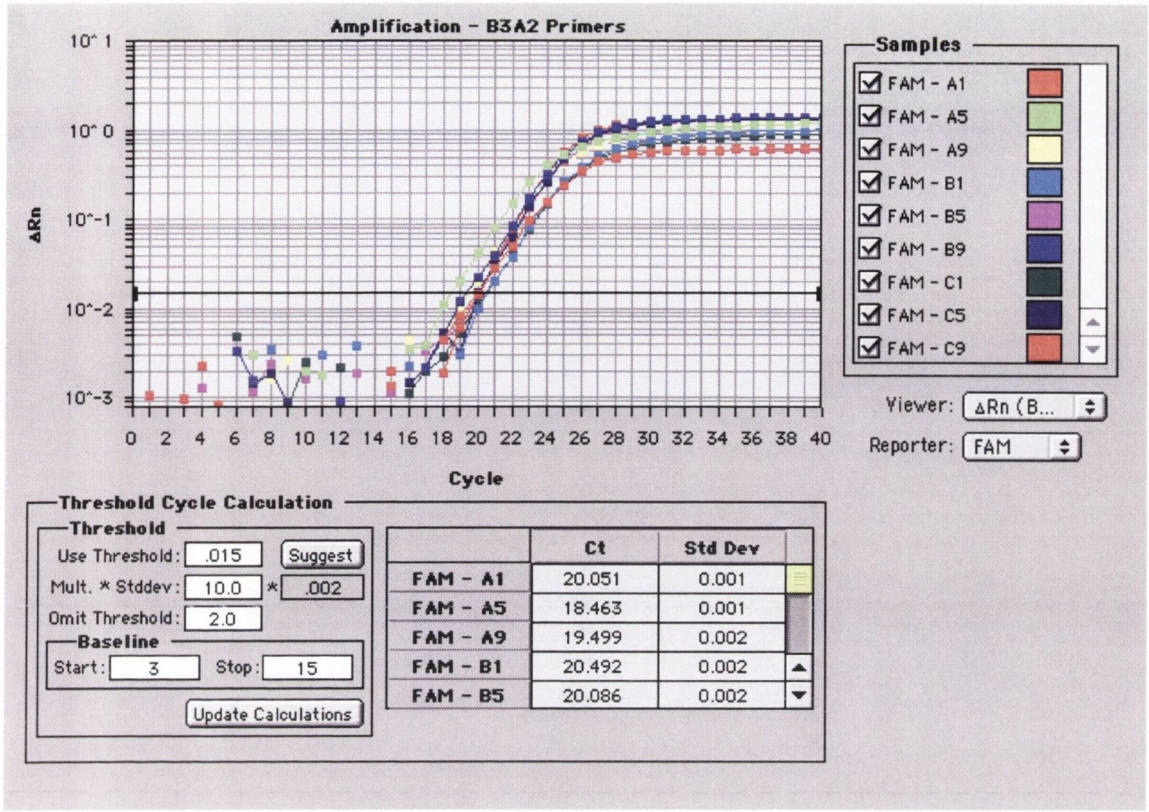


Figure A.1 A TaqMan plot showing amplification of bcr-abl using b3a2 specific primers

A.2 Multiplexing TaqMan Reactions

To facilitate exact comparisons in gene expression between different targets when possible both amplification reactions were performed in a single well. This could only occur if their probes were tagged with different fluorescent labels and increased the number of reactions per TaqMan plate. To this end, primer efficiencies were analysed alone and in duplex, using neat and diluted cDNA to assess any cross-reactions.

Table A.2 Ct values obtained using b2a2 and GAPDH primers alone and in duplex, and using cDNA neat and diluted one in ten.

Primers	c DNA	B2A2	GAPDH
B2A2	Neat	20.9575	-
	1/10 Dilution	24.92	-
GAPDH	Neat	-	15.5875
	1/10 Dilution	-	19.27
B2A2 + GAPDH	Neat	21.3775	15.6325
	1/10 Dilution	25.175	19.41

The b2a2 Ct value was marginally increased when primers were amplified in duplex with GAPDH primer sets. The change is insignificant and therefore the primers are suitable for multiplexing. There was also a slight decrease in the ΔR_n value for the reaction, however this change is not significant as ΔR_n value is not used for calculation of gene expression (Figure A.3).

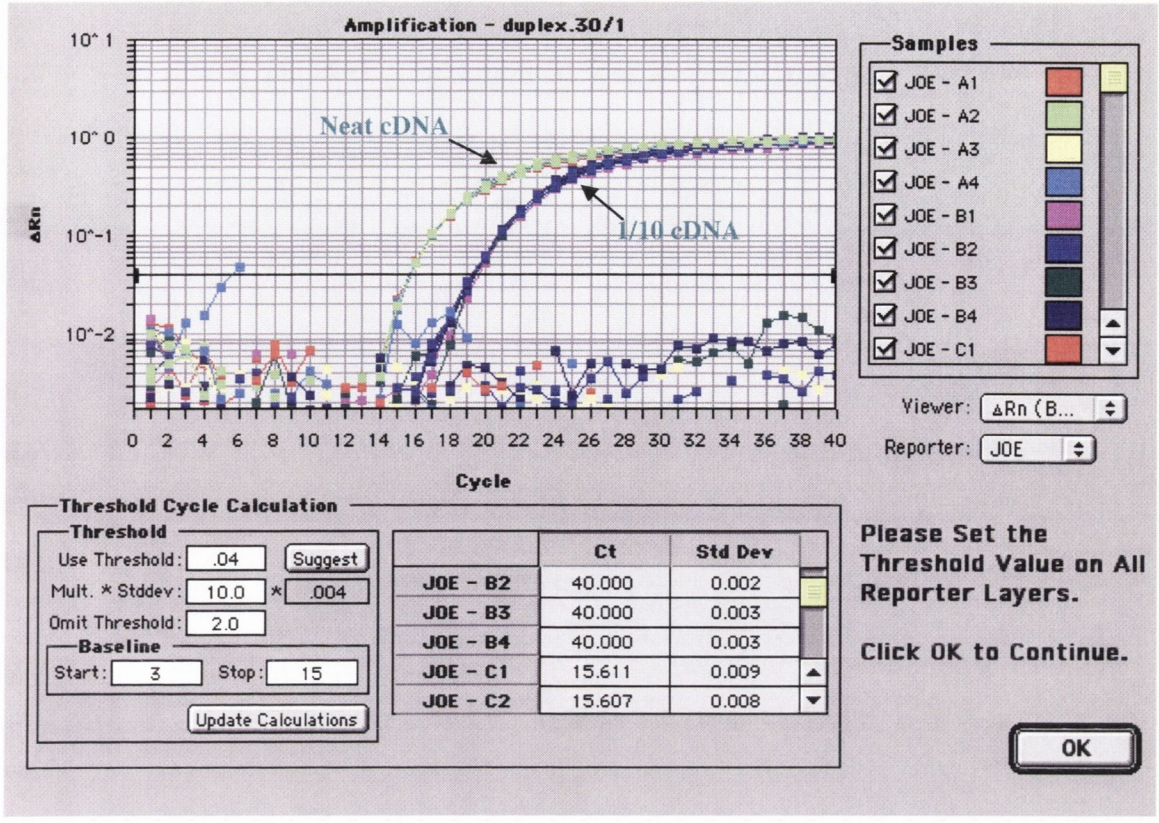


Figure A.2 GAPDH amplification in 1. Neat cDNA and 2. cDNA diluted 1/10 on the Ct value of GAPDH. ΔR_n remained constant

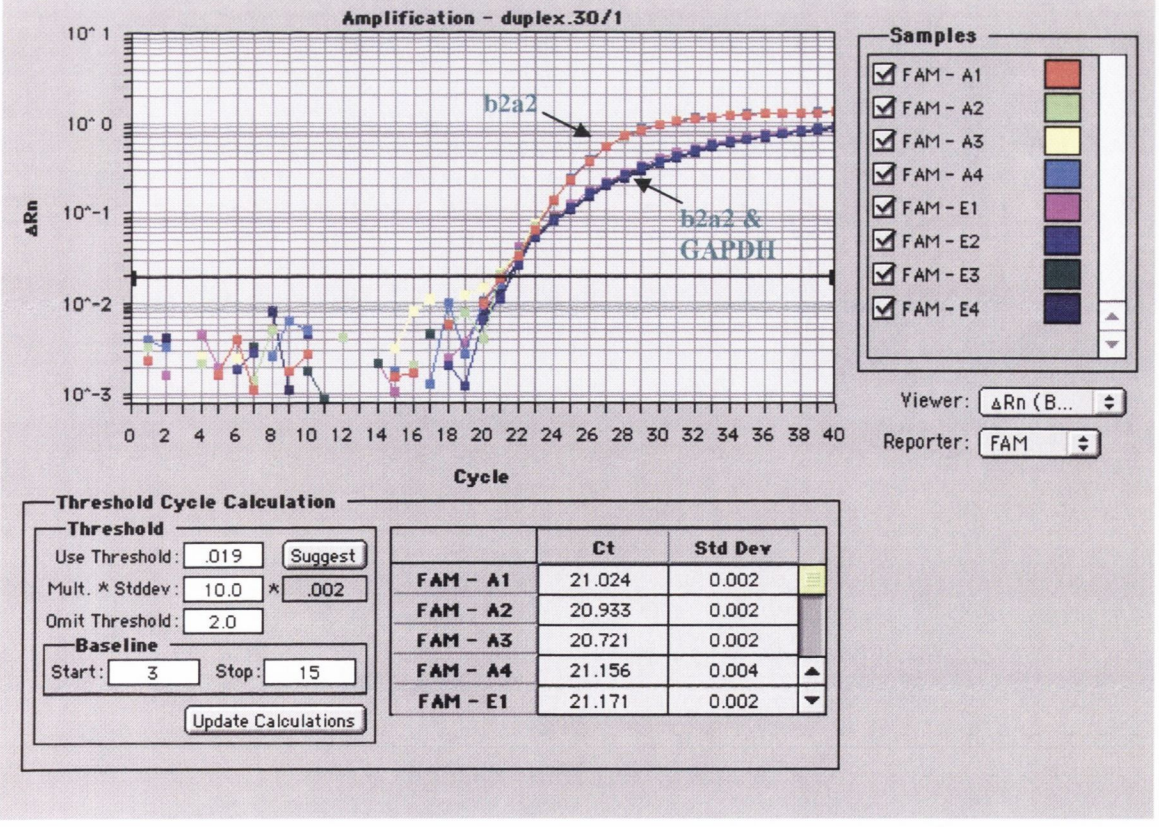


Figure A.3 Amplification of b2a2 primers alone and in the duplex with GAPDH primers. Ct values remain constant.

A.3 Efficiency Curve (Validation Experiment)

In order to compare levels of a target sequence with those of a standard housekeeping gene, both sets of primers need to amplify their respective targets with comparable efficiencies over a range of target concentrations. This is to allow for accurate comparisons between their expression at different concentrations of target. cDNA was serially diluted (1-1/1,000) and amplified using both sets of primers. The ΔCt over each dilution was calculated (Table A.3), and the graph of log dilution against ΔCt was plotted (Figure A.4). Primer sets are said to have comparable efficiency if the slope of this graph is less than 0.1.

Table A.3 ΔCt values for b2a2 and GAPDH following amplification with the serially diluted cDNA. ΔCt values for the serial dilution of cDNA.

cDNA	B2A2	GAPDH	ΔCt
Neat	21.9775	15.2375	6.74
1/2	22.64	16.2025	6.4375
1/5	24.08	17.495	6.585
1/10	25.7875	19.3775	6.41
1/20	27.7775	20.52	7.2575
1/50	27.81	21.8375	5.9725
1/100	29.2975	23.3875	5.91
1/200	30.7775	24.335	6.4425
1/500	32.3475	25.9875	6.36
1/1,000	32.5325	26.8925	5.64

The ΔCt values were plotted against the log fold dilution (Figure A.4). The slope of the graph was less than 0.1, therefore the primer sets amplified their targets with similar efficiencies and were suitable for comparative expression analysis.

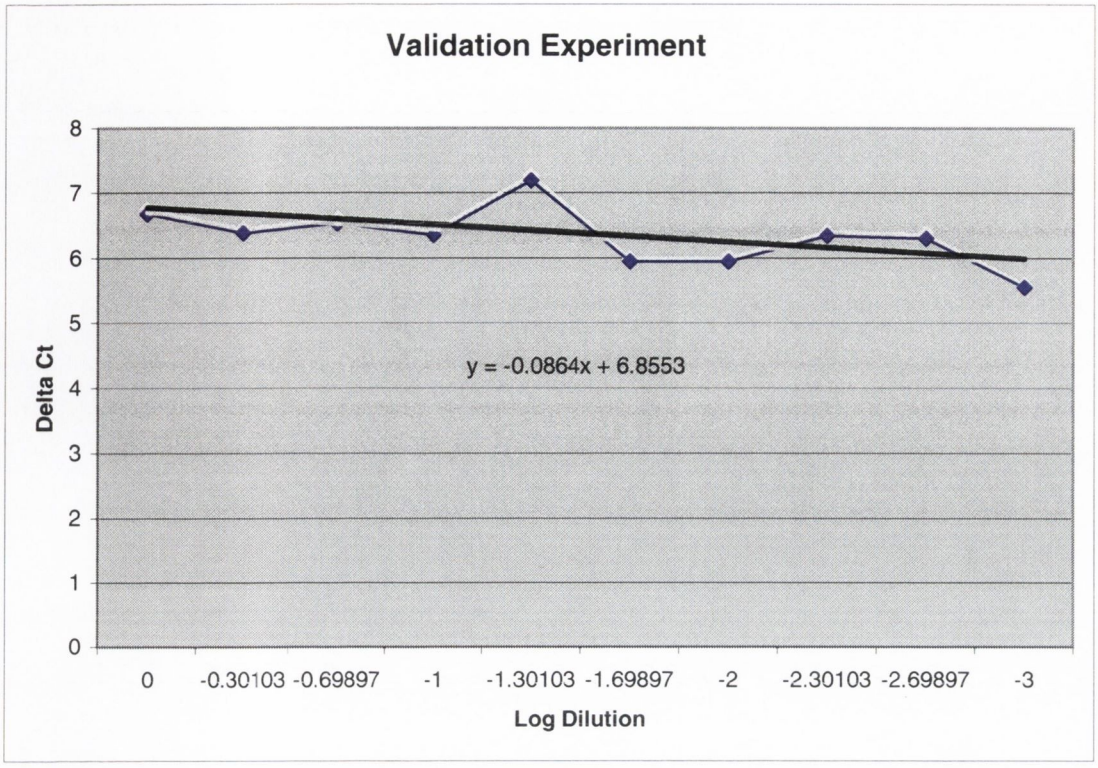


Figure A.4 The ΔCt values for the serially diluted cDNA plotted against the log dilution to examine the efficiency of amplification

References

Abe T, Takai K, Nakada S, Yokota T, Takaku H (1998) Specific inhibition of influenza virus RNA polymerase and nucleoprotein gene expression by circular dumbbell RNA/DNA chimeric oligonucleotides containing antisense phosphodiester oligonucleotides. *FEBS Lett* **425**, 91-6.

Afar DE, Goga A, McLaughlin J, Witte ON, Sawyers CL (1994) Differential complementation of Bcr-Abl point mutants with c-Myc. *Science* **264**, 424-6.

Agami R (2002) RNAi and related mechanisms and their potential use for therapy. *Curr Opin Chem Biol* **6**, 829-34.

Agarwal N, Gewirtz AM, Author (1999) Oligonucleotide therapeutics for hematologic disorders. *Biochim Biophys Acta* **1489**, 85-96.

Agrawal I, Kandimalla ER, Author (2000) Antisense therapeutics: is it as simple as complementary base recognition? *Mol Med Today* **6**, 72-81.

Agrawal N, Dasaradhi PVN - Mohmmed A, Mohmmed A FAU - Malhotra P, Malhotra P FAU - Bhatnagar RK, Bhatnagar RK FAU - Mukherjee SK, PST - ppublish SO - MSL-eP-JAP-UST-J-S-IE-M- (2003) RNA interference: biology, mechanism, and applications. *Microbiol Mol Biol Rev* **67(4):**, 657-85.

Agrawal S, Author (1999) Importance of nucleotide sequence and chemical modifications of antisense oligonucleotides. *Biochim Biophys Acta* **1489**, 53-68.

Agrawal S, Jiang Z, *et al.* (1997) Mixed-backbone oligonucleotides as second generation antisense oligonucleotides: in vitro and in vivo studies. *Proc Natl Acad Sci U S A* **94**, 2620-5.

Agrawal S, Zhao Q (1998) Antisense therapeutics. *Curr Opin Chem Biol* **2**, 519-28.

Ahlquist P (2002) RNA-dependent RNA polymerases, viruses, and RNA silencing. *Science* **296**, 1270-3.

Akhtar S, Hughes MD, Khan A, Bibby M, Hussain M, Nawaz Q, Double J, Sayyed P, Author (2000) The delivery of antisense therapeutics. *Adv Drug Deliv Rev* **44**, 3-21.

Akkina R, Banerjea A, Bai J, Anderson J, Li MJ, Rossi J (2003) siRNAs, ribozymes and RNA decoys in modeling stem cell-based gene therapy for HIV/AIDS. *Anticancer Res* **23**, 1997-2005.

Alisky JM, Davidson BL (2004) Towards therapy using RNA interference. *Am J Pharmacogenomics* **4**, 45-51.

Alley MC, Scudiero DA, *et al.* (1988) Feasibility of drug screening with panels of human tumor cell lines using a microculture tetrazolium assay. *Cancer Res* **48**, 589-601.

Alvarnas JC, Forman SJ (2004) Graft purging in autologous bone marrow transplantation: a promise not quite fulfilled. *Oncology (Huntingt)* **18**, 867-76; discussion 876-8, 881, 884.

Amarzguioui M, Brede G, Babaie E, Grotli M, Sproat B, Prydz H (2000) Secondary structure prediction and in vitro accessibility of mRNA as tools in the selection of target sites for ribozymes. *Nucleic Acids Res* **28**, 4113-24.

Amarzguioui M, Holen T, Babaie E, Prydz H (2003) Tolerance for mutations and chemical modifications in a siRNA. *Nucleic Acids Res* **31**, 589-95.

Ando K, Ajchenbaum-Cymbalista F, Griffin JD (1993) Regulation of G1/S transition by cyclins D2 and D3 in hematopoietic cells. *Proc Natl Acad Sci U S A* **90**, 9571-5.

Anselmet A, Mayat E, Wietek S, Layer PG, Payrastre B, Massoulie J (2002) Non-antisense cellular responses to oligonucleotides. *FEBS Lett* **510**, 175-80.

Arora V, Cate ML, Ghosh C, Iversen PL (2002) Phosphorodiamidate morpholino antisense oligomers inhibit expression of human cytochrome P450 3A4 and alter selected drug metabolism. *Drug Metab Dispos* **30**, 757-62.

Arora V, Devi GR, Iversen PL (2004) Neutrally charged phosphorodiamidate morpholino antisense oligomers: uptake, efficacy and pharmacokinetics. *Curr Pharm Biotechnol* **5**, 431-9.

Askari FK, McDonnell WM, Author (1996) Antisense-oligonucleotide therapy. *N Engl J Med* **334**, 316-8.

Baker BF, Condon TP, Koller E, McKay RA, Siwkowski AM, Vickers TA, Monia BP (2001) Discovery and analysis of antisense oligonucleotide activity in cell culture. *Methods* **23**, 191-8.

Barry EL, Gesek FA, Friedman PA (1993) Introduction of antisense oligonucleotides into cells by permeabilization with streptolysin O. *Biotechniques* **15**, 1016-8, 1020.

Bashir T, Pagano M (2003) Aberrant ubiquitin-mediated proteolysis of cell cycle regulatory proteins and oncogenesis. *Adv Cancer Res* **88**, 101-44.

Basye J, Trent JO, Gao D, Ebbinghaus SW (2001) Triplex formation by morpholino oligodeoxyribonucleotides in the HER-2/neu promoter requires the pyrimidine motif. *Nucleic Acids Res* **29**, 4873-80.

Beale G, Hollins AJ, Benboubetra M, Sohail M, Fox SP, Benter I, Akhtar S (2003) Gene silencing nucleic acids designed by scanning arrays: anti-EGFR activity of siRNA, ribozyme and DNA enzymes targeting a single hybridization-accessible region using the

same delivery system. *J Drug Target* **11**, 449-56.

Bedi A, Zehnbauer BA, Barber JP, Sharkis SJ, Jones RJ (1994) Inhibition of apoptosis by BCR-ABL in chronic myeloid leukemia. *Blood* **83**, 2038-44.

Beltinger C, Saragovi HU, *et al.* (1995) Binding, uptake, and intracellular trafficking of phosphorothioate-modified oligodeoxynucleotides. *J Clin Invest* **95**, 1814-23.

Bergan R, Neckers L (1996) How do antisense oligodeoxynucleotides inhibit the growth of chronic myelogenous leukemia cells? *Blood* **87**, 4019-20.

Bernstein E, Caudy AA, Hammond SM, Hannon GJ (2001) Role for a bidentate ribonuclease in the initiation step of RNA interference. *Nature* **409**, 363-6.

Bernstein E, Denli AM, Hannon GJ (2001) The rest is silence. *Rna* **7**, 1509-21.

Bernstein E, Kim SY, *et al.* (2003) Dicer is essential for mouse development. *Nat Genet* **35**, 215-7. Epub 2003 Oct 5.

Bhatia R, Munthe HA, Verfaillie CM (1998) Tyrphostin AG957, a tyrosine kinase inhibitor with anti-BCR/ABL tyrosine kinase activity restores beta1 integrin-mediated adhesion and inhibitory signaling in chronic myelogenous leukemia hematopoietic progenitors. *Leukemia* **12**, 1708-17.

Bhatia R, Verfaillie CM, Author (1998) Inhibition of BCR-ABL expression with antisense oligodeoxynucleotides restores beta1 integrin-mediated adhesion and proliferation inhibition in chronic myelogenous leukemia hematopoietic progenitors. *Blood* **91**, 3414-22.

BioPharma (2004) NeuGene Antisense Clinical Development Program. www.avibio.com.

Blalock WL, Weinstein-Oppenheimer C, *et al.* (1999) Signal transduction, cell cycle regulatory, and anti-apoptotic pathways regulated by IL-3 in hematopoietic cells: possible sites for intervention with anti-neoplastic drugs. *Leukemia* **13**, 1109-66.

Borthakur G, Cortes JE (2004) Imatinib mesylate in the treatment of chronic myelogenous leukemia. *Int J Hematol* **79**, 411-9.

Bouchard C, Dittrich O, Kiermaier A, Dohmann K, Menkel A, Eilers M, Luscher B (2001) Regulation of cyclin D2 gene expression by the Myc/Max/Mad network: Myc-dependent TRRAP recruitment and histone acetylation at the cyclin D2 promoter. *Genes Dev* **15**, 2042-7.

Bouchard C, Thieke K, *et al.* (1999) Direct induction of cyclin D2 by Myc contributes to cell cycle progression and sequestration of p27. *Embo J* **18**, 5321-33.

Boutla A, Delidakis C, Livadaras I, Tsagris M, Tabler M (2001) Short 5'-phosphorylated double-stranded RNAs induce RNA interference in Drosophila. *Curr Biol* **11**, 1776-80.

Braasch DA, Liu Y, Corey DR (2002) Antisense inhibition of gene expression in cells by oligonucleotides incorporating locked nucleic acids: effect of mRNA target sequence and chimera design. *Nucleic Acids Res* **30**, 5160-7.

Brand RM, Iversen PL, Author (2000) Transdermal delivery of antisense compounds. *Adv Drug Deliv Rev* **44**, 51-57.

Branford S, Hughes TP, Rudzki Z (2002) Dual transcription of b2a2 and b3a2 BCR-ABL transcripts in chronic myeloid leukaemia is confined to patients with a linked polymorphism within the BCR gene. *Br J Haematol* **117**, 875-7.

Brantl S (2002) Antisense-RNA regulation and RNA interference. *Biochim Biophys Acta* **1575**, 15-25.

Braun SE, Chen K, Battiwalla M, Cornetta K, Author (1997) Gene therapy strategies for leukemia. *Mol Med Today* **3**, 39-46.

Brooks AR, Shiffman D, Chan CS, Brooks EE, Milner PG (1996) Functional analysis of the human cyclin D2 and cyclin D3 promoters. *J Biol Chem* **271**, 9090-9.

Brooksband C (2001) ABL to resist. *Nature Rev can* **1**, 175.

Broughton CM, Spiller DG, Pender N, Komorovskaya M, Grzybowski J, Giles RV, Tidd DM, Clark RE, Author (1997) Preclinical studies of streptolysin-O in enhancing antisense oligonucleotide uptake in harvests from chronic myeloid leukaemia patients. *Leukemia* **11**, 1435-41.

Brown CM, Jacobs G, Stockwell P, Schreiber M (2003) Detection of signals in mRNAs that influence translation. *Appl Bioinformatics* **2**, S47-51.

Brown R, Plumb JA (2004) Demethylation of DNA by decitabine in cancer chemotherapy. *Expert Rev Anticancer Ther* **4**, 501-10.

Brummelkamp TR, Bernards R, Agami R (2002) A system for stable expression of short interfering RNAs in mammalian cells. *Science* **296**, 550-3. Epub 2002 Mar 21.

Buettner R, Mora LB, Jove R (2002) Activated STAT signaling in human tumors provides novel molecular targets for therapeutic intervention. *Clin Cancer Res* **8**, 945-54.

Burgess GS, Williamson EA, *et al.* (1998) Regulation of the c-jun gene in p210 BCR-ABL transformed cells corresponds with activity of JNK, the c-jun N-terminal kinase. *Blood* **92**, 2450-60.

Burns KH, Agno JE, Sicinski P, Matzuk MM (2003) Cyclin D2 and p27 are tissue-specific regulators of tumorigenesis in inhibin alpha knockout mice. *Mol Endocrinol* **17**, 2053-69. Epub 2003 Jul 10.

Cai Z, Lin M, Wuchter C, Ruppert V, Dorken B, Ludwig WD, Karawajew L (2001) Apoptotic response to homoharringtonine in human wt p53 leukemic cells is independent of reactive oxygen species generation and implicates Bax translocation, mitochondrial cytochrome c release and caspase activation. *Leukemia* **15**, 567-74.

Cambier N, Chopra R, Strasser A, Metcalf D, Elefanty AG (1998) BCR-ABL activates pathways mediating cytokine independence and protection against apoptosis in murine hematopoietic cells in a dose-dependent manner. *Oncogene* **16**, 335-48.

Campbell JD, Cook G, Holyoake TL (2001) Evolution of bone marrow transplantation--the original immunotherapy. *Trends Immunol* **22**, 88-92.

Caplen NJ, Fleenor J, Fire A, Morgan RA (2000) dsRNA-mediated gene silencing in cultured Drosophila cells: a tissue culture model for the analysis of RNA interference. *Gene* **252**, 95-105.

Carpousis AJ, Vanzo NF, Raynal LC (1999) mRNA degradation. A tale of poly(A) and multiprotein machines. *Trends Genet* **15**, 24-8.

Chalk AM, Sonnhammer EL (2002) Computational antisense oligo prediction with a neural network model. *Bioinformatics* **18**, 1567-75.

Chissoe SL, Bodenteich A, *et al.* (1995) Sequence and analysis of the human ABL gene, the BCR gene, and regions involved in the Philadelphia chromosomal translocation. *Genomics* **27**, 67-82.

Chiu YL, Rana TM (2003) siRNA function in RNAi: a chemical modification analysis. *Rna* **9**, 1034-48.

Cho-Chung YS (2004) Antisense protein kinase A RI alpha-induced tumor reversion: portrait of a microarray. *Biochim Biophys Acta* **1697**, 71-9.

Chomczynski P, Sacchi N (1987) Single-step method of RNA isolation by acid guanidinium thiocyanate-phenol-chloroform extraction. *Anal Biochem* **162**, 156-9.

Chopra R, Pu QQ, Elefanty AG, Author (1999) Biology of BCR-ABL. *Blood Rev* **13**, 211-29.

Cirino NM, Li G, Xiao W, Torrence PF, Silverman RH (1997) Targeting RNA decay with 2',5' oligoadenylate-antisense in respiratory syncytial virus-infected cells. *Proc Natl Acad Sci U S A* **94**, 1937-42.

Clark RE, Grzybowski J, Broughton CM, Pender NT, Spiller DG, Brammer CG, Giles RV, Tidd DM, Author (1999) Clinical use of streptolysin-O to facilitate antisense oligodeoxyribonucleotide delivery for purging autografts in chronic myeloid leukaemia. *Bone Marrow Transplant* **23**, 1303-8.

Cohen JS, Author (1992) Oligonucleotide therapeutics. *Trends Biotechnol* **10**, 87-91.

Corey DR, Abrams JM (2001) Morpholino antisense oligonucleotides: tools for investigating vertebrate development. *Genome Biol* **2**, REVIEWS1015.

Cotter FE, Johnson P, Hall P, Pocock C, al Mahdi N, Cowell JK, Morgan G, Author (1994) Antisense oligonucleotides suppress B-cell lymphoma growth in a SCID-hu mouse model. *Oncogene* **9**, 3049-55.

Cotter FE, Waters J, Cunningham D (1999) Human Bcl-2 antisense therapy for lymphomas. *Biochim Biophys Acta* **1489**, 97-106.

Cotter TG, Author (1995) BCR-ABL: an anti-apoptosis gene in chronic myelogenous leukemia. *Leuk Lymphoma* **18**, 231-6.

Couzin J (2002) Breakthrough of the year. Small RNAs make big splash. *Science* **298**, 2296-7.

Couzin J (2004) Molecular biology. RNAi shows cracks in its armor. *Science* **306**, 1124-5.

Crowder C, Dahle O, Davis RE, Gabrielsen OS, Rudikoff S (2004) PML mediates IFN{alpha} induced apoptosis in myeloma by regulating TRAIL induction. *Blood* **30**, 30.

Czauderna F, Fechtner M, Dames S, Aygun H, Klippel A, Pronk GJ, Giese K, Kaufmann J (2003) Structural variations and stabilising modifications of synthetic siRNAs in mammalian cells. *Nucleic Acids Res* **31**, 2705-16.

D R (1999) GEM 132. Gene expression modulation 132. *Drugs R D* **2**, 313-4.

Davidson TJ, Harel S, Arboleda VA, Prunell GF, Shelanski ML, Greene LA, Troy CM (2004) Highly efficient small interfering RNA delivery to primary mammalian neurons induces MicroRNA-like effects before mRNA degradation. *J Neurosci* **24**, 10040-6.

de Fabritiis P, Petti MC, *et al.* (1998) BCR-ABL antisense oligodeoxynucleotide in vitro purging and autologous bone marrow transplantation for patients with chronic myelogenous leukemia in advanced phase. *Blood* **91**, 3156-62.

Deininger MW, Druker BJ (2003) Specific targeted therapy of chronic myelogenous leukemia with imatinib. *Pharmacol Rev* **55**, 401-23. Epub 2003 Jul 17.

Deininger MW, Vieira SA, *et al.* (2001) Direct relation between BCR-ABL tyrosine kinase activity and cyclin D2 expression in lymphoblasts. *Cancer Res* **61**, 8005-13.

Delmer A, Ajchenbaum-Cymbalista F, Tang R, Ramond S, Faussat AM, Marie JP, Zittoun R (1995) Overexpression of cyclin D2 in chronic B-cell malignancies. *Blood* **85**, 2870-6.

DeLong RK, Yoo H, *et al.* (1999) Novel cationic amphiphiles as delivery agents for antisense oligonucleotides. *Nucleic Acids Res* **27**, 3334-41.

Demidov VV (2002) PNA comes of age: from infancy to maturity. *Drug Discov Today* **7**, 153-5.

Denisov AY, Noronha AM, Wilds CJ, Trempe JF, Pon RT, Gehring K, Damha MJ (2001) Solution structure of an arabinonucleic acid (ANA)/RNA duplex in a chimeric hairpin: comparison with 2'-fluoro-ANA/RNA and DNA/RNA hybrids. *Nucleic Acids Res* **29**, 4284-93.

Denli AM, Hannon GJ (2003) RNAi: an ever-growing puzzle. *Trends Biochem Sci* **28**, 196-201.

Der SD, Yang YL, Weissmann C, Williams BR (1997) A double-stranded RNA-activated protein kinase-dependent pathway mediating stress-induced apoptosis. *Proc Natl Acad Sci U S A* **94**, 3279-83.

Deshayes S, Gerbal-Chaloin S, Morris MC, Aldrian-Herrada G, Charnet P, Divita G, Heitz F (2004) On the mechanism of non-endosomial peptide-mediated cellular delivery of nucleic acids. *Biochim Biophys Acta* **1667**, 141-7.

Devroe E, Silver PA (2002) Retrovirus-delivered siRNA. *BMC Biotechnol* **2**, 15.

Dey A, Li W (2000) Cell cycle-independent induction of D1 and D2 cyclin expression, but not cyclin-Cdk complex formation or Rb phosphorylation, by IFNgamma in macrophages. *Biochim Biophys Acta* **1497**, 135-47.

Di Bacco A, Keeshan K, McKenna SL, Cotter TG (2000) Molecular abnormalities in chronic myeloid leukemia: deregulation of cell growth and apoptosis. *Oncologist* **5**, 405-15.

Dias N, Stein CA (2002) Potential roles of antisense oligonucleotides in cancer therapy. The example of Bcl-2 antisense oligonucleotides. *Eur J Pharm Biopharm* **54**, 263-9.

Dillin A (2003) The specifics of small interfering RNA specificity. *Proc Natl Acad Sci U S A* **100**, 6289-91.

Ding Y, Chan, C.Y. and Lawrence, C.E. (2004) RNA Interference Rational design of siRNAs with the Sfold software. In 'RNA Interference: from Basic Science to Drug Development'. (Ed. K Appasani). (Cambridge University Press)

Ding Y, Chan CY, Lawrence CE (2004) Sfold web server for statistical folding and rational design of nucleic acids. *Nucleic Acids Res* **32**, W135-41.

Ding Y, Lawrence CE (2001) Statistical prediction of single-stranded regions in RNA secondary structure and application to predicting effective antisense target sites and beyond. *Nucleic Acids Res* **29**, 1034-46.

Ding Y, Lawrence CE (2003) A statistical sampling algorithm for RNA secondary structure prediction. *Nucleic Acids Res* **31**, 7280-301.

Dokka S, Rojanasakul Y (2000) Novel non-endocytic delivery of antisense oligonucleotides. *Adv Drug Deliv Rev* **44**, 35-49.

Dorsett Y, Tuschl T (2004) siRNAs: applications in functional genomics and potential as therapeutics. *Nat Rev Drug Discov* **3**, 318-29.

Dorsey JF, Cunnick JM, Lanehart R, Huang M, Kraker AJ, Bhalla KN, Jove R, Wu J (2002) Interleukin-3 protects Bcr-Abl-transformed hematopoietic progenitor cells from apoptosis induced by Bcr-Abl tyrosine kinase inhibitors. *Leukemia* **16**, 1589-95.

Doshi KJ, Cannone JJ, Cobaugh CW, Gutell RR (2004) Evaluation of the suitability of free-energy minimization using nearest-neighbor energy parameters for RNA secondary structure prediction. *BMC Bioinformatics* **5**, 105.

Dougal D (2000) John Hughes Bennett 1812-1875.. (Department of Oncology, Faculty of Medicine, University of Edinburgh) http://www.onc.ed.ac.uk/jhbl/

Druker BJ, Sawyers CL, Kantarjian H, Resta DJ, Reese SF, Ford JM, Capdeville R, Talpaz M (2001) Activity of a specific inhibitor of the BCR-ABL tyrosine kinase in the blast crisis of chronic myeloid leukemia and acute lymphoblastic leukemia with the Philadelphia chromosome. *N Engl J Med* **344**, 1038-42.

Drummond MW, Holyoake TL (2001) Tyrosine kinase inhibitors in the treatment of chronic myeloid leukaemia: so far so good? *Blood Rev* **15**, 85-95.

Dykstra ML, Cherukuri A, Pierce SK (2001) Floating the raft hypothesis for immune receptors: access to rafts controls receptor signaling and trafficking. *Traffic* **2**, 160-6.

Elbashir SM, Harborth J, Lendeckel W, Yalcin A, Weber K, Tuschl T (2001) Duplexes of 21-nucleotide RNAs mediate RNA interference in cultured mammalian cells. *Nature* **411**, 494-8.

Elbashir SM, Lendeckel W, Tuschl T (2001) RNA interference is mediated by 21- and 22-nucleotide RNAs. *Genes Dev* **15**, 188-200.

Elbashir SM, Martinez J, Patkaniowska A, Lendeckel W, Tuschl T (2001) Functional anatomy of siRNAs for mediating efficient RNAi in Drosophila melanogaster embryo lysate. *Embo J* **20**, 6877-88.

Engelhard HH (1998) Antisense Oligodeoxynucleotide Technology: Potential Use for the Treatment of Malignant Brain Tumors. *Cancer Control* **5**, 163-170.

Eriksson M, Nielsen PE, Good L (2002) Cell permeabilization and uptake of antisense peptide-peptide nucleic acid (PNA) into Escherichia coli. *J Biol Chem* **277**, 7144-7. Epub 2001 Dec 05.

Faderl S, Talpaz M, Estrov Z, O'Brien S, Kurzrock R, Kantarjian HM (1999) The biology of chronic myeloid leukemia. *N Engl J Med* **341**, 164-72.

Fernandes RS, Gorman AM, McGahon A, Lawlor M, McCann S, Cotter TG, Author (1996) The repression of apoptosis by activated abl oncogenes in chronic myelogenous leukaemia. *Leukemia* **10**, s17-21.

Filmore D (2004) Assessing Antisense. *Modern Drug Discovery*, 49-50.

Fire A (1999) RNA-triggered gene silencing. *Trends Genet* **15**, 358-63.

Fire A, Xu S, Montgomery MK, Kostas SA, Driver SE, Mello CC (1998) Potent and specific genetic interference by double-stranded RNA in Caenorhabditis elegans. *Nature* **391**, 806-11.

Fischer H, Chen J, Skoog L, Lindblom A (2002) Cyclin D2 expression in familial and sporadic breast cancer. *Oncol Rep* **9**, 1157-61.

Fisher TL, Terhorst T, Cao X, Wagner RW (1993) Intracellular disposition and metabolism of fluorescently-labeled unmodified and modified oligonucleotides microinjected into mammalian cells. *Nucleic Acids Res* **21**, 3857-65.

Flaherty KT, Stevenson JP, O'Dwyer PJ (2001) Antisense therapeutics: lessons from early clinical trials. *Curr Opin Oncol* **13**, 499-505.

Flowers ME, Traina F, *et al.* (2004) Serious graft-versus-host disease after hematopoietic cell transplantation following nonmyeloablative conditioning. *Bone Marrow Transplant* **22**, 22.

Friedrichsen BN, Richter HE, Hansen JA, Rhodes CJ, Nielsen JH, Billestrup N, Moldrup A (2003) Signal transducer and activator of transcription 5 activation is sufficient to drive transcriptional induction of cyclin D2 gene and proliferation of rat pancreatic beta-cells.

Mol Endocrinol **17**, 945-58. Epub 2003 Feb 13.

Galderisi U, Cascino A, Giordano A, Author (1999) Antisense oligonucleotides as therapeutic agents. *J Cell Physiol* **181**, 251-7.

Garcia-Chaumont C, Seksek O, Grzybowska J, Borowski E, Bolard J, Author (2000) Delivery systems for antisense oligonucleotides. *Pharmacol Ther* **87**, 255-77.

Garcia-Chaumont C, Seksek O, Jolles B, Bolard J (2000) A cationic derivative of amphotericin B as a novel delivery system for antisense oligonucleotides. *Antisense Nucleic Acid Drug Dev* **10**, 177-84.

GeneTools (2004) Morpholino Oligonucleotide production & research. www.gene-tools.com. (James Summerton, Ph.D.)

Gesbert F, Griffin JD (2000) Bcr/Abl activates transcription of the Bcl-X gene through STAT5. *Blood* **96**, 2269-76.

Gewirtz AM, Sokol DL, Ratajczak MZ, Author (1998) Nucleic acid therapeutics: state of the art and future prospects. *Blood* **92**, 712-36.

Ghosh C, Iversen PL (2000) Intracellular delivery strategies for antisense phosphorodiamidate morpholino oligomers. *Antisense Nucleic Acid Drug Dev* **10**, 263-74.

Giannini CD, Roth WK, Piiper A, Zeuzem S, Author (1999) Enzymatic and antisense effects of a specific anti-Ki-ras ribozyme in vitro and in cell culture. *Nucleic Acids Res* **27**, 2737-44.

Giles R (2001) University of Liverpool Antisense Research Group http://www.liv.ac.uk/~giles/index.htm. In.

Giles RV, Spiller DG, Clark RE, Tidd DM (1999) Antisense morpholino oligonucleotide analog induces missplicing of C-myc mRNA. *Antisense Nucleic Acid Drug Dev* **9**, 213-20.

Giles RV, Spiller DG, Green JA, Clark RE, Tidd DM, Author (1995) Optimization of antisense oligodeoxynucleotide structure for targeting bcr-abl mRNA. *Blood* **86**, 744-54.

Giles RV, Spiller DG, Grzybowski J, Clark RE, Nicklin P, Tidd DM (1998) Selecting optimal oligonucleotide composition for maximal antisense effect following streptolysin O-mediated delivery into human leukaemia cells. *Nucleic Acids Res* **26**, 1567-75.

Giles RV, Spiller DG, Tidd DM (1995) Detection of ribonuclease H-generated mRNA fragments in human leukemia cells following reversible membrane permeabilization in the presence of antisense oligodeoxynucleotides. *Antisense Res Dev* **5**, 23-31.

Giles RV GJ, Spiller DG, Tidd DM (1997) Enhanced antisense effects resulting from an improved streptolysin-0 protocol for oligonucleotide delivery into human leukemia cells. *Nucleotides and Nucleotides* **16**, 1156-1163.

Goldman JM (1995) Bone marrow transplantation for chronic myeloid leukemia. *J Hematother* **4**, 62.

Goldman JM, Melo JV (2003) Chronic myeloid leukemia--advances in biology and new approaches to treatment. *N Engl J Med* **349**, 1451-64.

Gowher H, Jeltsch A (2004) Mechanism of Inhibition of DNA Methyltransfers by Cytidine Analogs in Cancer Therapy. *Cancer Biol Ther* **3**, 11.

Grace MJ, Lee S, *et al.* (2004) Site of pegylation and PEG molecule size attenuate interferon-alpha anti-viral and anti-proliferative activities through the JAK/STAT signaling pathway. *J Biol Chem* **13**, 13.

Grassi G, Dawson P, Guarnieri G, Kandolf R, Grassi M (2004) Therapeutic potential of hammerhead ribozymes in the treatment of hyper-proliferative diseases. *Curr Pharm Biotechnol* **5**, 369-86.

Griesshammer M, Hehlmann R, *et al.* (1993) Interferon in chronic myeloid leukemia. A workshop report. *Ann Hematol* **67**, 101-6.

Grunweller A, Wyszko E, Bieber B, Jahnel R, Erdmann VA, Kurreck J (2003) Comparison of different antisense strategies in mammalian cells using locked nucleic acids, 2'-O-methyl RNA, phosphorothioates and small interfering RNA. *Nucleic Acids Res* **31**, 3185-93.

Guilhot F, Roy L, Guilhot J, Millot F (2004) Interferon therapy in chronic myelogenous leukemia. *Hematol Oncol Clin North Am* **18**, 585-603, viii.

Gupta S, Schoer RA, Egan JE, Hannon GJ, Mittal V (2004) Inducible, reversible, and stable RNA interference in mammalian cells. *Proc Natl Acad Sci U S A* **4**, 4.

Guy-Caffey JK, Bodepudi V, Bishop JS, Jayaraman K, Chaudhary N (1995) Novel polyaminolipids enhance the cellular uptake of oligonucleotides. *J Biol Chem* **270**, 31391-6.

Hagstrom JE (2003) Plasmid-based gene delivery to target tissues in vivo: the intravascular approach. *Curr Opin Mol Ther* **5**, 338-44.

Hamar P, Song E, Kokeny G, Chen A, Ouyang N, Lieberman J (2004) Small interfering RNA targeting Fas protects mice against renal ischemia-reperfusion injury. *Proc Natl Acad Sci U S A* **101**, 14883-8. Epub 2004 Oct 04.

Hamilton AJ, Baulcombe DC (1999) A species of small antisense RNA in posttranscriptional gene silencing in plants. *Science* **286**, 950-2.

Hamzavi R, Dolle F, Tavitian B, Dahl O, Nielsen PE (2003) Modulation of the pharmacokinetic properties of PNA: preparation of galactosyl, mannosyl, fucosyl, N-acetylgalactosaminyl, and N-acetylglucosaminyl derivatives of aminoethylglycine peptide nucleic acid monomers and their incorporation into PNA oligomers. *Bioconjug Chem* **14**, 941-54.

Hannon GJ, Rossi JJ (2004) Unlocking the potential of the human genome with RNA interference. *Nature* **431**, 371-8.

Heasman J (2002) Morpholino oligos: making sense of antisense? *Dev Biol* **243**, 209-14.

Hehlmann R, Heimpel H, *et al.* (1993) Randomized comparison of busulfan and hydroxyurea in chronic myelogenous leukemia: prolongation of survival by hydroxyurea. The German CML Study Group. *Blood* **82**, 398-407.

Hernandez JC, Leon F, Quintana J, Estevez F, Bermejo J (2004) Icogenin, a new cytotoxic steroidal saponin isolated from Dracaena draco. *Bioorg Med Chem* **12**, 4423-9.

Ho SP, Bao Y, Lesher T, Malhotra R, Ma LY, Fluharty SJ, Sakai RR (1998) Mapping of RNA accessible sites for antisense experiments with oligonucleotide libraries. *Nat Biotechnol* **16**, 59-63.

Ho SP, Britton DH, Stone BA, Behrens DL, Leffet LM, Hobbs FW, Miller JA, Trainor GL (1996) Potent antisense oligonucleotides to the human multidrug resistance-1 mRNA are rationally selected by mapping RNA-accessible sites with oligonucleotide libraries. *Nucleic Acids Res* **24**, 1901-7.

Hochhaus A (2004) Imatinib mesylate (Glivec, Gleevec) in the treatment of chronic myelogenous leukemia (CML) and gastrointestinal stromal tumors (GIST). *Ann Hematol* **83**, S65-6.

Hohjoh H (2004) Enhancement of RNAi activity by improved siRNA duplexes. *FEBS Lett* **557**, 193-8.

Holen T, Amarzguioui M, Babaie E, Prydz H (2003) Similar behaviour of single-strand and double-strand siRNAs suggests they act through a common RNAi pathway. *Nucleic Acids Res* **31**, 2401-7.

Holen T, Amarzguioui M, Wiiger MT, Babaie E, Prydz H (2002) Positional effects of short interfering RNAs targeting the human coagulation trigger Tissue Factor. *Nucleic Acids Res* **30**, 1757-66.

Holyoake DT (2001) Recent advances in the molecular and cellular biology of chronic myeloid leukaemia: lessons to be learned from the laboratory. *Br J Haematol* **113**, 11-23.

Howard K (2003) Unlocking the money-making potential of RNAi. *Nat Biotechnol* **21**, 1441-6.

Hu Q, Bally MB, Madden TD (2002) Subcellular trafficking of antisense oligonucleotides and down-regulation of bcl-2 gene expression in human melanoma cells using a fusogenic liposome delivery system. *Nucleic Acids Res* **30**, 3632-41.

Hu Q, Shew CR, Bally MB, Madden TD (2001) Programmable fusogenic vesicles for intracellular delivery of antisense oligodeoxynucleotides: enhanced cellular uptake and biological effects. *Biochim Biophys Acta* **1514**, 1-13.

Hudziak RM, Barofsky E, Barofsky DF, Weller DL, Huang SB, Weller DD (1996) Resistance of morpholino phosphorodiamidate oligomers to enzymatic degradation. *Antisense Nucleic Acid Drug Dev* **6**, 267-72.

Hughes MD, Hussain M, Nawaz Q, Sayyed P, Akhtar S (2001) The cellular delivery of antisense oligonucleotides and ribozymes. *Drug Discov Today* **6**, 303-315.

Hussain M, Shchepinov M, Sohail M, Benter IF, Hollins AJ, Southern EM, Akhtar S (2004) A novel anionic dendrimer for improved cellular delivery of antisense oligonucleotides. *J Control Release* **99**, 139-55.

Hussain N (2000) Ligand-mediated tissue specific drug delivery. *Adv Drug Deliv Rev* **43**, 95-100.

Hutvagner G, Zamore PD (2002) RNAi: nature abhors a double-strand. *Curr Opin Genet Dev* **12**, 225-32.

Hutvagner G, Zamore PD (2002) A microRNA in a multiple-turnover RNAi enzyme complex. *Science* **297**, 2056-60.

Illmer T, Schaich M, *et al.* (2004) P-glycoprotein-mediated drug efflux is a resistance mechanism of chronic myelogenous leukemia cells to treatment with imatinib mesylate. *Leukemia* **18**, 401-8.

Indolfi C, Chiariello M, Avvedimento EV (1996) Selective gene therapy for proliferative disorders: sense and antisense. *Nat Med* **2**, 634-5.

Ireland NCRI (2004) The National Cancer Registry Ireland
Incidence, Mortality, Treatment and Survival. www.ncri.ie.

Islam A, Handley SL, Thompson KS, Akhtar S (2000) Studies on uptake, sub-cellular trafficking and efflux of antisense oligodeoxynucleotides in glioma cells using self-

assembling cationic lipoplexes as delivery systems. *J Drug Target* **7**, 373-82.

Iversen PL (2001) Phosphorodiamidate morpholino oligomers: favorable properties for sequence-specific gene inactivation. *Curr Opin Mol Ther* **3**, 235-8.

Iversen PL, Arora V, Acker AJ, Mason DH, Devi GR (2003) Efficacy of antisense morpholino oligomer targeted to c-myc in prostate cancer xenograft murine model and a Phase I safety study in humans. *Clin Cancer Res* **9**, 2510-9.

Jacque JM, Triques K, Stevenson M (2002) Modulation of HIV-1 replication by RNA interference. *Nature* **418**, 435-8.

Jahagirdar BN, Miller JS, Shet A, Verfaillie CM (2001) Novel therapies for chronic myelogenous leukemia. *Exp Hematol* **29**, 543-56.

Jain KK (2004) RNAi and siRNA in target validation. *Drug Discov Today* **9**, 307-9.

Jansen B, Zangemeister-Wittke U (2002) Antisense therapy for cancer--the time of truth. *Lancet Oncol* **3**, 672-83.

Jayaraman A, Walton SP, Yarmush ML, Roth CM (2001) Rational selection and quantitative evaluation of antisense oligonucleotides. *Biochim Biophys Acta* **1520**, 105-14.

Jena N, Deng M, Sicinska E, Sicinski P, Daley GQ (2002) Critical role for cyclin D2 in BCR/ABL-induced proliferation of hematopoietic cells. *Cancer Res* **62**, 535-41.

Jiang L, Wu JB, Yu K, Ni WH (2004) [Inhibitory effect of siRNA on bcr-abl gene expression in K562 cell line]. *Zhongguo Shi Yan Xue Ye Xue Za Zhi* **12**, 332-4.

Jiang Y, Zhao RC, Verfaillie CM (2000) Abnormal integrin-mediated regulation of chronic myelogenous leukemia CD34+ cell proliferation: BCR/ABL up-regulates the cyclin-dependent kinase inhibitor, p27Kip, which is relocated to the cell cytoplasm and incapable of regulating cdk2 activity. *Proc Natl Acad Sci U S A* **97**, 10538-43.

Johansson B, Fioretos T, Mitelman F (2002) Cytogenetic and molecular genetic evolution of chronic myeloid leukemia. *Acta Haematol* **107**, 76-94.

Kairemo KJ, Tenhunen M, Jekunen AP (1998) Gene therapy using antisense oligodeoxynucleotides labeled with Auger- emitting radionuclides. *Cancer Gene Ther* **5**, 408-12.

Kamath RS, Fraser AG, *et al.* (2003) Systematic functional analysis of the Caenorhabditis elegans genome using RNAi. *Nature* **421**, 231-7.

Karras JG, McKay RA, Dean NM, Monia BP (2000) Deletion of individual exons and

induction of soluble murine interleukin-5 receptor-alpha chain expression through antisense oligonucleotide-mediated redirection of pre-mRNA splicing. *Mol Pharmacol* **58**, 380-7.

Kato JY, Sherr CJ (1993) Inhibition of granulocyte differentiation by G1 cyclins D2 and D3 but not D1. *Proc Natl Acad Sci U S A* **90**, 11513-7.

Kay L, Heuhns E (1985) 'Clinical Blood Transfusion.' (Pitman Publishing Ltd)

Kearney P, Wright LA, Milliken S, Biggs JC (1995) Improved specificity of ribozyme-mediated cleavage of bcr-abl mRNA. *Exp Hematol* **23**, 986-9.

Keeshan K, Cotter TG, McKenna SL (2002) High Bcr-Abl expression prevents the translocation of Bax and Bad to the mitochondrion. *Leukemia* **16**, 1725-34.

Keeshan K, Cotter TG, McKenna SL (2003) Bcr-Abl upregulates cytosolic p21WAF-1/CIP-1 by a phosphoinositide-3-kinase (PI3K)-independent pathway. *Br J Haematol* **123**, 34-44.

Kehn K, Deng L, *et al.* (2004) The role of cyclin D2 and p21/waf1 in human T-cell leukemia virus type 1 infected cells. *Retrovirology* **1**, 6.

Kennedy S, Wang D, Ruvkun G (2004) A conserved siRNA-degrading RNase negatively regulates RNA interference in C. elegans. *Nature* **427**, 645-9.

Khan AU, Lal SK (2003) Ribozymes: a modern tool in medicine. *J Biomed Sci* **10**, 457-67.

Kindler T, Meyer RG, Fischer T (2002) BCR-ABL as a target for novel therapeutic interventions. *Expert Opin Ther Targets* **6**, 85-101.

Klejman A, Rushen L, Morrione A, Slupianek A, Skorski T (2002) Phosphatidylinositol-3 kinase inhibitors enhance the anti-leukemia effect of STI571. *Oncogene* **21**, 5868-76.

Kocisova E, Praus P, Rosenberg I, Seksek O, Sureau F, Stepanek J, Turpin PY (2004) Intracellular uptake of modified oligonucleotide studied by two fluorescence techniques. *Biopolymers* **74**, 110-4.

Kole R, Vacek M, Williams T (2004) Modification of alternative splicing by antisense therapeutics. *Oligonucleotides* **14**, 65-74.

Kolibaba KS, BJ D (2000) Current Status of Treatment for Chronic Myelogenous Leukemia. *Medscape Oncology* **3**, 2000.

Komatsu N, Watanabe T, *et al.* (2003) A member of Forkhead transcription factor FKHRL1 is a downstream effector of STI571-induced cell cycle arrest in BCR-ABL-

expressing cells. *J Biol Chem* **278**, 6411-9. Epub 2002 Nov 26.

Koppelhus U, Nielsen PE (2003) Cellular delivery of peptide nucleic acid (PNA). *Adv Drug Deliv Rev* **55**, 267-80.

Kretschmer-Kazemi Far R, Sczakiel G (2003) The activity of siRNA in mammalian cells is related to structural target accessibility: a comparison with antisense oligonucleotides. *Nucleic Acids Res* **31**, 4417-24.

Kurien BT, Scofield RH (2003) Protein blotting: a review. *J Immunol Methods* **274**, 1-15.

Kurzrock R, Kantarjian HM, Druker BJ, Talpaz M (2003) Philadelphia chromosome-positive leukemias: from basic mechanisms to molecular therapeutics. *Ann Intern Med* **138**, 819-30.

La Rosee P, O'Dwyer ME, Druker BJ (2002) Insights from pre-clinical studies for new combination treatment regimens with the Bcr-Abl kinase inhibitor imatinib mesylate (Gleevec/Glivec) in chronic myelogenous leukemia: a translational perspective. *Leukemia* **16**, 1213-9.

Laktionov PP, Dazard JE, Vives E, Rykova EY, Piette J, Vlassov VV, Lebleu B (1999) Characterisation of membrane oligonucleotide-binding proteins and oligonucleotide uptake in keratinocytes. *Nucleic Acids Res* **27**, 2315-24.

Larsen HJ, Bentin T, Nielsen PE (1999) Antisense properties of peptide nucleic acid. *Biochim Biophys Acta* **1489**, 159-66.

Laurent A, Naval M, Debart F, Vasseur JJ, Rayner B (1999) Chiral and steric effects in the efficient binding of alpha-anomeric deoxyoligonucleoside N-alkylphosphoramidates to ssDNA and RNA. *Nucleic Acids Res* **27**, 4151-9.

Lavorgna G, Dahary D, Lehner B, Sorek R, Sanderson CM, Casari G (2004) In search of antisense. *Trends Biochem Sci* **29**, 88-94.

Lebedeva I, Benimetskaya L, Stein CA, Vilenchik M (2000) Cellular delivery of antisense oligonucleotides. *Eur J Pharm Biopharm* **50**, 101-19.

Lebedeva I, Stein CA (2001) Antisense oligonucleotides: promise and reality. *Annu Rev Pharmacol Toxicol* **41**, 403-19.

LeDoan T, Etore F, Tenu JP, Letourneux Y, Agrawal S (1999) Cell binding, uptake and cytosolic partition of HIV anti-gag phosphodiester oligonucleotides 3'-linked to cholesterol derivatives in macrophages [In Process Citation]. *Bioorg Med Chem* **7**, 2263-9.

Leirdal M, Sioud M (2002) Gene silencing in mammalian cells by preformed small RNA

duplexes. *Biochem Biophys Res Commun* **295**, 744-8.

Leung YM, Ou YJ, Kwan CY, Loh TT (1997) Specific interaction between tetrandrine and Quillaja saponins in promoting permeabilization of plasma membrane in human leukemic HL-60 cells. *Biochim Biophys Acta* **1325**, 318-28.

Levin AA (1999) A review of the issues in the pharmacokinetics and toxicology of phosphorothioate antisense oligonucleotides. *Biochim Biophys Acta* **1489**, 69-84.

Lewin B (2003) 'Genes VIII.'

Li H, Grenet J, Kidd VJ (1995) Structure and gene expression of avian cyclin D2. *Gene* **167**, 341-2.

Li S, Gillessen S, Tomasson MH, Dranoff G, Gilliland DG, Van Etten RA (2001) Interleukin 3 and granulocyte-macrophage colony-stimulating factor are not required for induction of chronic myeloid leukemia-like myeloproliferative disease in mice by BCR/ABL. *Blood* **97**, 1442-50.

Lipardi C, Wei Q, Paterson BM (2001) RNAi as random degradative PCR: siRNA primers convert mRNA into dsRNAs that are degraded to generate new siRNAs. *Cell* **107**, 297-307.

Liu G, He J, Dou S, Gupta S, Vanderheyden JL, Rusckowski M, Hnatowich DJ (2004) Pretargeting in tumored mice with radiolabeled morpholino oligomer showing low kidney uptake. *Eur J Nucl Med Mol Imaging* **31**, 417-24. Epub 2003 Dec 23.

Liu J, Xiao N, DeFranco DB (1999) Use of digitonin-permeabilized cells in studies of steroid receptor subnuclear trafficking. *Methods* **19**, 403-9.

Lloyd BH, Giles RV, Spiller DG, Grzybowski J, Tidd DM, Sibson DR (2001) Determination of optimal sites of antisense oligonucleotide cleavage within TNFalpha mRNA. *Nucleic Acids Res* **29**, 3664-73.

Lochmann D, Jauk E, Zimmer A (2004) Drug delivery of oligonucleotides by peptides. *Eur J Pharm Biopharm* **58**, 237-51.

Lok CN, Viazovkina E, Min KL, Nagy E, Wilds CJ, Damha MJ, Parniak MA (2002) Potent gene-specific inhibitory properties of mixed-backbone antisense oligonucleotides comprised of 2'-deoxy-2'-fluoro-D-arabinose and 2'-deoxyribose nucleotides. *Biochemistry* **41**, 3457-67.

Lowenthal PR (2000) Leukaemia - A Historical Odyssey-Virchow. http://www.mnsu.edu/emuseum/information/biography/uvwxyz/virchow_rudolf.html.

Luger SM, O'Brien SG, Ratajczak J, Ratajczak MZ, Mick R, Stadtmauer EA, Nowell PC, Goldman JM, Gewirtz AM (2002) Oligodeoxynucleotide-mediated inhibition of c-myb gene expression in autografted bone marrow: a pilot study. *Blood* **99**, 1150-8.

Lukas J, Bartkova J, Welcker M, Petersen OW, Peters G, Strauss M, Bartek J (1995) Cyclin D2 is a moderately oscillating nucleoprotein required for G1 phase progression in specific cell types. *Oncogene* **10**, 2125-34.

Luzzatto L, Melo JV (2002) Acquired resistance to imatinib mesylate: selection for pre-existing mutant cells. *Blood* **100**, 1105.

Ma DD, Rede T, Naqvi NA, Cook PD (2000) Synthetic oligonucleotides as therapeutics: the coming of age. *Biotechnol Annu Rev* **5**, 155-96.

Macaluso M, Russo G, Cinti C, Bazan V, Gebbia N, Russo A (2002) Ras family genes: an interesting link between cell cycle and cancer. *J Cell Physiol* **192**, 125-30.

Mahon FX, Ripoche J, Pigeonnier V, Jazwiec B, Pigneux A, Moreau JF, Reiffers J (1995) Inhibition of chronic myelogenous leukemia cells harboring a BCR-ABL B3A2 junction by antisense oligonucleotides targeted at the B2A2 junction. *Exp Hematol* **23**, 1606-11.

Malumbres M, Pellicer A (1998) RAS pathways to cell cycle control and cell transformation. In. (Ed. A Pellicer) pp. d887-d912. (Front Biosci)

Mangos MM, Min KL, Viazovkina E, Galarneau A, Elzagheid MI, Parniak MA, Damha MJ (2003) Efficient RNase H-directed cleavage of RNA promoted by antisense DNA or 2'F-ANA constructs containing acyclic nucleotide inserts. *J Am Chem Soc* **125**, 654-61.

Mani S, Gu Y, Wadler S, Fingert H, Author (1999) Antisense therapeutics in oncology: points to consider in their clinical evaluation [In Process Citation]. *Antisense Nucleic Acid Drug Dev* **9**, 543-7.

Mani S, Rudin CM, Kunkel K, Holmlund JT, Geary RS, Kindler HL, Dorr FA, Ratain MJ (2002) Phase I clinical and pharmacokinetic study of protein kinase C-alpha antisense oligonucleotide ISIS 3521 administered in combination with 5-fluorouracil and leucovorin in patients with advanced cancer. *Clin Cancer Res* **8**, 1042-8.

Maran A, Waller CF, *et al.* (1998) 2',5'-Oligoadenylate-antisense chimeras cause RNase L to selectively degrade bcr/abl mRNA in chronic myelogenous leukemia cells. *Blood* **92**, 4336-43.

Marcucci G, Byrd JC, *et al.* (2002) Phase I and Pharmacodynamic Studies of G3139, a Bcl-2 Antisense Oligonucleotide, in Combination with Chemotherapy in Refractory or Relapsed Acute Leukemia. *Blood* **22**, 22.

Marley SB, Lewis JL, Schneider H, Rudd CE, Gordon MY (2004) Phosphatidylinositol-3 kinase inhibitors reproduce the selective antiproliferative effects of imatinib on chronic myeloid leukaemia progenitor cells. *Br J Haematol* **125**, 500-11.

Martiat P, Lewalle P, Taj AS, Philippe M, Larondelle Y, Vaerman JL, Wildmann C, Goldman JM, Michaux JL (1993) Retrovirally transduced antisense sequences stably suppress P210BCR-ABL expression and inhibit the proliferation of BCR/ABL-containing cell lines. *Blood* **81**, 502-9.

Martino A, Holmes JHt, Lord JD, Moon JJ, Nelson BH (2001) Stat5 and Sp1 regulate transcription of the cyclin D2 gene in response to IL-2. *J Immunol* **166**, 1723-9.

Mathews DH, Disney MD, Childs JL, Schroeder SJ, Zuker M, Turner DH (2004) Incorporating chemical modification constraints into a dynamic programming algorithm for prediction of RNA secondary structure. *Proc Natl Acad Sci U S A* **101**, 7287-92. Epub 2004 May 3.

Matulonis U, Salgia R, Okuda K, Druker B, Griffin JD (1993) Interleukin-3 and p210 BCR/ABL activate both unique and overlapping pathways of signal transduction in a factor-dependent myeloid cell line. *Exp Hematol* **21**, 1460-6.

Maury S, Belhadj K, Chami I, Kuentz M, Cordonnier C, Bories D (2001) Autologous reconstitution combined with durable leukemic remission after allogeneic BMT for CML: absence of persistence of a donor-derived T cell effector population. *Bone Marrow Transplant* **28**, 717-20.

Meehl MA, Caparon MG (2004) Specificity of streptolysin O in cytolysin-mediated translocation. *Mol Microbiol* **52**, 1665-76.

Meister G, Landthaler M, Dorsett Y, Tuschl T (2004) Sequence-specific inhibition of microRNA- and siRNA-induced RNA silencing. *Rna* **10**, 544-50.

Mello CC, Conte D, Jr. (2004) Revealing the world of RNA interference. *Nature* **431**, 338-42.

Mercatante DR, Kole R (2002) Control of alternative splicing by antisense oligonucleotides as a potential chemotherapy: effects on gene expression. *Biochim Biophys Acta* **1587**, 126-32.

Meyer O, Kirpotin D, Hong K, Sternberg B, Park JW, Woodle MC, Papahadjopoulos D (1998) Cationic liposomes coated with polyethylene glycol as carriers for oligonucleotides. *J Biol Chem* **273**, 15621-7.

Miller PS, Cassidy RA, Hamma T, Kondo NS (2000) Studies on anti-human immunodeficiency virus oligonucleotides that have alternating methylphosphonate/phosphodiester linkages. *Pharmacol Ther* **85**, 159-63.

Min KL, Viazovkina E, Galarneau A, Parniak MA, Damha MJ (2002) Oligonucleotides comprised of alternating 2'-deoxy-2'-fluoro-beta-D-arabinonucleosides and D-2'-deoxyribonucleosides (2'F-ANA/DNA 'altimers') induce efficient RNA cleavage mediated by RNase H. *Bioorg Med Chem Lett* **12**, 2651-4.

Minasov G, Teplova M, Nielsen P, Wengel J, Egli M (2000) Structural basis of cleavage by RNase H of hybrids of arabinonucleic acids and RNA. *Biochemistry* **39**, 3525-32.

Mollee P, Arthur C, *et al.* (2004) Interferon-{alpha}-2b and oral cytarabine ocfosfate for newly diagnosed chronic myeloid leukaemia. *Ann Oncol* **15**, 1810-1815.

Monia BP, Johnston JF, Sasmor H, Cummins LL (1996) Nuclease resistance and antisense activity of modified oligonucleotides targeted to Ha-ras. *J Biol Chem* **271**, 14533-40.

Moon JJ, Rubio ED, Martino A, Krumm A, Nelson BH (2004) A permissive role for phosphatidylinositol 3-kinase in the Stat5-mediated expression of cyclin D2 by the interleukin-2 receptor. *J Biol Chem* **279**, 5520-7. Epub 2003 Dec 02.

Morcos PA (2001) Achieving efficient delivery of morpholino oligos in cultured cells. *Genesis* **30**, 94-102.

Morris MC, Chaloin L, Mery J, Heitz F, Divita G (1999) A novel potent strategy for gene delivery using a single peptide vector as a carrier. *Nucleic Acids Res* **27**, 3510-7.

Morse MA (2001) Technology evaluation: ISIS-2503, Isis Pharmaceuticals. *Curr Opin Mol Ther* **3**, 589-94.

Moulton HM, Nelson MH, Hatlevig SA, Reddy MT, Iversen PL (2004) Cellular uptake of antisense morpholino oligomers conjugated to arginine-rich peptides. *Bioconjug Chem* **15**, 290-9.

Mullen P, McPhillips F, MacLeod K, Monia B, Smyth JF, Langdon SP (2004) Antisense oligonucleotide targeting of Raf-1: importance of raf-1 mRNA expression levels and raf-1-dependent signaling in determining growth response in ovarian cancer. *Clin Cancer Res* **10**, 2100-8.

Muotri AR, da Veiga Pereira L, dos Reis Vasques L, Menck CF (1999) Ribozymes and the anti-gene therapy: how a catalytic RNA can be used to inhibit gene function. *Gene* **237**, 303-10.

Muratovska A, Eccles MR (2004) Conjugate for efficient delivery of short interfering RNA (siRNA) into mammalian cells. *FEBS Lett* **558**, 63-8.

Nathan PC, Sung L, Crump M, Beyene J (2004) Consolidation therapy with autologous bone marrow transplantation in adults with acute myeloid leukemia: a meta-analysis. *J*

Natl Cancer Inst **96**, 38-45.

NCBI (2004) The BLASTn search tool http://www.ncbi.nlm.nih.gov/BLAST/. (NCBI)

Neshat MS, Raitano AB, Wang HG, Reed JC, Sawyers CL (2000) The survival function of the Bcr-Abl oncogene is mediated by Bad-dependent and -independent pathways: roles for phosphatidylinositol 3-kinase and Raf. *Mol Cell Biol* **20**, 1179-86.

Nichols BJ, Kenworthy AK, Polishchuk RS, Lodge R, Roberts TH, Hirschberg K, Phair RD, Lippincott-Schwartz J (2001) Rapid cycling of lipid raft markers between the cell surface and Golgi complex. *J Cell Biol* **153**, 529-41.

Nielsen PE (1995) DNA analogues with nonphosphodiester backbones. *Annu Rev Biophys Biomol Struct* **24**, 167-83.

Niewiarowski W, Gendaszewska E, Rebowski G, Wojcik M, Mikolajczyk B, Goss W, Soszynski M, Bartosz G (2000) Multidrug resistance-associated protein--reduction of expression in human leukaemia cells by antisense phosphorothioate oligonucleotides. *Acta Biochim Pol* **47**, 1183-8.

Novina CD, Murray MF, *et al.* (2002) siRNA-directed inhibition of HIV-1 infection. *Nat Med* **8**, 681-6.

Nowell PC, Hungerford DA (1960) A minute chromosome in human chronic granulocytic leukemia. *Science* **132**, 1497.

O'Brien SG, Kirkland MA, Melo JV, Rao MH, Davidson RJ, McDonald C, Goldman JM (1994) Antisense BCR-ABL oligomers cause non-specific inhibition of chronic myeloid leukemia cell lines. *Leukemia* **8**, 2156-62.

Oehlke J, Birth P, Klauschenz E, Wiesner B, Beyermann M, Oksche A, Bienert M (2002) Cellular uptake of antisense oligonucleotides after complexing or conjugation with cell-penetrating model peptides. *Eur J Biochem* **269**, 4025-32.

Olie RA, Hall J, Natt F, Stahel RA, Zangemeister-Wittke U (2002) Analysis of ribosyl-modified, mixed backbone analogs of a bcl-2/bcl-xL antisense oligonucleotide. *Biochim Biophys Acta* **1576**, 101-9.

Olsson-Stromberg U, Simonsson B, *et al.* (2004) Comparison of busulphan, hydroxyurea and allogeneic bone marrow transplantation (BMT) in chronic myeloid leukaemia: BMT prolongs survival. *Hematol J* **5**, 462-6.

Orr RM, Dorr FA (2005) Clinical studies of antisense oligonucleotides for cancer therapy. *Methods Mol Med* **106**, 85-111.

Oupicky D, Diwadkar V (2003) Stimuli-responsive gene delivery vectors. *Curr Opin Mol*

Ther **5**, 345-50.

Overfield J, Dawson M, D H (1999) 'Transfusion Science.' (Butterworth Heinemann Publishers)

Pannier AK, Arora V, Iversen PL, Brand RM (2004) Transdermal delivery of phosphorodiamidate Morpholino oligomers across hairless mouse skin. *Int J Pharm* **275**, 217-26.

Parada Y, Banerji L, *et al.* (2001) BCR-ABL and interleukin 3 promote haematopoietic cell proliferation and survival through modulation of cyclin D2 and p27Kip1 expression. *J Biol Chem* **276**, 23572-80.

Paterson BM, Roberts BE, Kuff EL (1977) Structural gene identification and mapping by DNA-mRNA hybrid-arrested cell-free translation. *Proc Natl Acad Sci U S A* **74**, 4370-4.

Patzel V, Steidl U, Kronenwett R, Haas R, Sczakiel G (1999) A theoretical approach to select effective antisense oligodeoxyribonucleotides at high statistical probability. *Nucleic Acids Res* **27**, 4328-34.

Pavithran K (2001) Treatment of Leukemia-An Update http://www.priory.com/med/leuk.htm. In.

Pedersen JS, Meyer IM, Forsberg R, Simmonds P, Hein J (2004) A comparative method for finding and folding RNA secondary structures within protein-coding regions. *Nucleic Acids Res* **32**, 4925-36. Print 2004.

Peracchi A (2004) Prospects for antiviral ribozymes and deoxyribozymes. *Rev Med Virol* **14**, 47-64.

Phillips MI (2005) Antisense therapeutics: a promise waiting to be fulfilled. *Methods Mol Med* **106**, 3-10.

Piatelli MJ, Wardle C, Blois J, Doughty C, Schram BR, Rothstein TL, Chiles TC (2004) Phosphatidylinositol 3-kinase-dependent mitogen-activated protein/extracellular signal-regulated kinase kinase 1/2 and NF-kappa B signaling pathways are required for B cell antigen receptor-mediated cyclin D2 induction in mature B cells. *J Immunol* **172**, 2753-62.

Pichon C, Monsigny M, Roche AC (1999) Intracellular localization of oligonucleotides: influence of fixative protocols. *Antisense Nucleic Acid Drug Dev* **9**, 89-93.

Piller G (2001) Leukaemia - a brief historical review from ancient times to 1950. *Br J Haematol* **112**, 282-92.

Plasterk RH (2002) RNA silencing: the genome's immune system. *Science* **296**, 1263-5.

Pooga M, Land T, Bartfai T, Langel U (2001) PNA oligomers as tools for specific modulation of gene expression. *Biomol Eng* **17**, 183-92.

Prater CE, Miller PS (2004) 3'-methylphosphonate-modified oligo-2'-O-methylribonucleotides and their Tat peptide conjugates: uptake and stability in mouse fibroblasts in culture. *Bioconjug Chem* **15**, 498-507.

Prochownik EV (2004) c-Myc as a therapeutic target in cancer. *Expert Rev Anticancer Ther* **4**, 289-302.

Qin G, Taylor M, Ning YY, Iversen P, Kobzik L (2000) In vivo evaluation of a morpholino antisense oligomer directed against tumor necrosis factor-alpha. *Antisense Nucleic Acid Drug Dev* **10**, 11-6.

Raab RM, Stephanopoulos G (2004) Dynamics of gene silencing by RNA interference. *Biotechnol Bioeng* **88**, 121-32.

Radosevic N, Delmer A, Tang R, Marie JP, Ajchenbaum-Cymbalista F (2001) Cell cycle regulatory protein expression in fresh acute myeloid leukemia cells and after drug exposure. *Leukemia* **15**, 559-66.

Raffo A, Lai JC, Stein CA, Miller P, Scaringe S, Khvorova A, Benimetskaya L (2004) Antisense RNA down-regulation of bcl-2 expression in DU145 prostate cancer cells does not diminish the cytostatic effects of G3139 (Oblimersen). *Clin Cancer Res* **10**, 3195-206.

Raitano AB, Halpern JR, Hambuch TM, Sawyers CL (1995) The Bcr-Abl leukemia oncogene activates Jun kinase and requires Jun for transformation. *Proc Natl Acad Sci U S A* **92**, 11746-50.

Raju J, Patlolla JM, Swamy MV, Rao CV (2004) Diosgenin, a steroid saponin of Trigonella foenum graecum (Fenugreek), inhibits azoxymethane-induced aberrant crypt foci formation in F344 rats and induces apoptosis in HT-29 human colon cancer cells. *Cancer Epidemiol Biomarkers Prev* **13**, 1392-8.

Ramaswamy G, Slack FJ (2002) siRNA. A guide for RNA silencing. *Chem Biol* **9**, 1053-5.

Ramirez MT, Sah VP, Zhao XL, Hunter JJ, Chien KR, Brown JH (1997) The MEKK-JNK pathway is stimulated by alpha1-adrenergic receptor and ras activation and is associated with in vitro and in vivo cardiac hypertrophy. *J Biol Chem* **272**, 14057-61.

Rapozzi V, Burm BE, Cogoi S, Van Der Marel GA, Van Boom JH, Quadrifoglio F, Xodo LE (2002) Antiproliferative effect in chronic myeloid leukaemia cells by antisense peptide nucleic acids. *Nucleic Acids Res* **30**, 3712-21.

Ray A, Norden B (2000) Peptide nucleic acid (PNA): its medical and biotechnical applications and promise for the future. *Faseb J* **14**, 1041-60.

Re RN, Cook JL, Giardina JF (2004) The inhibition of tumor growth by triplex-forming oligonucleotides. *Cancer Lett* **209**, 51-3.

Rebowski G, Wojcik M, Boczkowska M, Gendaszewska E, Soszynski M, Bartosz G, Niewiarowski W (2001) Antisense hairpin loop oligonucleotides as inhibitors of expression of multidrug resistance-associated protein 1: their stability in fetal calf serum and human plasma. *Acta Biochim Pol* **48**, 1061-76.

Reiter A, Hochhaus A, Berger U, Kuhn C, Hehlmann R (2001) AraC-based pharmacotherapy of chronic myeloid leukaemia. *Expert Opin Pharmacother* **2**, 1129-35.

Reynolds A, Leake D, Boese Q, Scaringe S, Marshall WS, Khvorova A (2004) Rational siRNA design for RNA interference. *Nat Biotechnol* **1**, 1.

Ribozyme PI (2002) http://www.rpi.com/hepc.jsp
Targeting Disease with nucleic acid technology-Heptazyme.. (Ribozyme Pharmaceuticals Inc.)

Ribozyme PI (2002) http://www.rpi.com/herzyme.jsp
Targeting Disease with nucleic acid technology-Herzyme. In. (Pharmaceuticals Inc Ribozyme)

Rodriguez-Puebla ML, LaCava M, Miliani De Marval PL, Jorcano JL, Richie ER, Conti CJ (2000) Cyclin D2 overexpression in transgenic mice induces thymic and epidermal hyperplasia whereas cyclin D3 expression results only in epidermal hyperplasia. *Am J Pathol* **157**, 1039-50.

Rossignol F, Vache C, Clottes E (2002) Natural antisense transcripts of hypoxia-inducible factor 1alpha are detected in different normal and tumour human tissues. *Gene* **299**, 135-40.

Rosti G, Bonifazi F, Trabacchi E, De Vivo A, Bassi S, Martinelli G, Testoni N, Russo D, Baccarani M (2003) A phase II study of alpha-interferon and oral arabinosyl cytosine (YNK01) in chronic myeloid leukemia. *Leukemia* **17**, 554-9.

Rouillard JM, Zuker M, Gulari E (2003) OligoArray 2.0: design of oligonucleotide probes for DNA microarrays using a thermodynamic approach. *Nucleic Acids Res* **31**, 3057-62.

Rowley JD (1973) A new consistent chromosomal abnormality in chronic myelogenous leukaemia identified by quinacrine fluorescence and Giemsa staining :Letter. *Nature* **243**, 290-3.

Rowley PT, Kosciolek BA, Kool ET (1999) Circular antisense oligonucleotides inhibit growth of chronic myeloid leukemia cells. *Mol Med* **5**, 693-700.

Rudin CM, Holmlund J, *et al.* (2001) Phase I Trial of ISIS 5132, an antisense oligonucleotide inhibitor of c-raf-1, administered by 24-hour weekly infusion to patients with advanced cancer. *Clin Cancer Res* **7**, 1214-20.

Rudin CM, Kozloff M, Hoffman PC, Edelman MJ, Karnauskas R, Tomek R, Szeto L, Vokes EE (2004) Phase I study of G3139, a bcl-2 antisense oligonucleotide, combined with carboplatin and etoposide in patients with small-cell lung cancer. *J Clin Oncol* **22**, 1110-7.

Saikawa Y, Kubota T, Otani Y, Kitajima M, Modlin IM (2001) Cyclin D1 antisense oligonucleotide inhibits cell growth stimulated by epidermal growth factor and induces apoptosis of gastric cancer cells. *Jpn J Cancer Res* **92**, 1102-9.

Salomoni P, Condorelli F, Sweeney SM, Calabretta B (2000) Versatility of BCR/ABL-expressing leukemic cells in circumventing proapoptotic BAD effects. *Blood* **96**, 676-84.

Samglik P (1998) Making sense of antisense. *The Scientist* **12**.

Sanchez-Garcia I, Martin-Zanca D (1997) Regulation of Bcl-2 gene expression by BCR-ABL is mediated by Ras. *J Mol Biol* **267**, 225-8.

Sasaki Y, Jensen CT, Karlsson S, Jacobsen SE (2004) Enforced expression of cyclin D2 enhances the proliferative potential of myeloid progenitors, accelerates in vivo myeloid reconstitution, and promotes rescue of mice from lethal myeloablation. *Blood* **104**, 986-92. Epub 2004 Apr 22.

Sattler M, Salgia R (1998) Role of the adapter protein CRKL in signal transduction of normal hematopoietic and BCR/ABL-transformed cells. *Leukemia* **12**, 637-44.

Savage DG, Antman KH (2002) Imatinib mesylate--a new oral targeted therapy. *N Engl J Med* **346**, 683-93.

Sawyers CL (1993) The role of myc in transformation by BCR-ABL. *Leuk Lymphoma* **11**, 45-6.

Sawyers CL (1997) Signal transduction pathways involved in BCR-ABL transformation. In 'Baillieres Clinical Haematology')

Sazani P, Gemignani F, Kang SH, Maier MA, Manoharan M, Persmark M, Bortner D, Kole R (2002) Systemically delivered antisense oligomers upregulate gene expression in mouse tissues. *Nat Biotechnol* **20**, 1228-33.

Sazani P, Vacek MM, Kole R (2002) Short-term and long-term modulation of gene

expression by antisense therapeutics. *Curr Opin Biotechnol* **13**, 468-72.

Schaff GW (1998) Fomivirsen approved for CMV retinitis: first antisense drug. *AIDS Treat News*, 7.

Scherr M, Battmer K, Winkler T, Heidenreich O, Ganser A, Eder M (2003) Specific inhibition of bcr-abl gene expression by small interfering RNA. *Blood* **101**, 1566-9.

Scherr M, Morgan MA, Eder M (2003) Gene silencing mediated by small interfering RNAs in mammalian cells. *Curr Med Chem* **10**, 245-56.

Scherr M, Steinmann D, Eder M (2004) RNA interference (RNAi) in hematology. *Ann Hematol* **83**, 1-8. Epub 2003 Oct 22.

Schiavone N, Donnini M, Nicolin A, Capaccioli S (2004) Antisense oligonucleotide drug design. *Curr Pharm Des* **10**, 769-84.

Schiffelers RM, Woodle MC, Scaria P (2004) Pharmaceutical prospects for RNA interference. *Pharm Res* **21**, 1-7.

Schmajuk G, Sierakowska H, Kole R (1999) Antisense oligonucleotides with different backbones. Modification of splicing pathways and efficacy of uptake. *J Biol Chem* **274**, 21783-9.

Schnapp E, Tamaka EM (2004) Quantitative evaluation of morpholino-mediated protein knockdown of GFP, MSX1, and PAX7 during tail regeneration in Ambystoma mexicanum. *Dev Dyn* **232**, 162-170.

Schutze N (2004) siRNA technology. *Mol Cell Endocrinol* **213**, 115-9.

Schwarz DS, Hutvagner G, Haley B, Zamore PD (2002) Evidence that siRNAs function as guides, not primers, in the Drosophila and human RNAi pathways. *Mol Cell* **10**, 537-48.

Schwarz DS, Tomari Y, Zamore PD (2004) The RNA-Induced Silencing Complex Is a Mg(2+)-Dependent Endonuclease. *Curr Biol* **14**, 787-91.

Scudiero DA, Shoemaker RH, Paull KD, Monks A, Tierney S, Nofziger TH, Currens MJ, Seniff D, Boyd MR (1988) Evaluation of a soluble tetrazolium/formazan assay for cell growth and drug sensitivity in culture using human and other tumor cell lines. *Cancer Res* **48**, 4827-33.

Sczakiel G (2000) Theoretical and experimental approaches to design effective antisense oligonucleotides. *Front Biosci* **5**, D194-201.

Sereni D, Tubiana R, *et al.* (1999) Pharmacokinetics and tolerability of intravenous

trecovirsen (GEM 91), an antisense phosphorothioate oligonucleotide, in HIV-positive subjects. *J Clin Pharmacol* **39**, 47-54.

Shen C, Buck AK, Liu X, Winkler M, Reske SN (2003) Gene silencing by adenovirus-delivered siRNA. *FEBS Lett* **539**, 111-4.

Shen C, Reske SN (2004) Adenovirus-delivered siRNA. *Methods Mol Biol* **252**, 523-32.

Sherr CJ (1996) Cancer cell cycles. *Science* **274**, 1672-7.

Shi F, Hoekstra D (2004) Effective intracellular delivery of oligonucleotides in order to make sense of antisense. *J Control Release* **97**, 189-209.

Shuai K, Halpern J, ten Hoeve J, Rao X, Sawyers CL (1996) Constitutive activation of STAT5 by the BCR-ABL oncogene in chronic myelogenous leukemia. *Oncogene* **13**, 247-54.

Shuey DJ, McCailus DE, Giordano T (2002) RNAi: gene-silencing in therapeutic intervention. *Drug Discov Today* **7**, 1040-6.

Sierig G, Cywes C, Wessels MR, Ashbaugh CD (2003) Cytotoxic effects of streptolysin o and streptolysin s enhance the virulence of poorly encapsulated group a streptococci. *Infect Immun* **71**, 446-55.

Silva JM, Sachidanandam R, Hannon GJ (2003) Free energy lights the path toward more effective RNAi. *Nat Genet* **35**, 303-5.

Simmer F, Tijsterman M, Parrish S, Koushika SP, Nonet ML, Fire A, Ahringer J, Plasterk RH (2002) Loss of the putative RNA-directed RNA polymerase RRF-3 makes C. elegans hypersensitive to RNAi. *Curr Biol* **12**, 1317-9.

Singer IO, Franklin IM (1998) Autografting as first line treatment for chronic myeloid leukaemia. *J Clin Pathol* **51**, 92-5.

Singer IO, Franklin IM, *et al.* (1998) Autologous transplantation in chronic myeloid leukaemia using peripheral blood stem cells. *Br J Haematol* **102**, 1359-62.

Singer NG, McCune WJ (1998) Update on immunosuppressive therapy. *Curr Opin Rheumatol* **10**, 169-73.

Sioud M (2004) Therapeutic siRNAs. *Trends Pharmacol Sci* **25**, 22-8.

Sioud M, Sorensen DR (2003) Cationic liposome-mediated delivery of siRNAs in adult mice. *Biochem Biophys Res Commun* **312**, 1220-5.

Skorski T, Nieborowska-Skorska M, Nicolaides NC, Szczylik C, Iversen P, Iozzo RV, Zon G, Calabretta B (1994) Suppression of Philadelphia1 leukemia cell growth in mice

by BCR-ABL antisense oligodeoxynucleotide. *Proc Natl Acad Sci U S A* **91**, 4504-8.

Smaglik P (1998) Making Sense of Antisense. *The Scientist* **12**.

Smetsers TF, Skorski T, van de Locht LT, Wessels HM, Pennings AH, de Witte T, Calabretta B, Mensink EJ (1994) Antisense BCR-ABL oligonucleotides induce apoptosis in the Philadelphia chromosome-positive cell line BV173. *Leukemia* **8**, 129-40.

Smetsers TF, van de Locht LT, Pennings AH, Wessels HM, de Witte TM, Mensink EJ (1995) Phosphorothioate BCR-ABL antisense oligonucleotides induce cell death, but fail to reduce cellular bcr-abl protein levels. *Leukemia* **9**, 118-30.

Smith L, Andersen KB, Hovgaard L, Jaroszewski JW (2000) Rational selection of antisense oligonucleotide sequences. *Eur J Pharm Sci* **11**, 191-8.

Sohail M (2001) Antisense technology: inaccessibility and non-specificity. *Drug Discov Today* **6**, 1260-1261.

Sohail M, Southern EM (2000) Selecting optimal antisense reagents. *Adv Drug Deliv Rev* **44**, 23-34.

Sohail M, Southern EM (2000) Hybridization of antisense reagents to RNA. *Curr Opin Mol Ther* **2**, 264-71.

Sohail M, Southern EM (2000) Antisense arrays. *Mol Cell Biol Res Commun* **3**, 67-72.

Solvason N, Wu WW, *et al.* (2000) Cyclin D2 is essential for BCR-mediated proliferation and CD5 B cell development. *Int Immunol* **12**, 631-8.

Sonoyama J, Matsumura I, *et al.* (2002) Functional cooperation among Ras, STAT5, and phosphatidylinositol 3-kinase is required for full oncogenic activities of BCR/ABL in K562 cells. *J Biol Chem* **277**, 8076-82. Epub 2002 Jan 04.

Spiekermann K, Pau M, Schwab R, Schmieja K, Franzrahe S, Hiddemann W (2002) Constitutive activation of STAT3 and STAT5 is induced by leukemic fusion proteins with protein tyrosine kinase activity and is sufficient for transformation of hematopoietic precursor cells. *Exp Hematol* **30**, 262-71.

Spiller DG, Giles RV, Grzybowski J, Tidd DM, Clark RE (1998) Improving the intracellular delivery and molecular efficacy of antisense oligonucleotides in chronic myeloid leukemia cells: a comparison of streptolysin-O permeabilization, electroporation, and lipophilic conjugation. *Blood* **91**, 4738-46.

Spiller DG, Tidd DM (1995) Nuclear delivery of antisense oligodeoxynucleotides through reversible permeabilization of human leukemia cells with streptolysin O. *Antisense Res Dev* **5**, 13-21.

Stein CA (1995) Does antisense exist? *Nat Med* **1**, 1119-21.

Stein CA (1996) Phosphorothioate antisense oligodeoxynucleotides: questions of specificity. *Trends Biotechnol* **14**, 147-9.

Stein CA (1999) Two problems in antisense biotechnology: in vitro delivery and the design of antisense experiments. *Biochim Biophys Acta* **1489**, 45-52.

Stein CA (2000) Is irrelevant cleavage the price of antisense efficacy? *Pharmacol Ther* **85**, 231-6.

Stein CA (2001) The experimental use of antisense oligonucleotides: a guide for the perplexed. *J Clin Invest* **108**, 641-4.

Stevenson JP, Yao KS, *et al.* (1999) Phase I clinical/pharmacokinetic and pharmacodynamic trial of the c-raf-1 antisense oligonucleotide ISIS 5132 (CGP 69846A). *J Clin Oncol* **17**, 2227-36.

Stevenson M (2004) Therapeutic potential of RNA interference. *N Engl J Med* **351**, 1772-7.

Stewart MJ, Litz-Jackson S, Burgess GS, Williamson EA, Leibowitz DS, Boswell HS (1995) Role for E2F1 in p210 BCR-ABL downstream regulation of c-myc transcription initiation. Studies in murine myeloid cells. *Leukemia* **9**, 1499-507.

Storz G (2002) An expanding universe of noncoding RNAs. *Science* **296**, 1260-3.

Storz G, Opdyke JA, Zhang A (2004) Controlling mRNA stability and translation with small, noncoding RNAs. *Curr Opin Microbiol* **7**, 140-4.

Sullenger BA, Gilboa E (2002) Emerging clinical applications of RNA. *Nature* **418**, 252-8.

Summerton J (1999) Morpholino antisense oligomers: the case for an RNase H-independent structural type. *Biochim Biophys Acta* **1489**, 141-58.

Summerton J, Weller D (1997) Morpholino antisense oligomers: design, preparation, and properties. *Antisense Nucleic Acid Drug Dev* **7**, 187-95.

Summerton JE (2003) Custom cancer therapies: safe and effective treatments for most or all cancers. *Ann N Y Acad Sci* **1002**, 189-96.

Suwanmanee T, Sierakowska H, Fucharoen S, Kole R (2002) Repair of a splicing defect in erythroid cells from patients with beta-thalassemia/HbE disorder. *Mol Ther* **6**, 718-26.

Suwanmanee T, Sierakowska H, Lacerra G, Svasti S, Kirby S, Walsh CE, Fucharoen S, Kole R (2002) Restoration of human beta-globin gene expression in murine and human IVS2-654 thalassemic erythroid cells by free uptake of antisense oligonucleotides. *Mol Pharmacol* **62**, 545-53.

t Hoen PA, Out R, Commandeur JN, Vermeulen NP, van Batenburg FH, Manoharan M, van Berkel TJ, Biessen EA, Bijsterbosch MK (2002) Selection of antisense oligodeoxynucleotides against glutathione S-transferase Mu. *Rna* **8**, 1572-83.

Takano Y, Kato Y, van Diest PJ, Masuda M, Mitomi H, Okayasu I (2000) Cyclin D2 overexpression and lack of p27 correlate positively and cyclin E inversely with a poor prognosis in gastric cancer cases. *Am J Pathol* **156**, 585-94.

Takei Y, Kadomatsu K, Yuasa K, Sato W, Muramatsu T (2004) Morpholino antisense oligomer targeting human midkine: Its application for cancer therapy. *Int J Cancer* **1**, 1.

Tamm I (2005) Antisense therapy in clinical oncology: preclinical and clinical experiences. *Methods Mol Med* **106**, 113-34.

Tamm I, Dorken B, Hartmann G (2001) Antisense therapy in oncology: new hope for an old idea? *Lancet* **358**, 489-97.

Tanaka M, Nyce JW (2001) Respirable antisense oligonucleotides: a new drug class for respiratory disease. *Respir Res* **2**, 5-9.

Tanguay DA, Chiles TC (1996) Regulation of the catalytic subunit (p34PSK-J3/cdk4) for the major D-type cyclin in mature B lymphocytes. *J Immunol* **156**, 539-48.

Tari AM, Tucker SD, Deisseroth A, Lopez-Berestein G (1994) Liposomal delivery of methylphosphonate antisense oligodeoxynucleotides in chronic myelogenous leukemia. *Blood* **84**, 601-7.

Tauchi T, Ohyashiki K (2004) Molecular mechanisms of resistance of leukemia to imatinib mesylate. *Leuk Res* **28**, S39-45.

Telegeev GD, Dubrovska AN, Dybkov MV, Maliuta SS (2004) Influence of BCR/ABL fusion proteins on the course of Ph leukemias. *Acta Biochim Pol* **51**, 845-9.

Teramoto N, Pokrovskaja K, Szekely L, Polack A, Yoshino T, Akagi T, Klein G (1999) Expression of cyclin D2 and D3 in lymphoid lesions. *Int J Cancer* **81**, 543-50.

Thijsen S, Schuurhuis G, van Oostveen J, Ossenkoppele G (1999) Chronic myeloid leukemia from basics to bedside. *Leukemia* **13**, 1646-74.

Thompson JD (2002) Applications of antisense and siRNAs during preclinical drug development. *Drug Discov Today* **7**, 912-7.

Thurston DE (1999) Nucleic acid targeting: therapeutic strategies for the 21st century. *Br J Cancer* **1**, 65-85.

Timmons L, Tabara H, Mello CC, Fire AZ (2003) Inducible systemic RNA silencing in Caenorhabditis elegans. *Mol Biol Cell* **14**, 2972-83.

Tipping AJ, Mahon FX, Lagarde V, Goldman JM, Melo JV (2001) Restoration of sensitivity to STI571 in STI571-resistant chronic myeloid leukemia cells. *Blood* **98**, 3864-7.

Tiscornia G, Singer O, Ikawa M, Verma IM (2003) A general method for gene knockdown in mice by using lentiviral vectors expressing small interfering RNA. *Proc Natl Acad Sci U S A* **100**, 1844-8.

Torigoe H, Kawahashi K, Tamura Y (2003) Promotion of triplex formation by morpholino modification: thermodynamic and kinetic studies. *Nucleic Acids Res Suppl*, 157-8.

Toschi N (2000) Influence of mRNA self-structure on hybridization: computational tools for antisense sequence selection. *Methods* **22**, 261-9.

Tourriere H, Chebli K, Tazi J (2002) mRNA degradation machines in eukaryotic cells. *Biochimie* **84**, 821-37.

Turchi L, Loubat A, Rochet N, Rossi B, Ponzio G (2000) Evidence for a direct correlation between c-Jun NH2 terminal kinase 1 activation, cyclin D2 expression, and G(1)/S phase transition in the murine hybridoma 7TD1 cells. *Exp Cell Res* **261**, 220-8.

Turhan AG, Solary E, Vainchenker W, Dusanter-Fourt I (1998) Molecular pathophysiology of chronic myelogenous leukemia. *Hematol Cell Ther* **40**, 217-21.

Tuschl T (2002) Expanding small RNA interference. *Nat Biotechnol* **20**, 446-8.

Tuschl T, Elbashir S, Harborth J, Weber K (2003) The siRNA User Guide: Selection of siRNA duplexes from the target mRNA sequence. In.

Uchida H, Tanaka T, *et al.* (2004) Adenovirus-mediated transfer of siRNA against survivin induced apoptosis and attenuated tumor cell growth in vitro and in vivo. *Mol Ther* **10**, 162-71.

Ueno Y, Ishihara S, Ito Y, Kitade Y (2004) Synthesis of 2',5'-oligoadenylate analogs containing an adenine acyclonucleoside and their ability to activate human RNase L. *Bioorg Med Chem Lett* **14**, 4431-4.

Van Etten RA (2004) Mechanisms of transformation by the BCR-ABL oncogene: new

perspectives in the post-imatinib era. *Leuk Res* **28**, S21-8.

Verfaillie CM, McIvor RS, Zhao RC (1999) Gene therapy for chronic myelogenous leukemia. *Mol Med Today* **5**, 359-66.

Vester B, Wengel J (2004) LNA (locked nucleic acid): high-affinity targeting of complementary RNA and DNA. *Biochemistry* **43**, 13233-41.

Vickers TA, Koo S, Bennett CF, Crooke ST, Dean NM, Baker BF (2003) Efficient reduction of target RNAs by small interfering RNA and RNase H-dependent antisense agents. A comparative analysis. *J Biol Chem* **278**, 7108-18.

Vickers TA, Wyatt JR, Freier SM (2000) Effects of RNA secondary structure on cellular antisense activity. *Nucleic Acids Res* **28**, 1340-7.

Villalona-Calero MA, Ritch P, *et al.* (2004) A phase I/II study of LY900003, an antisense inhibitor of protein kinase C-alpha, in combination with cisplatin and gemcitabine in patients with advanced non-small cell lung cancer. *Clin Cancer Res* **10**, 6086-93.

Virmani A, Rathi A, *et al.* (2003) Aberrant methylation of the cyclin D2 promoter in primary small cell, nonsmall cell lung and breast cancers. *Int J Cancer* **107**, 341-5.

Wagner E, Ogris M, Zauner W (1998) Polylysine-based transfection systems utilizing receptor-mediated delivery. *Adv Drug Deliv Rev* **30**, 97-113.

Wagner EG, Flardh K (2002) Antisense RNAs everywhere? *Trends Genet* **18**, 223-6.

Wagner RW, Flanagan WM (1997) Antisense technology and prospects for therapy of viral infections and cancer. *Mol Med Today* **3**, 31-8.

Wall NR, Shi Y (2003) Small RNA: can RNA interference be exploited for therapy? *Lancet* **362**, 1401-3.

Wang H, Cai Q, Zeng X, Yu D, Agrawal S, Zhang R (1999) Antitumor activity and pharmacokinetics of a mixed-backbone antisense oligonucleotide targeted to the RIalpha subunit of protein kinase A after oral administration. *Proc Natl Acad Sci U S A* **96**, 13989-94.

Wang H, Hang J, Shi Z, Li M, Yu D, Kandimalla ER, Agrawal S, Zhang R (2002) Antisense oligonucleotide targeted to RIalpha subunit of cAMP-dependent protein kinase (GEM231) enhances therapeutic effectiveness of cancer chemotherapeutic agent irinotecan in nude mice bearing human cancer xenografts: in vivo synergistic activity, pharmacokinetics and host toxicity. *Int J Oncol* **21**, 73-80.

Webb A, Cunningham D, Cotter F, Clarke PA, di Stefano F, Ross P, Corbo M, Dziewanowska Z (1997) BCL-2 antisense therapy in patients with non-Hodgkin

lymphoma. *Lancet* **349**, 1137-41.

Weinstein-Oppenheimer CR, Blalock WL, Steelman LS, Chang F, McCubrey JA (2000) The Raf signal transduction cascade as a target for chemotherapeutic intervention in growth factor-responsive tumors. *Pharmacol Ther* **88**, 229-79.

Weis S, Palmer M (2001) Streptolysin O: the C-terminal, tryptophan-rich domain carries functional sites for both membrane binding and self-interaction but not for stable oligomerization. *Biochim Biophys Acta* **1510**, 292-9.

Weng DE, Usman N (2001) Angiozyme: a novel angiogenesis inhibitor. *Curr Oncol Rep* **3**, 141-6.

Wertheim JA, Forsythe K, Druker BJ, Hammer D, Boettiger D, Pear WS (2002) BCR-ABL-induced adhesion defects are tyrosine kinase-independent. *Blood* **99**, 4122-30.

Wilds CJ, Damha MJ (2000) 2'-Deoxy-2'-fluoro-beta-D-arabinonucleosides and oligonucleotides (2'F-ANA): synthesis and physicochemical studies. *Nucleic Acids Res* **28**, 3625-35.

Williamson EA, Burgess GS, Eder P, Litz-Jackson S, Boswell HS (1997) Cyclic AMP negatively controls c-myc transcription and G1 cell cycle progression in p210 BCR-ABL transformed cells: inhibitory activity exerted through cyclin D1 and cdk4. *Leukemia* **11**, 73-85.

Wilson JA, Richardson CD (2003) Induction of RNA interference using short interfering RNA expression vectors in cell culture and animal systems. *Curr Opin Mol Ther* **5**, 389-96.

Wilson-Rawls J, Liu J, Laneuville P, Arlinghaus RB (1997) P210 Bcr-Abl interacts with the interleukin-3 beta c subunit and constitutively activates Jak2. *Leukemia* **3**, 428-31.

Winkler K (2004) Killing the messenger. *Nature Reviews Drug Discovery* **3**, 823-824.

Winston WM, Molodowitch C, Hunter CP (2002) Systemic RNAi in C. elegans requires the putative transmembrane protein SID-1. *Science* **295**, 2456-9. Epub 2002 Feb 07.

Witherell GW (2001) ISIS-14803 (Isis Pharmaceuticals). *Curr Opin Investig Drugs* **2**, 1523-9.

Wohlbold L, van der Kuip H, Miething C, Vornlocher HP, Knabbe C, Duyster J, Aulitzky WE (2003) Inhibition of bcr-abl gene expression by small interfering RNA sensitizes for imatinib mesylate (STI571). *Blood* **102**, 2236-9.

Wong SF-M, Jami, McLaughlin J FAU - Cheng D, Cheng D FAU - Shannon K (2003) IL-3 receptor signaling is dispensable for BCR-ABL-induced myeloproliferative disease.

PG - 11630-5. In.

Wood MJ, Trulzsch B, Abdelgany A, Beeson D (2003) Ribozymes and siRNA for the treatment of diseases of the nervous system. *Curr Opin Mol Ther* **5**, 383-8.

Wright L, Wilson SB, Milliken S, Biggs J, Kearney P (1993) Ribozyme-mediated cleavage of the bcr/abl transcript expressed in chronic myeloid leukemia. *Exp Hematol* **21**, 1714-8.

Xia H, Mao Q, Paulson HL, Davidson BL (2002) siRNA-mediated gene silencing in vitro and in vivo. *Nat Biotechnol* **20**, 1006-10.

Xie RL, Gupta S, Miele A, Shiffman D, Stein JL, Stein GS, van Wijnen AJ (2003) The tumor suppressor interferon regulatory factor 1 interferes with SP1 activation to repress the human CDK2 promoter. *J Biol Chem* **278**, 26589-96. Epub 2003 May 5.

Xie S, Lin H, Sun T, Arlinghaus RB (2002) Jak2 is involved in c-Myc induction by Bcr-Abl. *Oncogene* **21**, 7137-46.

Yacyshyn BR, Chey WY, *et al.* (2002) Double blind, placebo controlled trial of the remission inducing and steroid sparing properties of an ICAM-1 antisense oligodeoxynucleotide, alicaforsen (ISIS 2302), in active steroid dependent Crohn's disease. *Gut* **51**, 30-6.

Yamakawa H, Abe T, Saito T, Takai K, Yamamoto N, Takaku H (1998) Properties of nicked and circular dumbbell RNA/DNA chimeric oligonucleotides containing antisense phosphodiester oligodeoxynucleotides. *Bioorg Med Chem* **6**, 1025-32.

Yanagisawa K, Kosaka A, Iwahana H, Nakanishi M, Tominaga S (1999) Opposite regulation of the expression of cyclin-dependent kinase inhibitors during contact inhibition. *J Biochem (Tokyo)* **125**, 36-40.

Yinjun L, Jie J, Weilai X, Xiangming T (2004) Homoharringtonine mediates myeloid cell apoptosis via upregulation of pro-apoptotic bax and inducing caspase-3-mediated cleavage of poly(ADP-ribose) polymerase (PARP). *Am J Hematol* **76**, 199-204.

Yu J, Miehlke S, Ebert MP, Szokodi D, Wehvnignh B, Malfertheiner P, Ehninger G, Bayerdoerffer E (2002) Expression of cyclin genes in human gastric cancer and in first degree relatives. *Chin Med J (Engl)* **115**, 710-5.

Yuen AR, Sikic BI (2000) Clinical studies of antisense therapy in cancer. *Front Biosci* **5**, D588-93.

Zamaratski E, Pradeepkumar PI, Chattopadhyaya J (2001) A critical survey of the structure-function of the antisense oligo/RNA heteroduplex as substrate for RNase H. *J Biochem Biophys Methods* **48**, 189-208.

Zamore PD (2002) Ancient pathways programmed by small RNAs. *Science* **296**, 1265-9.

Zamore PD (2004) Plant RNAi: How a viral silencing suppressor inactivates siRNA. *Curr Biol* **14**, R198-200.

Zamore PD, Tuschl T, Sharp PA, Bartel DP (2000) RNAi: double-stranded RNA directs the ATP-dependent cleavage of mRNA at 21 to 23 nucleotide intervals. *Cell* **101**, 25-33.

Zender L, Kubicka S (2004) SiRNA based strategies for inhibition of apoptotic pathways in vivo--analytical and therapeutic implications. *Apoptosis* **9**, 51-4.

Zhang YC, Taylor MM, Samson WK, Phillips MI (2005) Antisense inhibition: oligonucleotides, ribozymes, and siRNAs. *Methods Mol Med* **106**, 11-34.

Zhao Q, Matson S, Herrera CJ, Fisher E, Yu H, Krieg AM (1993) Comparison of cellular binding and uptake of antisense phosphodiester, phosphorothioate, and mixed phosphorothioate and methylphosphonate oligonucleotides. *Antisense Res Dev* **3**, 53-66.

Zhao Q, Song X, Waldschmidt T, Fisher E, Krieg AM (1996) Oligonucleotide uptake in human hematopoietic cells is increased in leukemia and is related to cellular activation. *Blood* **88**, 1788-95.

Zhao RC, Jiang Y, Verfaillie CM (2001) A model of human p210(bcr/ABL)-mediated chronic myelogenous leukemia by transduction of primary normal human CD34(+) cells with a BCR/ABL-containing retroviral vector. *Blood* **97**, 2406-12.

Zheng R (1999) Technology evaluation: GEM-92, Hybridon Inc. *Curr Opin Mol Ther* **1**, 521-3.

Zuker M (2003) Mfold web server for nucleic acid folding and hybridization prediction. *Nucleic Acids Res* **31**, 3406-15.